DIOXYGEN ACTIVATION BY LOW VALENT COBALT COMPLEXES SUPPORTED BY FERROCENYL-SUBSTITUTED, REDOX ACTIVE HYDROTRIS(PYRAZOLYL)BORATE LIGANDS

by

Eric R. Sirianni

A dissertation submitted to the Faculty of the University of Delaware in partial fulfillment of the requirements for the degree of Doctor of Philosophy in Chemistry and Biochemistry

Fall 2014

ProQuest LLC.
789 East Eisenhower Parkway
P.O. Box 1346
Ann Arbor, MI 48106 - 1346

DIOXYGEN ACTIVATION BY LOW VALENT COBALT COMPLEXES SUPPORTED BY REDOX-ACTIVE, FERROCENYL-SUBSTITUTED HYDROTRIS(PYRAZOLYL)BORATE LIGANDS

by

Eric R. Sirianni

Approved: _____
Murray V. Johnston, Ph.D.
Chair of the Department of Chemistry and Biochemistry

Approved: _____
George H. Watson, Ph.D.
Dean of the College of Arts & Sciences

Approved: _____
James G. Richards, Ph.D.
Vice Provost for Graduate and Professional Education

I certify that I have read this dissertation and that in my opinion it meets the academic and professional standard required by the University as a dissertation for the degree of Doctor of Philosophy.

Signed: _____

Klaus H. Theopold, Ph.D.
Professor in charge of dissertation

I certify that I have read this dissertation and that in my opinion it meets the academic and professional standard required by the University as a dissertation for the degree of Doctor of Philosophy.

Signed: _____

Paul J. Fagan, Ph.D.
Member of dissertation committee

I certify that I have read this dissertation and that in my opinion it meets the academic and professional standard required by the University as a dissertation for the degree of Doctor of Philosophy.

Signed: _____

Charles G. Riordan, Ph.D.
Member of dissertation committee

I certify that I have read this dissertation and that in my opinion it meets the academic and professional standard required by the University as a dissertation for the degree of Doctor of Philosophy.

Signed: _____

Mary P. Watson, Ph.D.
Member of dissertation committee

Dedicated to my mother and father

ACKNOWLEDGMENTS

First and foremost I would like to extend my deep appreciation and thanks to my research advisor, Klaus Theopold, for the opportunity to work in his research group. Through his guidance, encouragement, and patience, I have been able to expand my knowledge of chemistry. His advice both in and out of the laboratory has been invaluable to me and has made my research experience a very rewarding one.

I would also like to thank the members of my dissertation committee, Dr. Charles Riordan, Dr. Mary Watson, and Dr. Paul Fagan for reviewing my research and providing me helpful advice during my graduate work. I am eternally grateful to Dr. Glenn Yap for his sage wisdom in X-ray crystallography and for his friendship. I would like to thank fellow group members, both past and present, for providing me with helpful discussion and counsel as we toiled in the Theopold lab together. A special thanks to both the Riordan lab and the Rosenthal lab for their help and friendships.

To my family, I cannot put into words how appreciative I am for all the sacrifices you have made to get me to where I am. Your love and support have inspired me through the toughest of times in my life. I am forever grateful.

Finally, I would like to thank Dr. Swiatoslaw Trofimenko. Although he had passed away before I joined the lab, I have come to know him through his work and our shared love of poly(pyrazolyl)borate chemistry. I hope that my small contribution to this area of chemistry will help to preserve the legacy of a man who made such a profound impact on our chemistry.

TABLE OF CONTENTS

LIST OF TABLES

LIST OF FIGURES

LIST OF SCHEMES

ABSTRACT

The successful synthesis and structural characterization of a new family of second and third generation ferrocenyl-substituted tris(pyrazolyl)borate ligands was achieved. These ligands employ ferrocenyl (Fc) moieties for increased C-H bond strengths as well as maintaining the steric demands necessary to remain "tetrahedral enforcers". The thallium(I) salts of the Tp^{Fc*} (**1**) and $Tp^{Fc,Me*}$ (**2**) ligands were isolated as N-confused asymmetric isomers. However, $Tp^{Fc,iPr}Tl$ (**3**) was isolated as the symmetric ligand as a dimer with an apparent Tl – Tl interaction. Cyclic voltammetry of **1**, **2**, and **3** revealed single, reversible, three electron redox processes which suggests a lack of electronic communication between the ferrocenyl moieties when bound to a hydrotris(pyrazolyl)borate ligand. Conversely, $Tp^{CF3,Fc}Tl$ (**4**) displays an irreversible redox process that is accompanied by decomposition during the oxidation wave of the CV.

Thallium salts **1** and **2** undergo borotropic rearrangements to form the symmetric $Tp^{Fc}Tl$ (**7**) and $Tp^{Fc,Me}Tl$ (**8**), respectively. These ligands react with CoX_2 (X: Cl, I) to form their symmetric TpCoX complexes. Salt metathesis of **3** with CoI_2 led to the isolation of $Tp^{Fc,iPr}CoI$ (**13**) as the only observable product. However, the reaction of **3** with $CoCl_2$ yielded an N-confused $Tp^{Fc,iPr*}CoCl$ (**14**) complex. The electronic characterization of $Tp^{Fc,R}$ (R: H, Me, *i*-Pr) has been sought through the synthesis of their corresponding copper(I) carbonyl complexes. Although the reaction of **7** and **8** with CuI under CO yields the symmetric $Tp^{Fc}Cu(CO)$ (**16**) and $Tp^{Fc,Me}Cu(CO)$ (**17**), respectively, the reaction of **3** with CuI under CO yielded the

singly N-confused $Tp^{Fc,iPr*}Cu(CO)$ (**19**) and doubly N-confused $Tp^{Fc,iPr**}Cu(CO)$ (**18**) complexes.

The $Tp^{Fc,Me}$ ligand has been employed in cobalt oxygen chemistry and has displayed its ability to resist C-H bond activation on the ligand. $Tp^{Fc,Me}Co(\eta^3\text{-}C_3H_5)$ (**22**) reacted with O_2 to form an apparent $Tp^{Fc,Me}CoOOC_3H_5$ intermediate which underwent O – O bond homolysis to form $Tp^{Fc,Me}CoOH$ (**21**). **22** reacted with CO to form $Tp^{Fc,Me}Co(CO)$ (**23**). **23** reacts with O_2 to form the side-on superoxo complex, $Tp^{Fc,Me}Co(O_2)$, which has been structurally characterized by X-ray diffraction. Furthermore, the terminal imido complex, $Tp^{Fc,Me}CoNAd$ (**25**), displayed greater thermal stability than its analogous alkyl-substituted $Tp^{tBu,Me}CoNR$ complexes.

Chapter 1

INTRODUCTION

Transition metal oxo complexes are believed to be the active species involved in many oxygen transfer reactions. Although terminal metal oxo complexes and their isoelectronic imido analogs are ubiquitous throughout the chemistry of early transition metals, there are few reported for late transition metals.[1] In the early 1960's, a molecular orbital diagram from the vanadyl ion, $VO(OH)_5^{2+}$, for tetragonal transition metal complexes containing a terminal oxo ligands was published by Ballhausen and Gray (Figure 1.1).[2]

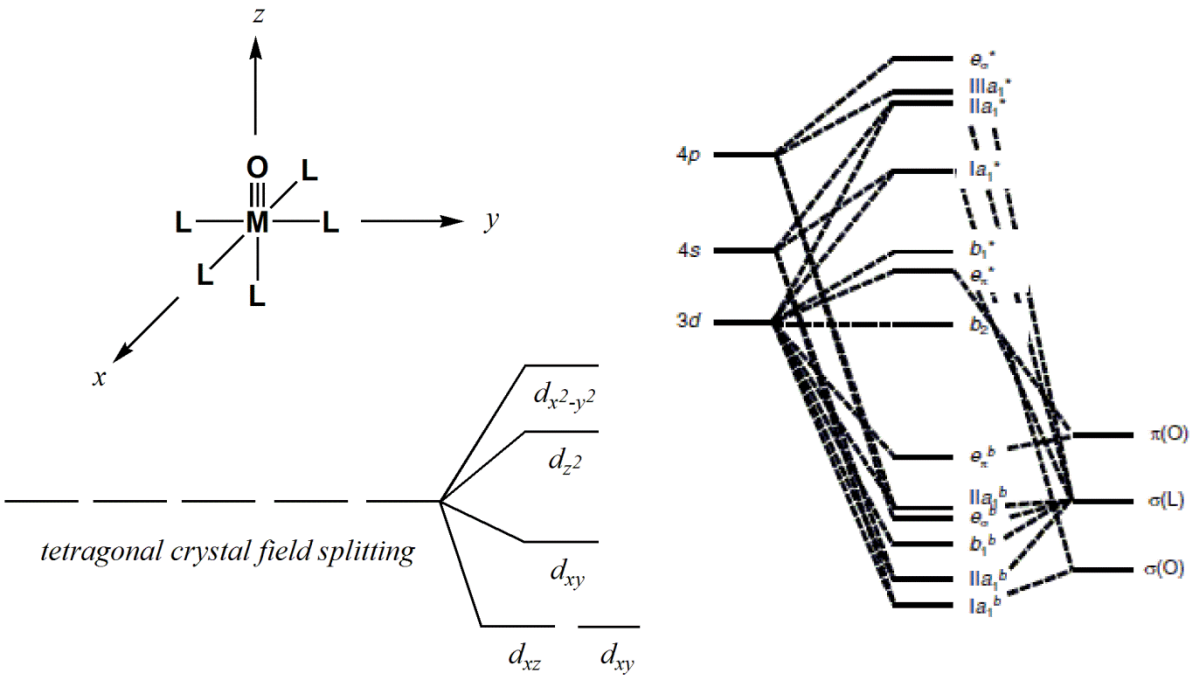

Figure 1.1: Molecular orbital model of the electronic structures of tetragonal metal-oxo complexes[3] and tetragonal crystal field splitting.

Based on this, they proposed that a terminal oxo complex in a tetragonal ligand field can have no more than five d-electrons. This is the highest number of d-electrons a complex can have and still maintain some metal oxo multiple bonding. This is due to the absence of π-bonding to the metal which causes the oxo to be extremely basic and unstable with respect to protonation or attack by electrophiles.[3] Achieving the low d-electron counts necessary for the metal-oxo multiple bonding becomes increasingly difficult for metals on the right half of the transition metal series. Ultimately, the metal oxidation states necessary for the formation of terminal metal-oxo complexes becomes so great that these complexes are unstable with respect to elimination of H_2O_2 or O_2.[3] Moreover, no tetragonal terminal oxo complexes or their isoelectronic imido analogs have been synthesized from group 9 onwards. This phenomenon is known as the "oxo wall" (Figure 1.2).[2,3]

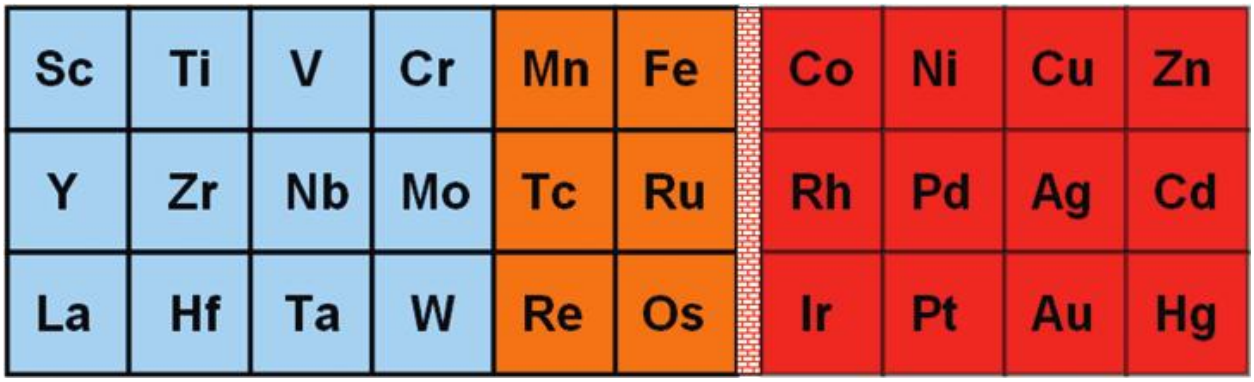

Figure 1.2: The oxo wall which divides group 8 and 9.[4]

In order to find complexes beyond the oxo wall, it is vital to alter the coordination geometry and reduce the coordination number to liberate orbitals to host nonbonding (or weakly antibonding) electrons. Multiply bonded metal-oxos and the isoelectronic metal-imido complexes of this type are not in violation of the oxo wall and remain consistent with the metal-ligand π-bonding principles dictated by Ballhausen and Gray.[3] Notably,

Wilkinson synthesized the first isolable late transition metal terminal oxo species, $Ir(O)(mes)_3$, in the early 1990's.[5] In this instance, the Ir atom is d^4 Ir(V) and is in a trigonal, not tetragonal, ligand field and therefore does not violate the oxo wall (Figure 1.3). Since then, complexes such as a the d^6 distorted square planar Pt(IV) oxo have been reported.[6]

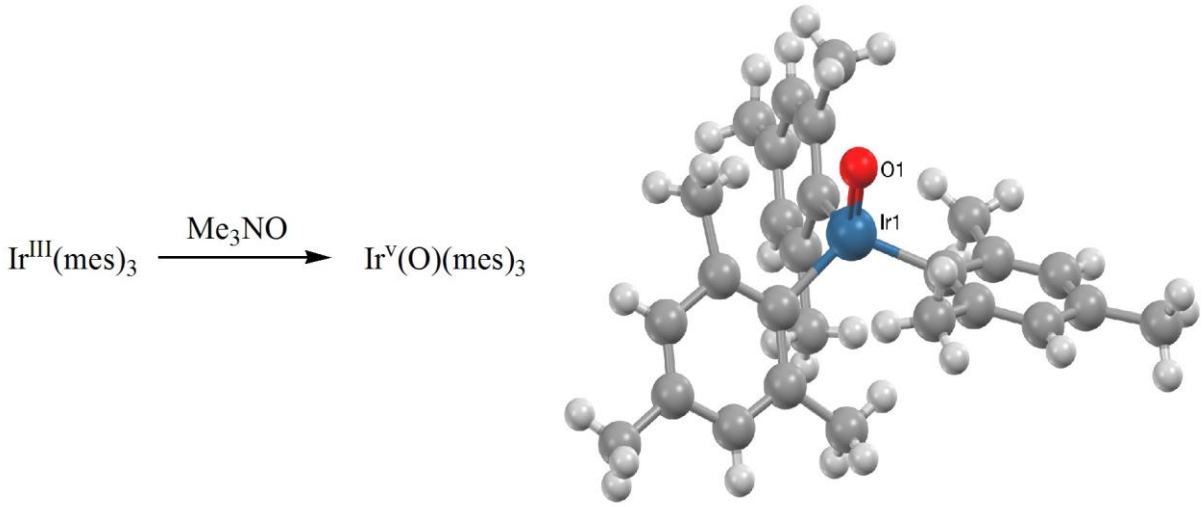

Figure 1.3: Synthesis and molecular structure of $Ir^{V}(O)(mes)_3$.

Of particular interest in this context is the coordination chemistry of cobalt. Although the latter has garnered interest since the time of Alfred Werner over a century ago,[7] inorganic and organometallic complexes of cobalt have continued to be studied due to their industrial applications[8] and biological relevance.[9] Much attention has been given to the study of the binding of dioxygen to Co(II). The chemical and physical properties of both peroxo and superoxo–bridged dicobalt(III) complexes have been extensively studied.[10] Under certain conditions, oxidation of a Co(II) species occurs to ultimately yield Co(III) dioxygen complexes. It was found that by manipulating the ligands, the peroxo and superoxo species could be isolated. For example $Co[(CN)_5]^{3-}$ reacts with oxygen to produce a bridged peroxo species. While the

peroxo bridge complex is isolable, it can be oxidized in a one-electron step to form the superoxide complex (Scheme 1.1).[11]

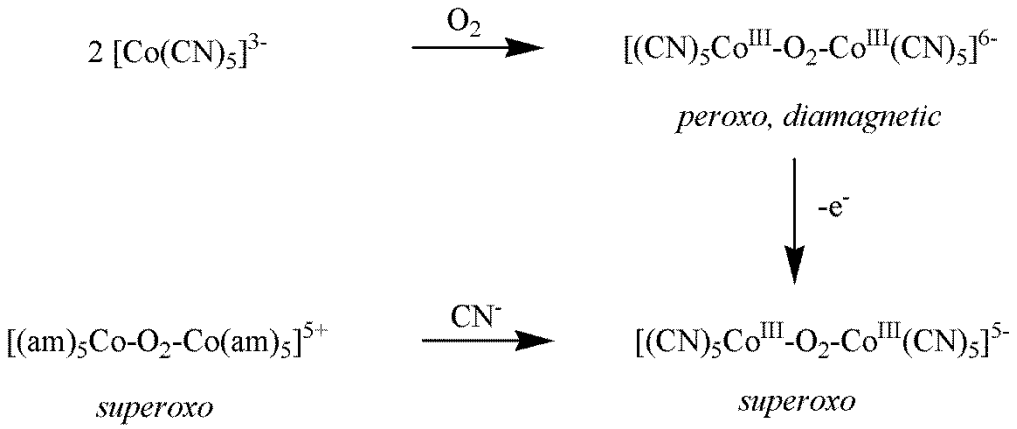

Scheme 1.1: Synthesis and oxidation of a superoxo–bridged dicobalt(III) complex.

More complicated polyfunctional ligands, such as the Schiff base ligand Co(II)(acacen) (acacen = ethylenediamineacetylacetonate) complex, show a reactivity towards dioxygen that is varied. At low temperatures, these complexes show reversible binding of oxygen (Scheme 1.2). However, at high temperatures, the complex is irreversibly oxidized to form the bridged peroxo or superoxo species.

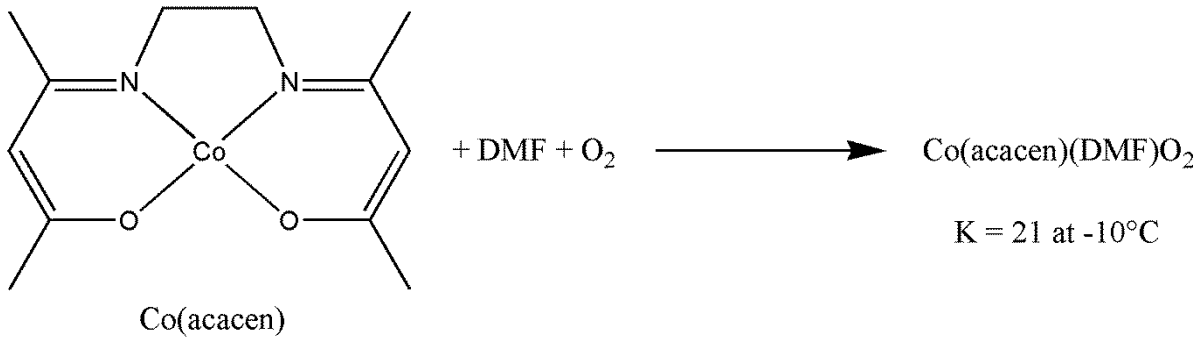

Scheme 1.2: Oxygen activation by a Co(II)(acacen) complex.

Nitrogen donor ligands such as tris(pyrazolyl)borate ligands (Tp) have been employed for over half a century in the stabilization of transition metal complexes.[12] Moro-oka,[13] Kitajima[14] and others have used these ligands to isolate and characterize several first-row transition metal oxygen species. In our laboratory, sterically hindered Tp ligands or "tetrahedral enforcers"[15] have been employed to design and synthesize cobalt complexes to be used as model systems to study and isolate intermediates of the oxidation process. The attempted isolation of a terminal cobalt-oxo complex and isoelectronic imido analogs has been a major focus of our research efforts for three decades. The choice of this ligand is significant because it maintains threefold symmetry and, in principle, allows for metal-oxo bonding for as many as seven d-electrons thus allowing the crossing of the oxo wall.[3] In particular, $Tp^{tBu,Me}$ and $Tp^{iPr,Me}$ (in which the 3-position is substituted with a *tert*-butyl or *iso*-propyl group, respectively, and the 5-position substituted with a methyl group) have been the two Tp ligands most often used in this laboratory.[16] While the bulkier *tert*-butyl groups stabilize monomeric metal complexes, the iso-propyl groups, being less sterically hindered, often allow the formation of dinuclear complexes. This flexibility has led to the synthesis and isolation of many cobalt oxygen complexes, through the reaction of low-valent TpCoL (where L is N_2 or CO) with dioxygen in solution or in the solid state. Among these novel compounds was the first example of a monomeric side-on bound superoxide transition metal complex elucidated through X-ray structural analysis.[16a] In order to unleash the oxidizing power of oxygen, it is imperative to cleave the O-O bond, thus generating a metal-oxo species. In the $Tp^{tBu,Me}Co(O_2)$ system, cleavage of the O-O bond was achieved through the addition of another equivalent of $Tp^{tBu,Me}Co(N_2)$. However, attempts to isolate the elusive 'TpCo=O' were marred by ligand decomposition via C-H bond activation and the only

isolable species was the TpCoOH. To date, no unstabilized terminal cobalt oxo species has been isolated.

Work then began on the exploration of the isoelectronic cobalt imido chemistry. Although stable terminal imido complexes of the late first row transition metals are rare,[17] their chemistry could help elucidate the reactivity of the cobalt oxo chemistry. Initial attempts to synthesize a stable cobalt imido began with the attempted synthesis of the trimethylsilyl imido complex, $Tp^{tBu,Me}Co{=}NTMS$.[18] When $Tp^{tBu,Me}Co(N_2)$ is exposed to one 1 equiv. of trimethylsilylazide, an immediate color change from brown to red with a concomitant evolution of nitrogen gas was observed. However, the isolated product was not the expected $Tp^{tBu,Me}Co{=}NTMS$, had undergone C-H bond activation on the ligand followed by radical collapse onto the metal center (Scheme 1.3).

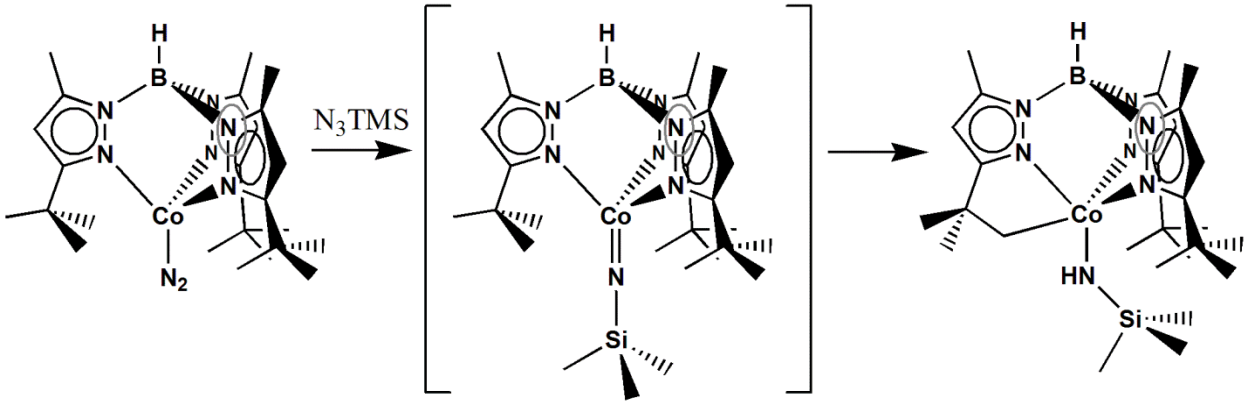

Scheme 1.3: Reaction of $Tp^{tBu,Me}Co(N_2)$ with N_3TMS.

The investigation of these compounds was furthered by replacing the trimethyl silyl group with various R groups (R: Me, Et, *t*-Bu and Ad). When $Tp^{tBu,Me}Co(N_2)$ was exposed to 1 equivalent of N_3R, an immediate color change from brown to green accompanied by the evolution of N_2 gas was observed and the expected terminal imido species were isolated.[19]

Notably, Tp$^{t\text{-Bu,Me}}$CoNAd was shown to be a spin-crossover compound between its diamagnetic ground state (S = 0) and its paramagnetic excited state (S = 1). However, this complex undergoes clean decomposition via C-H bond activation at elevated temperatures. This type of decomposition is reminiscent of the 'Tp^{tBu,Me}Co=NTMS' and 'Tp^{tBu,Me}Co=O' analogs.

Intramolecular C-H bond activation by highly reactive transition metal complexes extends beyond the research in our group. The decomposition *via* C-H bond activation of the ligand prevents the species from being viable catalysts in the oxidation of extraneous substrates. A representative example reported by Tolman is the intramolecular C-H bond activation of sterically hindered 1,4,7-triazacyclononaes linked by *m*-xylyl groups (*m*-XYL^{iPr4}) by a copper peroxo species.[20] In dilute solutions, the reaction of the Cu(I) starting material with oxygen at room temperatures generates the bridge Cu peroxo species (scheme 1.4). This species is responsible for the arene hydroxylation which results in the isolation of a product identified as [(*m*-XYL^{iPr4}-O)Cu$_2$(μ-OH)](SbF6)$_2$.

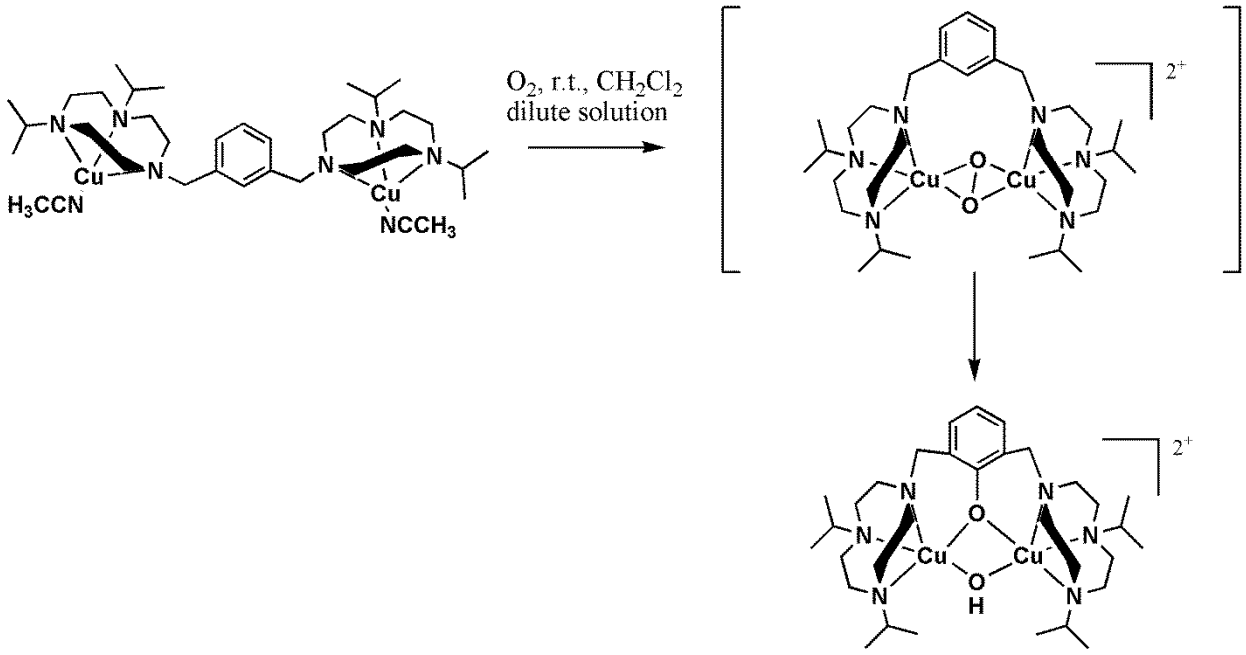

Scheme 1.4: Reaction of (*m*-XYL^{iPr4})Cu$_2$(NCCH$_3$)$_2$ with O$_2$.

Further, there are many examples of C-H bond activation in the Tp literature. The reaction of $Tp^{Ph,Me}Fe(\eta^1\text{-}O_2CC_6H_4\text{-}\rho\text{-}X)(pz^{Ph,Me}H)$ (where $Tp^{Ph,Me}$ = Hydrotris(3-phenyl-5-methylpyrazolyl)borate and X= Cl, H and OMe) and oxygen or hydrogen peroxide results in the insertion reaction by oxygen into the aromatic C-H bonds of the Tp ligand (Scheme 1.5).[21] In this reaction, dioxygen binds to the Fe center to form an end-on Fe(III) peroxo species, which abstracts a hydrogen from a phenyl group on the ligand *via* proton coupled electron transfer (PCET). The putative Fe(III) hydroperoxide species undergoes O-O bond homolysis to form the 'Fe(IV)-O•' species. The phenyl radical then combines with the 'Fe(IV)-O•' moiety to form the final product.

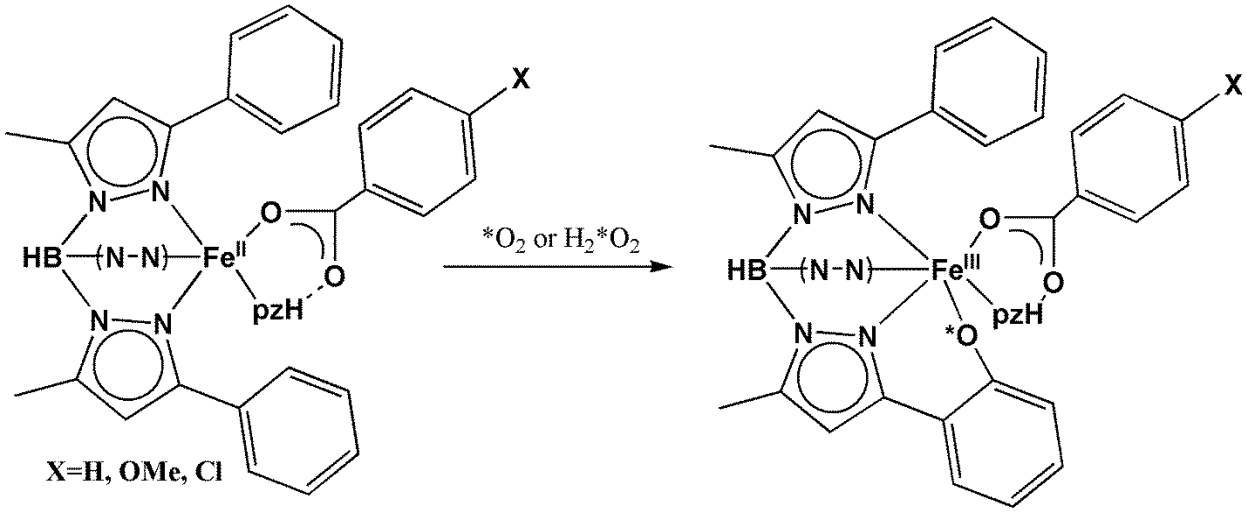

Scheme 1.5: Reaction of $Tp^{Ph,Me}Fe(\eta^1\text{-}O_2CC_6H_4\text{-}\rho\text{-}X)(pz^{Ph,Me}H)$ with O_2 or H_2O_2.

Examples specific to $Tp^{R,R'}Co$ of intramolecular C-H bond activation occur in the reaction of $[Tp^{iPr2}CoOH]_2$ with alkyl hydroperoxide or hydrogen peroxide.[13] Treatment of the hydroxo complex with alkyl hydroperoxide at low temperatures gave absorptions of 650 nm in the UV-Vis spectrum, characteristic of the high-spin Co(II) ion located in tetrahedral ligand

field. However, the thermal instability of this 'Tp^{iPr2}CoOOR' complex prevented the successful isolation of this complex. Instead, decomposition via C-H bond activation resulted in the intramolecular oxygenation of the isopropyl substituents proximal to the Co center to form a di-oxygenated species (Scheme 1.6). Likewise, treatment of [Tp^{iPr2}Co(μ-OH)]$_2$ with 1 equivalent of H_2O_2 led to the formation of a bridged peroxo species which undergoes C-H bond activation to form a mono-oxygenated species. Reactions with excess H_2O_2 resulted in the formation of the di-oxygenated species and a fully oxygenated species. Similar reactions have been observed when [Tp^{iPr2}Mn(μ-OH)]$_2$is exposed to oxygen resulting in the formation of {Mn[HB(3-OCMe$_2$-5-^{iPr}pz)(3,5-^{iPr2}pz)$_2$]}$_2$(μ-O).[22]

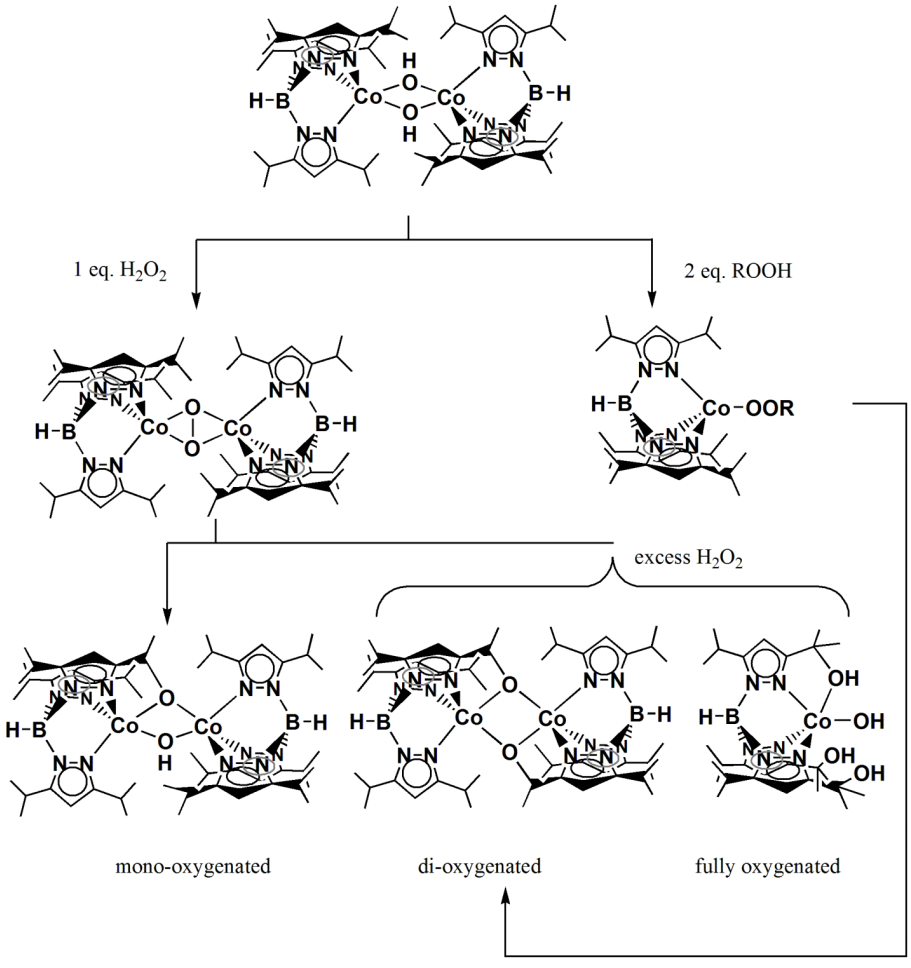

Scheme 1.6: Reaction of [Tp^{iPr2}Co(μ-OH)]$_2$ with peroxides.

For the reasons summarized above, several attempts have been made to overcome ligand decomposition by altering the substituents on the pyrazolyl rings (Scheme 1.7). Although the *t*-Bu group has relatively strong C-H bonds (98 kcal/mol),[23] they have proven vulnerable to activation. Exchanging the former for something with a considerably higher C-H bond strength may be advantageous in the prevention of ligand decomposition and allow for the activation of external substrates. The hydrotris(3-phenyl-5-methylpyrazolyl)borate ligand ($Tp^{Ph,Me}$) offers phenyl C-H bond strengths of 110kcal/mol[23], considerably higher than those of a *t*-Bu substituent. However, these substituents lack the steric bulk necessary to prevent the formation of Tp_2M complexes and are therefore not suitable for this chemistry. Furthermore, C-H bond activation has been shown to occur in the Fe - oxygen chemistry of this ligands.[21] Eliminating the free rotation of the Ph group by switching to a mesityl group affords a ligand that prevents the formation of bisligand complexes. Although the hydrotris(3-mesitylpyraozlyl)borate ligand (Tp^{Ms}) delivers the steric blocking needed to prevent the formation of Tp_2M complexes, it also presents vulnerable benzylic C-H bonds within activation distance of the metal center.[24] Perfluoroalkyl groups have also been investigated as suitable replacement. The hydrotris(3-(1,1,2,2,3,3,3-heptafluoropropyl)-5-methylpyrazolyl)borate ligand ($Tp^{n\text{-}C3F7,\ Me}$) provides C-F bonds of 119 kcal/mol.[23] However, the electron withdrawing ability of these groups causes it to be readily displaced from the metal center.[25] The results of these findings have led us to postulate that metallocences may serve as a suitable alternative to alkyl, aryl or perfluoroalkyl substituents of Tp ligands. Since ferrocene has a C-H bond strength of 117 kcal/mol[26] and the steric requirements necessary to prevent the formation of Tp_2M complexes, it is a fitting choice for the further investigation of this chemistry.

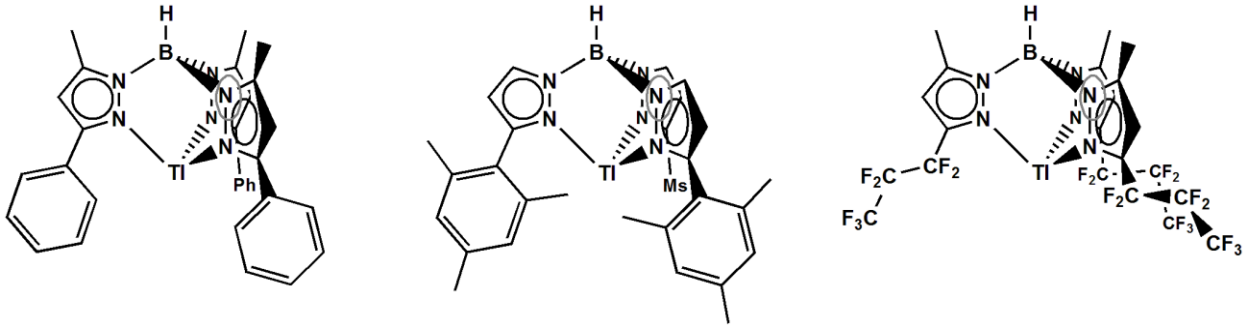

Scheme 1.7: The $Tp^{Ph,Me}Tl$, $Tp^{Ms}Tl$, and $Tp^{n\text{-}C3F7,\ Me}Tl$ complexes

The work described herein the synthesis of a new class of Tp ligands featuring ferrocenyl substituents, which have superior C-H bond strength over that of the parent $Tp^{tBu,Me}$ system. Also reported is the synthesis and characterization of low-valent cobalt (Co(I) and Co(II)) complexes bearing these sterically hindered Tp ligands and their reactivity towards dioxygen and other oxidants.

1.1 References

1. For examples see: a) Alsters, P. L., Teunissen, H. T.; Boersma, J., Spek, A. L., van Koten, G., *Organometallics* **1993**, *12*, 4691.; b) Khan, M. M. T., Chatterjee, D., Merchant, R. R., Bhatt, A.; Kumar, S. S., *J. Mol. Cat.,* **1991**, *66*, 289.; c) Limberg, C., *Angew. Chem. Int. Ed*. **2009**, *48*, 2270.; d) Mukerjee, S., Skogerson, K., DeGala, S., Caradonna, J. P., *Inorg. Chem. Acta.,* **2000**. *297*, 313-329.; e) Ballhausen, C. J.; Gray, H. B., *Inorg. Chem*. **1962**, *1*, 111.; f) Hay-Motherwell, R. S., Hussain-Bates, B.; Hursthouse, M. B., Wilkinson, G., *Polyhedron*. **1993**, *12*, 2009.; g). Glueck, D. S, Hollander, F. J., Bergman, R. G., *J. Am. Chem. Soc*. **1989**, *111*, 2719.; h) Glueck, D. S., Wu, J. X., Hollander, F. J., Bergman, R. G., *J. Am. Chem. Soc*. **1991**, *113*, 2041.; i) Mindiola, D. J., Hillhouse, G. L., *J. Am. Chem. Soc*. **2001**, *123*, 4623.; j) Jenkins, D. M., Betley, T. A., Peters, J. C., *J. Am. Chem. Soc*. **2002**, *124*, 11 238.; k) Betley, T. A., Peters, J. C., *J. Am. Chem. Soc*. **2003**, *125*, 10782; f) Dai, X., Kapoor, P., Warren, T. H., *J. Am. Chem. Soc.* **2004**, *126*, 4798.; l) King, E. R., Sazama, G. T. and Betley, T. A., *J. Am. Chem. Soc*. **2012**, *134*, 17858.; m) Geer, A. M., Tejel, C., López, J. A. and Ciriano, M. A., *Angew. Chem. Int. Ed*., **2014**, *53*, 1.
2. Ballhausen, C. J., Gray, H. B., *Inorg.Chem*. **1962**, *1*, 111.
3. Winkler, J. R.; Gray, H. B., *Struct Bond.*, **2012**, *142*, 17.
4. O'Halloran, K. P., Zhao, C., Ando, N. S.; Schultz, A. J.; Koetzle, T. F., Piccoli, P. M. B., Hedman, B.; Hodgson, K. O., Bobyr, E.; Kirk, M. L., Knottenbelt, S., Depperman, E. C., Stein, B., Anderson, T. M.; Cao, R., Geletii, Y. V., Hardcastle, K. I., Musaev, D. G., Neiwert, W. A., Fang, X.; Morokuma, K., Wu, S., Kögerler, P., Hill, C. L., *Inorg. Chem*. **2012**, *51*, 7025.

5. Hay-Motherwell, R. S., Hussain-Bates, B., Hursthouse, M. B., Wilkinson, G., *Polyhedron*, **1993**, *12*, 2009.
6. Poverenov, E., Efremenko, I.; Frenkel, A. I., Ben-David, Y., Shimon, L. J. W., Leitus, G., Konstantinovski, L., Martin, J. M. L., Milstein, D., *Nature*, **2008**, *455*, 1093.
7. a) Werner, A. *Chem. Ber*. **1914**, *47*, 3087.; b) Werner, A., *Chem. Ber.* **1911**, *44*, 1887.; c) Kauffman, G. B., Ed. Classics in Coordination Chemistry; Dover: New York, **1968**, 155.
8. For examples see: a) Cornils, B., Herrmann, W. A., Rasch, M., *Angew. Chem. Int. Ed*., **1994**, *33*, 2144.; b) Haumann, M., Jakuttis, M., Franke, R., Schonweiz, A., and Wasserscheid, P., *ChemCatChem*, **2011**, *2* ,1822.; c) Frohning, C. D., Kohlpaintner, C. W. , *Hydroformylation in Applied Homogeneous Catalysis with Organometallic Compounds* (Eds.: B. Cornils, W. A. Herrmann), Wiley-VCH, Weinheim, **2002**, 31.; d) Earl, R. A., Vollhardt, K. P. C., *J. Am. Chem. Soc*., **1983**, *105*, 6991.
9. For examples see: a) Hall, C. A., *Am. J. Hematol*., **1990**, *34*, 121.; b) Voet, D; Voet J.G. *Biochemistry*, John Wiley & Sons: New York, **1990**, 322.; c) Cotton, F. A.; Wilkinson, G. *Advanced Inorganic Chemistry*; John Wiley and Sons Inc.: New York, **1988**; 5th edition, 1369.
10. McLendon, G., Martell, A. E., *Coord. Chem. Rev*., **1976**, *19*, 1.
11. a) Casella, L, Gulotti, M., *Inorg. Chem*., **1986**, *25*, 1293.; b) Sasaki, T., Kikkawa, S., Hatakeyama, Y., Ueno, F. B., Saito, K., *Inorg. Chem*., **1985***, 24*, 4096.; c) Chen, D. C., Martell, A. E. *Inorg. Chem*., **1987**, *26*, 1026.; d) Taube, H., *Prog. Inorg. Chem*., **1986**, *34*, 607.

12. a) Trofimenko, S. Scorpionates, **1999**, London: Imperial College Press.; b) Pettinari, C. Scorpionates II: Chelating Borate Ligands, **2008**, London: Imperial College Press.

13. Hikichi, S., Komatsuzaki, H., Akita., M., and Moro-oka, Y., *J. Am. Chem. Soc*., **1998**. *120*, 4699.

14. Fujisawa, K., Tanaka, M., Moro-oka, Y., and Kitajima, N., J. Am. Chem. Soc., 1994, *116*, 12079.

15. Reinaud, O. M., Rheingold, A. L., and Theopold, K. H., *Inorg. Chem*., **1994**, *33*, 2306.

16. a) Egan, J. W. J.; Haggerty, B. S.; Rheingold, A. L.; Sendlinger, S. C.; Theopold, K. H., *J. Am. Chem. Soc.* **1990,** *112*, 2445.; b) Reinaud, O. M., Yap, G. P. A., Rheingold, A. L. and Theopold, K. H., *Angew. Chem. Int. Ed*., **1995**. *34*, 2051.; c) Qin, K.; Incarvito, C. D.; Rheingold, A. L.; Theopold, K. H., *J. Am. Chem. Soc.* **2002,** *124*, 14008.

17. a) Glueck, D. S., Hollander, F. J., Bergman, R. G., *J. Am. Chem. Soc*. **1989**, *111*, 2719; b) Glueck, D. S., Wu, J. X, Hollander, F. J., Bergman, R. G., *J. Am. Chem. Soc*. **1991**, 113, 2041; c) Mindiola, D. J., Hillhouse, G. L., *J. Am. Chem. Soc*. **2001**, *123*, 4623; d) Jenkins, D. M., Betley, T. A., Peters, J. C., *J. Am. Chem. Soc*. **2002**, *124*, 238; e) Betley, T. A., Peters, J. C., *J. Am. Chem. Soc*. **2003**, *125*, 10782; f) Dai, X., Kapoor, P., Warren, T. H., *J. Am. Chem. Soc.* **2004**, *126*, 4798.; g) King, E. R., Sazama, G. T. and Betley, T. A., *J. Am. Chem. Soc*. **2012**, *134*, 17858.

18. Thyagarajan, S., Shay, D. T., Incarvito, C. D., Rheingold, A. L., Theopold, K.H., *J. Am. Chem. Soc*. **2003**, *125*, 4440.

19. Shay, D. T., Yap, G. P. A., Zakharov, L. N., Rheingold, A. L. and Theopold, K. H., *Angew. Chem. Int. Ed.*, **2005**, *44*, 1508 .

20. Mahapartra, S., Kaderli, S., Llbet, A., Neuhold, Y., Palanché, T., Halfen, J. A., Young, V. G., Kaden, T. A., Que, L., Zuberbühler, A. D., and Tolman, W. B., Inorg. Chem., 1997, 36, 6343.

21. Fujisawa, K., Tada, N., Nishida, Y., Miyashita, Y., Okamoto, K., *Inorg. Chem. Commun*., **2008**, *11*, pp 381.

22. Kitajima, N., Osawa, M., Tanaka, M., Moro-oka, Y., *J. Am. Chem. Soc*., **1991**, *113*, 8952.

23. Blanksby, S. J., and Ellison, G. B., *Acc. Chem. Res*., **2003**, *36*, 255.

24. Pariya, C., Incarvito, C. D., Rheingold, A. L., Theopold, K. H., *Polyhedron*, **2004**, *23*, 439.

25. King, W. A., Yap, G. P. A., Incarvito, C. D., Rheingold, A. L., Theopold, K. H., *Inorg. Chim Acta*, **2009**, *362*, 4493.

26. Elihin, K., Larsson, K., *Thin Solid Films*, **2004**, *458*, 325.

Chapter 2

SYNTHESIS AND CHARACTERIZATION OF NOVEL FERROCENYL-SUBSTITUTED, REDOX ACTIVE TRIS(PYRAZOLYL)BORATE LIGANDS

2.1 Introduction

Since their inception in the late 1960's, poly(pyrazolyl)borate ligands or "scorpionates" have become ubiquitous throughout inorganic and coordination chemistry.[1,2] The term scorpionate stems from the way the metal is coordinated to the ligand. In much the same way a scorpion attacks its prey, two pyrazolyl arms grab the metal with the third arm (pz or R) acting as the stinger[3] (Scheme 2.1). First[4], second[5] (in which the pyrazolyl rings are substituted in the 3,4 and 5-position beyond a Me substituent) and third[6] generation (*R*Tp, in which the boron-bound hydride has been replaced by an alkyl or aryl group) tris(pyrazolyl)borate ligands have been employed extensively in synthesizing novel metal complexes for numerous transformations. These reactions have been studied in depth and have generated thousands of publications.

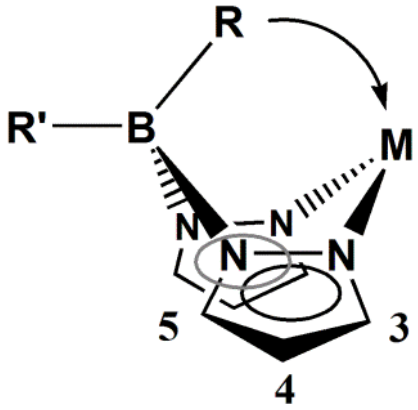

Scheme 2.1: The scorpionate ligand.

Like their cyclopentadienyl (Cp) analogs, tris(pyrazolyl)borate (Tp) ligands occupy three coordination sites, donate six electrons, and are monoanionic. Tp ligands can be sterically tuned by adding bulky substituents on the 3, 4 and 5 position of the pyrazolyl ring. The ability to adjust the steric bulk of the substituents of pyrazolyl rings allows for the control of the coordination geometry of the metal. Tp ligands with sterically demanding substituents such as *iso*-propyl[7] and *tert*-butyl[8] groups in the 3-position of the pyrazolyl ring have been deemed "tetrahedral enforcers"[9] due to their steric encumbrances, which often give rise to a pseudo- tetrahedral coordination geometry. Likewise, the Tp ligands can also be electronically tuned by substitution with electron withdrawing or donating groups. Ease of synthesis has also aided in the popularity of these ligands. Heating the corresponding pyrazoles in the presence of a metal borohydride (i.e., KBH_4) either neat or in a high boiling solvent yields the desired ligand after workup (Scheme 2.2). These characteristics have made them arguably more versatile than the Cp moiety.

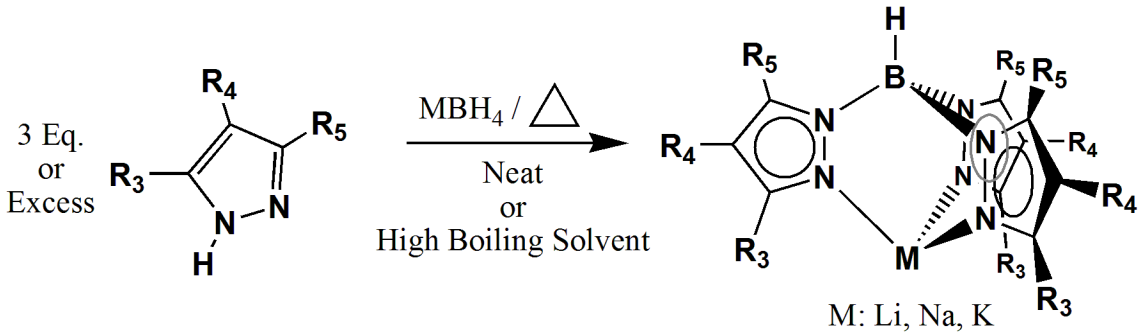

Scheme 2.2: Typical synthetic route for Tp ligands.

Redox-active ligands have gained popularity due to their ability to electronically modify the reactivity of the metal center.[10] It should come as no surprise that chemists would seek ways to combine tris(pyrazolyl)borates, which are mono-anionic ligands, with redox-active moieties. To date, only redox-active third generation tris(pyrazolyl)borates, in which ferrocene is

tethered to the boron, have been synthesized[11] along with a few examples of redox-active bis(pyrazolyl)borates[12,13] (Scheme 2.3). Since the borylation of

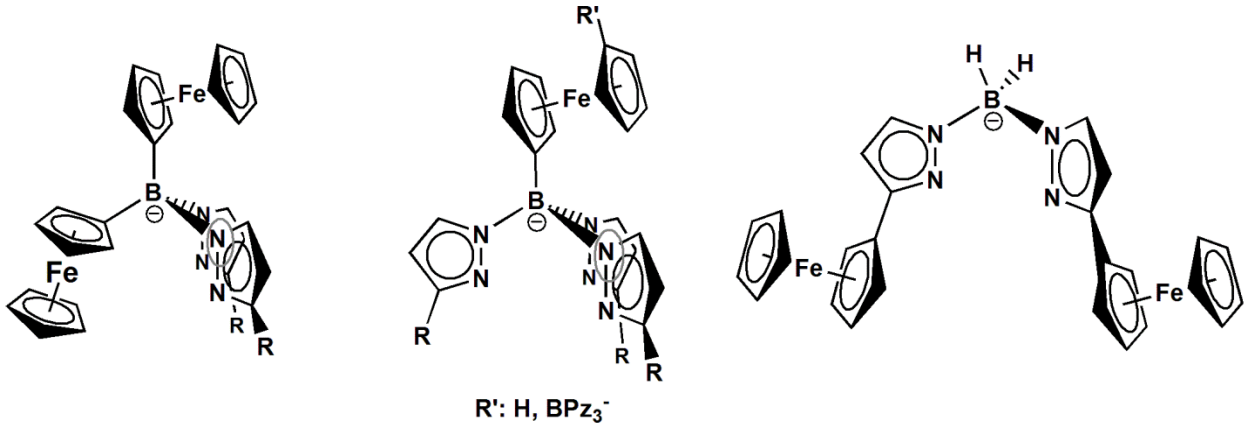

Scheme 2.3: Known redox active scorpionate ligands.

ferrocene is well known,[14] the ferrocenyl moiety has become an attractive building block on which to build redox-active Tp ligands. However, the synthesis of a second generation hydrotris(pyrazolyl)borate incorporating the ferrocenyl moiety has remained elusive. Trofimenko *et al.* reported the first example of bidentate bis(pyrazolyl)borate ligands in the early 90's.[13] Despite the successful synthesis of these ligands a hydrotris(pyrazolyl)borate species in which the ferrocenyl moieties are directly bound to the pyrazolyl subunits has never been synthesized prior to this work. Herein, the low-temperature synthesis and structural characterization of a new class of redox active Tp ligands of the type R'Tp^{Fc,R} (R: H, Me, *i*-Pr, CF3, Fc and R': H, Ph) are reported.

2.2 Results and Discussion

2.2.1 Synthesis and Characterization of $Tp^{Fc*}Tl$ and $Tp^{Fc,Me*}Tl$.

Although many tris(pyrazolyl)borate ligand syntheses appear to be quite trivial, the preparation of a Tp ligand with ferrocenyl groups tethered to the pyrazolyl moiety is not. Initial attempts to prepare the hydrotris(3-ferrocenylpyrazolyl)borate ligand by traditional methods resulted in the decomposition of the pyrazole. At high temperatures (over 170 ºC, neat or in high boiling solvents), ferrocenyl-substituted pyrazole undergoes ligand scrambling (Scheme 2.4) which is apparent in the ^{1}H NMR spectrum of the decomposition products. Such rearrangements are not unprecedented. Heating mono-substituted alkyl ferrocenes in the presence of aluminum chloride results in ligand scrambling to form the di-substituted ferrocene along with free ferrocene[15].

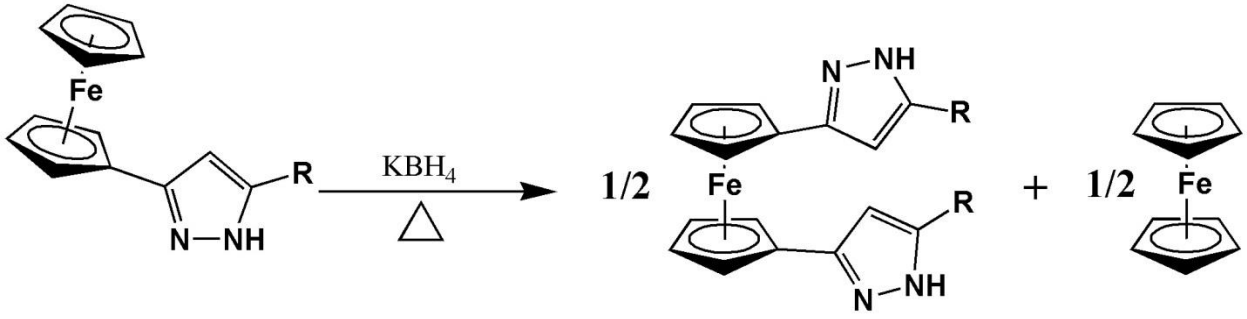

Scheme 2.4: Disproportionation of $Pz^{Fc,R}H$ at elevated temperatures.

A high boiling solvent (b.p. < 170 ºC) may be used to maintain temperatures that will not expedite the decomposition of the pyrazole. However, running these reactions with KBH_4 below the decomposition temperature of the pyrazole, even for extended periods of time, only resulted in the formation of a dihydrobis(pyrazolyl)borate species.[13] Therefore, an alternate route to the

formation of ferrocenyl-substituted Tp ligands was needed. There are several routes that potentially offer to overcome this synthetic challenge (Scheme 2.5).

The first route attempted was a metathesis of dichlorophenylborane with 3 equivalents of a metal pyrazolate, which can be done in toluene at room temperature or reflux[16]. Although toluene has a boiling point of 110ºC, this is well below the decomposition point of the ferrocenyl-substituted pyrazole and is considered "low-temperature" compared to the majority of tris(pyrazolyl)borate ligand syntheses.

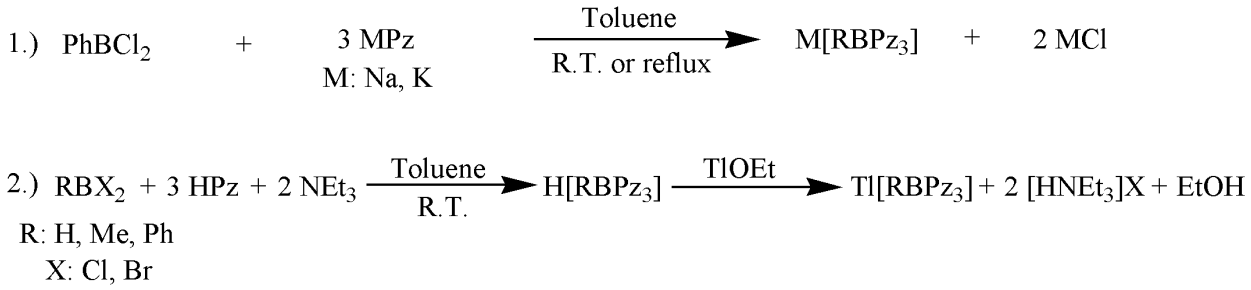

Scheme 2.5: Alternative tris(pyrazolyl)borate synthetic pathways.

Utilizing this synthetic route, we were able to generate only small amounts (< 5 %) of the corresponding tris(pyrazolyl)borate ligands. Although this engendered hope that these ligands could, in fact, be synthesized, the low yield of this procedure and the difficulty of recrystallizing boron-substituted tris(pyrazolyl)borate ligands[17,18] made the former unsuitable for large-scale, multi-gram syntheses. The second synthetic approach is a modification of the first,[19] wherein two equivalents of pyrazole are deprotonated *in situ* and react with an alkyl or aryl substituted dihalo-borane to form the tris(pyrazolyl)borate – acid complex ($H[RBPz_3]$). This compound is then reacted with a base, in this case TlOEt, to form the corresponding tris(pyrazolyl)borate thallium complex. Both synthetic approaches featured in scheme 1.5 suffered from low yields when

employed using ferrocenyl-substituted pyrazoles, and both of them yielded third-generation tris(pyrazolyl)borate ligands. Third-generation tris(pyrazolyl)borate ligands, which have sterically demanding substituents on their pyrazolyl rings tend to be less committed to binding κ^3 than their second-generation analogs in which the boron is substituted with a hydrogen.[18,19]

Jordan *et al*. reported a Lewis acid catalyzed low-temperature tris(pyrazolyl)borate synthesis.[20] The mechanism of this reaction involves a Lewis acid catalyzed protonolysis of the B-H bonds in the formation of $MeB(pz^R)_2H^-$ (Scheme 2.6), which reacts with another equivalent of pyrazole to form $Li[MeB(pz^R)_3]$. The coordination of the pyrazole to the Lewis acid (LA) decreases the pK_a of the pyrazole thereby increasing the rate of B-H protonolysis.[22]

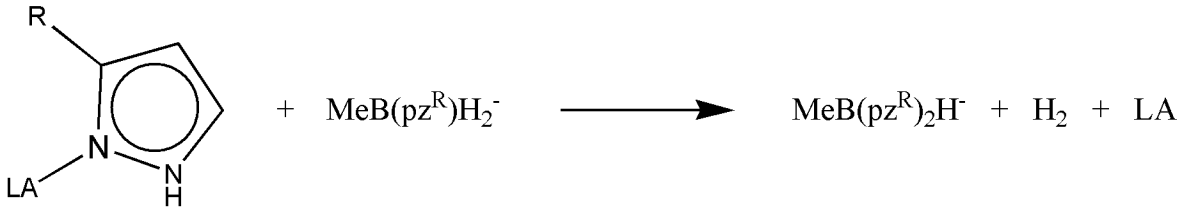

Scheme 2.6: Lewis acid catalyzed protonolysis.

Jordan's successful synthesis of third generation Tp ligands with sterically demanding substituents suggested that a modified procedure using lithium borohydride instead of $Li[MeBH_3]$ and the requisite ferrocenyl-substituted pyrazoles might result in the successful synthesis of the target compounds. However, in my hands, when 3 equivalents of 3-ferrocenylpyrazole, di(isopropoxy)methylborane ($MeB(O^iPr)_2$) (3 mol % vs. mol pyrazole), and $LiBH_4$ were heated in THF at 60 °C for three days, only the previously reported dihydrobis(3-ferrocenylpyrazolyl)borate ($Bp^{Fc}Tl$) was obtained (Figure 2.1). Although this was not the desired result, the yield of this reaction, i.e., 51%, was better than that of its previously reported synthesis.[13] X-ray quality crystals were grown by a slow diffusion of pentane into a saturated

solution of $Bp^{Fc}Tl$ in THF. The X-ray crystal structure of $Bp^{Fc}Tl$, which had not been reported, confirmed the configuration apparent in the ^{1}H NMR spectrum reported by Trofimenko. $Bp^{Fc}Tl$ crystallized in the monoclinic space group P_n. Figure 1.1 displays the molecular structure of the $Bp^{Fc}Tl$•THF complex in which Tl binds to the ligand in a trigonal pyramidal geometry with two pyrazolyl moieties binding to the Tl through the N atoms and the third coordination site being occupied by a molecule of THF solvent. The Tl-N distances (Table 2.1, note that the tables of bond distances and angles excludes those of the Fc fragments of this compound and all subsequent compounds) of complex $Bp^{Fc}Tl$•THF are 2.711(2)$Å_{avg}$ and the Tl-O distance is 2.674(2) Å. All other physical and spectroscopic data were consistent with the previously reported compound. Note that BpFcTl is not "N-confused", i.e., both Fc substituents are situated in the 3-position (away from the boron).

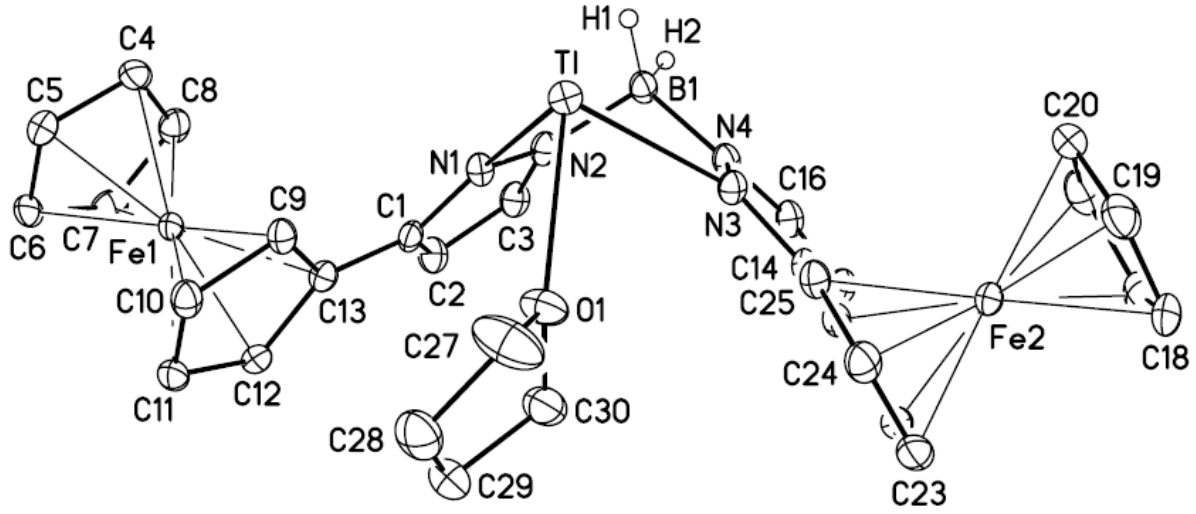

Figure 2.1: Molecular structure of $Bp^{Fc}Tl$ at 30% probability level. Hydrogen atoms (except H1 and H2) have been removed for clarity.

Table 2.1: Selected interatomic distances (Å) and angles (°) for $Bp^{Fc}Tl$

Distances (Å)

Tl-O(1)	2.674(2)	C(9)-C(10)	1.430(4)
Tl-N(3)	2.704(2)	C(9)-C(13)	1.445(4)
Tl-N(1)	2.719(2)	C(10)-C(11)	1.436(4)
B(1)-N(4)	1.554(4)	C(11)-C(12)	1.421(4)
B(1)-N(2)	1.562(4)	C(12)-C(13)	1.436(4)
N(1)-C(1)	1.355(4)	C(14)-C(15)	1.422(4)
N(1)-N(2)	1.365(3)	C(14)-C(26)	1.465(3)
N(2)-C(3)	1.353(4)	C(15)-C(16)	1.373(4)
N(3)-C(14)	1.340(3)	C(17)-C(18)	1.420(5)
N(3)-N(4)	1.367(3)	C(17)-C(21)	1.421(5)
N(4)-C(16)	1.359(4)	C(18)-C(19)	1.412(5)
O(1)-C(27)	1.420(5)	C(19)-C(20)	1.416(4)
O(1)-C(30)	1.422(4)	C(20)-C(21)	1.410(5)
C(1)-C(2)	1.412(5)	C(22)-C(26)	1.436(4)
C(1)-C(13)	1.456(4)	C(22)-C(23)	1.435(4)
C(2)-C(3)	1.382(4)	C(23)-C(24)	1.422(4)
C(4)-C(8)	1.422(4)	C(24)-C(25)	1.428(4)
C(4)-C(5)	1.424(4)	C(25)-C(26)	1.428(4)
C(5)-C(6)	1.428(4)	C(27)-C(28)	1.478(6)
C(6)-C(7)	1.420(4)	C(28)-C(29)	1.518(5)
C(7)-C(8)	1.421(4)	C(29)-C(30)	1.514(5)

Angles (°)

O(1)-Tl-N(3)	81.85(7)	N(3)-N(4)-B(1)	121.0(2)
O(1)-Tl-N(1)	87.50(8)	C(27)-O(1)-C(30)	105.1(3)
N(3)-Tl-N(1)	77.01(9)	C(27)-O(1)-Tl	124.5(2)
N(4)-B(1)-N(2)	107.4(3)	C(30)-O(1)-Tl	129.6(2)
C(1)-N(1)-N(2)	106.5(2)	N(1)-C(1)-C(2)	110.1(3)
C(1)-N(1)-Tl	140.5(2)	N(1)-C(1)-C(13)	122.0(3)
N(2)-N(1)-Tl	110.71(15)	C(2)-C(1)-C(13)	127.9(3)
C(3)-N(2)-N(1)	109.8(2)	C(3)-C(2)-C(1)	104.5(2)
C(3)-N(2)-B(1)	128.3(2)	N(2)-C(3)-C(2)	109.1(2)
N(1)-N(2)-B(1)	121.2(2)	C(8)-C(4)-C(5)	108.4(2)
C(14)-N(3)-N(4)	106.4(2)	C(4)-C(5)-C(6)	107.6(2)
C(14)-N(3)-Tl	140.52(18)	C(7)-C(6)-C(5)	108.0(3)
N(4)-N(3)-Tl	111.16(16)	C(6)-C(7)-C(8)	108.4(3)
C(16)-N(4)-N(3)	110.0(2)	C(4)-C(8)-C(7)	107.7(3)
C(16)-N(4)-B(1)	128.2(2)	C(10)-C(9)-C(13)	108.1(2)

C(9)-C(10)-C(11)	108.1(2)	C(21)-C(20)-C(19)	108.3(3)
C(12)-C(11)-C(10)	107.9(2)	C(20)-C(21)-C(17)	107.6(3)
C(11)-C(12)-C(13)	108.8(2)	C(26)-C(22)-C(23)	107.8(2)
C(12)-C(13)-C(9)	107.1(2)	C(24)-C(23)-C(22)	107.9(2)
C(12)-C(13)-C(1)	126.5(3)	C(23)-C(24)-C(25)	108.4(2)
C(9)-C(13)-C(1)	126.4(3)	C(26)-C(25)-C(24)	108.0(2)
N(3)-C(14)-C(15)	110.3(2)	C(25)-C(26)-C(22)	107.9(2)
N(3)-C(14)-C(26)	121.4(3)	C(25)-C(26)-C(14)	125.7(3)
C(15)-C(14)-C(26)	128.3(2)	C(22)-C(26)-C(14)	126.5(2)
C(16)-C(15)-C(14)	104.5(2)	O(1)-C(27)-C(28)	107.3(3)
N(4)-C(16)-C(15)	108.8(2)	C(27)-C(28)-C(29)	103.9(3)
C(18)-C(17)-C(21)	108.2(3)	C(30)-C(29)-C(28)	104.6(3)
C(19)-C(18)-C(17)	107.6(3)	O(1)-C(30)-C(29)	106.0(3)
C(18)-C(19)-C(20)	108.3(3)		

When the catalyst loading and the reaction temperature were increased, Tp ligands can be isolated (Scheme 2.7). Heating three equivalents of the parent pyrazole, 3-ferrocenylpyrazole, combined with $LiBH_4$ and $MeB(O^iPr)_2$ (6 mol % of pyrazole) in toluene for three days at 100 °C, the corresponding hydrobis(3-ferrocenylpyrazolyl)(5-ferrocenylpyrazolyl)borate (Tp^{Fc*})(* denotes 'N-confusion' or the 'asymmetric' ligand as defined by Trofimenko,[1] where one of the pyrazolyl moieties has the Fc-substituent occupying the 5-position) ligand can be precipitated as the lithium salt, as is indicated by the ^1H NMR spectrum. A metathesis between TlOAc and the lithium salt of the ligand allowed for the isolation of $Tp^{Fc*}Tl$ (**1**) complex as an orange solid in 51% yield. Excess pyrazole was removed by successive washings with methanol yielding **1**, the singly N-confused regioisomer, as the only observable product. **1** has an ^1H NMR spectrum, recorded in $CDCl_3$ at room temperature, with two sets of 5 well resolved signals in a ratio of 2:1 (Figure 2.2), which are assigned to the protons of the Tp^{Fc*} ligand.

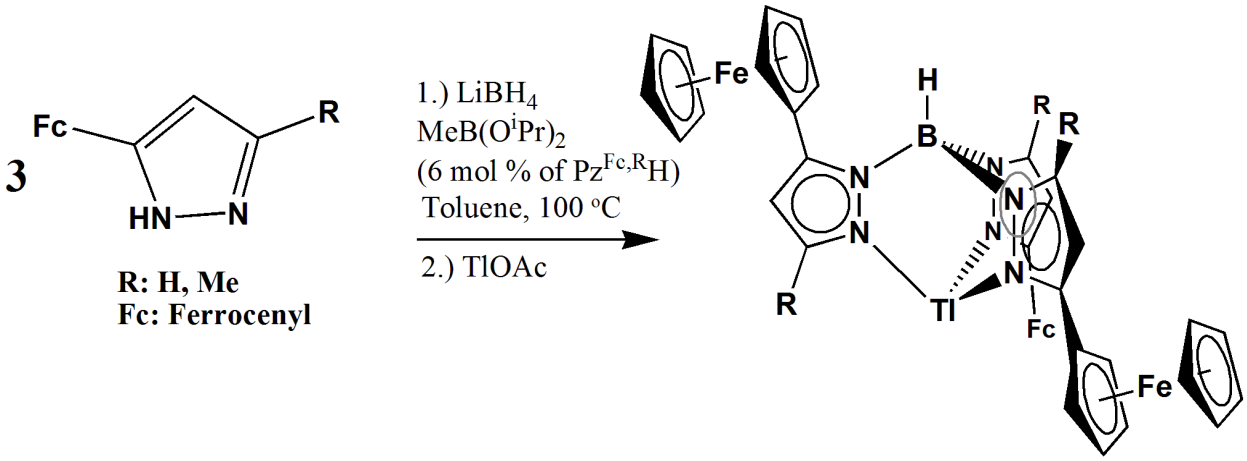

Scheme 2.7: Synthesis of $Tp^{Fc,R*}Tl$ ligands

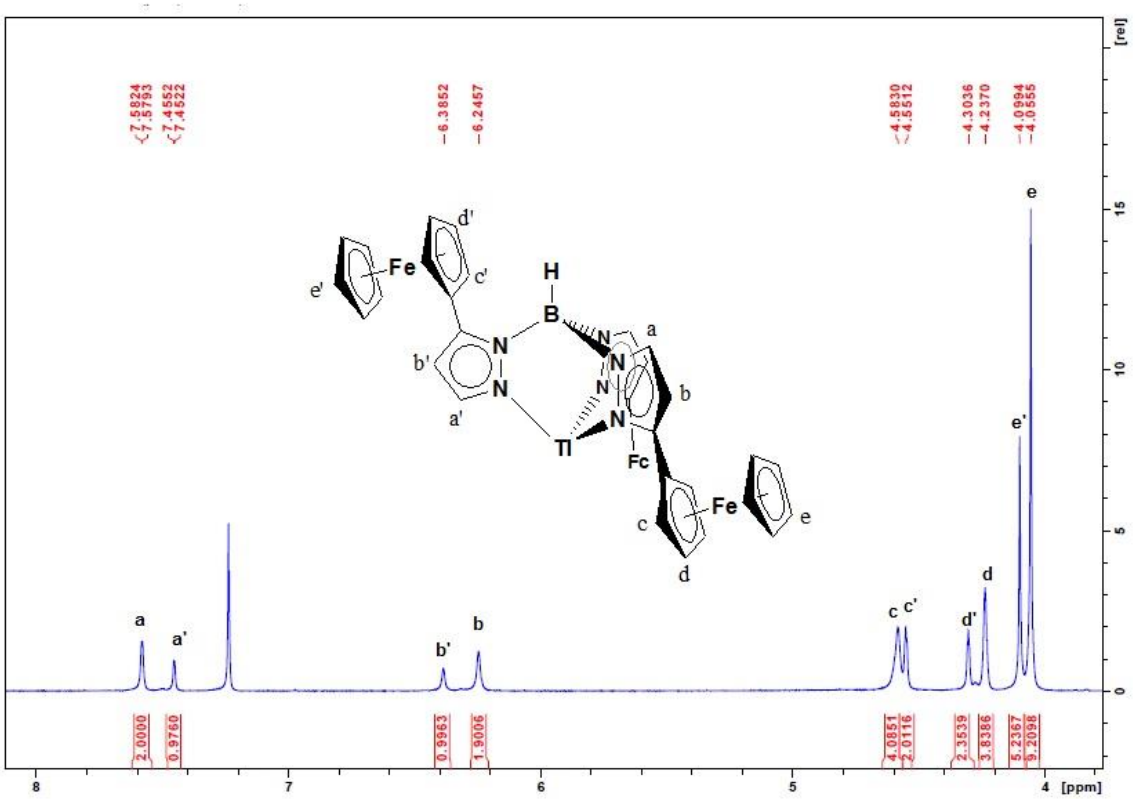

Figure 2.2: ^1H NMR spectrum of $Tp^{Fc*}Tl$ (1).

Cyclic voltammetry (CV) was used to investigate the number of accessible redox processes (Figure 2.3). Due to overlap with the usual reference compound (Fc), the solution was spiked with decamethylferrocene, which is oxidized by one electron at -0.59 V vs Fc/Fc^+ in CH_2Cl_2.[23] Through integration of the half waves of **1** and comparison to the half waves of decamethylferrocene, it was established that **1** undergoes a single three-electron redox process[24]. This suggests that the ferrocene moieties act independently and have no electronic communication between them. The difference in oxidation peak potential between **1** and Cp^*_2Fe, about 0.62 V, suggests that the electronic effect on the redox potential of ferrocenyl substituents is negligible. This is in agreement with attempts to establish the oxidation potential of **1** in solutions spiked with Cp_2Fe. The CV data of these experiments showed only a single, slightly broadened, redox wave rather than two peaks that would be expected if the redox potentials of **1** and Cp_2Fe were significantly different.

The X-ray crystal structure of **1** confirmed the singly N-confused configuration indicated by the ^1H NMR spectrum. Compound **1** crystallizes in the monoclinic space group $P2_1/c$. The molecular structure (Figure 2.4) shows the Tl binding to the ligand in a trigonal pyramidal geometry with κ^3-coordination. The average Tl-N distances (Table 2.2) of complex **1** are 2.62(4)Å, which is typical for TpTl complexes.[25] To better understand the steric effects of the ferrocenyl moieties on the Tp ligand, cone angles have been determined using the solid state structure (Table A1.1). Also of interest, was the position of the ferrocenyl moieties with respect to the plane of the pyrazole. The rotation of the Fc moieties with respect to the plane of the pyrazolyl ring can be determined from the X-ray crystal structures by measuring a relevant torsion angles. The torsion angles for **1** and all the following compounds in this chapter are defined in the appendix and can be viewed in Table A1.2.

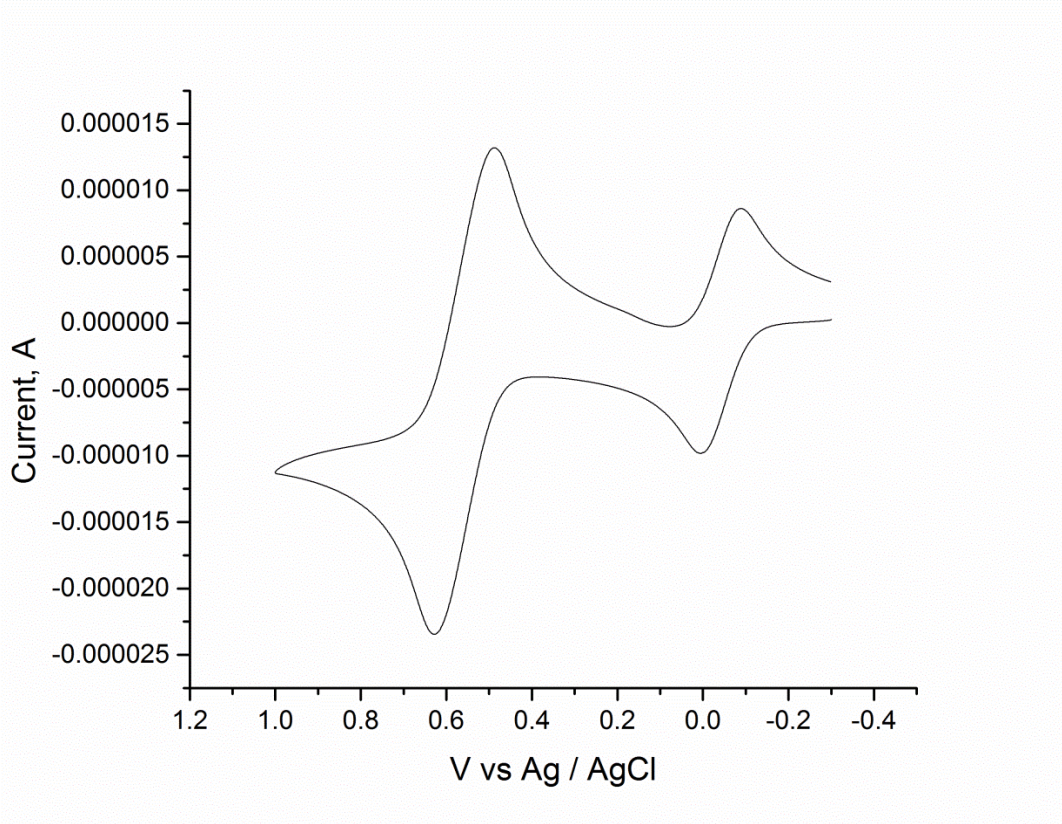

Figure 2.3: Cyclic voltammetric response of a 1.0 mM solution of $Tp^{Fc^*}Tl$ (1) recorded at a platinum electrode with at Ag/AgCl reference electrode in CH_2Cl_2 solutions containing 0.1 M $[NBu_4][PF_6]$ and Cp^*_2Fe using a scan rate of 100 mV/s.

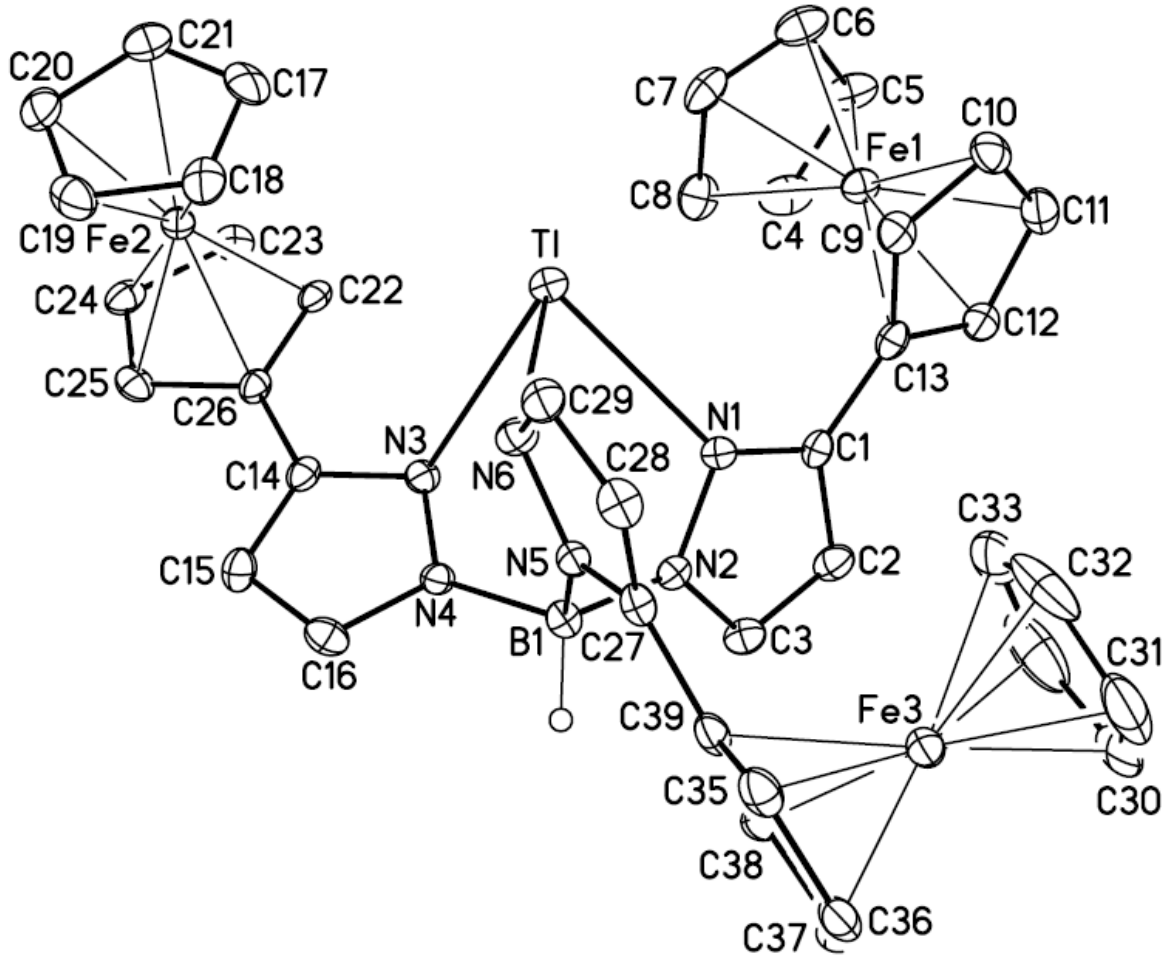

Figure 2.4: Molecular structure of $Tp^{Fc^*}Tl$ (1) at the 30% probability level. Hydrogen atoms (except the boron bound hydrogen, H1B) have been removed for clarity.

Table 2.2: Selected interatomic distances (Å) and angles (°) for $Tp^{Fc*}Tl$ (1) (Not included are the distances and angles of the Fc moieties).

Distances (Å)

Tl-N(1)	2.572(4)	C(14)-C(15)	1.383(7)
Tl-N(6)	2.642(4)	C(14)-C(26)	1.470(7)
Tl-N(3)	2.653(4)	C(15)-C(16)	1.367(7)
B(1)-N(2)	1.529(7)	C(17)-C(21)	1.398(9)
B(1)-N(4)	1.541(7)	C(17)-C(18)	1.414(8)
B(1)-N(5)	1.554(7)	C(18)-C(19)	1.409(8)
N(1)-C(1)	1.340(6)	C(19)-C(20)	1.415(9)
N(1)-N(2)	1.374(5)	C(20)-C(21)	1.412(8)
N(2)-C(3)	1.325(6)	C(22)-C(23)	1.417(7)
N(3)-C(14)	1.342(6)	C(22)-C(26)	1.433(7)
N(3)-N(4)	1.371(5)	C(23)-C(24)	1.421(7)
N(4)-C(16)	1.336(6)	C(24)-C(25)	1.401(7)
N(5)-C(27)	1.371(6)	C(25)-C(26)	1.435(7)
N(5)-N(6)	1.371(6)	C(27)-C(28)	1.381(7)
N(6)-C(29)	1.330(6)	C(27)-C(39)	1.454(7)
C(1)-C(2)	1.403(7)	C(28)-C(29)	1.380(7)
C(1)-C(13)	1.457(7)	C(30)-C(31)	1.409(13)
C(2)-C(3)	1.373(7)	C(30)-C(34)	1.415(13)
C(4)-C(8)	1.400(9)	C(31)-C(32)	1.364(12)
C(4)-C(5)	1.435(8)	C(32)-C(33)	1.342(10)
C(5)-C(6)	1.425(8)	C(33)-C(34)	1.354(11)
C(6)-C(7)	1.408(9)	C(35)-C(36)	1.411(8)
C(7)-C(8)	1.421(8)	C(35)-C(39)	1.425(7)
C(9)-C(10)	1.417(7)	C(36)-C(37)	1.398(9)
C(9)-C(13)	1.438(7)	C(37)-C(38)	1.431(7)
C(10)-C(11)	1.416(8)	C(38)-C(39)	1.426(7)
C(11)-C(12)	1.409(7)		
C(12)-C(13)	1.431(7)		

Angles (°)

N(1)-Tl-N(6)	75.31(13)	C(3)-N(2)-N(1)	109.5(4)
N(1)-Tl-N(3)	77.94(13)	C(3)-N(2)-B(1)	128.9(4)
N(6)-Tl-N(3)	75.55(13)	N(1)-N(2)-B(1)	121.2(4)
N(2)-B(1)-N(4)	112.0(4)	C(14)-N(3)-N(4)	105.5(4)
C(1)-N(1)-N(2)	106.7(4)	C(14)-N(3)-Tl	124.2(3)
C(1)-N(1)-Tl	129.1(3)	N(4)-N(3)-Tl	108.7(3)
N(2)-N(1)-Tl	114.3(3)	C(16)-N(4)-N(3)	109.8(4)

C(16)-N(4)-B(1)	125.1(4)	C(21)-C(17)-C(18)	108.3(5)
N(3)-N(4)-B(1)	124.9(4)	C(19)-C(18)-C(17)	108.0(6)
C(27)-N(5)-N(6)	109.9(4)	C(18)-C(19)-C(20)	107.6(5)
C(27)-N(5)-B(1)	130.6(4)	C(21)-C(20)-C(19)	108.1(6)
N(6)-N(5)-B(1)	119.5(4)	C(17)-C(21)-C(20)	108.0(6)
C(29)-N(6)-N(5)	106.2(4)	C(23)-C(22)-C(26)	108.2(5)
C(29)-N(6)-Tl	124.0(3)	C(22)-C(23)-C(24)	108.0(5)
N(5)-N(6)-Tl	113.3(3)	C(25)-C(24)-C(23)	108.4(5)
N(1)-C(1)-C(2)	109.5(5)	C(24)-C(25)-C(26)	108.6(5)
N(1)-C(1)-C(13)	121.8(5)	C(22)-C(26)-C(25)	106.7(4)
C(2)-C(1)-C(13)	128.6(5)	C(22)-C(26)-C(14)	129.3(5)
C(3)-C(2)-C(1)	104.9(5)	C(25)-C(26)-C(14)	124.0(5)
N(2)-C(3)-C(2)	109.4(5)	N(5)-C(27)-C(28)	106.7(5)
C(8)-C(4)-C(5)	109.6(6)	N(5)-C(27)-C(39)	126.6(5)
C(6)-C(5)-C(4)	105.5(6)	C(28)-C(27)-C(39)	126.7(5)
C(7)-C(6)-C(5)	109.5(6)	C(29)-C(28)-C(27)	106.2(5)
C(6)-C(7)-C(8)	107.7(6)	N(6)-C(29)-C(28)	111.0(5)
C(4)-C(8)-C(7)	107.7(6)	C(31)-C(30)-C(34)	105.4(7)
C(10)-C(9)-C(13)	107.9(5)	C(32)-C(31)-C(30)	107.7(8)
C(11)-C(10)-C(9)	108.3(5)	C(33)-C(32)-C(31)	109.5(8)
C(12)-C(11)-C(10)	108.3(5)	C(32)-C(33)-C(34)	109.4(8)
C(11)-C(12)-C(13)	108.5(5)	C(33)-C(34)-C(30)	108.1(8)
C(12)-C(13)-C(9)	106.9(5)	C(36)-C(35)-C(39)	108.8(5)
C(12)-C(13)-C(1)	126.7(5)	C(37)-C(36)-C(35)	108.6(5)
C(9)-C(13)-C(1)	126.2(5)	C(36)-C(37)-C(38)	107.8(5)
N(3)-C(14)-C(15)	110.8(5)	C(39)-C(38)-C(37)	108.2(5)
N(3)-C(14)-C(26)	122.6(5)	C(35)-C(39)-C(38)	106.6(5)
C(15)-C(14)-C(26)	126.6(5)	C(35)-C(39)-C(27)	121.3(5)
C(16)-C(15)-C(14)	105.1(5)	C(38)-C(39)-C(27)	131.9(5)
N(4)-C(16)-C(15)	108.9(5)		

In a similar fashion, heating three equivalents of 3-ferrocenyl-5-methylpyrazole, with $LiBH_4$ and $MeB(O^iPr)_2$ (6 mol % of pyrazole) in toluene at 100 °C for three days, resulted in the precipitation of the corresponding hydrobis(3-ferrocenyl-5-methylpyrazolyl)(5-ferrocenyl-3-methylpyrazolyl)borate ($Tp^{Fc,Me*}$) ligand as the lithium salt. After metathesis with TlOAc and work-up, $Tp^{Fc,Me*}Tl$ (**2**) ligand could be isolated as an orange solid in 73% yield. Like the $Tp^{Fc*}Tl$ analog, **2** was isolated as a singly N-confused regioisomer. **2** has an ^1H NMR spectrum with two sets of 5 well resolved signals in a ratio of 2:1 which are assigned to the protons of the $Tp^{Fc,Me*}$ ligand.

The solid state structure of **2**, as determined by X-ray diffraction, can be seen in Figure 2.5. X-ray quality crystals, grown by allowing a hot solution of **2** in dimethylsulfoxide (DMSO) to cool, crystallize in the triclinic crystal system in the space group P-1 with one molecule of DMSO per asymmetric unit. Like compound **1**, the Tl atom of compound **2** adopts a trigonal pyramidal geometry with a κ^3 bound ligand with an average Tl-N distance of 2.5232(17)Å (Table 2.3). Like compound **1**, CV analysis revealed that compound **2** undergoes a single three-electron redox process (Figure 2.6). Like **1**, the difference in oxidation peak potential between **2** and Cp^*_2Fe was 0.62 V.

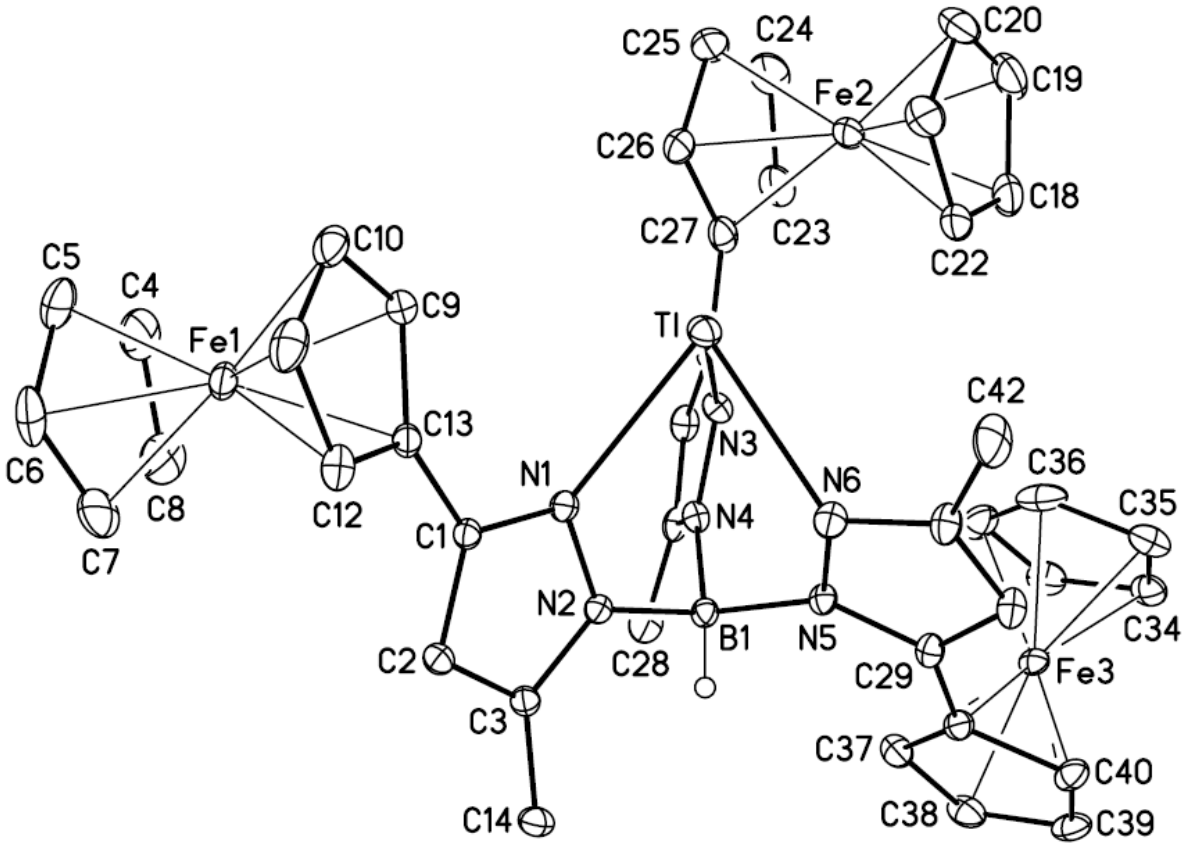

Figure 2.5: Molecular structure of $Tp^{Fc,Me*}Tl$ (2) at the 30% probability level. Hydrogen atoms (except the boron bound hydrogen, H1B) and a DMSO molecule of solvate have been removed for clarity.

Table 2.3: Selected interatomic bond distances (Å) and angles (°) for $Tp^{Fc,Me*}Tl$ (2).

Distances (Å)

Tl-N(1)	2.4964(17)	C(15)-C(16)	1.394(3)
Tl-N(6)	2.5222(18)	C(15)-C(27)	1.467(3)
Tl-N(3)	2.5514(17)	C(16)-C(17)	1.383(3)
B(1)-N(2)	1.549(3)	C(17)-C(28)	1.492(3)
B(1)-N(4)	1.553(3)	C(18)-C(19)	1.424(4)
B(1)-N(5)	1.564(3)	C(18)-C(22)	1.430(4)
N(1)-C(1)	1.336(3)	C(19)-C(20)	1.413(6)
N(1)-N(2)	1.367(2)	C(20)-C(21)	1.421(4)
N(2)-C(3)	1.359(2)	C(21)-C(22)	1.416(4)
N(3)-C(15)	1.341(3)	C(23)-C(24)	1.415(4)
N(3)-N(4)	1.371(2)	C(23)-C(27)	1.430(3)
N(4)-C(17)	1.361(3)	C(24)-C(25)	1.417(5)
N(5)-C(29)	1.363(2)	C(25)-C(26)	1.429(3)
N(5)-N(6)	1.371(2)	C(26)-C(27)	1.429(4)
N(6)-C(31)	1.333(3)	C(29)-C(30)	1.390(3)
C(1)-C(2)	1.403(3)	C(29)-C(41)	1.461(3)
C(1)-C(13)	1.468(3)	C(30)-C(31)	1.394(3)
C(2)-C(3)	1.378(3)	C(31)-C(42)	1.491(3)
C(3)-C(14)	1.495(3)	C(32)-C(33)	1.418(4)
C(4)-C(8)	1.414(4)	C(32)-C(36)	1.419(4)
C(4)-C(5)	1.417(4)	C(33)-C(34)	1.406(4)
C(5)-C(6)	1.411(4)	C(34)-C(35)	1.423(4)
C(6)-C(7)	1.407(4)	C(35)-C(36)	1.412(4)
C(7)-C(8)	1.410(4)	C(37)-C(38)	1.424(3)
C(9)-C(10)	1.423(3)	C(37)-C(41)	1.438(3)
C(9)-C(13)	1.437(3)	C(38)-C(39)	1.414(4)
C(10)-C(11)	1.417(4)	C(39)-C(40)	1.417(3)
C(11)-C(12)	1.417(3)	C(40)-C(41)	1.443(3)
C(12)-C(13)	1.433(3)		

Angles (°)

N(2)-B(1)-N(4)	110.48(16)	C(1)-N(1)-N(2)	106.77(16)
N(2)-B(1)-N(5)	110.25(16)	C(1)-N(1)-Tl	128.86(13)
N(4)-B(1)-N(5)	109.00(16)	N(2)-N(1)-Tl	120.83(11)
O(1)-S(1)-C(44)	106.3(2)	C(3)-N(2)-N(1)	109.68(15)
O(1)-S(1)-C(43)	108.02(15)	C(3)-N(2)-B(1)	128.17(17)
C(44)-S(1)-C(43)	95.96(19)	N(1)-N(2)-B(1)	122.11(15)

C(15)-N(3)-N(4)	106.30(17)	N(4)-C(17)-C(16)	107.28(19)
C(15)-N(3)-Tl	130.00(14)	N(4)-C(17)-C(28)	124.7(2)
N(4)-N(3)-Tl	120.54(12)	C(16)-C(17)-C(28)	128.0(2)
C(17)-N(4)-N(3)	110.19(17)	C(19)-C(18)-C(22)	107.1(3)
C(17)-N(4)-B(1)	130.03(17)	C(20)-C(19)-C(18)	108.3(3)
N(3)-N(4)-B(1)	119.69(16)	C(19)-C(20)-C(21)	108.5(3)
C(29)-N(5)-N(6)	109.19(16)	C(22)-C(21)-C(20)	107.6(3)
C(29)-N(5)-B(1)	131.89(17)	C(21)-C(22)-C(18)	108.5(2)
N(6)-N(5)-B(1)	118.91(15)	C(24)-C(23)-C(27)	108.3(3)
C(31)-N(6)-N(5)	107.24(17)	C(23)-C(24)-C(25)	108.4(2)
C(31)-N(6)-Tl	123.84(15)	C(24)-C(25)-C(26)	107.9(3)
N(5)-N(6)-Tl	119.21(12)	C(27)-C(26)-C(25)	108.1(2)
N(1)-C(1)-C(2)	110.18(17)	C(26)-C(27)-C(23)	107.3(2)
N(1)-C(1)-C(13)	121.58(18)	C(26)-C(27)-C(15)	128.3(2)
C(2)-C(1)-C(13)	128.09(18)	C(23)-C(27)-C(15)	124.4(2)
C(3)-C(2)-C(1)	105.29(17)	N(5)-C(29)-C(30)	107.81(18)
N(2)-C(3)-C(2)	108.08(17)	N(5)-C(29)-C(41)	126.92(18)
N(2)-C(3)-C(14)	123.80(18)	C(30)-C(29)-C(41)	125.10(18)
C(2)-C(3)-C(14)	128.12(18)	C(29)-C(30)-C(31)	105.36(18)
C(8)-C(4)-C(5)	107.3(3)	N(6)-C(31)-C(30)	110.38(19)
C(6)-C(5)-C(4)	108.2(3)	N(6)-C(31)-C(42)	121.2(2)
C(7)-C(6)-C(5)	108.0(3)	C(30)-C(31)-C(42)	128.4(2)
C(6)-C(7)-C(8)	108.1(3)	C(33)-C(32)-C(36)	107.4(2)
C(4)-C(8)-C(7)	108.3(3)	C(34)-C(33)-C(32)	108.4(2)
C(10)-C(9)-C(13)	107.9(2)	C(33)-C(34)-C(35)	108.2(2)
C(11)-C(10)-C(9)	108.3(2)	C(36)-C(35)-C(34)	107.4(2)
C(12)-C(11)-C(10)	108.4(2)	C(35)-C(36)-C(32)	108.5(2)
C(11)-C(12)-C(13)	108.2(2)	C(38)-C(37)-C(41)	108.2(2)
C(12)-C(13)-C(9)	107.26(19)	C(39)-C(38)-C(37)	108.6(2)
C(12)-C(13)-C(1)	124.48(19)	C(38)-C(39)-C(40)	108.11(19)
C(9)-C(13)-C(1)	128.25(19)	C(39)-C(40)-C(41)	108.6(2)
N(3)-C(15)-C(16)	110.26(19)	C(37)-C(41)-C(40)	106.46(18)
N(3)-C(15)-C(27)	122.8(2)	C(37)-C(41)-C(29)	131.09(19)
C(16)-C(15)-C(27)	126.9(2)	C(40)-C(41)-C(29)	122.10(19)
C(17)-C(16)-C(15)	105.97(18)		

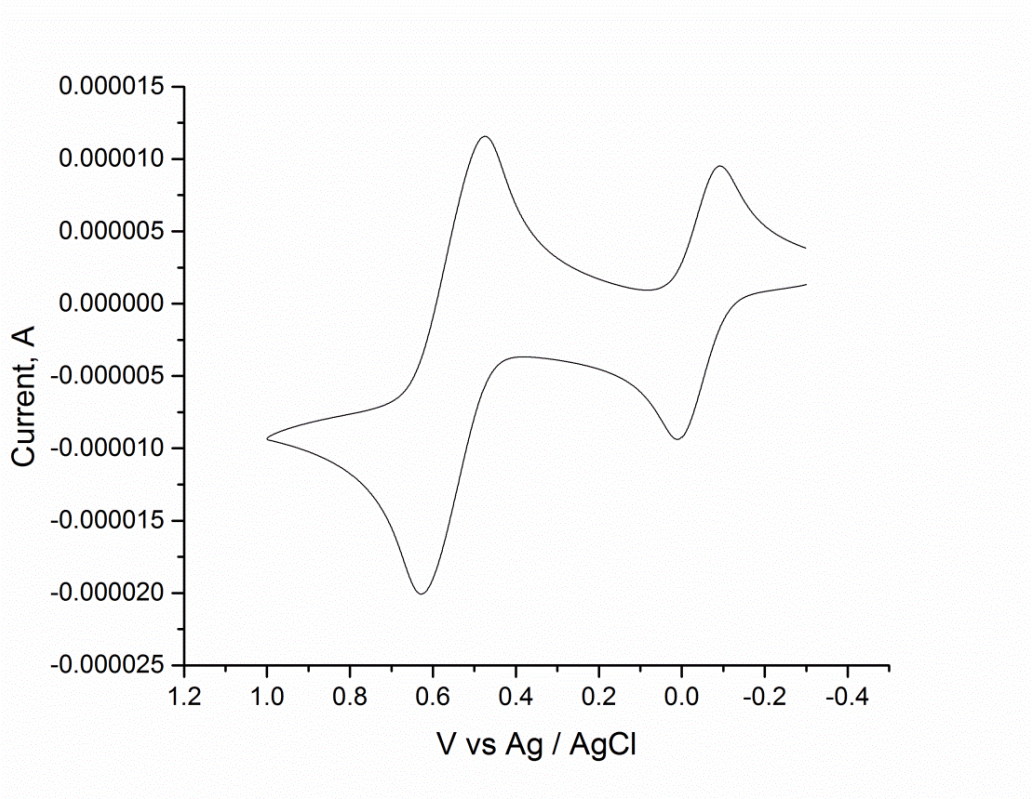

Figure 2.6: Cyclic voltammetric response of a 1.0 mM solution of $Tp^{Fc,Me*}Tl$ (2) recorded at a platinum electrode with a Ag/AgCl reference electrode in CH_2Cl_2 solutions containing 0.1 M $[NBu_4][PF_6]$ and Cp^*_2Fe using a scan rate of 100 mV/s.

2.2.2 Synthesis and Characterization of $Tp^{Fc,iPr}Tl$.

In an attempt to circumvent the problem of N-confusion in this new class of tris(pyrazolyl)borate ligands, several additional representative examples have been synthesized. We began to synthesize pyrazoles that contained larger substituents in the 5-position, such as the 3-ferrocenyl-5-*iso*-propylpyrazole, in an attempt to inhibit N-confusion. Larger substituents may prevent the formation of N-confused products by sterically crowding the boron atom. A solution of three equivalents of 3-ferrocenyl-5-*iso*-propylpyrazole, $LiBH_4$, and $MeB(O^iPr)_2$ (6 mol % of mol pyrazole) in toluene was heated for three days at 100 °C. After metathesis with TlOAc and work-up, $Tp^{Fc,iPr}Tl$ (**3**) can be isolated as an orange solid in 64% yield (Scheme 2.8). Complex **3**

has an ^{1}H NMR spectrum, recorded in $CDCl_3$ at room temperature, with one set of 6 well resolved signals that are easily assigned to the protons of the $Tp^{Fc,iPr}$ ligand (Figure 2.7).

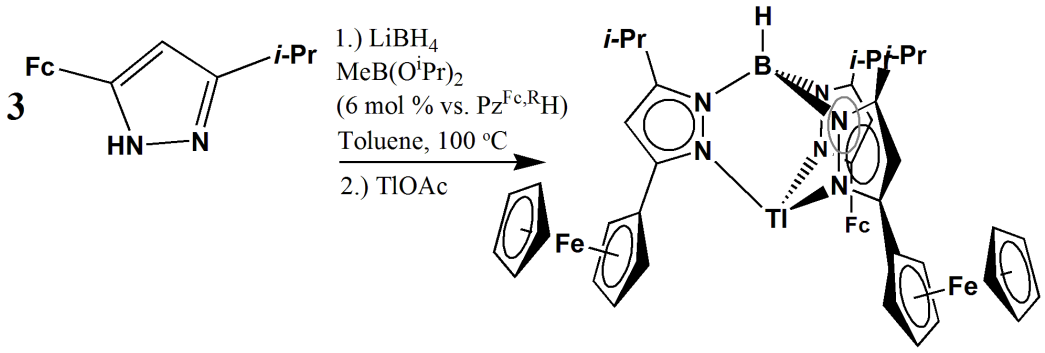

Scheme 2.8: Synthesis of $Tp^{Fc,iPr}Tl$ ligands.

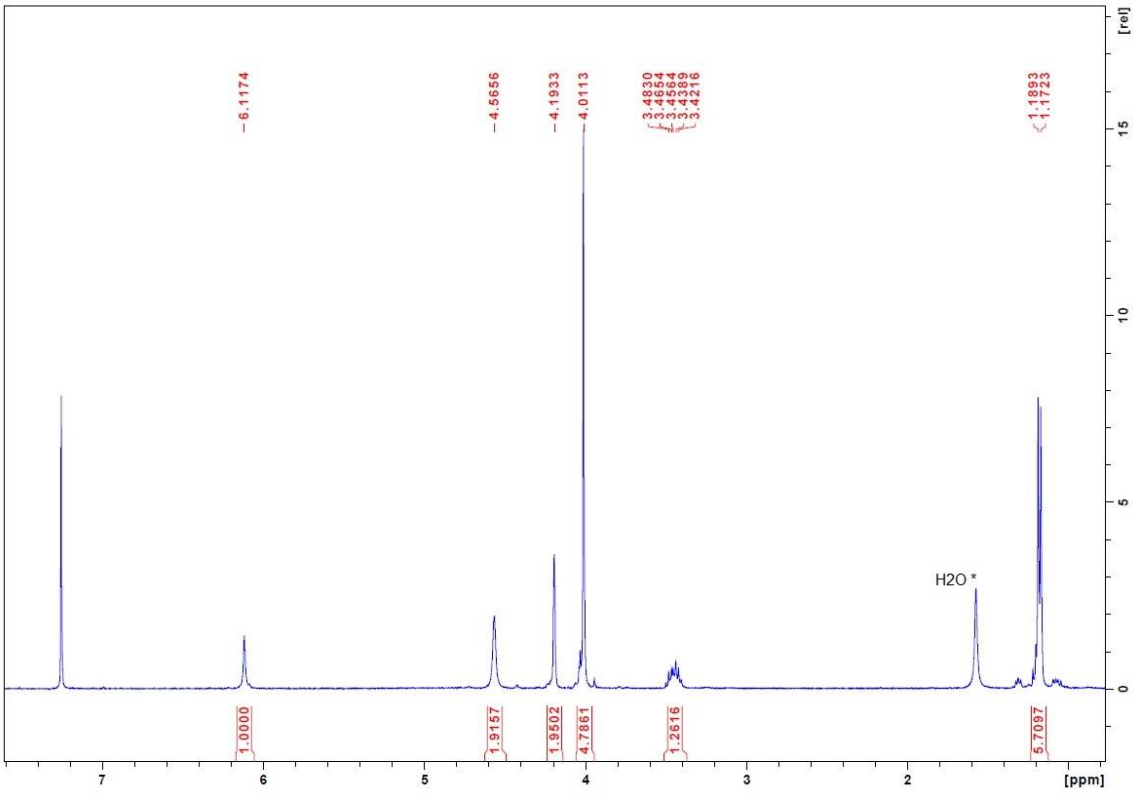

Figure 2.7: ^{1}H NMR spectrum of $Tp^{Fc,iPr}Tl$ (3) recorded in $CDCl_3$ at 400 MHz.

The X-ray crystal structure of **3** confirmed the symmetric structure of the ligand, which was suggested by the ^{1}H NMR spectrum. **3** crystallized in the rhombohedral space group R-3. The Tl salt of the ligand crystallizes as a dimer with an apparent Tl-Tl bond of 3.5372(10) Å (Figure 2.8).[26] For clarity, Figure 2.9 displays the molecular structure of the monomer of $Tp^{Fc,iPr}$ Tl in which Tl binds to the ligand in a trigonal pyramidal geometry with κ^3-coordination. The Tl-N distances (Table 2.4) of **3** are 2.572(4) Å. Once again, CV was used to investigate the number of accessible redox processes (Figure 2.10). The solutions was spiked with an equimolar amount of decamethylferrocene, by which it can be established that compound **3** undergoes a single three-electron redox process, similar to that of compounds **1** and **2**. Like **1** and **2**, the difference in oxidation peak potential between **3** and Cp^*_2Fe is 0.62 V. The increase in the electron donating ability of the 5-position substituents on the pyrazolyl ring does not significantly influence the potential at which the ferrocenyl moieties oxidize.

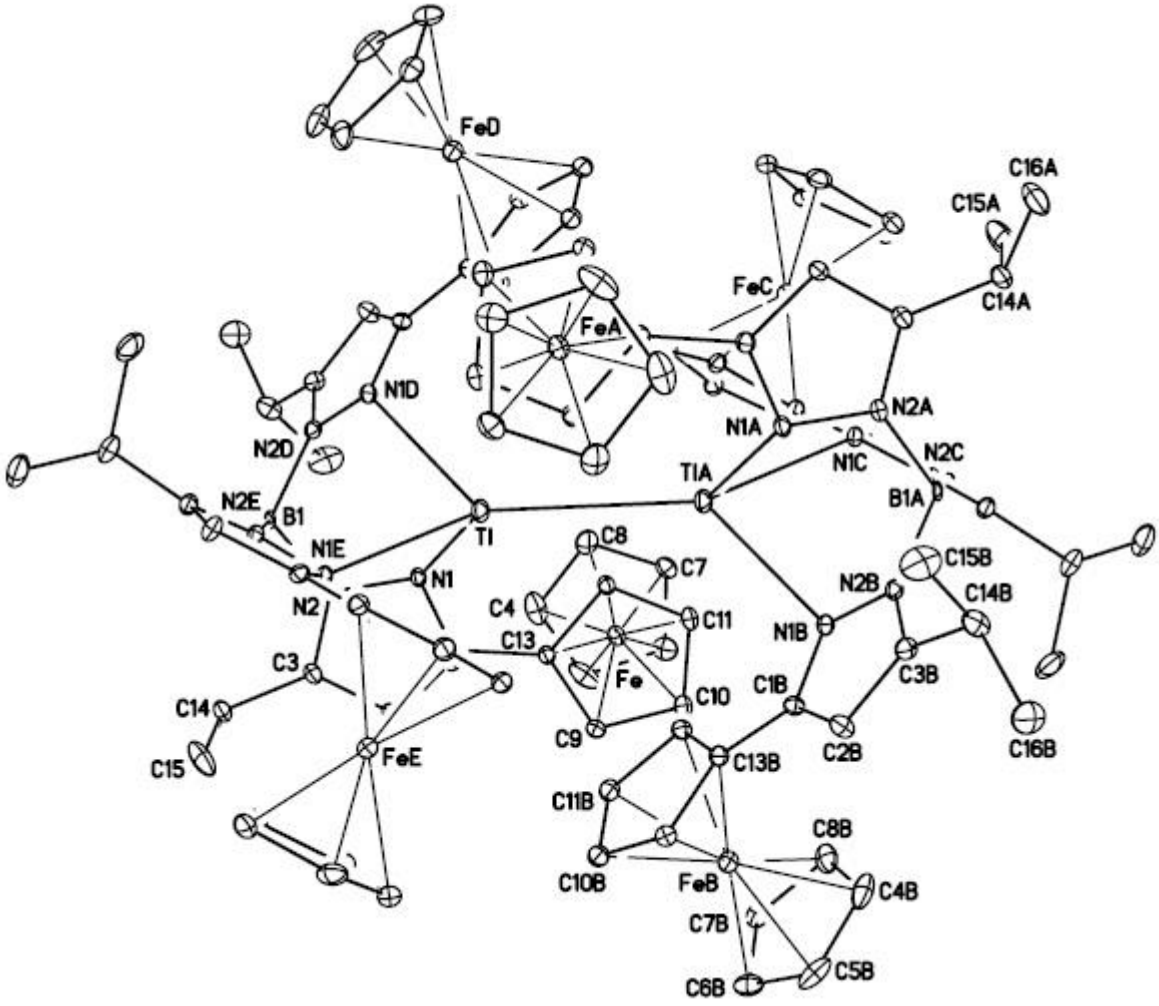

Figure 2.8: Molecular structure of $Tp^{Fc,iPr}Tl$ (3) dimer at the 30% probability level. Hydrogen atoms have been removed for clarity.

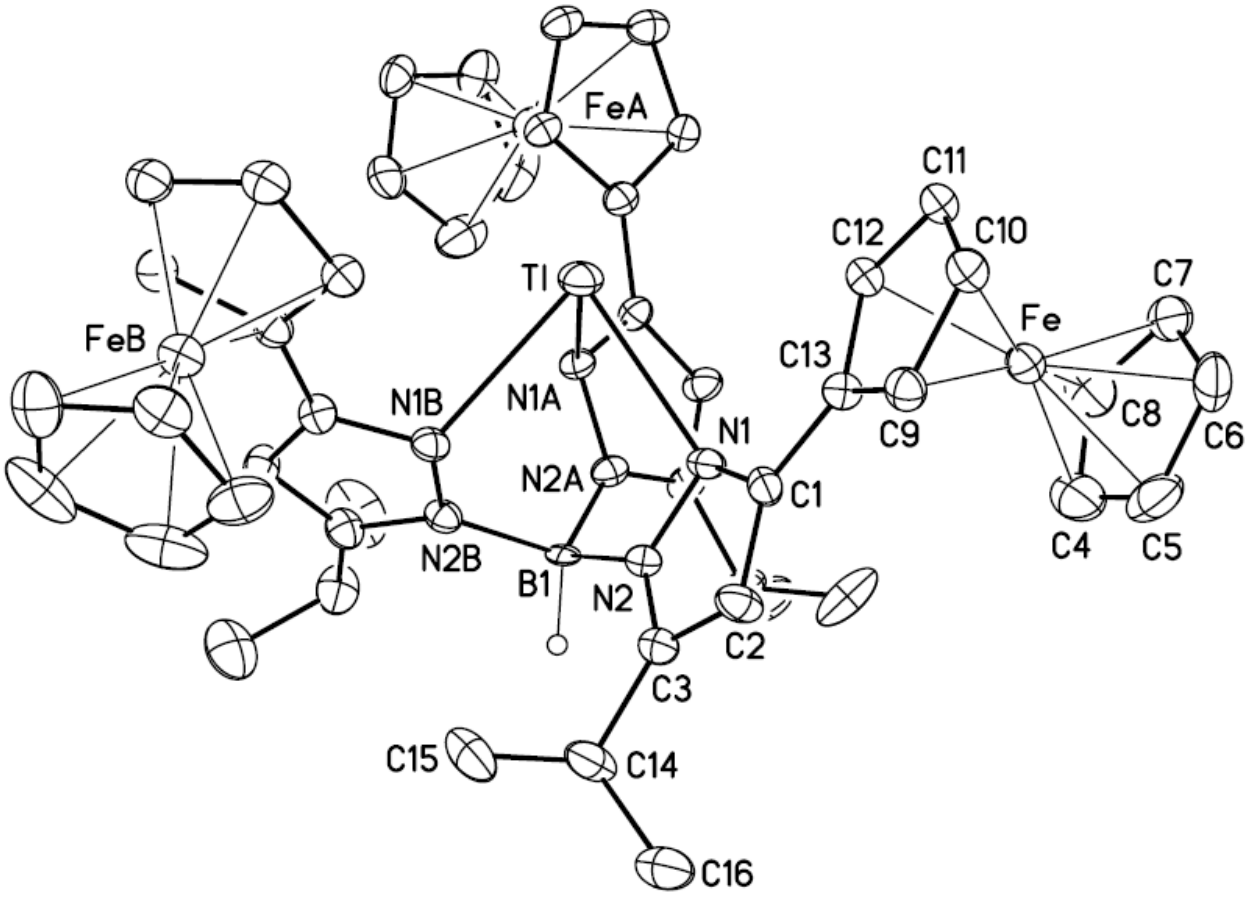

Figure 2.9: Molecular structure of $Tp^{Fc,iPr}Tl$ (3) monomer at 30% probability level. Hydrogen atoms (except the boron bound hydrogen, H1B) have been removed for clarity.

Table 2.4: Selected interatomic bond distances (Å) and angles (°) for $Tp^{Fc,iPr}Tl$ (3).

Distances (Å)

Tl-N(1)#1	2.572(4)	N(1)-N(2)	1.370(5)
Tl-N(1)	2.572(4)	N(2)-C(3)	1.348(6)
Tl-N(1)#2	2.572(4)	C(1)-C(2)	1.393(7)
Tl-Tl#3	3.5372(10)	C(1)-C(13)	1.463(7)
Fe-C(4)	2.027(7)	C(2)-C(3)	1.388(7)
Fe-C(8)	2.038(6)	C(3)-C(14)	1.505(7)
Fe-C(5)	2.040(6)	C(4)-C(8)	1.393(9)
Fe-C(6)	2.040(5)	C(4)-C(5)	1.433(10)
Fe-C(9)	2.042(5)	C(5)-C(6)	1.412(9)
Fe-C(12)	2.043(5)	C(6)-C(7)	1.400(8)
Fe-C(11)	2.043(5)	C(7)-C(8)	1.399(8)
Fe-C(7)	2.044(5)	C(9)-C(10)	1.415(7)
Fe-C(10)	2.046(5)	C(9)-C(13)	1.433(7)
Fe-C(13)	2.048(5)	C(10)-C(11)	1.412(7)
B(1)-N(2)#2	1.549(5)	C(11)-C(12)	1.420(7)
B(1)-N(2)	1.549(5)	C(12)-C(13)	1.437(7)
B(1)-N(2)#1	1.549(5)	C(14)-C(16)	1.511(8)
N(1)-C(1)	1.331(6)	C(14)-C(15)	1.527(9)

Angles (°)

N(1)A-Tl-N(1)	76.22(13)	C(9)-Fe-C(12)	68.8(2)
N(1)A-Tl-N(1)B	76.22(13)	C(4)-Fe-C(11)	158.0(3)
N(1)-Tl-N(1)B	76.22(13)	C(8)-Fe-C(11)	122.4(2)
C(4)-Fe-C(8)	40.1(3)	C(5)-Fe-C(11)	158.9(3)
C(4)-Fe-C(5)	41.3(3)	C(6)-Fe-C(11)	122.6(2)
C(8)-Fe-C(5)	68.1(3)	C(9)-Fe-C(11)	68.0(2)
C(4)-Fe-C(6)	68.5(3)	C(12)-Fe-C(11)	40.66(19)
C(8)-Fe-C(6)	67.8(3)	C(4)-Fe-C(7)	67.7(3)
C(5)-Fe-C(6)	40.5(3)	C(8)-Fe-C(7)	40.1(2)
C(4)-Fe-C(9)	123.0(3)	C(5)-Fe-C(7)	67.7(2)
C(8)-Fe-C(9)	156.7(2)	C(6)-Fe-C(7)	40.1(2)
C(5)-Fe-C(9)	110.1(2)	C(9)-Fe-C(7)	162.6(2)
C(6)-Fe-C(9)	127.0(2)	C(12)-Fe-C(7)	119.5(2)
C(4)-Fe-C(12)	121.4(3)	C(11)-Fe-C(7)	107.4(2)
C(8)-Fe-C(12)	104.7(2)	C(4)-Fe-C(10)	159.6(3)
C(5)-Fe-C(12)	160.0(3)	C(8)-Fe-C(10)	159.8(2)
C(6)-Fe-C(12)	155.9(2)	C(5)-Fe-C(10)	124.3(3)

C(6)-Fe-C(10)	110.1(2)	C(6)-C(5)-C(4)	107.1(6)
C(9)-Fe-C(10)	40.5(2)	C(6)-C(5)-Fe	69.8(4)
C(12)-Fe-C(10)	68.6(2)	C(4)-C(5)-Fe	68.9(4)
C(11)-Fe-C(10)	40.4(2)	C(7)-C(6)-C(5)	108.0(6)
C(7)-Fe-C(10)	125.3(2)	C(7)-C(6)-Fe	70.1(3)
C(4)-Fe-C(13)	106.2(3)	C(5)-C(6)-Fe	69.7(4)
C(8)-Fe-C(13)	119.5(2)	C(8)-C(7)-C(6)	108.6(6)
C(5)-Fe-C(13)	124.8(3)	C(8)-C(7)-Fe	69.7(3)
C(6)-Fe-C(13)	162.6(2)	C(6)-C(7)-Fe	69.8(3)
C(9)-Fe-C(13)	41.02(19)	C(4)-C(8)-C(7)	108.5(7)
C(12)-Fe-C(13)	41.15(18)	C(4)-C(8)-Fe	69.6(4)
C(11)-Fe-C(13)	68.6(2)	C(7)-C(8)-Fe	70.2(3)
C(7)-Fe-C(13)	154.8(2)	C(10)-C(9)-C(13)	108.6(4)
C(10)-Fe-C(13)	68.8(2)	C(10)-C(9)-Fe	69.9(3)
N(2)B-B(1)-N(2)	109.2(3)	C(13)-C(9)-Fe	69.7(3)
N(2)B-B(1)-N(2)A	109.2(3)	C(11)-C(10)-C(9)	107.9(5)
N(2)-B(1)-N(2)A	109.2(3)	C(11)-C(10)-Fe	69.7(3)
C(1)-N(1)-N(2)	106.4(4)	C(9)-C(10)-Fe	69.6(3)
C(1)-N(1)-Tl	117.1(3)	C(10)-C(11)-C(12)	108.9(5)
N(2)-N(1)-Tl	112.0(3)	C(10)-C(11)-Fe	69.9(3)
C(3)-N(2)-N(1)	110.2(4)	C(12)-C(11)-Fe	69.6(3)
C(3)-N(2)-B(1)	130.7(4)	C(11)-C(12)-C(13)	107.6(5)
N(1)-N(2)-B(1)	118.7(4)	C(11)-C(12)-Fe	69.7(3)
N(1)-C(1)-C(2)	110.5(4)	C(13)-C(12)-Fe	69.6(3)
N(1)-C(1)-C(13)	118.8(4)	C(9)-C(13)-C(12)	107.0(4)
C(2)-C(1)-C(13)	130.6(4)	C(9)-C(13)-C(1)	127.0(4)
C(3)-C(2)-C(1)	105.3(4)	C(12)-C(13)-C(1)	125.9(4)
N(2)-C(3)-C(2)	107.5(4)	C(9)-C(13)-Fe	69.3(3)
N(2)-C(3)-C(14)	122.2(5)	C(12)-C(13)-Fe	69.2(3)
C(2)-C(3)-C(14)	130.1(5)	C(1)-C(13)-Fe	129.9(4)
C(8)-C(4)-C(5)	107.8(6)	C(3)-C(14)-C(16)	111.6(5)
C(8)-C(4)-Fe	70.4(4)	C(3)-C(14)-C(15)	111.0(5)
C(5)-C(4)-Fe	69.9(4)	C(16)-C(14)-C(15)	111.1(5)

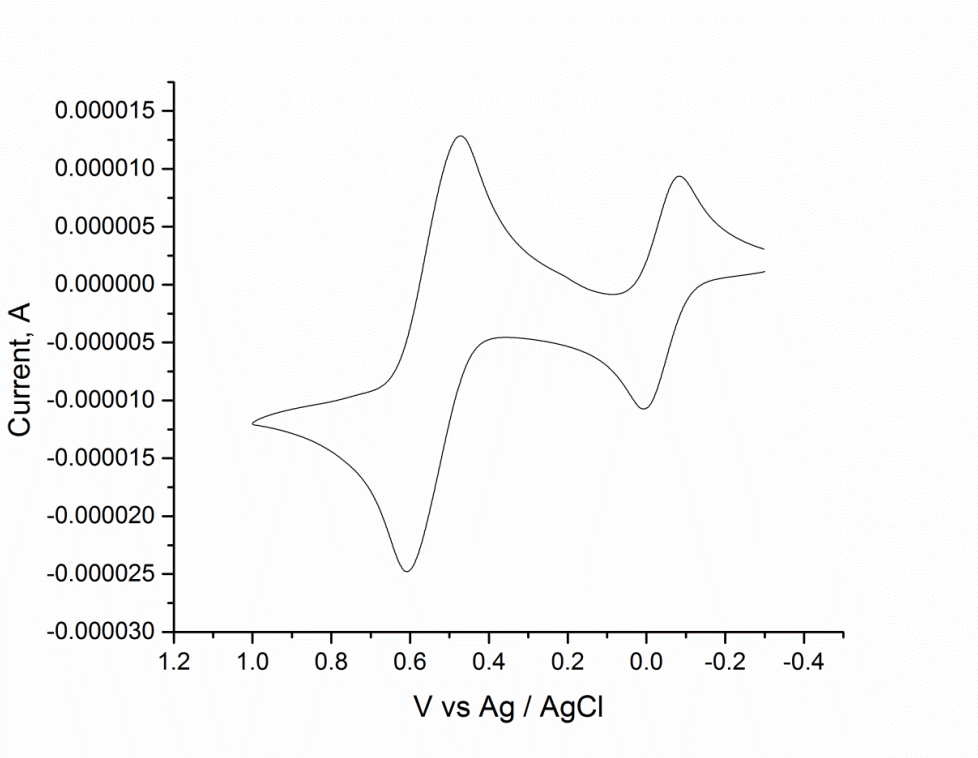

Figure 2.10: Cyclic voltammetric response of a 1.0 mM solution of $Tp^{Fc,iPr}Tl$ (3) recorded at a platinum electrode with a Ag/AgCl reference electrode in CH_2Cl_2 solutions containing 0.1 M $[NBu_4][PF_6]$ and Cp^*_2Fe using a scan rate of 100 mV/s.

2.2.3 Synthesis and Characterization of $Tp^{CF3,Fc}Tl$..

With the successful synthesis of hydrotris(pyrazolyl)borate ligands containing pyrazoles with both ferrocene and electron donating alkyl substituents, the scope of the reaction was then tested with pyrazoles containing both ferrocene and electron withdrawing groups. Heating three equivalents of 3-ferrocenyl-5-trifluoromethylpyrazole, combined with $LiBH_4$ and $MeB(O^iPr)_2$ (6 mol % of pyrazole) in toluene for three days produced the corresponding hydrotris(3-trifluoromethyl-5-ferrocenylpyrazolyl)borate ($Tp^{CF3,Fc}$) ligand, which was isolated as an orange solid after workup with TlOAc in 53% yield (Scheme 2.9). The ^1H NMR spectrum in CD_2Cl_2 revealed only three well resolved proton resonances instead of the expected four (or eight if N-

confused). This apparently arises from the coincidental overlap of a proton resonance from the ferrocenyl Cp-protons which are tethered to the pyrazolyl ring and the proton resonances of the unsubstituted ferrocenyl Cp ring.

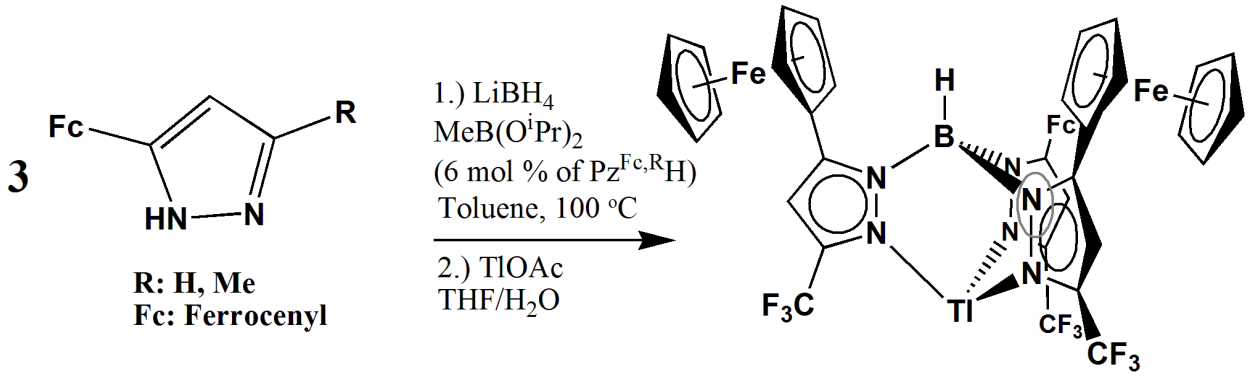

Scheme 2.9: Synthesis of $Tp^{CF3,Fc}Tl$ (4).

X-ray quality crystals were grown by slow diffusion of methanol into a saturated solution of **4** in CH_2Cl_2. The X-ray crystal structure of **4** (Figure 2.10) showed the symmetric binding of the ligand that was apparent in the ^1H NMR spectrum. However, it also revealed that all of the ferrocenyl substituents are in the 5-position and that the trifluoromethyl groups occupy the 3-positions of the pyrazole rings. Similar hydrotris(pyrazolyl)borate with bulky substituents, namely hydrotris[3-trifluoromethyl-5-(2-thienyl)pyrazolyl]borate thallium(I) ($Tp^{CF3,Tn}Tl$)[27] and hydrotris(3-trifluoromethyl-5-phenylpyrazolyl)borate ($Tp^{CF3,Ph}Tl$),[28] also display the trifluoromethyl groups in the 3-position of the pyrazolyl groups. This would suggest that the more electron rich nitrogen of the pyrazole preferentially binds to the boron atom during the ligand formation. Curiously, the X-ray crystallographic analysis of a dihydrobis(3-ferrocenyl-5-trifluoromethylpyrazolyl)borate thallium(I) ($Bp^{Fc,CF3}Tl$) complex (Figure A1.1) (synthesized in dimethylacetamide instead of toluene) shows the ferrocenyl substituents in the 3-position while the trifluoromethyl groups occupy the 5-position of the pyrazolyl groups. This observation

suggests that the boron initially binds preferentially to the N with the least amount of steric encumbrance. Once complexed in its hydrotris(pyrazolyl)borate form, ligand undergoes an apparent borotropic rearrangement to form a hydrotris(pyrazolyl)borate ligand with the trifluoromethyl groups now in the 3-position and the ferrocenyl groups occupying the 5-position (Scheme 2.12). The CV of **4** (Figure 2.12) reveals an increased oxidation potential with a peak separation of 0.7 V from Cp^*_2Fe, greater than that of **1** – **3** at 0.62 V. This is due to the introduction of more electron withdrawing groups which make it more difficult to oxidize the complex. However, upon oxidation, **4** undergoes decomposition which results in an irreversible redox wave.

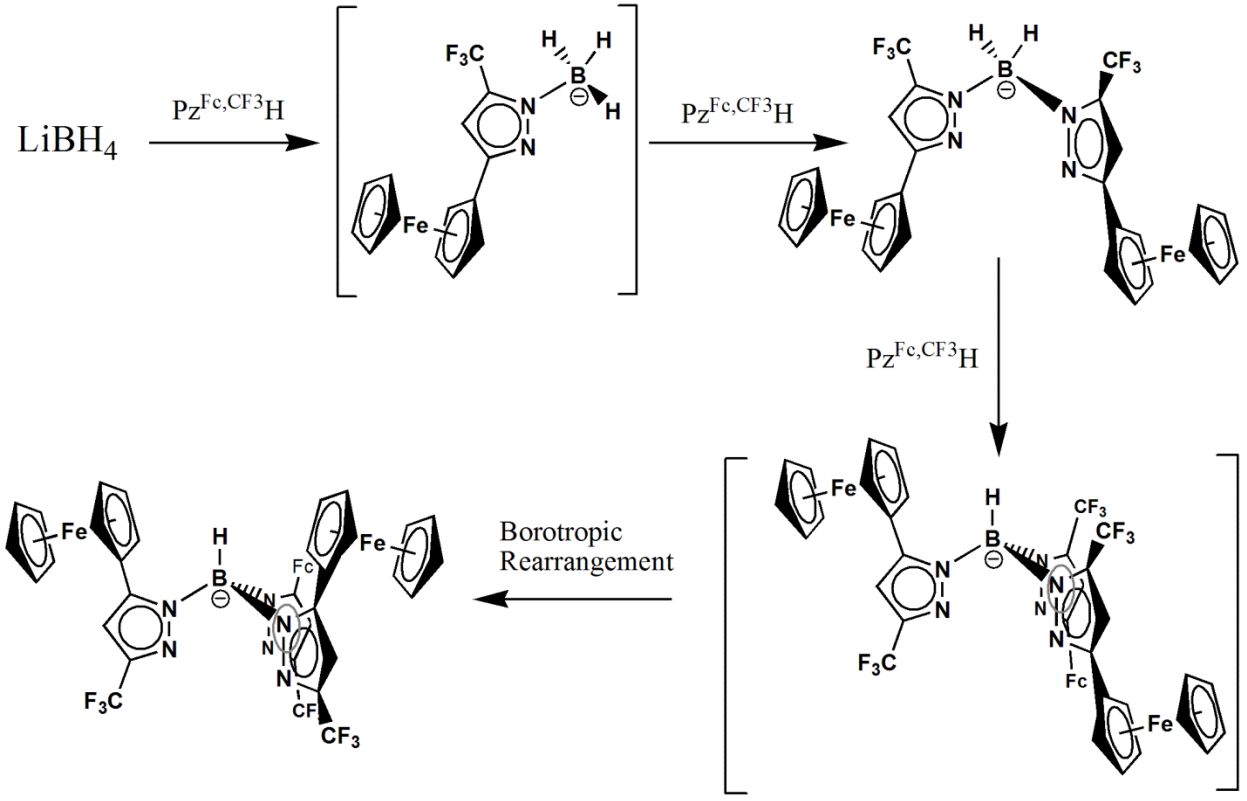

Scheme 2.10: Synthesis and proposed borotropic rearrangement of the $Tp^{CF3,Fc}$ ligand.

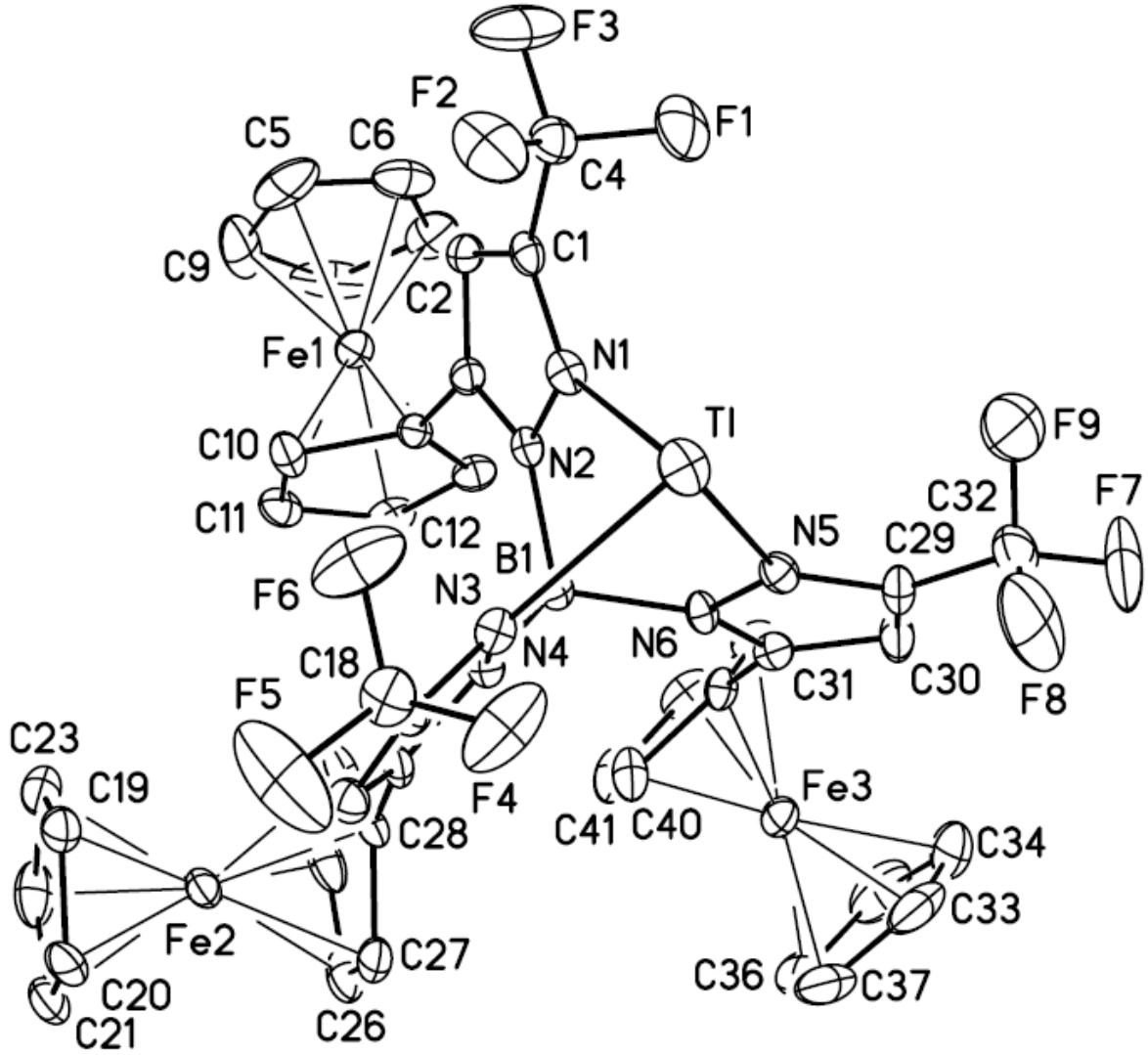

Figure 2.11: Molecular structure of $Tp^{CF3,Fc}Tl$ (4) at 30% probability level. Hydrogen atoms have been removed for clarity.

Table 2.5: Selected interatomic distances (Å) and angles (°) for $Tp^{CF3,Fc}Tl$ (4).

Distances (Å)

Tl-N(1)	2.587(5)	C(8)-C(9)	1.440(13)
Tl-N(3)	2.587(4)	C(10)-C(11)	1.416(8)
Tl-N(5)	2.635(5)	C(10)-C(14)	1.449(7)
B(1)-N(2)	1.544(8)	C(11)-C(12)	1.393(9)
B(1)-N(4)	1.548(8)	C(12)-C(13)	1.411(8)
B(1)-N(6)	1.569(7)	C(13)-C(14)	1.422(8)
F(1)-C(4)	1.338(7)	C(15)-C(16)	1.390(8)
F(2)-C(4)	1.321(8)	C(15)-C(18)	1.488(8)
F(3)-C(4)	1.318(7)	C(16)-C(17)	1.379(8)
F(4)-C(18)	1.318(7)	C(17)-C(28)	1.459(8)
F(5)-C(18)	1.293(7)	C(19)-C(20)	1.391(8)
F(6)-C(18)	1.311(7)	C(19)-C(23)	1.410(9)
F(4')-C(18)	1.286(15)	C(20)-C(21)	1.396(10)
F(5')-C(18)	1.289(15)	C(21)-C(22)	1.412(10)
F(6')-C(18)	1.302(15)	C(22)-C(23)	1.396(10)
F(7)-C(32)	1.311(8)	C(24)-C(25)	1.422(9)
F(8)-C(32)	1.292(8)	C(24)-C(28)	1.435(8)
F(9)-C(32)	1.318(8)	C(25)-C(26)	1.391(10)
N(1)-C(1)	1.330(7)	C(26)-C(27)	1.440(9)
N(1)-N(2)	1.357(6)	C(27)-C(28)	1.430(8)
N(2)-C(3)	1.366(7)	C(29)-C(30)	1.371(9)
N(3)-C(15)	1.326(7)	C(29)-C(32)	1.493(8)
N(3)-N(4)	1.368(6)	C(30)-C(31)	1.379(8)
N(4)-C(17)	1.378(7)	C(31)-C(42)	1.469(8)
N(5)-C(29)	1.333(7)	C(33)-C(37)	1.374(12)
N(5)-N(6)	1.359(6)	C(33)-C(34)	1.384(13)
N(6)-C(31)	1.371(7)	C(34)-C(35)	1.399(13)
C(1)-C(2)	1.384(7)	C(35)-C(36)	1.412(13)
C(1)-C(4)	1.480(8)	C(36)-C(37)	1.376(13)
C(2)-C(3)	1.382(7)	C(38)-C(39)	1.417(9)
C(3)-C(14)	1.484(7)	C(38)-C(42)	1.426(8)
C(5)-C(6)	1.353(12)	C(39)-C(40)	1.414(10)
C(5)-C(9)	1.363(13)	C(40)-C(41)	1.401(9)
C(6)-C(7)	1.344(10)	C(41)-C(42)	1.427(8)
C(7)-C(8)	1.416(12)		

Angles (°)

N(1)-Tl-N(3)	71.01(14)	C(5)-C(9)-C(8)	106.6(7)
N(1)-Tl-N(5)	70.48(14)	C(11)-C(10)-C(14)	106.8(6)
N(3)-Tl-N(5)	77.10(14)	C(12)-C(11)-C(10)	109.1(5)
N(2)-B(1)-N(4)	110.6(5)	C(11)-C(12)-C(13)	108.8(6)
N(2)-B(1)-N(6)	109.7(4)	C(12)-C(13)-C(14)	108.0(6)
N(4)-B(1)-N(6)	111.7(4)	C(13)-C(14)-C(10)	107.3(5)
C(1)-N(1)-N(2)	105.6(4)	C(13)-C(14)-C(3)	128.6(5)
C(1)-N(1)-Tl	131.0(3)	C(10)-C(14)-C(3)	124.0(5)
N(2)-N(1)-Tl	123.3(3)	N(3)-C(15)-C(16)	111.2(5)
N(1)-N(2)-C(3)	110.3(4)	N(3)-C(15)-C(18)	120.1(5)
N(1)-N(2)-B(1)	121.9(4)	C(16)-C(15)-C(18)	128.6(6)
C(3)-N(2)-B(1)	127.8(5)	C(17)-C(16)-C(15)	105.9(5)
C(15)-N(3)-N(4)	106.2(4)	N(4)-C(17)-C(16)	106.6(5)
C(15)-N(3)-Tl	129.5(4)	N(4)-C(17)-C(28)	124.7(5)
N(4)-N(3)-Tl	123.2(3)	C(16)-C(17)-C(28)	128.6(5)
N(3)-N(4)-C(17)	110.0(4)	F(4')-C(18)-F(5')	109.0(17)
N(3)-N(4)-B(1)	120.5(4)	F(4')-C(18)-F(5)	127(2)
C(17)-N(4)-B(1)	129.2(5)	F(5')-C(18)-F(5)	57(2)
C(29)-N(5)-N(6)	105.4(5)	F(4')-C(18)-F(6')	107.0(16)
C(29)-N(5)-Tl	131.9(4)	F(5')-C(18)-F(6')	106.9(16)
N(6)-N(5)-Tl	122.6(3)	F(5)-C(18)-F(6')	51(2)
N(5)-N(6)-C(31)	110.1(4)	F(4')-C(18)-F(6)	44(2)
N(5)-N(6)-B(1)	121.0(5)	F(5')-C(18)-F(6)	137(3)
C(31)-N(6)-B(1)	128.2(4)	F(5)-C(18)-F(6)	107.7(6)
N(1)-C(1)-C(2)	112.2(5)	F(6')-C(18)-F(6)	66(2)
N(1)-C(1)-C(4)	119.4(5)	F(4')-C(18)-F(4)	60(2)
C(2)-C(1)-C(4)	128.4(5)	F(5')-C(18)-F(4)	55(2)
C(1)-C(2)-C(3)	104.5(5)	F(5)-C(18)-F(4)	106.3(6)
N(2)-C(3)-C(2)	107.5(5)	F(6')-C(18)-F(4)	142(3)
N(2)-C(3)-C(14)	122.1(5)	F(6)-C(18)-F(4)	103.3(6)
C(2)-C(3)-C(14)	130.3(5)	F(4')-C(18)-C(15)	120(2)
F(3)-C(4)-F(2)	106.6(6)	F(5')-C(18)-C(15)	110(3)
F(3)-C(4)-F(1)	106.8(6)	F(5)-C(18)-C(15)	112.9(6)
F(2)-C(4)-F(1)	104.1(5)	F(6')-C(18)-C(15)	104(2)
F(3)-C(4)-C(1)	112.7(5)	F(6)-C(18)-C(15)	112.8(5)
F(2)-C(4)-C(1)	113.3(5)	F(4)-C(18)-C(15)	113.2(5)
F(1)-C(4)-C(1)	112.7(5)	C(20)-C(19)-C(23)	108.0(6)
C(6)-C(5)-C(9)	109.5(9)	C(19)-C(20)-C(21)	108.0(7)
C(7)-C(6)-C(5)	110.5(8)	C(20)-C(21)-C(22)	108.5(6)
C(6)-C(7)-C(8)	107.6(8)	C(23)-C(22)-C(21)	107.1(7)
C(7)-C(8)-C(9)	105.9(7)	C(22)-C(23)-C(19)	108.4(6)

C(25)-C(24)-C(28)	107.7(6)	F(7)-C(32)-F(9)	105.3(6)
C(26)-C(25)-C(24)	108.8(6)	F(8)-C(32)-C(29)	113.8(6)
C(25)-C(26)-C(27)	108.8(6)	F(7)-C(32)-C(29)	112.2(6)
C(28)-C(27)-C(26)	107.0(6)	F(9)-C(32)-C(29)	113.3(6)
C(27)-C(28)-C(24)	107.7(5)	C(37)-C(33)-C(34)	110.7(9)
C(27)-C(28)-C(17)	123.3(5)	C(33)-C(34)-C(35)	105.6(9)
C(24)-C(28)-C(17)	129.0(5)	C(34)-C(35)-C(36)	108.5(10)
N(5)-C(29)-C(30)	112.2(5)	C(37)-C(36)-C(35)	107.5(9)
N(5)-C(29)-C(32)	119.1(6)	C(33)-C(37)-C(36)	107.6(9)
C(30)-C(29)-C(32)	128.7(6)	C(39)-C(38)-C(42)	107.8(6)
C(29)-C(30)-C(31)	105.1(6)	C(40)-C(39)-C(38)	108.0(6)
N(6)-C(31)-C(30)	107.2(5)	C(41)-C(40)-C(39)	108.6(6)
N(6)-C(31)-C(42)	123.3(5)	C(40)-C(41)-C(42)	108.2(6)
C(30)-C(31)-C(42)	129.4(6)	C(38)-C(42)-C(41)	107.4(5)
F(8)-C(32)-F(7)	106.9(6)	C(38)-C(42)-C(31)	124.0(5)
F(8)-C(32)-F(9)	104.5(7)	C(41)-C(42)-C(31)	128.6(5)

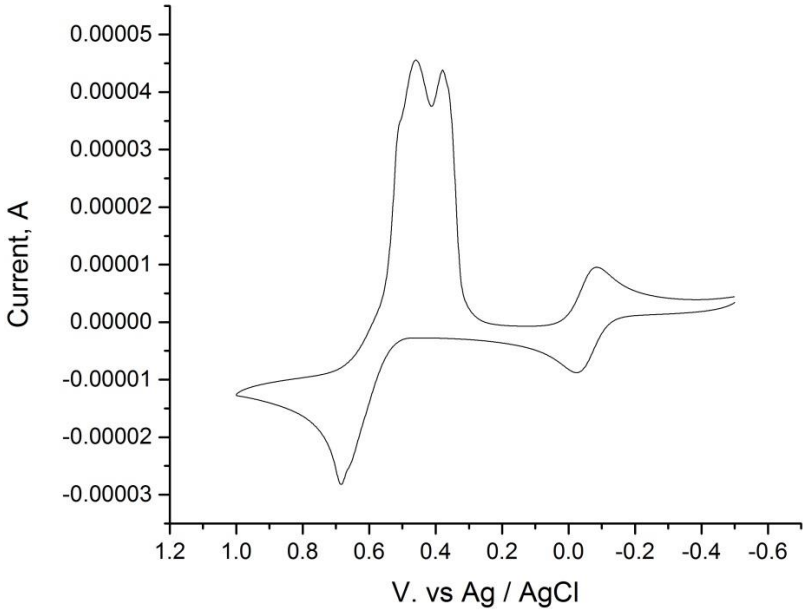

Figure 2.12: Cyclic voltammetric response of a 1.0 mM solution of $Tp^{CF3,Fc}Tl$ (4) recorded at a platinum electrode with a Ag/AgCl reference electrode in CH_2Cl_2 solutions containing 0.1 M $[NBu_4][PF_6]$ and Cp^*_2Fe using a scan rate of 100 mV/s.

2.2.4 Synthesis and Characterization of $PhTp^{Fc}Tl$.

The scope of this synthetic method can be extended further beyond that of the second generation tris(pyrazolyl)borates. Heating three equivalents of 3-ferrocenylpyrazole, with $Li(PhBH_3)$ and $MeB(O^iPr)_2$ (6 mol % vs. pyrazole) in toluene for three days, resulted in the precipitation of the corresponding phenyltris(3-ferrocenylpyrazolyl)borate ($PhTp^{Fc}$) ligand as the lithium salt. After work up with TlOAc, $PhTp^{Fc}Tl$ (**5**) can be isolated in 78% yield as an orange solid (Scheme 2.11). ^1H NMR in $CDCl_3$ revealed 7 well resolved resonances that can be assigned to the $PhTp^{Fc}$ ligand.

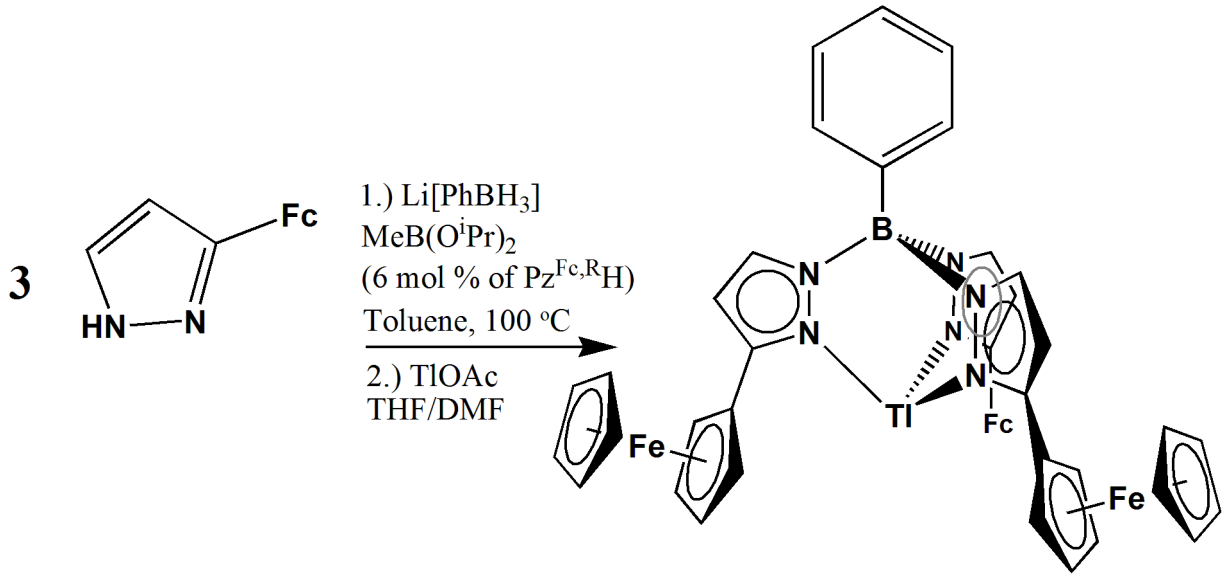

Scheme 2.11: Synthesis of the $PhTp^{Fc}Tl$ (5).

However, X-ray analysis (Figure 2.13) reveals a solid state structure with the Tl metal bonding to two N atoms of the ligand with a distances of 2.582(3) Å (Table 2.6) and a third interaction between the π system of the phenyl ring and the Tl metal center. The third pyrazolyl arm appears not to be bonding to the Tl. However, in solution, **5** apparently equilibrates between isomers which differ according to whether the uncoordinated pyrazolyl group is located

axially or equatorially relative to the six-membered, BN4Tl, ring and appear chemically equivalent in the ^{1}H NMR spectrum (Scheme 2.12). This type of coordination is not uncommon for phenyltris(pyrazolyl)borate ligands with bulky substituted pyrazoles.[18,19] It also displays the flexibility in coordination of bulky phenyltris(pyrazolyl)borate ligands compared to the more rigid second generation $Tp^{Fc,R}$ analoges.

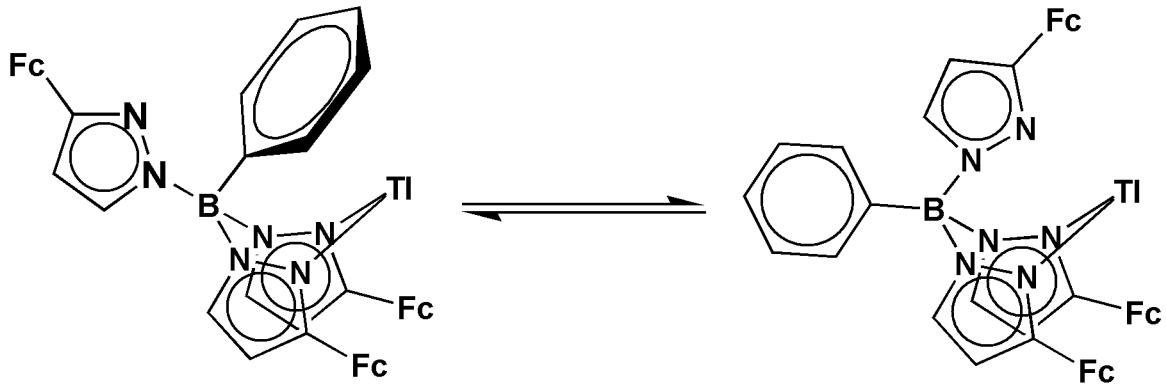

(equatorial) (axial)

Scheme 2.12: Exchange between axial and equatorial position in solution of 5.

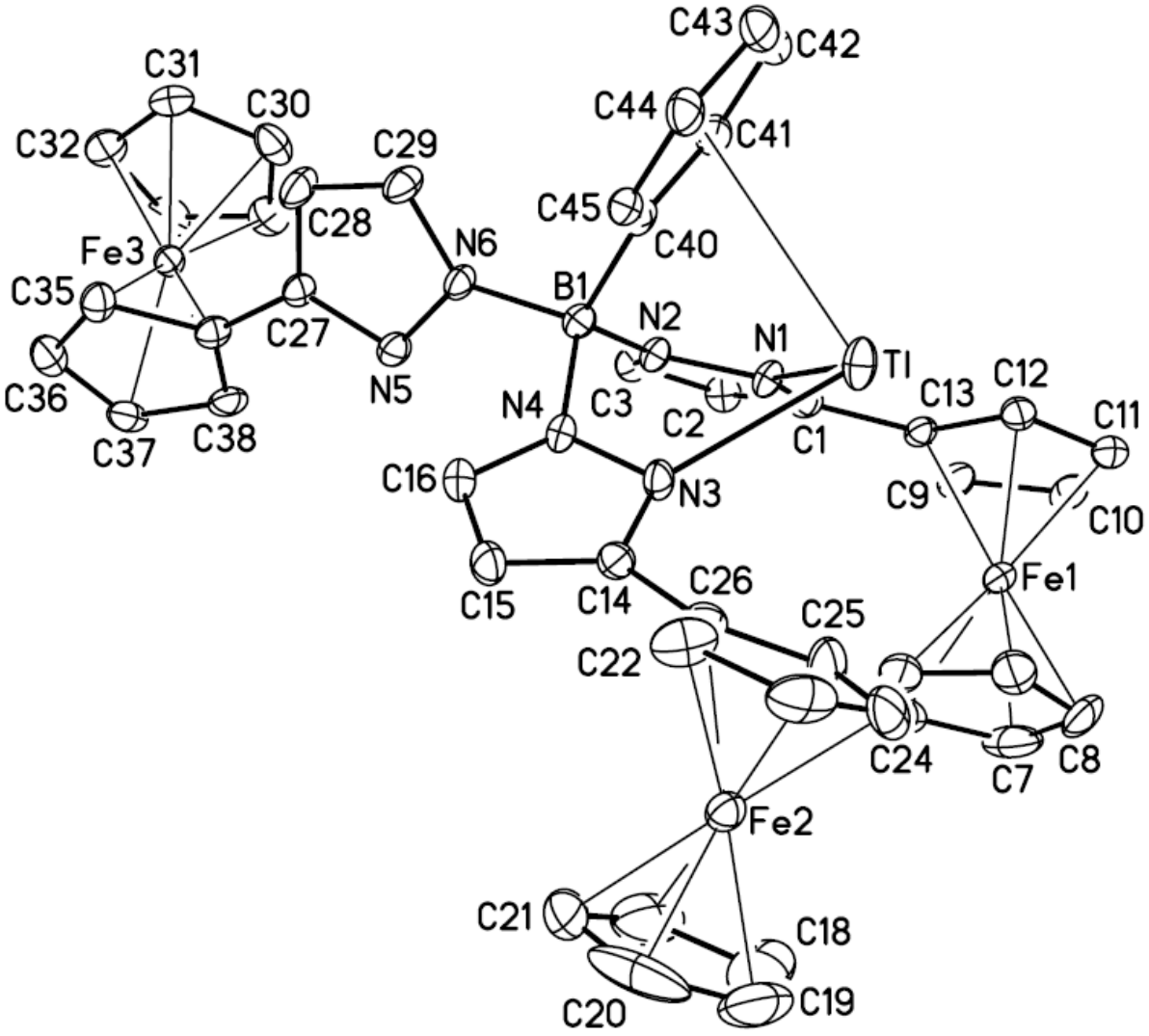

Figure 2.13: Molecular structure of PhTp^{Fc}Tl (5) at the 30% probability level. Hydrogen atoms have been removed for clarity.

Table 2.6: Selected interatomic distances (Å) and angles (°) for $PhTp^{Fc}Tl$ (5).

Distances (Å)

Tl-N(1)	2.570(3)	C(15)-C(16)	1.369(5)
Tl-N(3)	2.594(3)	C(17)-C(21)	1.357(10)
B(1)-N(6)	1.541(4)	C(17)-C(18)	1.358(8)
B(1)-N(2)	1.552(5)	C(18)-C(19)	1.315(9)
B(1)-N(4)	1.572(5)	C(19)-C(20)	1.360(9)
B(1)-C(45)	1.623(5)	C(20)-C(21)	1.462(10)
N(1)-C(1)	1.334(5)	C(22)-C(23)	1.417(6)
N(1)-N(2)	1.379(4)	C(22)-C(26)	1.410(6)
N(2)-C(3)	1.346(4)	C(23)-C(24)	1.397(8)
N(3)-C(14)	1.346(4)	C(24)-C(25)	1.430(6)
N(3)-N(4)	1.365(4)	C(25)-C(26)	1.414(6)
N(4)-C(16)	1.342(4)	C(27)-C(28)	1.394(5)
N(5)-C(27)	1.339(4)	C(27)-C(39)	1.469(5)
N(5)-N(6)	1.384(4)	C(28)-C(29)	1.367(5)
N(6)-C(29)	1.352(4)	C(30)-C(34)	1.390(6)
C(1)-C(2)	1.395(5)	C(30)-C(31)	1.417(6)
C(1)-C(13)	1.465(5)	C(31)-C(32)	1.414(6)
C(2)-C(3)	1.367(5)	C(32)-C(33)	1.399(6)
C(4)-C(5)	1.409(6)	C(33)-C(34)	1.412(6)
C(4)-C(8)	1.426(7)	C(35)-C(39)	1.430(5)
C(5)-C(6)	1.407(6)	C(35)-C(36)	1.427(5)
C(6)-C(7)	1.390(7)	C(36)-C(37)	1.402(6)
C(7)-C(8)	1.389(8)	C(37)-C(38)	1.432(5)
C(9)-C(13)	1.417(5)	C(38)-C(39)	1.425(5)
C(9)-C(10)	1.408(5)	C(40)-C(41)	1.399(5)
C(10)-C(11)	1.407(5)	C(40)-C(45)	1.398(5)
C(11)-C(12)	1.406(5)	C(41)-C(42)	1.373(6)
C(12)-C(13)	1.434(5)	C(42)-C(43)	1.382(6)
C(14)-C(15)	1.396(5)	C(43)-C(44)	1.382(6)
C(14)-C(26)	1.465(5)	C(44)-C(45)	1.402(5)

Angles (°)

N(1)-Tl-N(3)	73.10(9)	N(4)-B(1)-C(45)	108.1(3)
N(6)-B(1)-N(2)	110.9(3)	C(1)-N(1)-N(2)	106.2(3)
N(6)-B(1)-N(4)	107.9(3)	C(1)-N(1)-Tl	135.2(2)
N(2)-B(1)-N(4)	109.1(3)	N(2)-N(1)-Tl	118.5(2)
N(6)-B(1)-C(45)	110.5(3)	C(3)-N(2)-N(1)	109.1(3)
N(2)-B(1)-C(45)	110.3(3)	C(3)-N(2)-B(1)	131.9(3)

N(1)-N(2)-B(1)	118.9(3)	C(18)-C(19)-C(20)	112.2(6)
C(14)-N(3)-N(4)	106.5(3)	C(19)-C(20)-C(21)	104.6(6)
C(14)-N(3)-Tl	130.7(2)	C(17)-C(21)-C(20)	105.0(6)
N(4)-N(3)-Tl	118.5(2)	C(23)-C(22)-C(26)	108.4(5)
C(16)-N(4)-N(3)	109.6(3)	C(24)-C(23)-C(22)	108.0(4)
C(16)-N(4)-B(1)	130.1(3)	C(23)-C(24)-C(25)	108.3(4)
N(3)-N(4)-B(1)	118.4(3)	C(26)-C(25)-C(24)	107.4(5)
C(27)-N(5)-N(6)	104.8(3)	C(22)-C(26)-C(25)	107.9(4)
C(29)-N(6)-N(5)	110.2(3)	C(22)-C(26)-C(14)	124.0(4)
C(29)-N(6)-B(1)	126.6(3)	C(25)-C(26)-C(14)	127.9(4)
N(5)-N(6)-B(1)	123.0(3)	N(5)-C(27)-C(28)	111.5(3)
N(1)-C(1)-C(2)	110.6(3)	N(5)-C(27)-C(39)	121.3(3)
N(1)-C(1)-C(13)	122.2(3)	C(28)-C(27)-C(39)	127.2(3)
C(2)-C(1)-C(13)	127.2(3)	C(29)-C(28)-C(27)	105.2(3)
C(3)-C(2)-C(1)	105.0(3)	N(6)-C(29)-C(28)	108.4(3)
N(2)-C(3)-C(2)	109.0(3)	C(34)-C(30)-C(31)	108.2(4)
C(5)-C(4)-C(8)	105.9(5)	C(30)-C(31)-C(32)	107.6(4)
C(6)-C(5)-C(4)	108.8(4)	C(33)-C(32)-C(31)	107.7(4)
C(7)-C(6)-C(5)	108.0(5)	C(34)-C(33)-C(32)	108.4(4)
C(8)-C(7)-C(6)	108.4(5)	C(30)-C(34)-C(33)	108.1(4)
C(7)-C(8)-C(4)	108.9(4)	C(39)-C(35)-C(36)	107.7(4)
C(13)-C(9)-C(10)	108.8(3)	C(37)-C(36)-C(35)	108.7(3)
C(11)-C(10)-C(9)	108.3(4)	C(36)-C(37)-C(38)	108.0(4)
C(10)-C(11)-C(12)	108.0(3)	C(39)-C(38)-C(37)	108.0(4)
C(11)-C(12)-C(13)	108.5(3)	C(38)-C(39)-C(35)	107.5(3)
C(9)-C(13)-C(12)	106.4(3)	C(38)-C(39)-C(27)	127.1(3)
C(9)-C(13)-C(1)	125.4(3)	C(35)-C(39)-C(27)	125.3(3)
C(12)-C(13)-C(1)	128.1(3)	C(41)-C(40)-C(45)	121.8(4)
N(3)-C(14)-C(15)	109.7(3)	C(42)-C(41)-C(40)	119.6(4)
N(3)-C(14)-C(26)	119.2(3)	C(41)-C(42)-C(43)	119.8(4)
C(15)-C(14)-C(26)	130.8(3)	C(44)-C(43)-C(42)	120.6(4)
C(16)-C(15)-C(14)	105.3(3)	C(43)-C(44)-C(45)	121.4(4)
N(4)-C(16)-C(15)	108.8(3)	C(40)-C(45)-C(44)	116.7(3)
C(21)-C(17)-C(18)	110.7(6)	C(40)-C(45)-B(1)	121.1(3)
C(19)-C(18)-C(17)	107.4(7)	C(44)-C(45)-B(1)	122.2(3)

2.3 Conclusions

The synthesis and structural characterization of several second generation as well as a third generation ferrocenyl-substituted hydrotris(pyrazolyl)borate complexes has been achieved via a low-temperature Lewis-acid catalyzed synthetic pathway. The structures of the thallium(I) salts of the Tp^{Fc*} and $Tp^{Fc,Me*}$ ligands display a singly N-confused motif in which one of the pyrazole groups exhibited the Fc-substituent in the 5-position – adjacent to boron. In contrast, the thallium(I) salts of the $Tp^{Fc,iPr}$ and $Tp^{CF3,Fc}$ ligands do not feature N-confusion resulting from the low-temperature synthesis. All the thallium(I) salts of the second generation tris(pyrazolyl)borate display adopt a κ^3-coordination mode with the Tl bound in a trigonal pyramidal coordination geometry. In the third generation ligand, the bulky phenyl substituent prevents the N-confusion of the ligand, directing all the ferrocenyl groups to the 3-position of the pyrazole. In the solid state, the ligand binds κ^2 to the thallium through the N atoms of two pyrazolyl groups of the $PhTp^{Fc}$ ligand with an interaction between the Tl metal and the π system of the phenyl ring. However, the pyrazolyl rings appear to be magnetically equivalent in solution suggesting an exchange between the pyrazolyl arms that is fast on the ^1H NMR timescale. Cyclic voltammetry of $Tp^{Fc*}Tl$, $Tp^{Fc,Me*}Tl$, and $Tp^{Fc,iPr}Tl$ revealed single, reversible, three electron redox processes which suggests a lack of electronic communication between the ferrocenyl moieties when complexed in a hydrotris(pyrazolyl)borate ligand. Conversely, $Tp^{CF3,Fc}Tl$ displays an irreversible redox processes that is accompanied by decomposition during the oxidation wave of the CV.

2.4 Experimental

All reactions were run under a nitrogen atmosphere using standard glovebox and Schlenk techniques unless otherwise stated. Diethyl ether, pentane, tetrahydrofuran (THF), and toluene were distilled over Na or K-benzophenone ketyl under nitrogen atmosphere, or by passing the solvent through activated alumina columns followed by a nitrogen purge to remove dissolved oxygen[27]. Organic chemicals were bought from Aldrich or Acros and acetylferrocene was purchased from Strem. NMR spectra were obtained on Bruker AVIII-400 or AV 600 spectrometers and were referenced to the residual protons of the solvent (CD_2Cl_2, 5.32 ppm; $CDCl_3$, 7.27 ppm; C_6D_6, 7.15 ppm). ^{11}B NMR were referenced to $BF_3 \bullet Et_2O$ (0.0 ppm). ^{19}F NMR were referenced to $CFCl_3$ (0.00 ppm). FT-IR spectra were recorded on Matteson Alpha Centauri or Nicolet Magna-IR 560 spectrometers with a resolution of 4 cm^{-1}. Mass spectra were obtained by the University of Delaware Mass Spectrometry. X-ray crystallographic studies were conducted in the University of Delaware X-ray crystallographic facility. Elemental analyses were obtained from Robertson Microlit, Ledgewood, NJ 07852 or Intertek Pharmaceutical Services, Whitehouse, NJ 08888. 3-ferrocenylpyrazole,[13] 3-ferrocenyl-5-methylpyrazole,[29] 3-ferrocenyl-5-trifluoromethylpyrazole,[30] and $Li[PhBH_3] \bullet 2THF$[31] were prepared by literature procedures.

2.4.1 General Considerations

General considerations for X-ray diffraction studies: Unless specified otherwise, single crystal X-ray diffraction studies were performed under the following conditions. Crystals were selected, sectioned as required, and mounted on glass fibers or MiTeGen™ plastic mesh with viscous oil and flash-cooled to the data collection temperature. Diffraction data were collected on a Brüker-AXS CCD diffractometer with graphite-monochromated Mo-Kα radiation (λ=0.71073

Å). The data-sets were treated with absorption corrections based on redundant multiscan data[32]. The structures were solved using direct methods and refined with full-matrix, least-squares procedures on F^2. Unit cell parameters were determined by sampling three different sections of the Ewald sphere. Nonhydrogen atoms were refined with anisotropic displacement parameters. Hydrogen atoms were treated as idealized contributions with geometrically calculated positions and with U_{iso} equal to 1.2, or 1.5 for methyl, U_{eq} of the attached atom. Structure factors and anomalous dispersion coefficients are contained in the SHELXTL program library[33].

Single crystal X-ray diffraction studies. No symmetry higher than triclinic was observed for **kla0244** (**2**) and **kla0226** (**4**). The systematic absences in the diffraction data, unit cell parameters and equivalent reflections are consistent with *R*3 and *R*-3 for **klat967** (**3**), uniquely, for $P2_1/c$ for **kla0004** (**1**) and **kla0030** (**5**). For the triclinic and trigonal cases, solution in the centrosymmetric space group option yielded chemically reasonable and computationally stable results of refinement. The dimeric structure of **klat967** (**3**) is centered at six-fold rotoinversion. A dimethyl sulfoxide solvent molecule was located in the asymmetric unit of **kla0244** (**2**). A trifluoro methyl group in **kla0226** (**4**) was located disordered in two positions with 54/46 refined site occupancies, treated with geometrical restraints, and constrained to have equal atomic displacement between chemically equivalent disordered contributions. Slight yet significant disorder in cyclopentadienide ligands that could not be resolved was observed, one Cp each, in **kla0004** (**1**) and **kla0030** (**5**). The disordered groups were treated with rigid-bond *U* restraints. All non-hydrogen atoms were refined with anisotropic displacement parameters. Borohydride H-atoms on **kla0004** (**1**) and **klat967** (**3**) were located from the difference map and constrained to U_{iso} equal to 1.2 B-atom U_{eq}.

2.4.2 3-ferrocenyl-5-isopropylpyrazole, $pz^{Fc,iPr}H$.

In a glovebox, 15 g (0.066 mol) of acetylferrocene was dissolved in 100 mL of THF in a round bottom flask equipped with a magnetic stir bar. 2.63 g (0.066 mol) of KH was added in small increments and the mixture was allowed to stir for four hours. The resulting orange precipitate was collected on a frit and washed with THF until the washings were no longer colored. The orange solid was dried under vacuum yielding 16.6 g (95 %) of the K salt of the ferrocenylenolate. Under a constant purge of N_2, a round bottom equipped with a stir bar was charged with 16.6 g (0.062 mol) of the K salt of the ferrocenylenolate and 50 mL of ethyl isobutyrate was heated at 40°C for 12 hours. The resulting solid was filtered quickly in air on a frit and washed with pentanes before being dissolved in methanol. 4.27 g (0.062 mol) of hydrazine monohydrochloride was added and the solution was refluxed for 6 hours. The solution was added to 100 mL of water and the mixture was extracted with methylene chloride. The methylene chloride fraction was stripped and the resulting residue was dissolved in methanol. 1.55 mL (0.031 mol) of hydrazine monohydrate was added and the solution was refluxed for 1 hour. The solution was poured into ice water and allowed to stir for 1 hour. The solid was collected on a frit and washed with copious amounts of water. The solid was dried under vacuum overnight yielding 11.1 (61 %) of the product. ^{1}H NMR (400 MHz, $CDCl_3$): 6.08 (s, 1 H), 4.57 (s, 2 H), 4.24 (s, 2 H), 4.06 (s, 5 H), 2.98 (m, 1 H), 1.3 (d, J = 6.59 Hz, 6 H) ppm. IR (KBR): 3093 (w), 2967 (s), 2927 (w), 1595 (s), 1577 (s), 1488 (s), 1362(s), 1129 (s), 1105 (s), 1061 (s), 1026 (s), 813 (w), 525 (s), 503 (s), 488 (s), 454 (s) cm^{-1}. Mp: 160 – 162 °C. Mass Spectrum (ESI) m/z, (%): 294, (100, M^+). Anal Calcd for $C_{16}H_{18}N_2Fe$: C, 65.33; H, 6.17; N, 9.52. Found: C, 65.09; H, 6.25; N, 9.47.

2.4.3 Dihydrobis(3-ferrocenylpyrazolyl)borato-thallium(I), $Bp^{Fc}Tl$.

7.0 g (0.028 mol) of 3-ferrocenylpyrazole, 0.2 (9.0 mmol) g of $LiBH_4$, 25 mL of THF and 0.3 mL (1.7 mmol) of di(isopropoxy)methylborane were combined inside a thick walled glass vessel under N_2 atmosphere. The solution was allowed to heat at 60°C for 3 days. The solution was then transferred to a round bottom flask and 2.5 g (9.5 mmol) of thallium acetate was added and allowed to stir over night. The solution was filtered through celite and the solvent was removed. The residue was triturated with methanol until an orange solid formed. The solid was collected on a frit and washed with water to remove excess thallium salts. The material was then washed with several more portions of hot methanol until the washings were colorless, removing excess pyrazole. The resulting product was allowed to dry at 100°C for 3 hours under vacuum yielding 3.34 g (51%) of $Bp^{Fc}Tl$. ^1H NMR and ^{11}B NMR consistent with previously reported $Bp^{Fc}Tl$.[13] X-ray quality crystals were grown from slow diffusion of pentane into a saturated solution of $Bp^{Fc}Tl$ in THF. ^1H NMR(400 MHz, CD_2Cl_2): 7.44 (s 2 H), 6.25 (s, 2 H), 4.53 (s, 2 H), 4.26 (s, 2 H), 4.05 (s, 10 H) ppm. ^{11}B NMR: -8.8 ppm.

2.4.4 Hydrobis(3-ferrocenylpyrazolyl)(5-ferrocenylpyrazolyl)borato-thallium(I), $Tp^{Fc*}Tl$ (1).

7.05 g (0.028 mol) of 3-ferrocenylpyrazole, 0.20 (9.0 mmol) g of $LiBH_4$, 25 mL of toluene and 0.3 mL(1.7 mmol) of di(isopropoxy)methylborane were combined inside a thick walled glass ampule under inert atmosphere. The solution was allowed to heat at 110°C for 3 days during which a precipitate formed. The solution was transferred to a round bottom flask and the solvent stripped. The residue was dissolved in a minimum amount of THF. An aqueous solution of 2.50 g (9.5 mmol) of thallium acetate was added and allowed to stir over night. During the course of the reaction, an orange precipitate formed. The solid was collected on a frit,

washed with several portions of water to remove the lithium acetate and washed with hot methanol to remove excess pyrazole. The resulting product was allowed to dry at 100°C for 3 hours under vacuum yielding 4.51 g (51 %) of product. ^{1}H NMR (400 MHz, $CDCl_3$): 7.58 (s, 2 H), 7.45 (s, 1 H), 6.38 (s 1 H), 6.24 (s, 2 H), 4.58 (s, 4 H), 4.55 (s, 2 H), 4.30 (s, 2 H), 4.24 (s, 4 H), 4.09 (s, 5 H), 4.05 (s, 10 H) ppm. ^{11}B NMR: -3.23 ppm. IR (KBR): 3086 (w), 2483 (w, B-H), 1547 (s), 1489 (s), 1424 (m), 1240 (s), 1189 (w), 938 (s), 870 (s), 818 (w), 763 (m), 718 (m), 647 (s), 623 (s), 505 (w), 443 (s) cm^{-1}. Mp: 192 – 194 °C. Mass Spectrum (LIFDI) m/z, (%): 970.074, (100, M^+). Elemental analysis for isomer ($Tp^{Fc}Tl$) found on page 133.

2.4.5 Hydrobis(3-ferrocenyl-5-methylpyrazolyl)(3-methyl-5-ferrocenylpyrazolyl)borato-thallium(I), $Tp^{Fc,Me*}Tl$ (2).

7.50 g (0.028 mol) of 3-ferrocenyl-5-methylpyrazole, 0.20 g (9.0 mmol) of $LiBH_4$, 25 mL of toluene and 0.3 mL (1.7 mmol) of di(isopropoxy)methylborane were combined inside a thick walled glass ampule under inert atmosphere. The solution was allowed to heat at 110°C for 3 days during which a precipitate formed. The orange solid was collected on a frit and washed with several portions of hot toluene followed by pentane and dried. The solid was then added to a round bottom flask containing 2.50 g (9.5 mmol) of thallium acetate and 150 mL of THF and allowed to stir over night. The solution was filtered through a bed of Celite and the solvent removed under vacuum. 150 mL of methanol was added to the orange tar and allowed to stir until an orange solid formed. The solid was collected on a frit, washed with several portions of methanol and dried at 100°C for 3 hours under vacuum yielding 6.76 g (73 %) of product. ^{1}H NMR (400 MHz, CD_2Cl_2): 6.32 (s 1 H), 6.14 (s, 2 H), 4.58 (s, 4 H), 4.51 (s, 2 H), 4.34 (s, 2 H), 4.29 (s, 4 H), 4.17 (s, 5 H), 4.12 (s, 10 H), 2.39 (s, 3 H) 2.27 (s, 6 H) ppm. ^{11}B NMR: -7.31 ppm. IR (KBR): 3086 (w), 2918 (s), 2546 (w, B-H), 1646 (m), 1553 (s) 1424 (w), 1401 (s), 1362 (s),

1314 (s), 1225 (s), 1181 (w), 1027 (s), 1000 (s), 911 (s), 882 (s), 818 (s), 740 (s), 673 (s), 648 (s) 505 (s), 437 (m) cm^{-1}. Mp: 248 – 252 °C (blackening with melting). Mass Spectrum (LIFDI) m/z, (%): 1012.121, (100, M^+). Elemental analysis for isomer ($Tp^{Fc,Me}Tl$) found on page 134.

2.4.6 Hydrotris(3-ferrocenyl-5-iso-propylpyrazolyl)borato-thallium(I), $Tp^{Fc,iPr}Tl$ (3).

10.0 g (0.034 mol) of 3-ferrocenyl-5-*iso*-propylpyrazole, 0.26 g (0.011 mol) of $LiBH_4$ and 0.38 mL(2.0 mmol) of $MeB(OiPr)_2$ were combined in a thick walled pressure vessel along with 60 mL of toluene. The reaction was allowed to stir overnight at room temperature and then heated at 100°C for 3 days. The vessel was carefully vented and the toluene removed under vacuum and gentle heating. The residue was dissolved in a minimum amount of THF and transferred to a 250 mL round bottom. To this solution, 3.0 g (0.011 mol) of TlOAc was added and the mixture was allowed to stir overnight. The solution was filtered through a bed of Celite and the solvent removed under vacuum. The resulting residue was triturated with methanol until a precipitate formed. The orange solid was collected on a frit, washed with several portions of hot methanol until the washing were colorless, and dried under vacuum yielding 7.7 g (64 %) of product. ^1H NMR (400 MHz, C_6D_6): 6.29 (s, 3 H), 4.58 (s, 6 H), 4.01 (s, 6 H), 3.98 (s, 15 H), 3.64 (m, 3 H), 1.24 (d, J =5.05 Hz, 18 H) ppm. ^{11}B NMR: -7.57 ppm. IR (KBr): 3435 (w), 3092 (s), 2962 (s), 2927 (s), 2868 (s), 2504 (w, B-H), 1652 (m), 1555 (s), 1460 (m), 1398 (s), 1294 (s), 1175 (s), 1105 (s), 1047 (m), 1000 (s), 975 (s), 817 (w), 785 (s), 503 (w) cm^{-1}. Mp: 178 – 180 °C. Anal Calcd for $C_{48}H_{52}N_6BFe_3Tl$: C, 52.62; H, 4.78; N, 7.67. Found: C, 52.15; H, 4.62; N, 7.59.

2.4.7 Hydrotris(3-trifluoromethyl-5-ferrocenylpyrazolyl)borato-thallium(I), $Tp^{CF3,Fc}Tl$ (4).

8.00 g (0.025 mol) of 3-ferrocenyl-5-trifluoromethylpyrazole, 0.18 g (0.008 mol) of lithium borohydride, and 0.28 mL (1.5 mmol) of $MeB(OiPr)_2$ were combined in a thick walled pressure vessel along with 15 mL of toluene. The reaction was allowed to heat at 100 °C for 3 days. The resulting mixture was stripped of toluene and dissolved in a minimum amount of THF and 2.20 g (8.0 mmol) of TlOAc was added and the solution was allowed to stir over night. The solution was filtered through Celite and the THF stripped. The resulting residue was triturated with methanol and the solid collected on a frit, washed with hot methanol until the washing were colorless, and dried under vacuum yielding 4.96 g (53 %) of product. ^{1}H NMR (600 MHz, CD_2Cl_2): 6.64 (s, 3H), 4.02 (s, 12 H), 3.88 (s, 15 H) ppm. ^{19}F NMR: 59.17 (d, $J_{F\text{-}Tl}$ = 820.65 Hz, 9 F) ppm. ^{11}B NMR: -6.39 ppm. IR (KBr): 3123 (s), 3093 (w), 2630 (w, B-H), 1646 (m), 1561 (s), 1508 (s), 1462 (s), 1369 (s), 1261 (s), 1123 (m), 1067 (w), 983 (s), 885 (s), 812 (m), 755 (s), 505 (s) cm^{-1}. Mp: 268 – 270 °C. Anal Calcd for $C_{42}H_{31}N_6BF_9Fe_3Tl$: C, 42.99; H, 2.66; N, 7.16. Found: C, 42.81; H, 2.55; N, 7.06.

2.4.8 Phenyltris(3-ferrocenylpyrazolyl)borato-Thallium(I), $PhTp^{Fc}Tl$ (5).

In a thick walled pressure vessel equipped with a magnetic stir bar, a mixture of 2.1 g (8.67 mmol) $Li[PhBH_3]$•2THF, 6.8 g (0.026 mol) 3-ferrocenylpyrazole , and 0.28 mL (1.6 mmol) $MeB(OiPr)_2$ in toluene (30 mL) was stirred at 100°C for 3 days. The orange precipitate was filtered, washed with hot toluene (3 x 15 mL), and dried *in vacuo*. A mixture of the crude $PhTp^{Fc}Li$ and 1.1 g (4.0 mmol) TlOAc in 50/50 mix of THF/DMF (100 mL) was stirred at room temperature for 1 day. The solution was filtered through Celite and the solvent removed from the filtrate under vacuum. The resulting residue was triturated with methanol and the solid collected

on a frit, washed with several portions of methanol until the washings were colorless and dried under vacuum yielding 7.06g (78 %) of the product. ^{1}H NMR (400 MHz, $CDCl_3$): 7.47 (s, 3 H), 7.40 (s, 3H), 7.16 (m, 2 H), 6.40 (s, 3 H), 4.66 (s, 6 H), 4.32 (s, 6 H), 4.13 (s, 15 H) ppm. ^{11}B NMR: 1.11 ppm. IR (KBr): 3090 (s), 2923 (s), 2852 (w), 1652 (w), 1551 (s), 1489 (s), 1314 (w), 1193 (s), 1175 (s), 1001, (s), 964 (w), 870 (s), 817 (s), 706 (w), 506 (s), 486 (s) cm^{-1}. Mp: 217 – 219 °C. Anal Calcd for $C_{45}H_{38}N_6BFe_3Tl$: C, 51.69; H, 3.66; N, 8.04. Found: C, 51.00; H, 3.27; N, 7.79.

2.5 References

1. Trofimenko, S. Scorpionates, 1999, London: Imperial College Press.
2. Pettinari, C. *Scorpionates II: Chelating Borate Ligands*, **2008**, London: Imperial College Press.
3. Trofimenko, S. *Chem. Rev.*, **1993**, *93*, 943.
4. a) Trofimenko, S. *J. Am. Chem. Soc.,* **1966**, *88*, 1842.; b) Trofimenko, S., *J. Am. Chem. Soc.*, **1967**, 6288.
5. Calabrese, J. C., Trofimenko, S.; Thompson, J. S., *J. Chem. Soc., Chem. Commun*., **1986**, 1122.
6. Reger, D. L., Gardinier, J. R.; Gemmill, W. R., Smith, M. D.; Shahin, A. M.; Long, G. J.; Rebbouh, L., Grandjean, F., *J. Am. Chem. Soc.*, **2005**, *127*, 2303.
7. Reinaud, O. M., Rheingold, A. L., and Theopold, K. H., *Inorg. Chem*., **1994**, *33*, 2306.
8. Egan, J. W. Jr, Haggerty, B. S., Rheingold, A. L., Sendlinger, S. C. & Theopold, K. H. *J. Am. Chem. Soc.,* **1990**. *112*, 2445.
9. a) Lyaskovskyy, V., de Bruin, B. *ACS Catalysis*, **2012**, 2, 270.; b) Luca, O. R., Crabtree, R. H. *Chem. Soc. Rev*., **2013**, *42*, 1440.
10. a) F. Jäkle, K. Polborn, M. Wagner. Chem. Ber., **1996**, *129*, 603.; b) F. Fabrizi de Biani, F. Ja¨kle, M. Spiegler, M. Wagner, P. Zanello, *Inorg. Chem.*, **1997**, *36* 2103.; c) E. Herdtweck, F. Peters, W. Scherer, M. Wagner, *Polyhedron*, **1998**, *17*, 1149.; d) S.L. Guo, F. Peters, F. Fabrizi de Biani, J.W. Bats, E. Herdtweck, P. Zanello, M. Wagner, *Inorg. Chem*. **2001**, *40*, 4928.

11. a) Ilkhechi, A. H., Bolte, M., Lerner, H. W., Wagner, M., *J. Organomet. Chem*., **2005**, *690*, 1971-1977.; b) Kaufmann, L., Illkhechi, A. H., Vitze, H., Bolte, M., Lerner, H. and Wagner, M., *J. Organomet. Chem*., **2009**, *694*, 466.

12. Niedenzu, K., Serwatowski, J., Trofimenko, S., *Inorg. Chem*., **1991**, *30*, 524.

13. Ruf, W., Fueller, M., and Siebert, W., *J. Organomet. Chem.*, **1974**, *64*, C45.

14. Hayashi, T., Okada, T., and Shimizu, S., *Transition Met. Chem.*, **1996**, *21*, 418.

15. Baird, B., Pawlikowski, A. V., Su, J. Wiench, J. W., Pruski, M., and Sadow, A. D., *Inorg. Chem*., **2008**, *47*, 10208.

16. S. Trofimenko, *J. Am. Chem. Soc.*, **1967**, *89*, 6288.

17. a) D. L. White and J. W. Faller, *J. Am. Chem. Soc.*., **1982**, 104, 1548.; b) D. L. Reger and M. E. Tarquini, *Inorg. Chem*., **1982**, *21*, 84.

18. Janiak, C., Braun, L., Girgsdies, F., *J. Chem. Soc*., *Dalton Trans.,* **1999**, 3133.

19. a) Kisko, J. L., Hascall, and Parkin, G.*, J. Am. Chem. Soc.*, **1998**, *120*, 10561.; b) Kisko, J. L., Hascall, T., Kimblin, C., and Parkin, G.*, J. Chem. Soc., Dalton Trans.*, **1999**, 1929.

20. Chen, C., Jordan, R., *Organometallics*, **2010**, *29*, 3679.

21. a) Johnson, C. R., Henderson, W. W., Shepherd, R. E., *Inorg. Chem*. **1984**, *23*, 2754.; b) Evans, C. A., Rabenstein, D. L., Geier, G.; Erni, I.W., *J. Am. Chem. Soc.,* **1977**, *99*, 8106.; c) Johnson, C. R., Shepherd, R. E., Marr, B., Donnell, S. O., Dressick,W., *J. Am. Chem. Soc*., **1980**, *102*, 6227.; d) Hoq, M. F., Shepherd, R. E., *Inorg. Chem*., **1984**, *23*, 1851.; e) Evans, E., *J. Chem. Educ*., **2004**, *81*, 1191.

22. Connelly, N. G. and Geiger, W. E., *Chem. Rev.*, **1996**, *96*, 877.

23. Bard, A. J.; Faulkner, L. R. *Electrochemical Methods Fundamentals and Applications 2nd edition*, **2001**, Hoboken, NJ: John Wiley & Sons.

24. King, W. A., Yap, G. P. A., Incarvito, C. D., Rheingold, A. L., Theopold, K. H., *Inorg. Chim. Acta*, **2009**, *362*, 4493.

25. Rheingold, A. L., Liable-Samds, L. M., and Trofimenko, S., *Chem. Commun*., **1997**, 1691.

26. Han, R., Ghosh, P., Desrosiers, P. J., Trofimenko, S., and Parkin, G.*, J. Chem. Soc., Dalton Trans.*, **1997**, 3713.

27. Dias, H. V. R., Goh, T. K. H. H., *Polyhedron*, **2004**, *23*, 273.

28. Pangborn, A. B., Giardello, M. A. Grubbs, R. H. Rosen, R. K.; Timmers, F. J., *Organometallic*, **1996**, *15*, 1518.

29. Chabert, N., Jacquet, L., Marzin, C., and Tarrago, G., *New J. Chem*., **1995**, *19*, 443.

30. Zhang, Q., Song, W., Hossain, A. M. S., Liu, Z., Hu, G., Tian, Y., Wu, J., Jin, B., Zhou, H., Yang, J. and Zhang, S., *Dalton. Trans.*, **2011**, *40*, 3510.

31. Tsoureas, N., Bevis, T., Butts, C. P., Hamilton, A., and Owen, G. R., *Organometallics*, **2009**, 28, 5222.

32. Apex2, Bruker-AXS Inc, Madison, WI, **2007**.

33. Sheldrick, G.M., *Acta Cryst*., **2008**, A64, 112.

Chapter 3

BOROTROPIC REARRANGEMENTS IN $Tp^{Fc,R}$ LIGANDS

3.1 Introduction

The regiochemistry of the B-N bond formation can become a critical issue in the synthesis of hydrotris(pyrazolyl)borate ligands, especially when employing pyrazoles substituted with sterically demanding functional groups.[1,2] Typically, the high temperatures employed during synthesis leads to the symmetric ligand in which the larger substituents end up in the 3-position of the pyrazolyl ring, relatively distant from the B-N bond (Scheme 3.1). Typically, the regioselectivity during B-N bond formation is most prominent when the steric differences between 3-position substituent and the 5-position substituent are large as in the case of hydrotris(3-phenylpyrazolyl)borate (Tp^{Ph}) and hydrotris(3-*tert*-butylpyrazolyl)borate ($Tp^{t\text{-}Bu}$) ligands.[3,4]

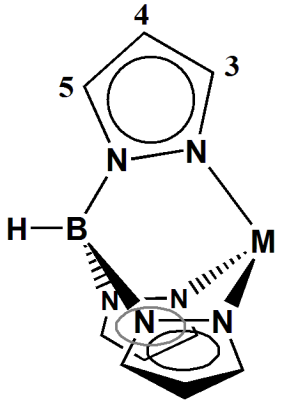

Scheme 3.1: Substitution position numbering on the pyrazolyl ring of a hydrotris(pyrazolyl)borate ligand.

In cases where the steric differences between the 3 and 5-position are not so stark, a mixture of regioisomers can be formed. For example, reaction of 3-*iso*-propyl-5-methylpyrazole with KBH_4 results in the formation of hydrotris(3-*iso*-propyl-5-methylpyrazolyl)borate ($Tp^{i\text{-}Pr,Me}$) and its regioisomer hydrobis(3-isopropyl-5-methylpyrazolyl)(3-methyl-5-*iso*-propylpyrazolyl)borate ($Tp^{iPr,Me*}$) in an approximate ratio of 4:1[5] when in its Tl salt. When complexed with cobalt(II) iodide, the ^1H NMR indicated the appearance of three regioisomers in a ratio of 3:3:1.[6] However, in the synthesis of the more sterically demanding hydrotris(3-*tert*-butyl-5-methylpyrazolyl)borate ($Tp^{t\text{-}Bu,Me}$) analog where the steric differences between the tert-butyl group and methyl group is more substantial, only one isomer is observed.[7]

The influence of steric effects during the course of ligand synthesis is especially evident in the preparation of the hydrotris(3-mesitylpyrazolyl)borate (Tp^{Ms}) ligand.[8] In a typical reaction with pyrazoles which are only substituted in the 3-position, high-boiling solvents are employed to control stoichiometry and prevent the formation of tetrakis(pyrazolyl)borate species. Since the reaction temperature is not high enough to drive the reaction to the more thermodynamically favored symmetric ligand completely, the asymmetric hydrobis(3-mesitylpyrazolyl)(5-mesitylpyrazolyl)borate (Tp^{Ms*}) ligand is the major product. However, the asymmetric product can be converted to the symmetric ligand through thermal isomerization. A similar situation occurs in the synthesis of hydrotris(3-neopentylpyrazolyl)borate (Tp^{Np})[9] and hydrotris(3-(9-anthryl)pyrazolyl)borate (Tp^{Ant})[10] ligands. However, the N-confused asymmetric ligands are observed as minor impurities.

Sometimes an isomerically pure, non N-confused Tp^R undergoes borotropic rearrangement to Tp^{R*} (* denotes a regioisomer in which one R group occupies the 5-position on the pyrazolyl ring relative to the boron) ligands during the course of complex formation. Such is

the case for hydrotris(3-*iso*-propylpyrazolyl)borate (Tp^{iPr})and hydrotris(3-*iso*-propyl-4-bromopyrazolyl)borate ($Tp^{iPr,4Br}$) ligands. Although the *iso*-propyl group is large enough to prevent the formation of bis-ligand complexes (i.e. Tp_2M), octahedral cobalt(II) complexes will form if a borotropic rearrangements occurs in the ligands to yield Tp^{iPr*} and $Tp^{iPr,4Br}$*, respectively.[11] Typically, these rearrangements are induced thermally and are a result of relieving steric interactions to allow for the more preferred octahedral geometry in Co(II) complexes. Borotropic rearrangements have also been cited for other Tp complexes of other transition metals such as Ti[12], Fe[9], Ni[9] and Mo[13] where the rearrangements occur to form octahedral metal complexes. Most commonly, rearrangements in first-row transition metal complexes take place at elevated temperatures, e.g., when the complexes are heated to their melting points to yield the isomerized products. A less common rearrangement involves complexes maintaining a tetrahedral or square planar coordination geometry, most occurring in late or second and third row transition metals.[14] Herein are reported several examples of borotropic rearrangement in $Tp^{Fc,R}$ (R: H, Me, *i*-Pr) complexes. These rearrangements occur within the Tl salts of the ligands as well as the Co and Cu complexes.

3.2 Results and Discussion

3.2.1 Borotropic Rearrangement of $Tp^{Fc*}Tl$ (1) to $Tp^{Fc}Tl$.

Most syntheses in which regioisomerization of the tris(pyrazolyl)borate is observed heavily favor the symmetric isomer over the asymmetric ones; in such cases, trace amounts of the asymmetric ligand can be removed with minimal effort. However, in the case of the

sterically demanding hydrotris(3-mesitylpyrazolyl)borate, the N-confused ligand is the major species.[8] Since solvent must be employed to control stoichiometry and prevent the formation of tetrakis(pyrazolyl)borate complexes[1], the resulting mixture of regioisomers heavily favors the N-confused kinetic product. The mixture of non N-confused and N-confused Tp^{Ms} ligands can be separated via fractional crystallization. It has also been shown that it is possible to convert the kinetically favored regioisomer (Tp^{Ms*}) to the thermodynamically favored symmetric isomer (Tp^{Ms}), via thermal isomerization. Solid samples of isomerically pure N-confused Tl salt of the ligand were heated above its melting point and the heating maintained at 260 °C for an hour. After cooling, the resulting sample contained only the thermodynamically favored symmetric ligand as shown through the shift of the B-H stretching frequency.[8]

Since the products of the low-temperature reactions for 3-ferrocenylpyrazole and 3-ferrocenyl-5-methylpyrazole favor the N-confused motif and could be isolated cleanly, these ligands seemed suitable candidates for thermal isomerization to their symmetric isomers (Scheme 3.2). Accordingly, a solid sample of $Tp^{Fc*}Tl$ (**1**) was heated to 220ºC under vacuum and kept at that temperature for one hour. After cooling to room temperature, the sample had been completely converted to the symmetric ligand $Tp^{Fc}Tl$ (**7**) as indicated by ^{1}H-NMR spectroscopy (Figure 3.1).

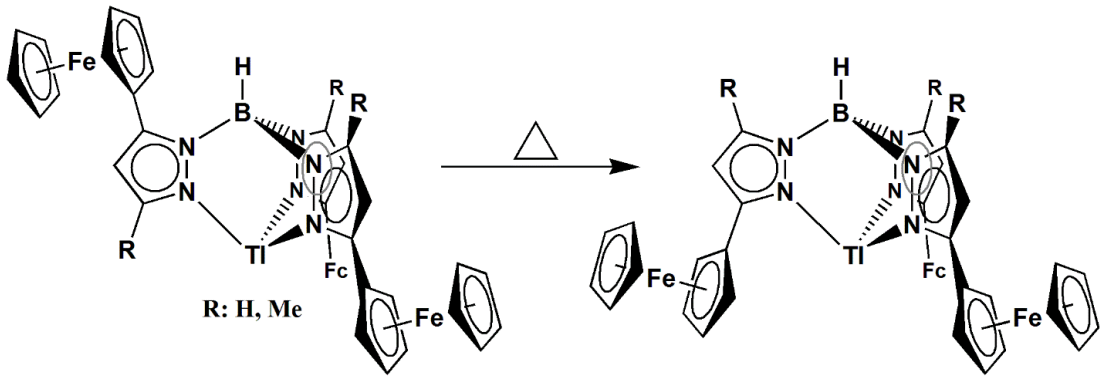

Scheme 3.2: Thermal isomerization of $Tp^{Fc*}Tl$ (1)/$Tp^{Fc,Me}$*Tl (2) to $Tp^{Fc}Tl$ (7)/$Tp^{Fc,Me}Tl$ (8).

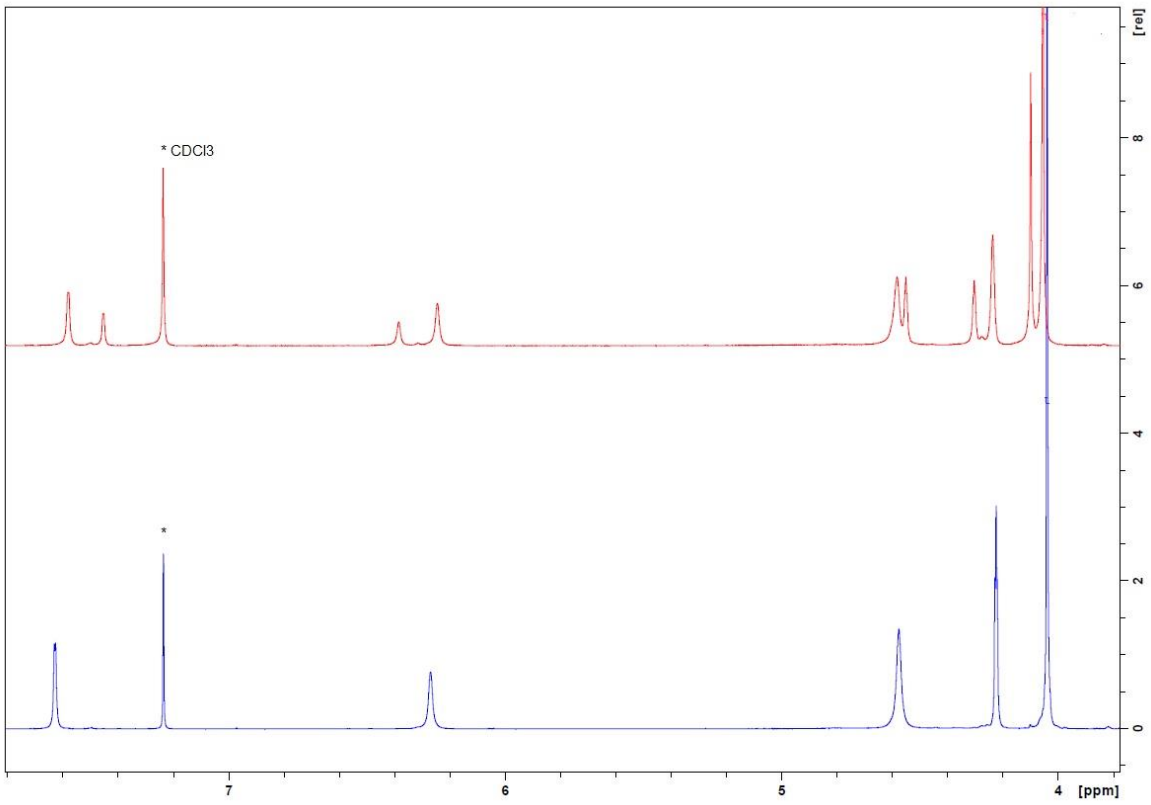

Figure 3.1: NMR spectral comparison of $Tp^{Fc*}Tl$ (top) and $Tp^{Fc}Tl$ (bottom).

In addition to ^{1}H NMR, a shift in the ^{11}B NMR resonance from -3.23 ppm in the N-confused ligand to -1.23 in the symmetric ligand was observed. Moreover, IR spectroscopy revealed a shift in the B-H stretching frequency from 2483 cm^{-1} in $Tp^{Fc*}Tl$ to 2420 cm^{-1} in $Tp^{Fc}Tl$. The X-ray crystal structure of **7** confirms the symmetric configuration suggested by the ^{1}H-NMR spectrum. **7** crystallized in the triclinic space group P-1. The molecular structure of $Tp^{Fc}Tl$ (Figure 3.2) has the ligand binding κ^3 to the Tl metal center in a trigonal pyramidal geometry. The average Tl-N distance (Table 3.1) of complex **7** are 2.569(4)Å. Cyclic voltammetry (CV) of **7** was shown to be identical to that of **1** at a potential of 0.62 V relative to Cp^*_2Fe. Apparently, the position of the ferrocene on the pyrazole does not affect the potential at which the ferrocenyl moiety is oxidized.

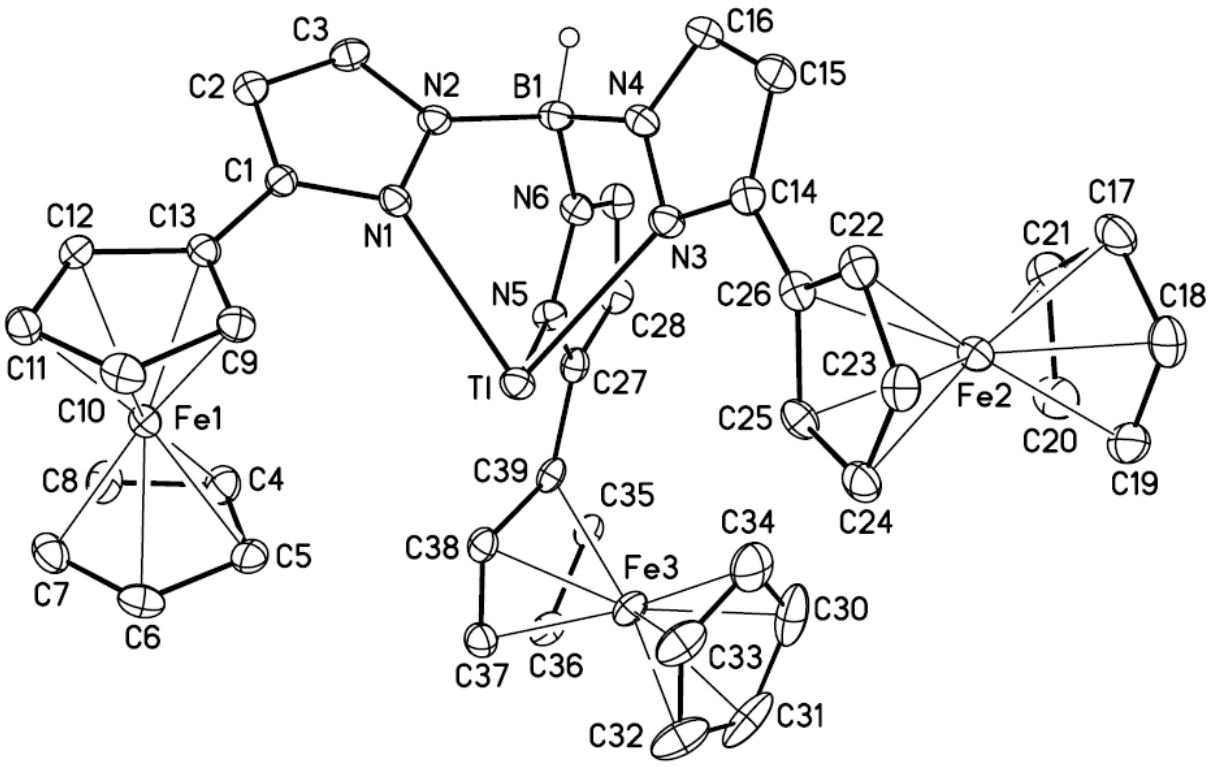

Figure 3.2: Molecular structure of $Tp^{Fc}Tl$ (7) at the 30% probability level. Hydrogen atoms (except the boron bound hydrogen, H1B) have been removed for clarity.

Table 3.1: Selected interatomic distances (Å) and angles (°) for $Tp^{Fc}Tl$ (7).

Distance (Å)

Tl-N(3)	2.549(3)	C(12)-C(13)	1.422(4)
Tl-N(1)	2.564(3)	C(14)-C(15)	1.393(5)
Tl-N(5)	2.595(3)	C(14)-C(26)	1.470(5)
B(1)-N(2)	1.541(5)	C(15)-C(16)	1.365(5)
B(1)-N(6)	1.547(5)	C(17)-C(21)	1.411(5)
B(1)-N(4)	1.550(5)	C(17)-C(18)	1.412(5)
N(1)-C(1)	1.339(4)	C(18)-C(19)	1.408(5)
N(1)-N(2)	1.369(3)	C(19)-C(20)	1.410(5)
N(2)-C(3)	1.340(4)	C(20)-C(21)	1.425(5)
N(3)-C(14)	1.343(4)	C(22)-C(23)	1.413(5)
N(3)-N(4)	1.369(4)	C(22)-C(26)	1.428(4)
N(4)-C(16)	1.340(4)	C(23)-C(24)	1.418(5)
N(5)-C(27)	1.337(4)	C(24)-C(25)	1.418(5)
N(5)-N(6)	1.372(4)	C(25)-C(26)	1.428(5)
N(6)-C(29)	1.341(4)	C(27)-C(28)	1.405(5)
C(1)-C(2)	1.390(4)	C(27)-C(39)	1.466(5)
C(1)-C(13)	1.468(4)	C(28)-C(29)	1.369(5)
C(2)-C(3)	1.369(5)	C(30)-C(34)	1.418(6)
C(4)-C(8)	1.407(5)	C(30)-C(31)	1.423(7)
C(4)-C(5)	1.413(5)	C(31)-C(32)	1.410(6)
C(5)-C(6)	1.415(5)	C(32)-C(33)	1.412(6)
C(6)-C(7)	1.420(5)	C(33)-C(34)	1.406(6)
C(7)-C(8)	1.414(5)	C(35)-C(36)	1.416(5)
C(9)-C(10)	1.420(5)	C(35)-C(39)	1.425(4)
C(9)-C(13)	1.434(4)	C(36)-C(37)	1.420(5)
C(10)-C(11)	1.417(5)	C(37)-C(38)	1.413(5)
C(11)-C(12)	1.418(5)	C(38)-C(39)	1.437(5)

Angles (°)

N(3)-Tl-N(1)	76.95(8)	C(3)-N(2)-N(1)	109.3(3)
N(3)-Tl-N(5)	75.95(8)	C(3)-N(2)-B(1)	128.0(3)
N(1)-Tl-N(5)	75.35(8)	N(1)-N(2)-B(1)	122.7(3)
N(2)-B(1)-N(6)	110.3(3)	C(14)-N(3)-N(4)	106.8(3)
N(2)-B(1)-N(4)	110.5(3)	C(14)-N(3)-Tl	129.5(2)
N(6)-B(1)-N(4)	110.1(3)	N(4)-N(3)-Tl	118.22(19)
C(1)-N(1)-N(2)	106.5(2)	C(16)-N(4)-N(3)	109.1(3)
C(1)-N(1)-Tl	131.4(2)	C(16)-N(4)-B(1)	128.0(3)
N(2)-N(1)-Tl	118.63(18)	N(3)-N(4)-B(1)	122.9(3)

C(27)-N(5)-N(6)	106.5(3)	C(19)-C(18)-C(17)	108.7(3)
C(27)-N(5)-Tl	132.8(2)	C(18)-C(19)-C(20)	107.9(3)
N(6)-N(5)-Tl	117.32(18)	C(19)-C(20)-C(21)	107.7(3)
C(29)-N(6)-N(5)	109.1(3)	C(17)-C(21)-C(20)	108.1(3)
C(29)-N(6)-B(1)	128.0(3)	C(23)-C(22)-C(26)	108.6(3)
N(5)-N(6)-B(1)	122.8(3)	C(22)-C(23)-C(24)	108.0(3)
N(1)-C(1)-C(2)	110.1(3)	C(25)-C(24)-C(23)	108.2(3)
N(1)-C(1)-C(13)	122.4(3)	C(24)-C(25)-C(26)	108.2(3)
C(2)-C(1)-C(13)	127.4(3)	C(22)-C(26)-C(25)	107.0(3)
C(3)-C(2)-C(1)	105.2(3)	C(22)-C(26)-C(14)	124.2(3)
N(2)-C(3)-C(2)	108.9(3)	C(25)-C(26)-C(14)	128.7(3)
C(8)-C(4)-C(5)	108.4(3)	N(5)-C(27)-C(28)	110.3(3)
C(4)-C(5)-C(6)	107.8(3)	N(5)-C(27)-C(39)	122.3(3)
C(5)-C(6)-C(7)	107.8(3)	C(28)-C(27)-C(39)	127.2(3)
C(8)-C(7)-C(6)	107.9(3)	C(29)-C(28)-C(27)	104.4(3)
C(4)-C(8)-C(7)	108.0(3)	N(6)-C(29)-C(28)	109.6(3)
C(10)-C(9)-C(13)	108.3(3)	C(34)-C(30)-C(31)	107.6(4)
C(11)-C(10)-C(9)	107.9(3)	C(32)-C(31)-C(30)	107.6(4)
C(10)-C(11)-C(12)	108.2(3)	C(31)-C(32)-C(33)	108.5(5)
C(11)-C(12)-C(13)	108.5(3)	C(34)-C(33)-C(32)	107.9(4)
C(12)-C(13)-C(9)	107.0(3)	C(33)-C(34)-C(30)	108.4(4)
C(12)-C(13)-C(1)	124.8(3)	C(36)-C(35)-C(39)	108.9(3)
C(9)-C(13)-C(1)	128.0(3)	C(35)-C(36)-C(37)	107.5(3)
N(3)-C(14)-C(15)	109.5(3)	C(38)-C(37)-C(36)	108.7(3)
N(3)-C(14)-C(26)	121.6(3)	C(37)-C(38)-C(39)	108.0(3)
C(15)-C(14)-C(26)	128.9(3)	C(35)-C(39)-C(38)	106.9(3)
C(16)-C(15)-C(14)	105.5(3)	C(35)-C(39)-C(27)	125.0(3)
N(4)-C(16)-C(15)	109.1(3)	C(38)-C(39)-C(27)	128.0(3)
C(21)-C(17)-C(18)	107.6(3)		

3.2.2 Borotropic Rearrangement of $Tp^{Fc,Me*}Tl$ (2) to $Tp^{Fc,Me}Tl$.

In a similar manner, a solid sample of the kinetically formed $Tp^{Fc,Me*}Tl$ was heated to 250 ºC under vacuum for one hour. After cooling to room temperature, the sample had been completely converted to the symmetric isomer $Tp^{Fc,Me}Tl$ (**8**) as apparent by ^1H NMR spectroscopy. The starting material, **2**, has two sets of proton resonances for the pyrazolyl rings in a ratio of 2:1. After 20 minutes of heating, the appearance of a third set of proton resonances

attributed to the formation of **8** was observed. When the reaction had been completed after an hour, only five well resolved proton resonances remained in the ^{1}H NMR spectrum (Figure 3.3). The ^{11}B NMR resonance shifts from -7.31 ppm in the asymmetric ligand, **2**, to -7.84 in compound **8**. IR spectroscopy also reveals a shift in the B-H stretching frequency from 2546 cm^{-1} in Tp^{Fc,Me*}Tl to 2523 cm^{-1} in Tp^{Fc,Me}Tl. X-ray quality crystals were obtained by the slow cooling of a solution of **8** in DMSO.

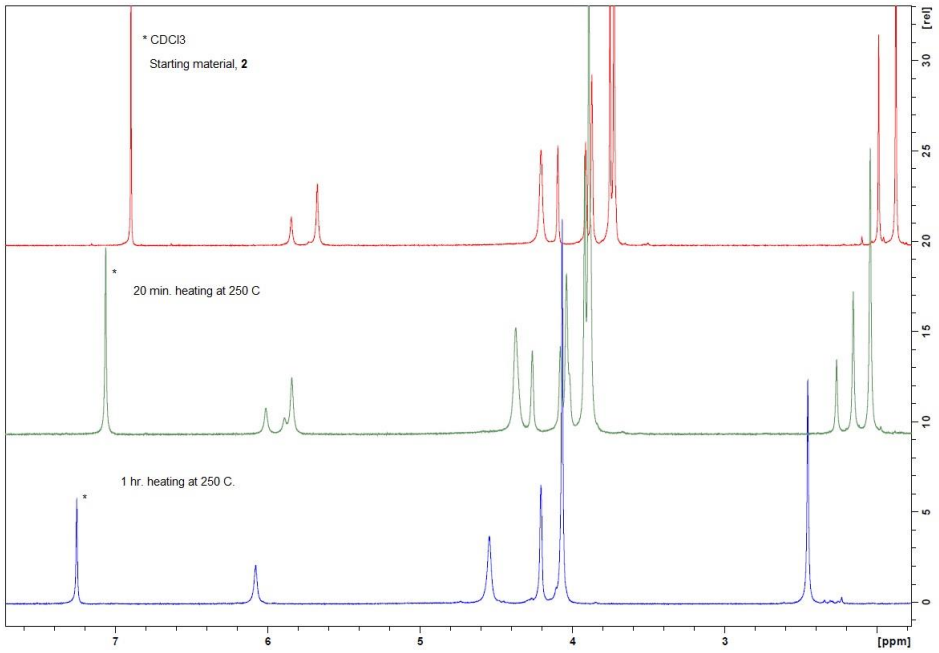

Figure 3.3: NMR spectral comparison of Tp^{Fc,Me*}Tl (2) (top), Tp^{Fc,Me*}Tl/Tp^{Fc,Me}Tl (middle), and Tp^{Fc,Me}Tl (8) (bottom).

The X-ray crystal structure of **8** confirms the symmetric configuration apparent in the ^{1}H NMR spectrum (Figure 3.4). Compound **8** crystallizes in the triclinic space group P-1. Figure 2.4 displays the molecular structure of Tp^{Fc,Me}Tl in which the ligand binds κ^3 to the Tl metal center in a trigonal pyramidal geometry. The average Tl-N distance (Table 3.2) of complex **8** is 2.554 Å. The ferrocenyl moieties appear to prefer to orient themselves in the solid state with two Fc

substituents with the same orientation (either clockwise or counter clockwise) relative to the pyrazolyl ring (torsion angles for $Tp^{Fc,R}MX$ compounds in this chapter can be found in Table A2.1). The third Fc substituent rotates in the opposite direction of the other Fc moieties. Similar to the $Tp^{Fc}Tl$ system, the CV of **8** was shown to be indistinguishable from that of **2** (Figure 3.5).

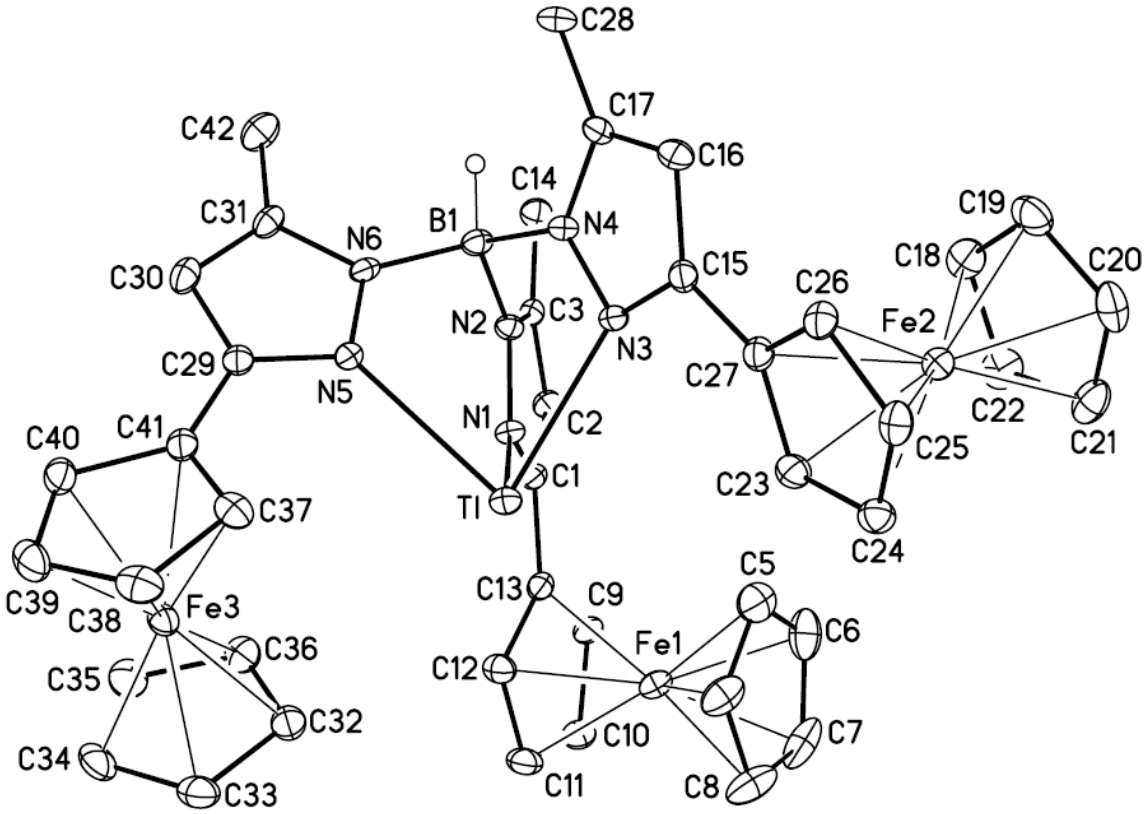

Figure 3.4: Molecular structure of $Tp^{Fc,Me}Tl$ (8) at 30% probability level. Hydrogen atoms (except the boron bound hydrogen, H1B) have been removed for clarity.

Table 3.2: Selected interatomic distances (Å) and angles (°) for $Tp^{Fc,Me}Tl$ (8).

Distances (Å)

Tl-N(3)	2.529(3)	C(15)-C(16)	1.401(5)
Tl-N(5)	2.553(3)	C(15)-C(27)	1.467(5)
Tl-N(1)	2.582(3)	C(16)-C(17)	1.368(5)
B(1)-N(4)	1.539(5)	C(17)-C(28)	1.490(5)
B(1)-N(6)	1.546(5)	C(18)-C(22)	1.411(6)
B(1)-N(2)	1.545(5)	C(18)-C(19)	1.415(6)
N(1)-C(1)	1.339(4)	C(19)-C(20)	1.417(6)
N(1)-N(2)	1.370(4)	C(20)-C(21)	1.405(6)
N(2)-C(3)	1.357(4)	C(21)-C(22)	1.420(6)
N(3)-C(15)	1.336(4)	C(23)-C(24)	1.420(5)
N(3)-N(4)	1.376(4)	C(23)-C(27)	1.431(5)
N(4)-C(17)	1.354(4)	C(24)-C(25)	1.417(5)
N(5)-C(29)	1.331(4)	C(25)-C(26)	1.418(5)
N(5)-N(6)	1.376(4)	C(26)-C(27)	1.431(5)
N(6)-C(31)	1.349(4)	C(29)-C(30)	1.388(5)
C(1)-C(2)	1.398(5)	C(29)-C(41)	1.473(5)
C(1)-C(13)	1.462(5)	C(30)-C(31)	1.378(5)
C(2)-C(3)	1.377(5)	C(31)-C(42)	1.489(5)
C(3)-C(14)	1.497(5)	C(32)-C(33)	1.413(5)
C(4)-C(5)	1.407(6)	C(32)-C(36)	1.415(6)
C(4)-C(8)	1.419(6)	C(33)-C(34)	1.420(6)
C(5)-C(6)	1.422(6)	C(34)-C(35)	1.406(6)
C(6)-C(7)	1.409(7)	C(35)-C(36)	1.412(6)
C(7)-C(8)	1.422(7)	C(37)-C(38)	1.423(5)
C(9)-C(10)	1.421(5)	C(37)-C(41)	1.427(5)
C(9)-C(13)	1.432(5)	C(38)-C(39)	1.414(6)
C(10)-C(11)	1.415(5)	C(39)-C(40)	1.411(6)
C(11)-C(12)	1.421(5)	C(40)-C(41)	1.434(5)
C(12)-C(13)	1.427(5)		

Angles (°)

N(3)-Tl-N(5)	78.03(9)	N(6)-B(1)-H(1B)	111.7(18)
N(3)-Tl-N(1)	75.44(9)	N(2)-B(1)-H(1B)	107.0(18)
N(5)-Tl-N(1)	75.51(9)	C(1)-N(1)-N(2)	106.6(3)
N(4)-B(1)-N(6)	109.7(3)	C(1)-N(1)-Tl	133.5(2)
N(4)-B(1)-N(2)	112.2(3)	N(2)-N(1)-Tl	118.26(19)
N(6)-B(1)-N(2)	110.4(3)	C(3)-N(2)-N(1)	109.7(3)
N(4)-B(1)-H(1B)	105.9(18)	C(3)-N(2)-B(1)	128.1(3)

N(1)-N(2)-B(1)	122.0(3)	C(17)-C(16)-C(15)	106.0(3)
C(15)-N(3)-N(4)	106.3(3)	N(4)-C(17)-C(16)	107.8(3)
C(15)-N(3)-Tl	127.2(2)	N(4)-C(17)-C(28)	123.1(3)
N(4)-N(3)-Tl	117.6(2)	C(16)-C(17)-C(28)	129.1(3)
C(17)-N(4)-N(3)	109.9(3)	C(22)-C(18)-C(19)	108.2(4)
C(17)-N(4)-B(1)	127.5(3)	C(18)-C(19)-C(20)	107.4(4)
N(3)-N(4)-B(1)	122.3(3)	C(21)-C(20)-C(19)	108.7(4)
C(29)-N(5)-N(6)	106.4(3)	C(20)-C(21)-C(22)	107.6(4)
C(29)-N(5)-Tl	132.1(2)	C(18)-C(22)-C(21)	108.1(4)
N(6)-N(5)-Tl	119.05(19)	C(24)-C(23)-C(27)	108.3(3)
C(31)-N(6)-N(5)	109.7(3)	C(25)-C(24)-C(23)	107.8(3)
C(31)-N(6)-B(1)	128.4(3)	C(24)-C(25)-C(26)	108.7(3)
N(5)-N(6)-B(1)	121.8(3)	C(25)-C(26)-C(27)	107.9(3)
N(1)-C(1)-C(2)	110.1(3)	C(23)-C(27)-C(26)	107.3(3)
N(1)-C(1)-C(13)	122.7(3)	C(23)-C(27)-C(15)	128.2(3)
C(2)-C(1)-C(13)	127.2(3)	C(26)-C(27)-C(15)	124.4(3)
C(3)-C(2)-C(1)	105.6(3)	N(5)-C(29)-C(30)	110.3(3)
N(2)-C(3)-C(2)	107.9(3)	N(5)-C(29)-C(41)	122.8(3)
N(2)-C(3)-C(14)	123.5(3)	C(30)-C(29)-C(41)	126.8(3)
C(2)-C(3)-C(14)	128.6(3)	C(29)-C(30)-C(31)	105.9(3)
C(5)-C(4)-C(8)	108.2(4)	N(6)-C(31)-C(30)	107.7(3)
C(4)-C(5)-C(6)	108.3(4)	N(6)-C(31)-C(42)	122.9(3)
C(7)-C(6)-C(5)	107.6(4)	C(30)-C(31)-C(42)	129.4(3)
C(6)-C(7)-C(8)	108.5(4)	C(33)-C(32)-C(36)	108.2(4)
C(4)-C(8)-C(7)	107.4(4)	C(32)-C(33)-C(34)	107.5(4)
C(10)-C(9)-C(13)	108.6(3)	C(35)-C(34)-C(33)	108.2(4)
C(11)-C(10)-C(9)	107.9(3)	C(34)-C(35)-C(36)	108.2(4)
C(10)-C(11)-C(12)	108.2(3)	C(35)-C(36)-C(32)	107.8(4)
C(11)-C(12)-C(13)	108.5(3)	C(38)-C(37)-C(41)	108.2(4)
C(12)-C(13)-C(9)	106.8(3)	C(39)-C(38)-C(37)	107.8(4)
C(12)-C(13)-C(1)	128.8(3)	C(38)-C(39)-C(40)	108.8(3)
C(9)-C(13)-C(1)	124.4(3)	C(39)-C(40)-C(41)	108.0(4)
N(3)-C(15)-C(16)	110.0(3)	C(37)-C(41)-C(40)	107.2(3)
N(3)-C(15)-C(27)	121.3(3)	C(37)-C(41)-C(29)	128.0(3)
C(16)-C(15)-C(27)	128.7(3)	C(40)-C(41)-C(29)	124.6(3)

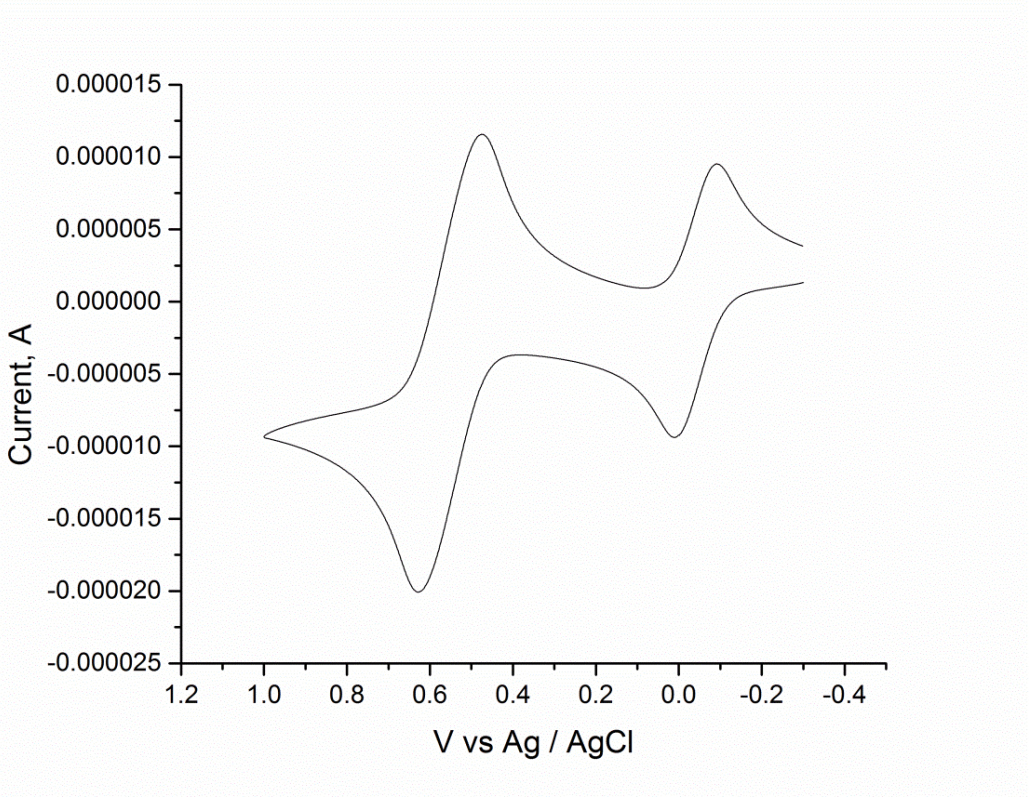

Figure 3.5: Cyclic voltammetric response of a 1.0 mM solution of $Tp^{Fc,Me}Tl$ (8) recorded at a platinum electrode with a Ag/AgCl reference electrode in CH_2Cl_2 solutions containing 0.1 M $[NBu_4][PF_6]$ and Cp^*_2Fe using a scan rate of 100 mV/s.

3.2.3 Borotropic Rearrangement of $Tp^{Fc,iPr}Tl$ to a Mixture of Regioisomers.

Unlike the $Tp^{Fc*}Tl$ and $Tp^{Fc,Me*}Tl$ analogs, the $Tp^{Fc,iPr}Tl$ species was the isolated product. Heating a solid sample of sample of the symmetric ligand under vacuum at 250 °C for 1 hour leads to the appearance of two new Tp complexes as indicated by ^1H NMR spectroscopy. Each new complex contained two sets of pyrazole resonances in a ratio of 2:1. This suggests the formation of two new regioisomers, presumably the hydrobis(3-ferrocenyl-5-*iso*-propylpyrazolyl)(3-*iso*-propyl-5-ferrocenylpyrazolyl)borate and the hydrobis(3-*iso*-propyl-5-ferrocenylpyrazolyl)(3-ferrocenyl-5-*iso*-propylpyrazolyl)borate (Scheme 3.3 and Figure 3.6).

However, it is difficult to establish the ratio of isomers due to peak overlap in the ^{1}H and ^{11}B NMR spectra. Attempts to isolate the pure N-confused isomers proved unsuccessful.

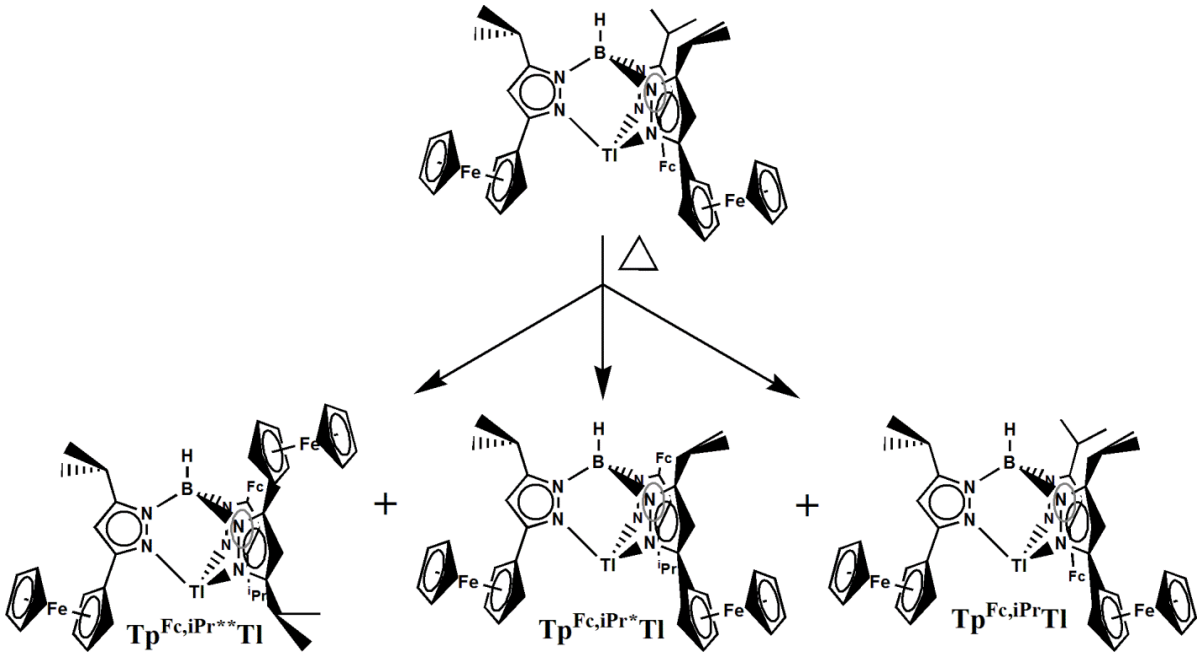

Scheme 3.3: Thermal isomerization of $Tp^{Fc,iPr}Tl$ to regioisomers.

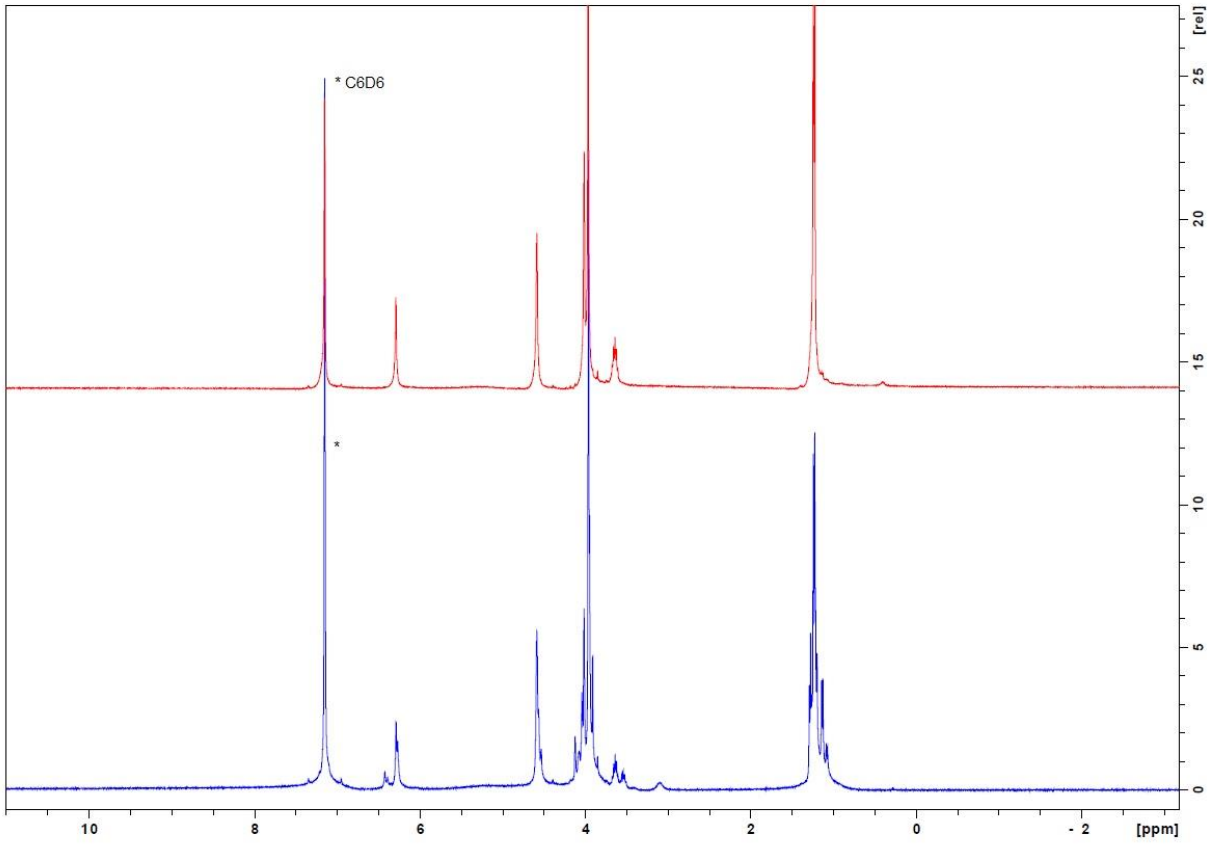

Figure 3.6: ^{1}H NMR spectral comparison of Tp^{Fc,iPr}Tl (3) (top) and its regioisomers (bottom).

3.2.4 Synthesis and Characterization of Tp^{Fc}Co(II) Halide Complexes.

The cobalt halide complexes provide important starting materials for the exploration of all chemistry in the various TpCo systems. Tp^{Fc}CoI (**9**) and Tp^{Fc}CoCl (**10**) were obtained through salt metathesis of the corresponding cobalt(II) halides and the Tl salt of the ligand in THF at room temperature. After solvent removal and recrystallization from cooled solutions (-30 °C) of the metal complexes in THF / pentanes mixture, **9** and **10** could be isolated as green crystals in 72% and 68 % yield, respectively. ^{1}H NMR spectra, recorded in C_6D_6 at room

temperature, displayed 5 well resolved signals ranging from 68 ppm to 3 ppm, which were assigned to the protons of the Tp^{Fc} ligand. A sixth, broad resonance can be observed around -20 ppm which can be assigned to the proton attached to the boron. The molecular structures of **9** (Figure 3.7) and **10** (Figure 3.8) display the expected pseudo tetrahedral coordination geometry with the ligand bound κ^3 to the Co and the fourth coordination site occupied by the halide. Complex **9** has a Co-I bond distances of 2.5236(7) Å (Table 3.3), while complex **10** has a Co-Cl bond distance of 2.1958(6) Å (Table 3.4). **9** and **10** have magnetic moments of 4.3 μ_B and 4.4 μ_B, respectively, indicative of a Co(II) species with three unpaired electrons.

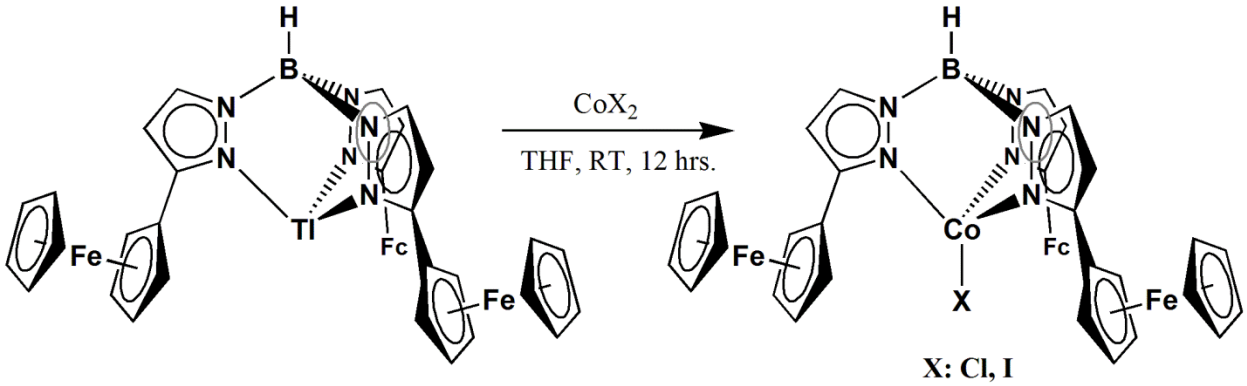

Scheme 3.4: Syntheses of $Tp^{Fc}CoX$ complexes.

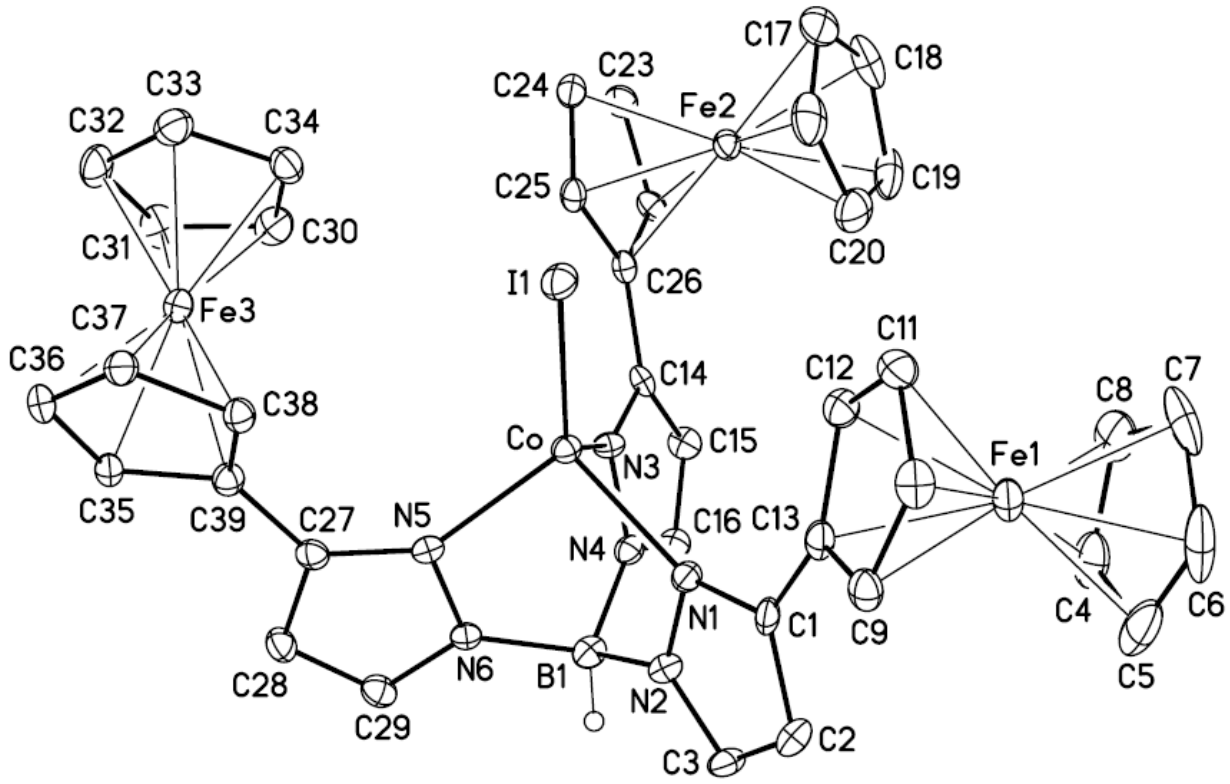

Figure 3.7: Molecular structure of $Tp^{Fc}CoI$ (9) at the 30% probability level. Hydrogen atoms (except the boron bound hydrogen, H1B) have been removed for clarity.

Table 3.3: Selected interatomic distances (Å) and angles (°) for $Tp^{Fc}CoI$ (9).

Distances (Å)

Co-N(5)	2.044(4)	C(12)-C(13)	1.433(6)
Co-N(1)	2.060(4)	C(14)-C(15)	1.407(6)
Co-N(3)	2.061(4)	C(14)-C(26)	1.455(6)
Co-I(1)	2.5236(7)	C(15)-C(16)	1.360(6)
B(1)-N(2)	1.539(6)	C(17)-C(21)	1.385(8)
B(1)-N(6)	1.542(6)	C(17)-C(18)	1.416(8)
B(1)-N(4)	1.547(6)	C(18)-C(19)	1.413(8)
N(1)-C(1)	1.353(5)	C(19)-C(20)	1.396(8)
N(1)-N(2)	1.375(5)	C(20)-C(21)	1.398(7)
N(2)-C(3)	1.340(5)	C(22)-C(23)	1.414(6)
N(3)-C(14)	1.342(5)	C(22)-C(26)	1.434(6)
N(3)-N(4)	1.378(5)	C(23)-C(24)	1.424(6)
N(4)-C(16)	1.346(5)	C(24)-C(25)	1.420(6)
N(5)-C(27)	1.351(5)	C(25)-C(26)	1.428(6)
N(5)-N(6)	1.383(5)	C(27)-C(28)	1.407(6)
N(6)-C(29)	1.341(5)	C(27)-C(39)	1.474(6)
C(1)-C(2)	1.405(6)	C(28)-C(29)	1.369(6)
C(1)-C(13)	1.466(6)	C(30)-C(31)	1.412(7)
C(2)-C(3)	1.356(6)	C(30)-C(34)	1.416(7)
C(4)-C(5)	1.411(8)	C(31)-C(32)	1.405(7)
C(4)-C(8)	1.411(8)	C(32)-C(33)	1.420(7)
C(5)-C(6)	1.381(9)	C(33)-C(34)	1.415(7)
C(6)-C(7)	1.412(9)	C(35)-C(36)	1.416(6)
C(7)-C(8)	1.413(8)	C(35)-C(39)	1.431(6)
C(9)-C(10)	1.403(6)	C(36)-C(37)	1.423(6)
C(9)-C(13)	1.439(6)	C(37)-C(38)	1.419(6)
C(10)-C(11)	1.422(6)	C(38)-C(39)	1.428(6)
C(11)-C(12)	1.426(6)		

Angles (°)

N(5)-Co-N(1)	99.88(14)	N(6)-B(1)-N(4)	109.3(4)
N(5)-Co-N(3)	91.08(14)	N(4)-B(1)-H(1B)	109(2)
N(1)-Co-N(3)	94.66(14)	C(1)-N(1)-N(2)	106.4(3)
N(5)-Co-I(1)	122.15(10)	C(1)-N(1)-Co	143.3(3)
N(1)-Co-I(1)	111.72(10)	N(2)-N(1)-Co	108.5(2)
N(3)-Co-I(1)	130.72(10)	C(3)-N(2)-N(1)	109.3(4)
N(2)-B(1)-N(6)	111.2(4)	C(3)-N(2)-B(1)	129.8(4)
N(2)-B(1)-N(4)	108.1(4)	N(1)-N(2)-B(1)	120.8(4)

C(14)-N(3)-N(4)	106.7(3)	C(15)-C(14)-C(26)	126.6(4)
C(14)-N(3)-Co	143.4(3)	C(16)-C(15)-C(14)	105.7(4)
N(4)-N(3)-Co	108.0(3)	N(4)-C(16)-C(15)	109.1(4)
C(16)-N(4)-N(3)	109.1(4)	C(21)-C(17)-C(18)	108.8(5)
C(16)-N(4)-B(1)	129.9(4)	C(19)-C(18)-C(17)	107.3(5)
N(3)-N(4)-B(1)	120.7(3)	C(20)-C(19)-C(18)	107.0(5)
C(27)-N(5)-N(6)	106.6(3)	C(19)-C(20)-C(21)	109.5(6)
C(27)-N(5)-Co	144.2(3)	C(17)-C(21)-C(20)	107.4(5)
N(6)-N(5)-Co	108.3(3)	C(23)-C(22)-C(26)	108.6(4)
C(29)-N(6)-N(5)	109.6(4)	C(22)-C(23)-C(24)	107.9(4)
C(29)-N(6)-B(1)	128.0(4)	C(25)-C(24)-C(23)	108.0(4)
N(5)-N(6)-B(1)	122.2(3)	C(24)-C(25)-C(26)	108.4(4)
N(1)-C(1)-C(2)	109.1(4)	C(25)-C(26)-C(22)	106.9(4)
N(1)-C(1)-C(13)	124.1(4)	C(25)-C(26)-C(14)	128.9(4)
C(2)-C(1)-C(13)	126.8(4)	C(22)-C(26)-C(14)	124.2(4)
C(3)-C(2)-C(1)	105.7(4)	N(5)-C(27)-C(28)	109.0(4)
N(2)-C(3)-C(2)	109.4(4)	N(5)-C(27)-C(39)	126.7(4)
C(5)-C(4)-C(8)	107.9(6)	C(28)-C(27)-C(39)	124.2(4)
C(6)-C(5)-C(4)	108.5(6)	C(29)-C(28)-C(27)	106.0(4)
C(5)-C(6)-C(7)	108.5(6)	N(6)-C(29)-C(28)	108.8(4)
C(8)-C(7)-C(6)	107.8(6)	C(31)-C(30)-C(34)	108.1(4)
C(4)-C(8)-C(7)	107.4(5)	C(32)-C(31)-C(30)	107.8(5)
C(10)-C(9)-C(13)	108.3(4)	C(31)-C(32)-C(33)	108.7(5)
C(9)-C(10)-C(11)	108.6(4)	C(34)-C(33)-C(32)	107.1(5)
C(10)-C(11)-C(12)	108.0(4)	C(33)-C(34)-C(30)	108.2(4)
C(11)-C(12)-C(13)	107.8(4)	C(36)-C(35)-C(39)	108.3(4)
C(12)-C(13)-C(9)	107.2(4)	C(35)-C(36)-C(37)	108.2(4)
C(12)-C(13)-C(1)	129.2(4)	C(37)-C(38)-C(39)	108.4(4)
C(9)-C(13)-C(1)	123.7(4)	C(38)-C(39)-C(35)	107.2(4)
N(3)-C(14)-C(15)	109.4(4)	C(38)-C(39)-C(27)	129.0(4)
N(3)-C(14)-C(26)	123.7(4)	C(35)-C(39)-C(27)	123.2(4)

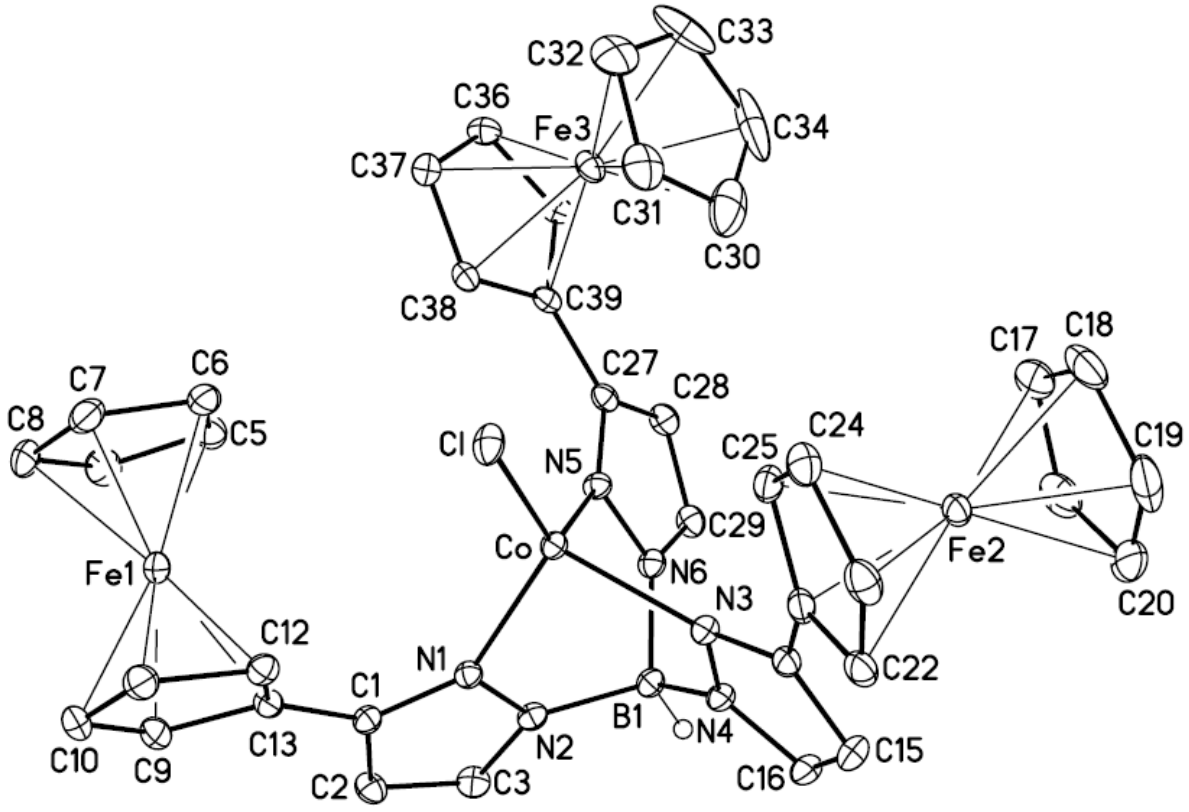

Figure 3.8: Molecular structure of $Tp^{Fc}CoCl$ (10) at the 30% probability level. Hydrogen atoms (except the boron bound hydrogen, H1B) have been removed for clarity.

Table 3.4: Selected interatomic distances (Å) and angles (°) for $Tp^{Fc}CoCl$ (10).

Distances (Å)

Co-N(1)	2.0441(16)	C(12)-C(13)	1.431(3)
Co-N(3)	2.0482(16)	C(14)-C(15)	1.404(3)
Co-N(5)	2.0539(16)	C(14)-C(26)	1.467(3)
Co-Cl(1)	2.1958(6)	C(15)-C(16)	1.369(3)
B(1)-N(4)	1.541(3)	C(17)-C(21)	1.414(3)
B(1)-N(2)	1.545(3)	C(17)-C(18)	1.419(4)
B(1)-N(6)	1.556(3)	C(18)-C(19)	1.405(4)
N(1)-C(1)	1.347(2)	C(19)-C(20)	1.408(4)
N(1)-N(2)	1.379(2)	C(20)-C(21)	1.416(4)
N(2)-C(3)	1.342(2)	C(22)-C(23)	1.421(3)
N(3)-C(14)	1.344(2)	C(22)-C(26)	1.438(3)
N(3)-N(4)	1.374(2)	C(23)-C(24)	1.427(3)
N(4)-C(16)	1.345(2)	C(24)-C(25)	1.419(3)
N(5)-C(27)	1.346(2)	C(25)-C(26)	1.432(3)
N(5)-N(6)	1.380(2)	C(27)-C(28)	1.402(3)
N(6)-C(29)	1.344(2)	C(27)-C(39)	1.462(3)
C(1)-C(2)	1.402(3)	C(28)-C(29)	1.374(3)
C(1)-C(13)	1.469(3)	C(30)-C(34)	1.393(5)
C(2)-C(3)	1.372(3)	C(30)-C(31)	1.395(4)
C(4)-C(5)	1.418(3)	C(31)-C(32)	1.394(4)
C(4)-C(8)	1.420(3)	C(32)-C(33)	1.423(4)
C(5)-C(6)	1.415(3)	C(33)-C(34)	1.431(5)
C(6)-C(7)	1.420(3)	C(35)-C(36)	1.422(3)
C(7)-C(8)	1.421(3)	C(35)-C(39)	1.433(3)
C(9)-C(10)	1.420(3)	C(36)-C(37)	1.425(3)
C(9)-C(13)	1.436(3)	C(37)-C(38)	1.425(3)
C(10)-C(11)	1.426(3)	C(38)-C(39)	1.430(3)
C(11)-C(12)	1.426(3)		

Angles (°)

N(1)-Co-N(3)	97.44(6)	N(2)-B(1)-N(6)	108.38(15)
N(1)-Co-N(5)	92.55(6)	C(1)-N(1)-N(2)	106.68(15)
N(3)-Co-N(5)	94.83(6)	C(1)-N(1)-Co	142.97(13)
N(1)-Co-Cl(1)	123.04(5)	N(2)-N(1)-Co	109.01(11)
N(3)-Co-Cl(1)	114.65(5)	C(3)-N(2)-N(1)	109.57(15)
N(5)-Co-Cl(1)	127.33(5)	C(3)-N(2)-B(1)	128.56(16)
N(4)-B(1)-N(2)	110.56(16)	N(1)-N(2)-B(1)	121.84(15)
N(4)-B(1)-N(6)	108.43(15)	C(14)-N(3)-N(4)	106.82(15)

C(14)-N(3)-Co	142.35(13)	C(16)-C(15)-C(14)	105.82(18)
N(4)-N(3)-Co	109.05(11)	N(4)-C(16)-C(15)	108.62(18)
C(16)-N(4)-N(3)	109.49(16)	C(21)-C(17)-C(18)	108.2(2)
C(16)-N(4)-B(1)	129.06(17)	C(19)-C(18)-C(17)	107.6(2)
N(3)-N(4)-B(1)	121.44(15)	C(18)-C(19)-C(20)	108.6(2)
C(27)-N(5)-N(6)	106.51(15)	C(19)-C(20)-C(21)	108.1(2)
C(27)-N(5)-Co	143.31(13)	C(17)-C(21)-C(20)	107.5(2)
N(6)-N(5)-Co	109.14(11)	C(23)-C(22)-C(26)	108.09(18)
C(29)-N(6)-N(5)	109.36(15)	C(22)-C(23)-C(24)	108.21(18)
C(29)-N(6)-B(1)	129.88(16)	C(25)-C(24)-C(23)	108.03(18)
N(5)-N(6)-B(1)	120.53(15)	C(24)-C(25)-C(26)	108.44(18)
N(1)-C(1)-C(2)	109.16(17)	C(25)-C(26)-C(22)	107.22(18)
N(1)-C(1)-C(13)	124.91(17)	C(25)-C(26)-C(14)	129.52(17)
C(2)-C(1)-C(13)	125.81(17)	C(22)-C(26)-C(14)	123.23(18)
C(3)-C(2)-C(1)	106.03(17)	N(5)-C(27)-C(28)	109.74(17)
N(2)-C(3)-C(2)	108.55(17)	N(5)-C(27)-C(39)	122.78(16)
C(5)-C(4)-C(8)	108.1(2)	C(28)-C(27)-C(39)	127.21(17)
C(6)-C(5)-C(4)	107.98(19)	C(29)-C(28)-C(27)	105.38(17)
C(5)-C(6)-C(7)	108.22(19)	N(6)-C(29)-C(28)	108.98(17)
C(8)-C(7)-C(6)	107.83(19)	C(34)-C(30)-C(31)	108.6(3)
C(7)-C(8)-C(4)	107.91(19)	C(32)-C(31)-C(30)	108.8(3)
C(10)-C(9)-C(13)	108.02(18)	C(31)-C(32)-C(33)	108.0(3)
C(9)-C(10)-C(11)	108.42(18)	C(32)-C(33)-C(34)	106.6(3)
C(12)-C(11)-C(10)	107.86(18)	C(30)-C(34)-C(33)	108.0(2)
C(11)-C(12)-C(13)	108.22(17)	C(36)-C(35)-C(39)	107.97(17)
C(12)-C(13)-C(9)	107.46(17)	C(35)-C(36)-C(37)	108.46(17)
C(12)-C(13)-C(1)	128.49(17)	C(38)-C(37)-C(36)	107.71(18)
C(9)-C(13)-C(1)	123.49(17)	C(37)-C(38)-C(39)	108.40(17)
N(3)-C(14)-C(15)	109.25(18)	C(38)-C(39)-C(35)	107.46(16)
N(3)-C(14)-C(26)	123.90(17)	C(38)-C(39)-C(27)	128.79(17)
C(15)-C(14)-C(26)	126.84(18)	C(35)-C(39)-C(27)	123.64(17)

3.2.5 Synthesis and Characterization of $Tp^{Fc,Me}Co(II)$ Halide Complexes.

In a similar manner to the Tp^{Fc} system, the cobalt halide complexes of $Tp^{Fc,Me}$ can be obtained through salt metathesis of the corresponding cobalt(II) halides and the Tl salt of the $Tp^{Fc,Me}$ ligand (**8**) in THF at room temperature or refluxing in CH_2Cl_2 for an hour (Scheme 3.5). After solvent removal and recrystallization from cooled solutions of the metal complexes in a CH_2Cl_2 / ether mixture, green crystals of $Tp^{Fc,Me}CoI$ (**11**) and $Tp^{Fc,Me}CoCl$ (**12**) were isolated in 81% and 75 % yield, respectively. The ^1H NMR spectra, recorded in C_6D_6 at room temperature, showed 5 well resolved resonances that were readily assigned to the protons of the $Tp^{Fc,Me}$ ligand.

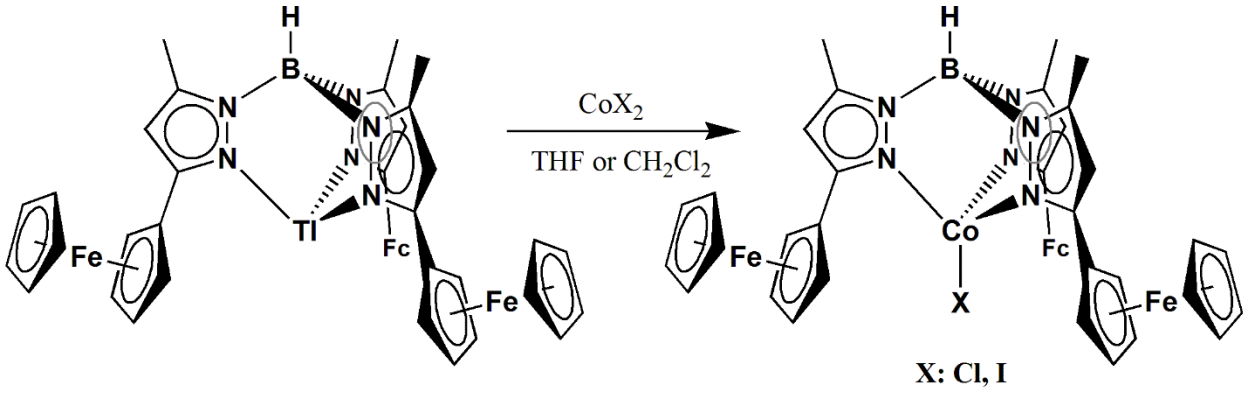

Scheme 3.5: Synthesis of $Tp^{Fc,Me}CoX$ complexes.

X-ray analysis revealed that both compounds crystallize in the triclinic space group P-1. The molecular structures of **11** (Figure 3.9) and **12** (Figure 3.10) exhibit pseudo-tetrahedral coordination geometry. The Co-I bond distance of **11** (Table 3.5) is 2.5443(4) Å, which is slightly longer than that of **9**. The Co-Cl bond distances of **12** is 2.2049(7) Å (Table 3.6).

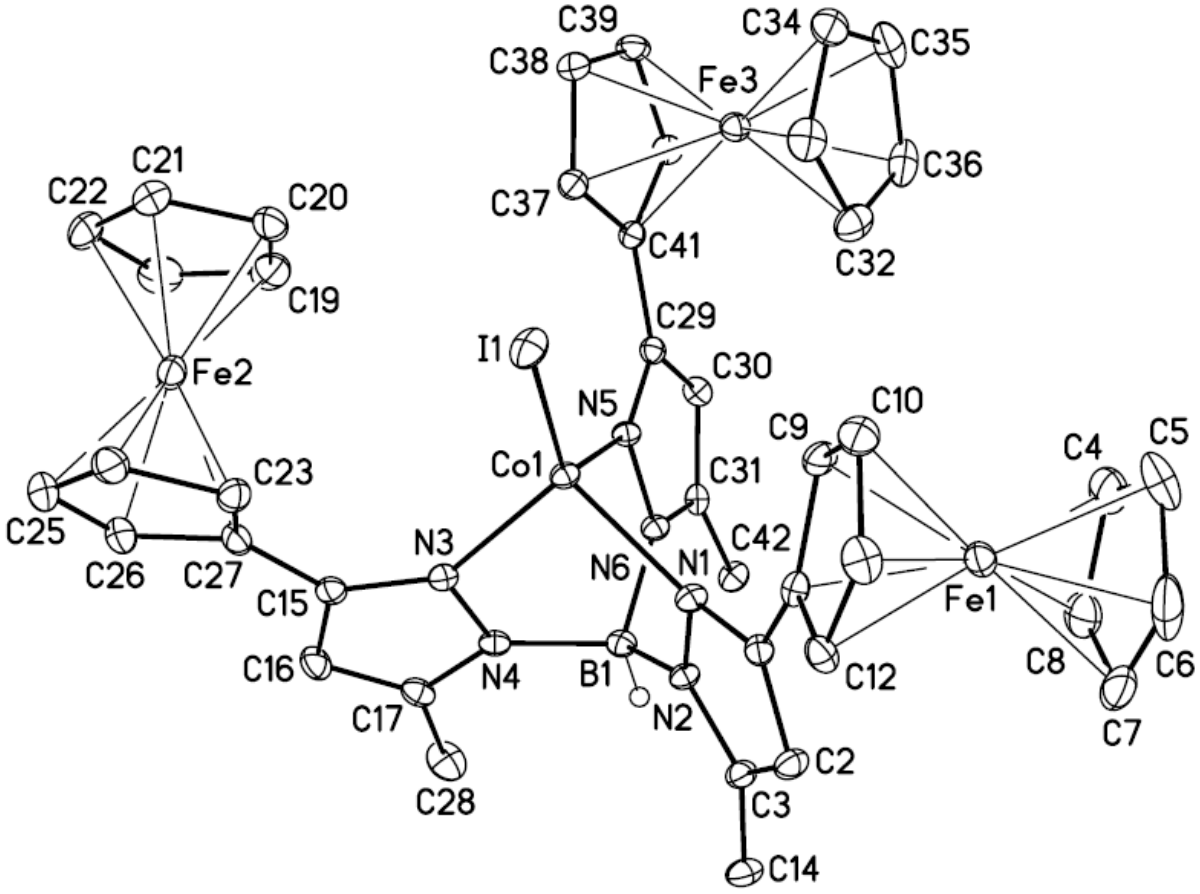

Figure 3.9: Molecular structure of $Tp^{Fc,Me}CoI$ (11) at the 30% probability level. Hydrogen atoms (except the boron bound hydrogen, H1B) have been removed for clarity.

Table 3.5: Selected interatomic distances (Å) and angles (°) for $Tp^{Fc,Me}CoI$ (11).

Distances (Å)

Co(1)-N(1)	2.042(2)	C(12)-C(13)	1.436(4)
Co(1)-N(5)	2.047(2)	C(15)-C(16)	1.395(4)
Co(1)-N(3)	2.053(2)	C(15)-C(27)	1.469(4)
Co(1)-I(1)	2.5443(4)	C(16)-C(17)	1.374(4)
B(1)-N(2)	1.541(4)	C(17)-C(28)	1.497(4)
B(1)-N(6)	1.555(4)	C(18)-C(19)	1.405(5)
B(1)-N(4)	1.555(4)	C(18)-C(22)	1.405(5)
N(1)-C(1)	1.351(3)	C(19)-C(20)	1.418(5)
N(1)-N(2)	1.384(3)	C(20)-C(21)	1.418(4)
N(2)-C(3)	1.349(3)	C(21)-C(22)	1.419(5)
N(3)-C(15)	1.347(4)	C(23)-C(24)	1.427(4)
N(3)-N(4)	1.388(3)	C(23)-C(27)	1.435(4)
N(4)-C(17)	1.349(3)	C(24)-C(25)	1.418(5)
N(5)-C(29)	1.346(3)	C(25)-C(26)	1.415(5)
N(5)-N(6)	1.388(3)	C(26)-C(27)	1.442(4)
N(6)-C(31)	1.349(3)	C(29)-C(30)	1.405(4)
C(1)-C(2)	1.397(4)	C(29)-C(41)	1.469(4)
C(1)-C(13)	1.461(4)	C(30)-C(31)	1.378(4)
C(2)-C(3)	1.367(4)	C(31)-C(42)	1.500(4)
C(3)-C(14)	1.501(4)	C(32)-C(33)	1.405(4)
C(4)-C(5)	1.406(5)	C(32)-C(36)	1.417(4)
C(4)-C(8)	1.416(5)	C(33)-C(34)	1.411(4)
C(5)-C(6)	1.407(5)	C(34)-C(35)	1.407(5)
C(6)-C(7)	1.402(6)	C(35)-C(36)	1.415(5)
C(7)-C(8)	1.403(5)	C(37)-C(38)	1.417(4)
C(9)-C(10)	1.419(4)	C(37)-C(41)	1.430(4)
C(9)-C(13)	1.431(4)	C(38)-C(39)	1.420(4)
C(10)-C(11)	1.421(4)	C(39)-C(40)	1.420(4)
C(11)-C(12)	1.408(4)	C(40)-C(41)	1.429(4)

Angles (°)

N(1)-Co(1)-N(5)	93.17(9)	N(2)-B(1)-N(4)	110.1(2)
N(1)-Co(1)-N(3)	99.14(9)	N(6)-B(1)-N(4)	108.0(2)
N(5)-Co(1)-N(3)	91.92(9)	C(1)-N(1)-N(2)	106.4(2)
N(1)-Co(1)-I(1)	110.53(6)	C(1)-N(1)-Co(1)	140.28(19)
N(5)-Co(1)-I(1)	131.57(6)	N(2)-N(1)-Co(1)	109.71(16)
N(3)-Co(1)-I(1)	123.11(6)	C(3)-N(2)-N(1)	109.5(2)
N(2)-B(1)-N(6)	110.4(2)	C(3)-N(2)-B(1)	130.8(2)

N(1)-N(2)-B(1)	119.7(2)	N(4)-C(17)-C(28)	122.8(3)
C(15)-N(3)-N(4)	106.3(2)	C(16)-C(17)-C(28)	129.2(3)
C(15)-N(3)-Co(1)	143.26(19)	C(19)-C(18)-C(22)	108.1(3)
N(4)-N(3)-Co(1)	109.30(16)	C(18)-C(19)-C(20)	108.4(3)
C(17)-N(4)-N(3)	109.6(2)	C(21)-C(20)-C(19)	107.6(3)
C(17)-N(4)-B(1)	128.9(2)	C(20)-C(21)-C(22)	107.5(3)
N(3)-N(4)-B(1)	121.3(2)	C(18)-C(22)-C(21)	108.5(3)
C(29)-N(5)-N(6)	106.5(2)	C(24)-C(23)-C(27)	107.7(3)
C(29)-N(5)-Co(1)	143.56(18)	C(25)-C(24)-C(23)	108.3(3)
N(6)-N(5)-Co(1)	109.78(15)	C(26)-C(25)-C(24)	108.7(3)
C(31)-N(6)-N(5)	109.7(2)	C(25)-C(26)-C(27)	107.9(3)
C(31)-N(6)-B(1)	129.5(2)	C(23)-C(27)-C(26)	107.4(3)
N(5)-N(6)-B(1)	120.3(2)	C(23)-C(27)-C(15)	129.0(3)
N(1)-C(1)-C(2)	109.2(2)	C(26)-C(27)-C(15)	123.1(3)
N(1)-C(1)-C(13)	123.2(2)	N(5)-C(29)-C(30)	109.5(2)
C(2)-C(1)-C(13)	127.6(3)	N(5)-C(29)-C(41)	123.6(2)
C(3)-C(2)-C(1)	106.6(2)	C(30)-C(29)-C(41)	126.9(2)
N(2)-C(3)-C(2)	108.3(2)	C(31)-C(30)-C(29)	106.2(2)
N(2)-C(3)-C(14)	122.6(3)	N(6)-C(31)-C(30)	108.2(2)
C(2)-C(3)-C(14)	129.1(3)	N(6)-C(31)-C(42)	123.1(2)
C(5)-C(4)-C(8)	108.2(3)	C(30)-C(31)-C(42)	128.7(2)
C(6)-C(5)-C(4)	108.0(4)	C(33)-C(32)-C(36)	108.0(3)
C(7)-C(6)-C(5)	107.8(3)	C(34)-C(33)-C(32)	108.1(3)
C(8)-C(7)-C(6)	108.8(3)	C(33)-C(34)-C(35)	108.2(3)
C(7)-C(8)-C(4)	107.2(3)	C(34)-C(35)-C(36)	107.9(3)
C(10)-C(9)-C(13)	108.2(3)	C(35)-C(36)-C(32)	107.7(3)
C(9)-C(10)-C(11)	107.9(3)	C(38)-C(37)-C(41)	108.4(2)
C(12)-C(11)-C(10)	108.6(3)	C(37)-C(38)-C(39)	108.0(3)
C(11)-C(12)-C(13)	108.2(3)	C(40)-C(39)-C(38)	108.1(2)
C(9)-C(13)-C(12)	107.1(2)	C(39)-C(40)-C(41)	108.3(2)
C(9)-C(13)-C(1)	128.8(2)	C(37)-C(41)-C(40)	107.1(2)
C(12)-C(13)-C(1)	124.1(3)	C(37)-C(41)-C(29)	128.5(2)
N(3)-C(15)-C(16)	109.5(3)	C(40)-C(41)-C(29)	124.3(2)
N(3)-C(15)-C(27)	126.2(3)	C(37)-C(41)-Fe(3)	69.43(16)
C(16)-C(15)-C(27)	124.3(3)	C(40)-C(41)-Fe(3)	69.61(16)
C(17)-C(16)-C(15)	106.6(3)	C(29)-C(41)-Fe(3)	125.91(19)
N(4)-C(17)-C(16)	108.0(3)		

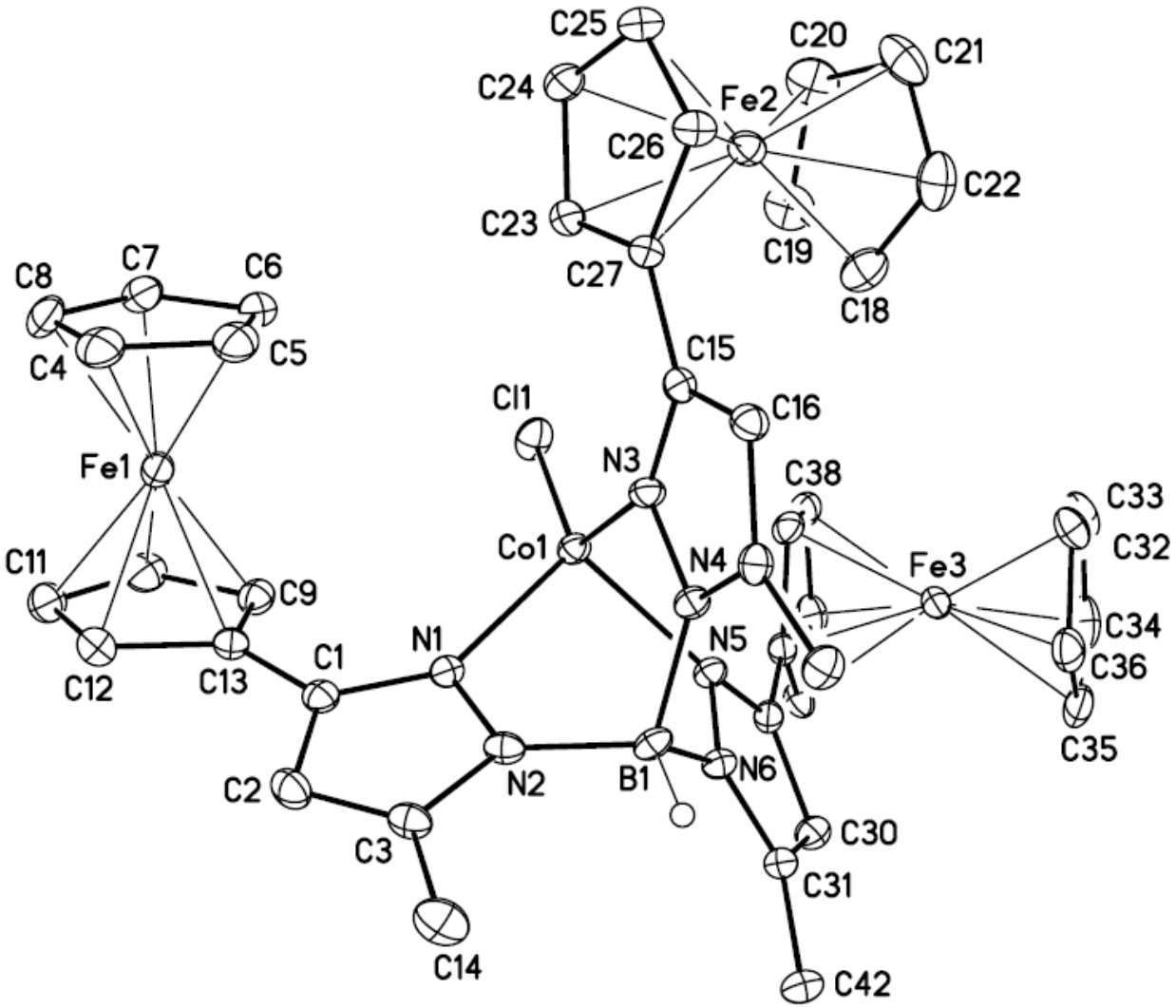

Figure 3.10: Molecular structure of $Tp^{Fc,Me}CoCl$ (12) at the 30% probability level. Hydrogen atoms (except the boron bound hydrogen, H1B) have been removed for clarity.

Table 3.6: Selected interatomic distances (Å) and angles (°) for $Tp^{Fc,Me}CoCl$ (12).

Distances (Å)

Co(1)-N(5)	2.037(2)	C(12)-C(13)	1.438(4)
Co(1)-N(1)	2.047(2)	C(15)-C(16)	1.401(3)
Co(1)-N(3)	2.052(2)	C(15)-C(27)	1.467(3)
Co(1)-Cl(1)	2.2049(7)	C(16)-C(17)	1.378(3)
B(1)-N(2)	1.532(3)	C(17)-C(28)	1.496(3)
B(1)-N(6)	1.553(3)	C(18)-C(22)	1.402(4)
B(1)-N(4)	1.574(3)	C(18)-C(19)	1.409(4)
N(1)-C(1)	1.351(3)	C(19)-C(20)	1.406(4)
N(1)-N(2)	1.385(3)	C(20)-C(21)	1.409(4)
N(2)-C(3)	1.358(3)	C(21)-C(22)	1.431(4)
N(3)-C(15)	1.339(3)	C(23)-C(24)	1.420(4)
N(3)-N(4)	1.384(3)	C(23)-C(27)	1.421(4)
N(4)-C(17)	1.356(3)	C(24)-C(25)	1.419(4)
N(5)-C(29)	1.342(3)	C(25)-C(26)	1.416(4)
N(5)-N(6)	1.390(3)	C(26)-C(27)	1.438(3)
N(6)-C(31)	1.345(3)	C(29)-C(30)	1.400(3)
C(1)-C(2)	1.398(3)	C(29)-C(41)	1.471(3)
C(1)-C(13)	1.470(3)	C(30)-C(31)	1.375(4)
C(2)-C(3)	1.374(4)	C(31)-C(42)	1.497(3)
C(3)-C(14)	1.491(3)	C(32)-C(33)	1.407(4)
C(4)-C(5)	1.410(4)	C(32)-C(36)	1.413(4)
C(4)-C(8)	1.420(4)	C(33)-C(34)	1.419(4)
C(5)-C(6)	1.422(4)	C(34)-C(35)	1.409(4)
C(6)-C(7)	1.424(4)	C(35)-C(36)	1.425(4)
C(7)-C(8)	1.412(4)	C(37)-C(38)	1.419(3)
C(9)-C(13)	1.428(4)	C(37)-C(41)	1.425(3)
C(9)-C(10)	1.429(4)	C(38)-C(39)	1.432(4)
C(10)-C(11)	1.428(4)	C(39)-C(40)	1.418(4)
C(11)-C(12)	1.418(4)	C(40)-C(41)	1.430(3)

Angles (°)

N(5)-Co(1)-N(1)	97.49(8)	N(2)-B(1)-N(6)	110.7(2)
N(5)-Co(1)-N(3)	94.14(8)	N(2)-B(1)-N(4)	108.19(19)
N(1)-Co(1)-N(3)	92.72(8)	N(6)-B(1)-N(4)	109.1(2)
N(5)-Co(1)-Cl(1)	112.77(6)	C(1)-N(1)-N(2)	106.41(19)
N(1)-Co(1)-Cl(1)	123.50(6)	C(1)-N(1)-Co(1)	142.64(17)
N(3)-Co(1)-Cl(1)	128.90(6)	N(2)-N(1)-Co(1)	109.86(14)

C(3)-N(2)-N(1)	109.4(2)	C(16)-C(15)-C(27)	127.2(2)
C(3)-N(2)-B(1)	129.4(2)	C(17)-C(16)-C(15)	106.1(2)
N(1)-N(2)-B(1)	121.17(19)	N(4)-C(17)-C(16)	108.0(2)
C(15)-N(3)-N(4)	106.94(19)	N(4)-C(17)-C(28)	122.9(2)
C(15)-N(3)-Co(1)	143.39(16)	C(16)-C(17)-C(28)	129.1(2)
N(4)-N(3)-Co(1)	109.45(14)	C(22)-C(18)-C(19)	108.4(3)
C(17)-N(4)-N(3)	109.28(19)	C(20)-C(19)-C(18)	108.2(3)
C(17)-N(4)-B(1)	129.5(2)	C(19)-C(20)-C(21)	108.2(3)
N(3)-N(4)-B(1)	120.59(18)	C(20)-C(21)-C(22)	107.5(3)
C(29)-N(5)-N(6)	106.30(19)	C(18)-C(22)-C(21)	107.6(3)
C(29)-N(5)-Co(1)	140.36(17)	C(24)-C(23)-C(27)	108.6(2)
N(6)-N(5)-Co(1)	109.98(14)	C(25)-C(24)-C(23)	108.0(2)
C(31)-N(6)-N(5)	109.60(19)	C(26)-C(25)-C(24)	108.2(2)
C(31)-N(6)-B(1)	130.4(2)	C(25)-C(26)-C(27)	108.1(2)
N(5)-N(6)-B(1)	119.93(18)	C(23)-C(27)-C(26)	107.1(2)
N(1)-C(1)-C(2)	109.8(2)	C(23)-C(27)-C(15)	128.8(2)
N(1)-C(1)-C(13)	124.8(2)	C(26)-C(27)-C(15)	124.1(2)
C(2)-C(1)-C(13)	125.3(2)	N(5)-C(29)-C(30)	109.6(2)
C(3)-C(2)-C(1)	106.2(2)	N(5)-C(29)-C(41)	122.7(2)
N(2)-C(3)-C(2)	108.3(2)	C(30)-C(29)-C(41)	127.6(2)
N(2)-C(3)-C(14)	122.3(2)	C(31)-C(30)-C(29)	106.2(2)
C(2)-C(3)-C(14)	129.4(2)	N(6)-C(31)-C(30)	108.2(2)
C(5)-C(4)-C(8)	107.7(3)	N(6)-C(31)-C(42)	122.4(2)
C(4)-C(5)-C(6)	108.2(3)	C(30)-C(31)-C(42)	129.4(2)
C(5)-C(6)-C(7)	107.8(3)	C(33)-C(32)-C(36)	108.5(3)
C(8)-C(7)-C(6)	107.6(3)	C(32)-C(33)-C(34)	108.0(3)
C(7)-C(8)-C(4)	108.6(3)	C(35)-C(34)-C(33)	108.0(3)
C(13)-C(9)-C(10)	108.2(2)	C(34)-C(35)-C(36)	108.0(3)
C(11)-C(10)-C(9)	107.9(3)	C(32)-C(36)-C(35)	107.6(3)
C(12)-C(11)-C(10)	108.2(3)	C(38)-C(37)-C(41)	108.4(2)
C(11)-C(12)-C(13)	108.2(3)	C(37)-C(38)-C(39)	107.7(2)
C(9)-C(13)-C(12)	107.5(2)	C(40)-C(39)-C(38)	108.2(2)
C(9)-C(13)-C(1)	128.6(2)	C(39)-C(40)-C(41)	108.0(2)
C(12)-C(13)-C(1)	123.6(2)	C(37)-C(41)-C(40)	107.8(2)
N(3)-C(15)-C(16)	109.6(2)	C(37)-C(41)-C(29)	128.2(2)
N(3)-C(15)-C(27)	123.2(2)	C(40)-C(41)-C(29)	123.9(2)

3.2.6 Synthesis and Characterization of TpFc,iPrCo(II) Halide Complexes.

$Tp^{Fc,iPr}CoI$ (**13**). was readily accessible by metathesis of anhydrous CoI_2 with $Tp^{Fc,iPr}Tl$ in THF at room temperature. Subsequent work-up of the reaction mixture and recrystallization from a cooled solution of the metal complex in a THF/pentane mixture, produced green crystals of **13** in 71% isolated yield. Its ^1H NMR spectrum in C_6D_6 had six well resolved resonances that are assigned to the protons of the $Tp^{Fc,iPr}$ ligand. X-ray crystallographic analysis (Figure 3.11) reveals the Tp ligand bound κ^3 to the pseudotetrahedral Co center with the fourth coordination site occupied by the I atom. Compound **13** has a Co-I distance of 2.5233(8) Å (Table 3.7). However in an unexpected development, when compound **13** was crystallized from chloroform it quantitatively underwent halide exchange accompanied by borotropic rearrangement yielding $Tp^{Fc,iPr*}CoCl$ (**14**) (Scheme 3.6). **14** is also accessible by the salt metathesis of the symmetric $Tp^{Fc,iPr}Tl$ with $CoCl_2$ in THF at room temperature. $Tp^{Fc,iPr*}CoCl$ maintains a pseudo tetrahedral geometry in the solid state (Figure 3.12) despite the rearrangement. To investigate the scope of N-confusion in the chloride compounds of the first-row transition series, several other examples of $Tp^{Fc,iPr}MCl$ (M: Cr, Mn, Zn) compounds have been synthesized all of which display the N-confused motif (Figures A2.1 - 3). However, iodide complexes, such as the $Tp^{Fc,iPr}CoI$ and $Tp^{Fc,iPr}FeI(THF)$ (Figure A2.4), remain symmetric. The isolations of several N-confused chloride complexes suggests that rearrangement of the $Tp^{Fc,iPr}MCl$ complexes is ubiquitous throughout the series and not specific to the cobalt case. This unusual room temperature isomerization differs from the borotropic rearrangements of Tp^{iPr} and $Tp^{iPr,4-Br}$, which undergo thermal isomerization in refluxing toluene to the octahedral geometry by rotating one of the *iso*-propyl substituents to the 5-position.[11] N-confusion in these cases can be attributed to the steric bulk of the co-ligand. In the case of iodide, The average N-N-Co bond angle is 109.5(3)° (Table 3.7),

compared to 111.3(2)° in the case of **14** (Table 3.8). The differences in the average N-N-Co bond angle may suggest that the steric interaction between a larger co-ligand causes the Fc moieties to be pushed further away from the co-ligand which, in turn, causes steric crowding between the substituents in the 5-position leaving less room for rearrangement. However, the smaller co-ligand alleviates this strain allowing a relaxation in the steric interaction between the *iso*-propyl groups, allowing room for the borotropic rearrangement to occur (Figure 3.13). This is also apparent in the average distance between the ipso carbons for the Fc moieties (6.472 Å in $Tp^{Fc,iPr}CoI$ (**13**)) and the average distance between the ipso carbons of the Fc moieties and the tertiary carbon of the *iso*-propyl group (6.401 Å in $Tp^{Fc,iPr*}CoCl$ (**14**)) which surround the Co metal center. Borotropic rearrangement only occurs at room temperature when the difference in steric bulk of the 3 and 5-position on the pyrazolyl ring is less pronounced. The space filling model for **13** and **14** (Figure 3.14) show that in the case of the **13**, the *iso*-propyl groups are closer together causing more steric crowding around the boron. However, in the space filling model of **14**, the interaction between the iso-propyl groups has been relaxed.

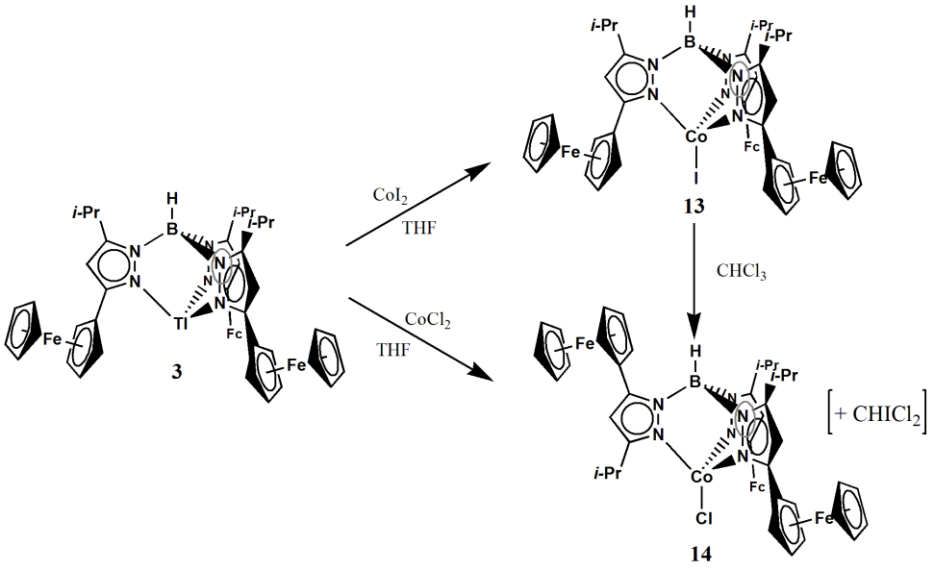

Scheme 3.6: Synthesis of $Tp^{Fc,iPr}CoX$ complexes.

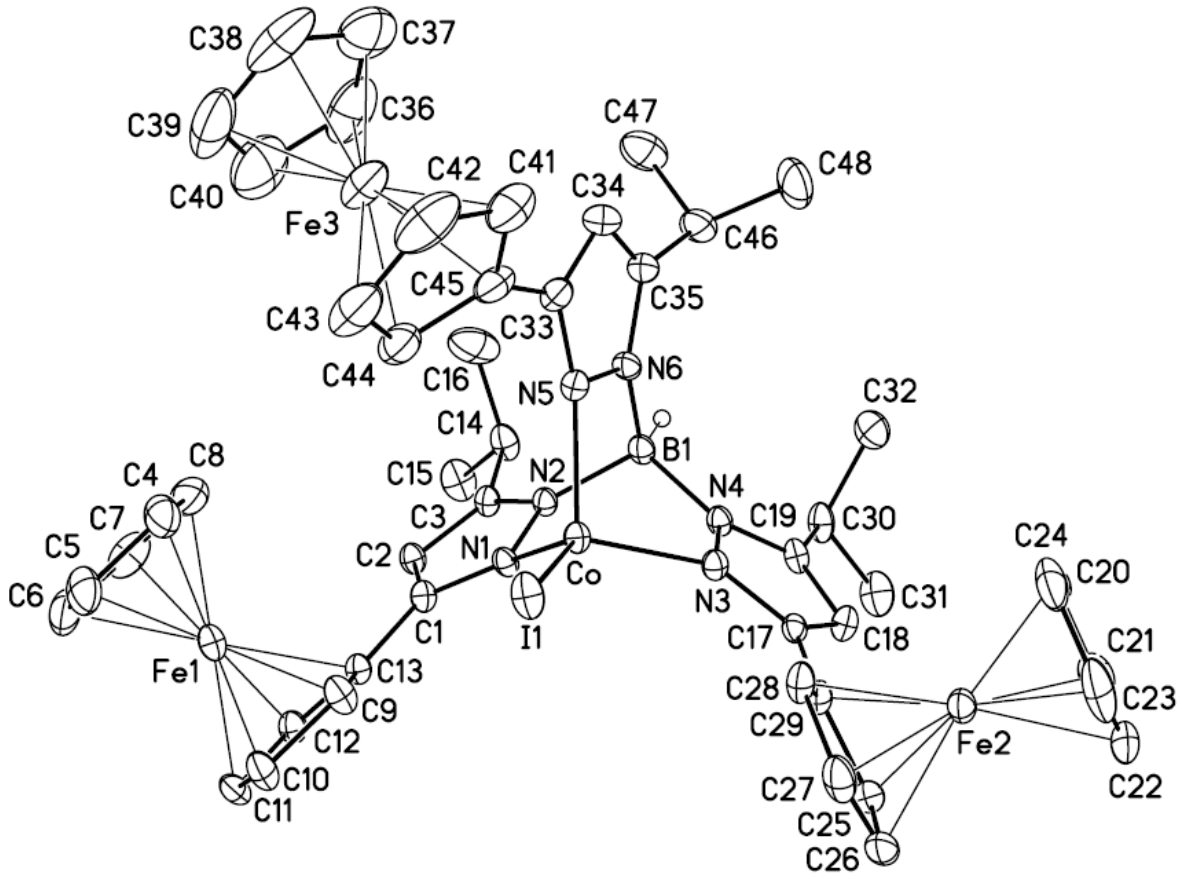

Figure 3.11: Molecular structure of $Tp^{Fc,iPr}CoI$ (13) at the 30% probability level. Hydrogen atoms (except the boron bound hydrogen, H1B) have been removed for clarity.

Table 3.7: Selected interatomic distances (Å) and angles (°) for $Tp^{Fc,iPr}CoI$ (13).

Distances (Å)

Co-N(3)	2.021(3)	C(17)-C(18)	1.401(6)
Co-N(1)	2.033(3)	C(17)-C(29)	1.466(6)
Co-N(5)	2.035(4)	C(18)-C(19)	1.380(6)
Co-I(1)	2.5233(8)	C(19)-C(30)	1.510(6)
B(1)-N(6)	1.545(6)	C(20)-C(21)	1.374(8)
B(1)-N(4)	1.547(6)	C(20)-C(24)	1.422(8)
B(1)-N(2)	1.554(6)	C(21)-C(22)	1.374(8)
N(1)-C(1)	1.337(5)	C(22)-C(23)	1.395(8)
N(1)-N(2)	1.387(4)	C(23)-C(24)	1.429(9)
N(2)-C(3)	1.360(5)	C(25)-C(26)	1.417(7)
N(3)-C(17)	1.351(5)	C(25)-C(29)	1.434(6)
N(3)-N(4)	1.393(4)	C(26)-C(27)	1.404(8)
N(4)-C(19)	1.356(5)	C(27)-C(28)	1.420(7)
N(5)-C(33)	1.343(6)	C(28)-C(29)	1.427(6)
N(5)-N(6)	1.384(5)	C(30)-C(31)	1.523(7)
N(6)-C(35)	1.360(6)	C(30)-C(32)	1.532(7)
C(1)-C(2)	1.403(6)	C(33)-C(34)	1.393(7)
C(1)-C(13)	1.466(6)	C(33)-C(45)	1.456(7)
C(2)-C(3)	1.372(6)	C(34)-C(35)	1.374(7)
C(3)-C(14)	1.516(6)	C(35)-C(46)	1.515(7)
C(4)-C(5)	1.395(7)	C(36)-C(37)	1.403(11)
C(4)-C(8)	1.403(8)	C(36)-C(40)	1.427(12)
C(5)-C(6)	1.400(8)	C(37)-C(38)	1.397(11)
C(6)-C(7)	1.397(8)	C(38)-C(39)	1.407(13)
C(7)-C(8)	1.419(9)	C(39)-C(40)	1.439(13)
C(9)-C(10)	1.410(6)	C(41)-C(42)	1.386(9)
C(9)-C(13)	1.428(6)	C(41)-C(45)	1.428(8)
C(10)-C(11)	1.422(6)	C(42)-C(43)	1.438(11)
C(11)-C(12)	1.411(6)	C(43)-C(44)	1.386(8)
C(12)-C(13)	1.435(6)	C(44)-C(45)	1.433(8)
C(14)-C(16)	1.519(8)	C(46)-C(47)	1.504(8)
C(14)-C(15)	1.534(7)	C(46)-C(48)	1.539(8)

Angles (°)

N(3)-Co-N(1)	95.47(13)	N(1)-Co-I(1)	129.47(9)
N(3)-Co-N(5)	97.90(14)	N(5)-Co-I(1)	114.43(11)
N(1)-Co-N(5)	91.57(14)	N(6)-B(1)-N(4)	110.0(4)
N(3)-Co-I(1)	120.67(10)	N(6)-B(1)-N(2)	107.7(3)

N(4)-B(1)-N(2)	110.1(3)	C(18)-C(17)-C(29)	126.3(4)
C(1)-N(1)-N(2)	107.0(3)	C(19)-C(18)-C(17)	106.6(4)
C(1)-N(1)-Co	141.8(3)	N(4)-C(19)-C(18)	108.0(4)
N(2)-N(1)-Co	108.5(2)	N(4)-C(19)-C(30)	123.3(4)
C(3)-N(2)-N(1)	108.8(3)	C(18)-C(19)-C(30)	128.7(4)
C(3)-N(2)-B(1)	130.0(3)	C(21)-C(20)-C(24)	108.4(5)
N(1)-N(2)-B(1)	121.2(3)	C(20)-C(21)-C(22)	109.4(5)
C(17)-N(3)-N(4)	106.7(3)	C(21)-C(22)-C(23)	108.7(5)
C(17)-N(3)-Co	141.5(3)	C(22)-C(23)-C(24)	107.6(5)
N(4)-N(3)-Co	109.6(2)	C(20)-C(24)-C(23)	106.0(5)
C(19)-N(4)-N(3)	109.3(3)	C(26)-C(25)-C(29)	107.4(5)
C(19)-N(4)-B(1)	130.2(4)	C(27)-C(26)-C(25)	108.6(4)
N(3)-N(4)-B(1)	120.5(3)	C(26)-C(27)-C(28)	108.8(4)
C(33)-N(5)-N(6)	107.0(4)	C(27)-C(28)-C(29)	107.3(4)
C(33)-N(5)-Co	140.9(3)	C(28)-C(29)-C(25)	107.9(4)
N(6)-N(5)-Co	110.4(3)	C(28)-C(29)-C(17)	128.3(4)
C(35)-N(6)-N(5)	109.4(4)	C(25)-C(29)-C(17)	123.8(4)
C(35)-N(6)-B(1)	132.0(4)	C(19)-C(30)-C(31)	111.4(4)
N(5)-N(6)-B(1)	118.0(3)	C(19)-C(30)-C(32)	109.6(4)
N(1)-C(1)-C(2)	109.8(4)	C(31)-C(30)-C(32)	111.6(4)
N(1)-C(1)-C(13)	124.4(4)	N(5)-C(33)-C(34)	109.0(4)
C(2)-C(1)-C(13)	125.7(4)	N(5)-C(33)-C(45)	121.3(4)
C(3)-C(2)-C(1)	106.0(4)	C(34)-C(33)-C(45)	129.7(5)
N(2)-C(3)-C(2)	108.5(4)	C(35)-C(34)-C(33)	107.2(5)
N(2)-C(3)-C(14)	123.0(4)	N(6)-C(35)-C(34)	107.3(4)
C(2)-C(3)-C(14)	128.4(4)	N(6)-C(35)-C(46)	123.6(5)
C(5)-C(4)-C(8)	108.0(5)	C(34)-C(35)-C(46)	129.0(5)
C(4)-C(5)-C(6)	108.4(5)	C(37)-C(36)-C(40)	110.2(8)
C(7)-C(6)-C(5)	108.3(5)	C(38)-C(37)-C(36)	107.0(9)
C(6)-C(7)-C(8)	107.5(6)	C(37)-C(38)-C(39)	109.4(9)
C(4)-C(8)-C(7)	107.8(5)	C(38)-C(39)-C(40)	108.2(9)
C(10)-C(9)-C(13)	108.6(4)	C(36)-C(40)-C(39)	105.1(9)
C(9)-C(10)-C(11)	108.3(4)	C(42)-C(41)-C(45)	108.7(6)
C(12)-C(11)-C(10)	107.8(4)	C(41)-C(42)-C(43)	108.2(6)
C(11)-C(12)-C(13)	108.7(4)	C(44)-C(43)-C(42)	107.8(6)
C(9)-C(13)-C(12)	106.6(4)	C(43)-C(44)-C(45)	108.9(6)
C(9)-C(13)-C(1)	129.8(4)	C(41)-C(45)-C(44)	106.5(5)
C(12)-C(13)-C(1)	123.5(4)	C(41)-C(45)-C(33)	126.7(5)
C(3)-C(14)-C(16)	109.9(4)	C(44)-C(45)-C(33)	126.8(5)
C(3)-C(14)-C(15)	111.3(4)	C(47)-C(46)-C(35)	112.4(5)
C(16)-C(14)-C(15)	110.2(4)	C(47)-C(46)-C(48)	109.6(5)
N(3)-C(17)-C(18)	109.3(4)	C(35)-C(46)-C(48)	108.8(5)
N(3)-C(17)-C(29)	124.3(4)		

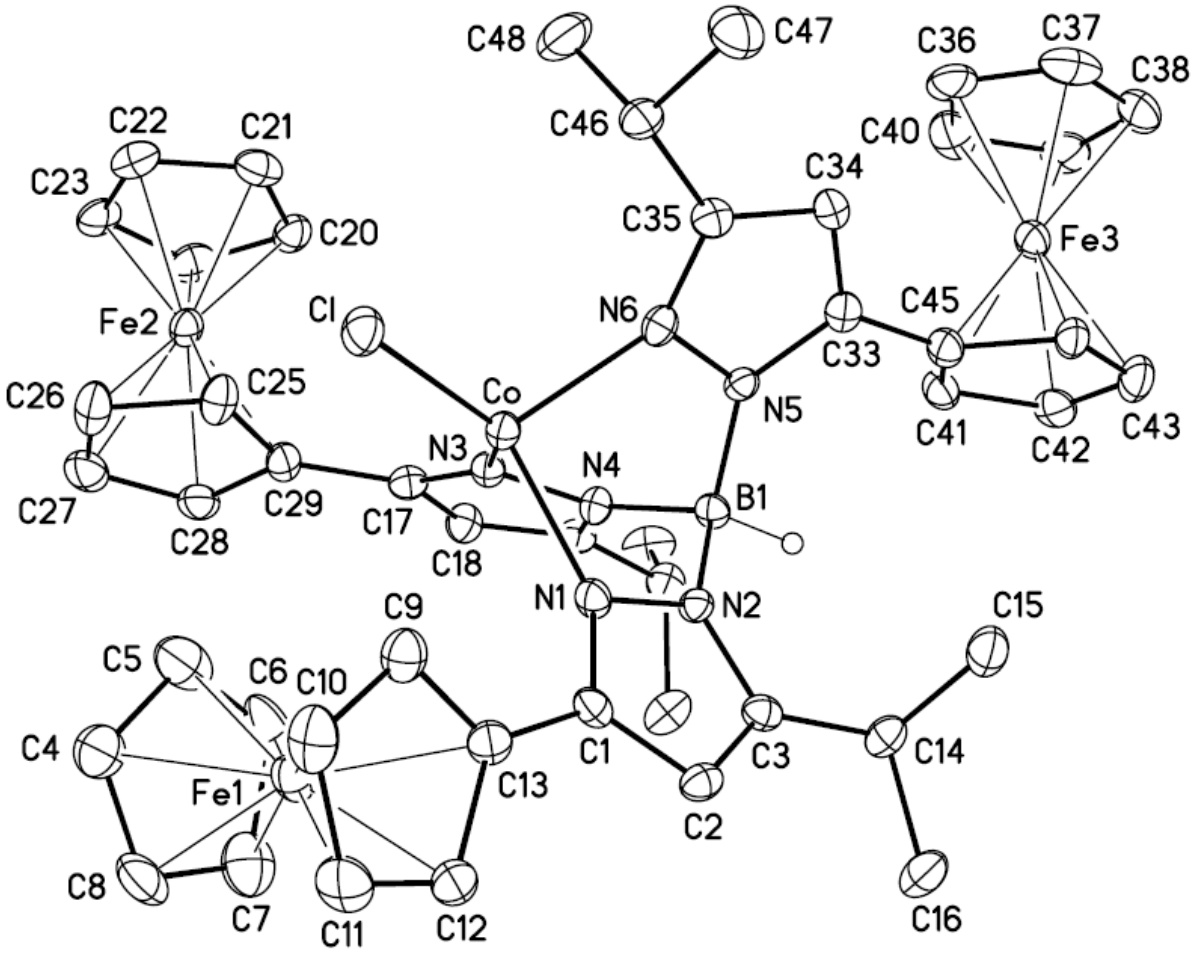

Figure 3.12: Molecular structure of $Tp^{Fc,iPr*}CoCl$ (14) at the 30% probability level. Hydrogen atoms (except the boron bound hydrogen, H1B) have been removed for clarity.

Table 3.8: Selected interatomic distances (Å) and angles (°) for $Tp^{Fc,iPr*}CoCl$ (14).

Distances (Å)

Co-N(6)	2.017(4)	C(17)-C(29)	1.448(6)
Co-N(1)	2.030(4)	C(18)-C(19)	1.372(7)
Co-N(3)	2.029(4)	C(19)-C(30)	1.485(7)
Co-Cl	2.2114(15)	C(20)-C(21)	1.416(7)
B(1)-N(5)	1.531(6)	C(20)-C(24)	1.430(7)
B(1)-N(2)	1.555(6)	C(21)-C(22)	1.409(8)
B(1)-N(4)	1.553(6)	C(22)-C(23)	1.378(8)
N(1)-C(1)	1.352(6)	C(23)-C(24)	1.404(7)
N(1)-N(2)	1.373(5)	C(25)-C(26)	1.412(7)
N(2)-C(3)	1.361(5)	C(25)-C(29)	1.419(7)
N(3)-C(17)	1.347(6)	C(26)-C(27)	1.417(8)
N(3)-N(4)	1.397(5)	C(27)-C(28)	1.403(8)
N(4)-C(19)	1.364(6)	C(28)-C(29)	1.432(7)
N(5)-C(33)	1.362(5)	C(30)-C(32)	1.527(7)
N(5)-N(6)	1.397(5)	C(30)-C(31)	1.535(7)
N(6)-C(35)	1.338(6)	C(33)-C(34)	1.353(6)
C(1)-C(2)	1.397(6)	C(33)-C(45)	1.478(7)
C(1)-C(13)	1.465(6)	C(34)-C(35)	1.398(6)
C(2)-C(3)	1.365(6)	C(35)-C(46)	1.488(6)
C(3)-C(14)	1.513(7)	C(36)-C(37)	1.407(9)
C(4)-C(5)	1.391(8)	C(36)-C(40)	1.399(9)
C(4)-C(8)	1.406(8)	C(37)-C(38)	1.396(8)
C(5)-C(6)	1.384(10)	C(38)-C(39)	1.402(8)
C(6)-C(7)	1.426(9)	C(39)-C(40)	1.414(8)
C(7)-C(8)	1.386(9)	C(41)-C(42)	1.414(7)
C(9)-C(10)	1.408(7)	C(41)-C(45)	1.429(7)
C(9)-C(13)	1.415(7)	C(42)-C(43)	1.398(7)
C(10)-C(11)	1.425(8)	C(43)-C(44)	1.411(7)
C(11)-C(12)	1.400(8)	C(44)-C(45)	1.430(7)
C(12)-C(13)	1.434(7)	C(46)-C(48)	1.513(7)
C(14)-C(16)	1.523(7)	C(46)-C(47)	1.503(7)
C(14)-C(15)	1.518(7)	C(49)-C(50)	1.500(10)
C(17)-C(18)	1.383(7)	C(51)-C(52)	1.487(10)

Angles (°)

N(6)-Co-N(1)	96.56(16)	N(6)-Co-Cl	110.51(12)
N(6)-Co-N(3)	94.52(16)	N(1)-Co-Cl	125.81(12)
N(1)-Co-N(3)	91.68(16)	N(3)-Co-Cl	129.73(12)

N(5)-B(1)-N(2)	110.0(4)	C(4)-C(8)-Fe(1)	69.4(3)
N(5)-B(1)-N(4)	109.9(4)	C(10)-C(9)-C(13)	109.1(5)
N(2)-B(1)-N(4)	108.6(4)	C(10)-C(9)-Fe(1)	70.7(3)
C(49)-O(1)-C(51)	116.4(7)	C(13)-C(9)-Fe(1)	70.5(3)
C(1)-N(1)-N(2)	106.7(4)	C(9)-C(10)-C(11)	107.2(5)
C(1)-N(1)-Co	142.2(3)	C(9)-C(10)-Fe(1)	68.7(3)
N(2)-N(1)-Co	110.8(3)	C(11)-C(10)-Fe(1)	68.8(3)
C(3)-N(2)-N(1)	109.7(4)	C(12)-C(11)-C(10)	108.7(5)
C(3)-N(2)-B(1)	129.5(4)	C(12)-C(11)-Fe(1)	70.0(3)
N(1)-N(2)-B(1)	120.4(4)	C(10)-C(11)-Fe(1)	70.2(3)
C(17)-N(3)-N(4)	107.3(4)	C(11)-C(12)-C(13)	108.0(5)
C(17)-N(3)-Co	142.0(3)	C(11)-C(12)-Fe(1)	69.6(3)
N(4)-N(3)-Co	110.2(3)	C(13)-C(12)-Fe(1)	69.8(3)
C(19)-N(4)-N(3)	108.6(4)	C(9)-C(13)-C(12)	107.0(5)
C(19)-N(4)-B(1)	130.3(4)	C(9)-C(13)-C(1)	129.7(5)
N(3)-N(4)-B(1)	121.0(4)	C(12)-C(13)-C(1)	123.3(5)
C(33)-N(5)-N(6)	107.4(4)	C(9)-C(13)-Fe(1)	68.7(3)
C(33)-N(5)-B(1)	133.7(4)	C(12)-C(13)-Fe(1)	69.0(3)
N(6)-N(5)-B(1)	118.3(4)	C(1)-C(13)-Fe(1)	128.2(3)
C(35)-N(6)-N(5)	107.8(4)	C(3)-C(14)-C(16)	110.0(4)
C(35)-N(6)-Co	139.0(3)	C(3)-C(14)-C(15)	109.9(4)
N(5)-N(6)-Co	113.0(3)	C(16)-C(14)-C(15)	110.3(4)
N(1)-C(1)-C(2)	109.0(4)	N(3)-C(17)-C(18)	108.6(4)
N(1)-C(1)-C(13)	124.0(4)	N(3)-C(17)-C(29)	122.3(4)
C(2)-C(1)-C(13)	127.0(4)	C(18)-C(17)-C(29)	128.9(5)
C(3)-C(2)-C(1)	106.9(4)	C(19)-C(18)-C(17)	108.2(4)
N(2)-C(3)-C(2)	107.7(4)	N(4)-C(19)-C(18)	107.3(4)
N(2)-C(3)-C(14)	122.6(4)	N(4)-C(19)-C(30)	123.2(4)
C(2)-C(3)-C(14)	129.1(4)	C(18)-C(19)-C(30)	129.3(4)
C(5)-C(4)-C(8)	108.1(7)	C(21)-C(20)-C(24)	107.4(5)
C(5)-C(4)-Fe(1)	69.7(4)	C(22)-C(21)-C(20)	106.9(5)
C(8)-C(4)-Fe(1)	70.0(3)	C(23)-C(22)-C(21)	109.8(5)
C(6)-C(5)-C(4)	108.7(7)	C(22)-C(23)-C(24)	108.2(5)
C(6)-C(5)-Fe(1)	70.5(4)	C(23)-C(24)-C(20)	107.7(5)
C(4)-C(5)-Fe(1)	70.0(3)	C(26)-C(25)-C(29)	108.9(5)
C(5)-C(6)-C(7)	107.4(6)	C(27)-C(26)-C(25)	108.0(5)
C(5)-C(6)-Fe(1)	69.5(4)	C(28)-C(27)-C(26)	107.7(5)
C(7)-C(6)-Fe(1)	69.6(4)	C(27)-C(28)-C(29)	109.2(5)
C(8)-C(7)-C(6)	107.8(7)	C(25)-C(29)-C(28)	106.2(5)
C(8)-C(7)-Fe(1)	69.9(4)	C(25)-C(29)-C(17)	129.4(5)
C(6)-C(7)-Fe(1)	69.3(4)	C(28)-C(29)-C(17)	124.4(5)
C(7)-C(8)-C(4)	107.9(6)	C(19)-C(30)-C(32)	111.8(4)
C(7)-C(8)-Fe(1)	70.2(4)	C(19)-C(30)-C(31)	110.3(4)

C(32)-C(30)-C(31)	110.7(4)	C(38)-C(39)-C(40)	108.0(6)
C(34)-C(33)-N(5)	109.2(4)	C(36)-C(40)-C(39)	107.2(6)
C(34)-C(33)-C(45)	129.4(5)	C(42)-C(41)-C(45)	108.5(5)
N(5)-C(33)-C(45)	121.4(4)	C(43)-C(42)-C(41)	108.2(5)
C(33)-C(34)-C(35)	107.0(4)	C(42)-C(43)-C(44)	108.6(5)
N(6)-C(35)-C(34)	108.7(4)	C(43)-C(44)-C(45)	108.4(5)
N(6)-C(35)-C(46)	122.6(4)	C(44)-C(45)-C(41)	106.3(5)
C(34)-C(35)-C(46)	128.5(5)	C(44)-C(45)-C(33)	124.3(5)
C(37)-C(36)-C(40)	108.8(6)	C(41)-C(45)-C(33)	129.3(5)
C(36)-C(37)-C(38)	107.6(6)	C(35)-C(46)-C(48)	110.4(4)
C(39)-C(38)-C(37)	108.4(6)	C(35)-C(46)-C(47)	112.1(4)

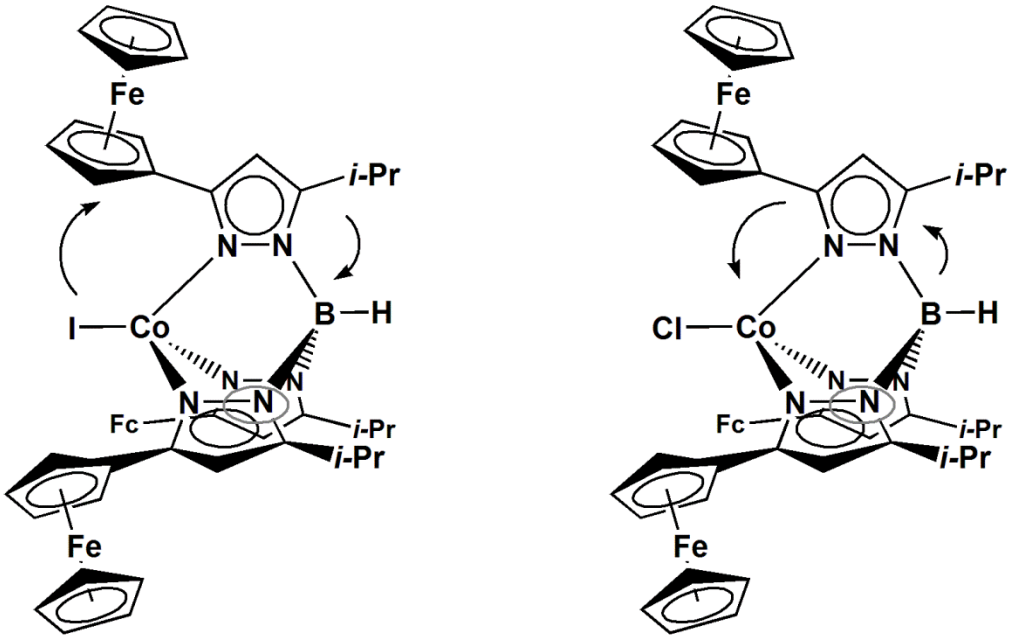

Figure 3.13: Co-ligand steric effect on $Tp^{Fc,iPr}Co$ complexes.

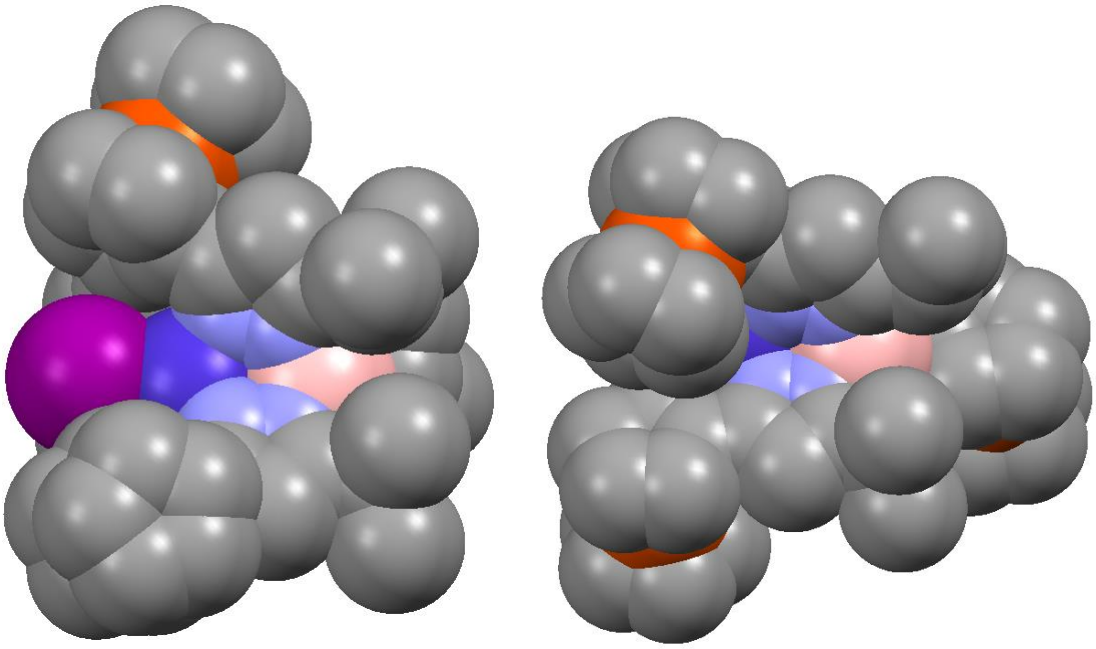

Figure 3.14: Space filling model of $Tp^{Fc,iPr}CoI$ (14) (left) and $Tp^{Fc,iPr*}CoCl$ (15) (right)

3.2.7 Thermal Isomerization of $Tp^{Fc,Me}CoI$.

The unusual room temperature isomerization of $Tp^{Fc,iPr}CoI$ to $Tp^{Fc,iPr*}CoCl$ complex when exposed to chloroform led to the investigation of the rearrangement of the analogus $Tp^{Fc,Me}$ ligand. It had already been established that $Tp^{Fc,Me}CoI$ does not suffer from halide exchange that plagues the *iso*-propyl analog when recrystallized from $CHCl_3$. Metathesis of the $Tp^{Fc,Me}$ ligand with CoI_2 in refluxing CH_2Cl_2 leads to the clean isolation of $Tp^{Fc,Me}CoI$. However, when a solid sample of $Tp^{Fc,Me}CoI$ is heated under vacuum to 250 °C for 1 minute the appearance of new resonances in the ^1H NMR spectrum was observed. Likewise, after 24 hours at 100 ^0C in C_6D_6 the NMR spectrum begins to show signs of borotropic rearrangement accompanied by other unidentified decomposition products. After a period of 72 hrs at 80 °C, the major product, $Tp^{Fc,Me*}CoI$ (**15**), begins to crystallize out of solution. The N-confusion of $Tp^{Fc,Me}CoI$ to

$Tp^{Fc,Me*}CoI$ differs from what is considered a thermodynamic versus kinetic product in the case of the rearrangement of $Tp^{Fc,Me*}Tl$ to $Tp^{Fc,Me}Tl$.

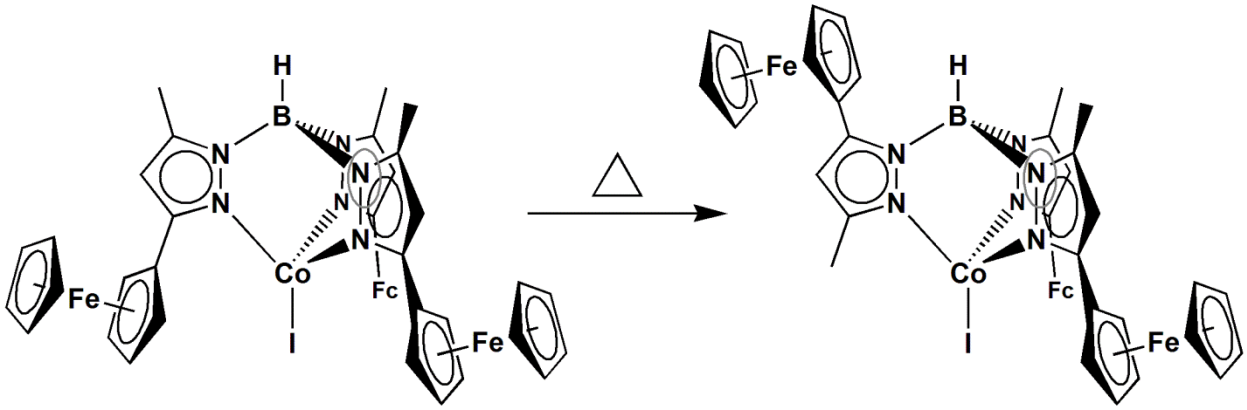

Scheme 3.7: Thermal isomerization of $Tp^{Fc,Me}CoI$ (11) to $Tp^{Fc,Me*}CoI$.

X-ray crystallographic analysis confirms the identity of the major product of this rearrangement as the singly N-confused $Tp^{Fc,Me*}CoI$ (Figure 3.15). $Tp^{Fc,Me*}CoI$ crystallizes in the triclinic spacegroup P-1 and shows the same four coordinate pseudo tetrahedral geometry as its $Tp^{Fc,Me}CoI$ analog with a Co-I bond distance that is negligibly elongated from 2.5443(4) Å in the symmetric ligand to 2.5716(10) Å in the N-confused $Tp^{Fc,Me*}CoI$ complex (Table 3.9).

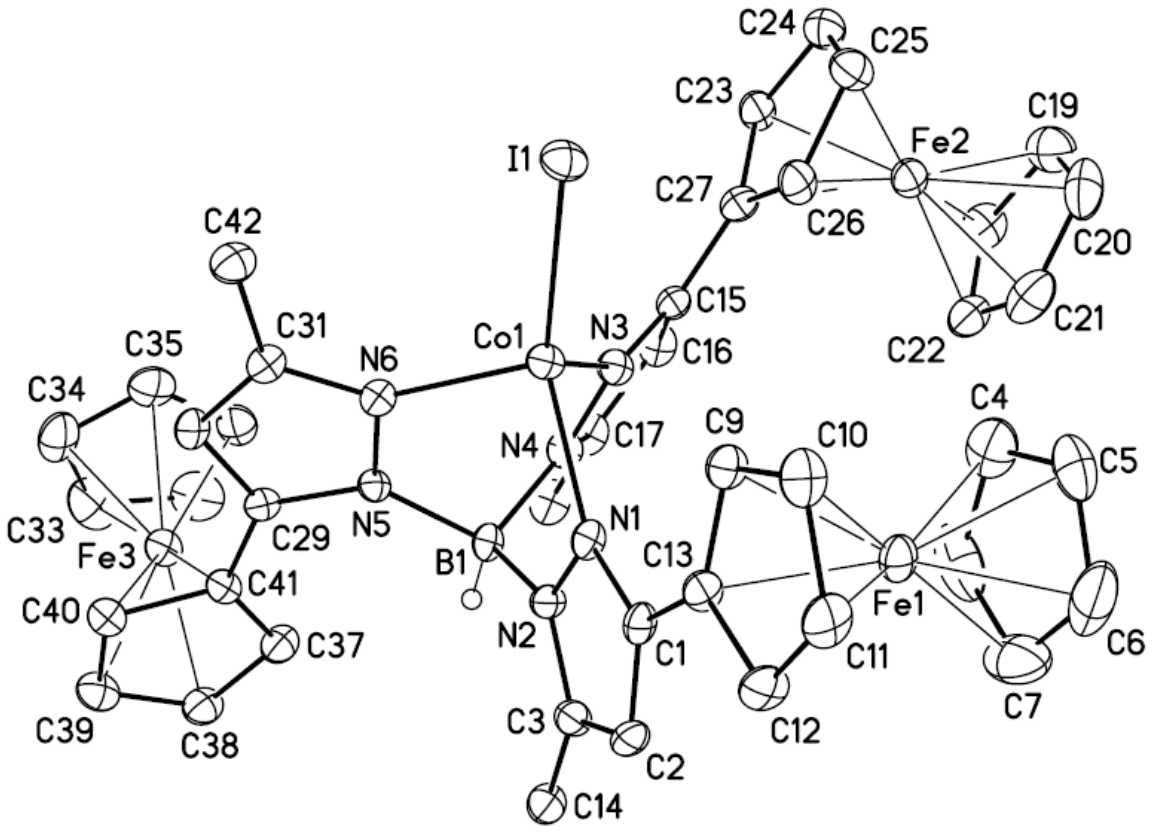

Figure 3.15: Molecular structure of $Tp^{Fc,Me*}CoI$ (15) at the 30% probability level. Hydrogen atoms (except the boron bound hydrogen, H1B) have been removed for clarity.

Table 3.9: Selected interatomic distances (Å) and angles (°) for $Tp^{Fc,Me*}$Col (15).

Distances (Å)

Co(1)-N(6)	2.033(4)	C(12)-C(13)	1.452(7)
Co(1)-N(3)	2.035(5)	C(15)-C(16)	1.395(8)
Co(1)-N(1)	2.060(4)	C(15)-C(27)	1.474(8)
Co(1)-I(1)	2.5716(10)	C(16)-C(17)	1.395(8)
B(1)-N(2)	1.547(7)	C(17)-C(28)	1.480(8)
B(1)-N(4)	1.553(7)	C(18)-C(22)	1.393(9)
B(1)-N(5)	1.554(7)	C(18)-C(19)	1.394(10)
N(1)-C(1)	1.345(7)	C(19)-C(20)	1.411(10)
N(1)-N(2)	1.396(6)	C(20)-C(21)	1.407(10)
N(2)-C(3)	1.359(7)	C(21)-C(22)	1.423(10)
N(3)-C(15)	1.352(7)	C(23)-C(24)	1.428(8)
N(3)-N(4)	1.377(6)	C(23)-C(27)	1.437(8)
N(4)-C(17)	1.356(7)	C(24)-C(25)	1.411(9)
N(5)-C(29)	1.370(6)	C(25)-C(26)	1.426(8)
N(5)-N(6)	1.378(6)	C(26)-C(27)	1.413(8)
N(6)-C(31)	1.339(7)	C(29)-C(30)	1.398(7)
C(1)-C(2)	1.390(8)	C(29)-C(41)	1.469(7)
C(1)-C(13)	1.464(7)	C(30)-C(31)	1.379(7)
C(2)-C(3)	1.369(8)	C(31)-C(42)	1.501(7)
C(3)-C(14)	1.514(8)	C(32)-C(33)	1.382(10)
C(4)-C(5)	1.387(10)	C(32)-C(36)	1.404(10)
C(4)-C(8)	1.396(11)	C(33)-C(34)	1.442(11)
C(5)-C(6)	1.366(12)	C(34)-C(35)	1.415(10)
C(6)-C(7)	1.455(13)	C(35)-C(36)	1.411(9)
C(7)-C(8)	1.394(13)	C(37)-C(38)	1.423(8)
C(9)-C(13)	1.417(8)	C(37)-C(41)	1.436(8)
C(9)-C(10)	1.420(8)	C(38)-C(39)	1.421(8)
C(10)-C(11)	1.433(9)	C(39)-C(40)	1.404(8)
C(11)-C(12)	1.417(8)	C(40)-C(41)	1.445(7)

Angles (°)

N(6)-Co(1)-N(3)	96.07(18)	N(2)-B(1)-N(5)	108.9(4)
N(6)-Co(1)-N(1)	94.13(17)	N(4)-B(1)-N(5)	108.6(5)
N(3)-Co(1)-N(1)	91.90(18)	C(1)-N(1)-N(2)	106.8(4)
N(6)-Co(1)-I(1)	113.41(13)	C(1)-N(1)-Co(1)	144.6(4)
N(3)-Co(1)-I(1)	119.30(13)	N(2)-N(1)-Co(1)	108.5(3)
N(1)-Co(1)-I(1)	133.86(12)	C(3)-N(2)-N(1)	108.1(4)
N(2)-B(1)-N(4)	109.9(4)	C(3)-N(2)-B(1)	128.7(5)

N(1)-N(2)-B(1)	123.2(4)	N(4)-C(17)-C(16)	106.8(5)
C(15)-N(3)-N(4)	107.1(4)	N(4)-C(17)-C(28)	123.6(5)
C(15)-N(3)-Co(1)	140.2(4)	C(16)-C(17)-C(28)	129.5(5)
N(4)-N(3)-Co(1)	110.6(3)	C(22)-C(18)-C(19)	108.4(7)
C(17)-N(4)-N(3)	110.2(4)	C(18)-C(19)-C(20)	109.0(7)
C(17)-N(4)-B(1)	128.8(5)	C(21)-C(20)-C(19)	106.8(7)
N(3)-N(4)-B(1)	121.1(4)	C(20)-C(21)-C(22)	108.2(7)
C(29)-N(5)-N(6)	108.5(4)	C(18)-C(22)-C(21)	107.6(7)
C(29)-N(5)-B(1)	133.5(4)	C(24)-C(23)-C(27)	106.6(5)
N(6)-N(5)-B(1)	118.0(4)	C(25)-C(24)-C(23)	109.1(6)
C(31)-N(6)-N(5)	108.0(4)	C(24)-C(25)-C(26)	107.7(6)
C(31)-N(6)-Co(1)	137.9(4)	C(27)-C(26)-C(25)	108.2(5)
N(5)-N(6)-Co(1)	113.9(3)	C(26)-C(27)-C(23)	108.4(5)
N(1)-C(1)-C(2)	109.9(5)	C(26)-C(27)-C(15)	127.9(5)
N(1)-C(1)-C(13)	122.8(5)	C(23)-C(27)-C(15)	123.7(5)
C(2)-C(1)-C(13)	127.3(5)	N(5)-C(29)-C(30)	107.3(4)
C(3)-C(2)-C(1)	106.2(5)	N(5)-C(29)-C(41)	126.4(5)
N(2)-C(3)-C(2)	109.0(5)	C(30)-C(29)-C(41)	126.3(5)
N(2)-C(3)-C(14)	122.4(5)	C(31)-C(30)-C(29)	106.5(5)
C(2)-C(3)-C(14)	128.5(5)	N(6)-C(31)-C(30)	109.7(5)
C(5)-C(4)-C(8)	107.9(8)	N(6)-C(31)-C(42)	122.6(5)
C(6)-C(5)-C(4)	109.1(8)	C(30)-C(31)-C(42)	127.7(5)
C(5)-C(6)-C(7)	108.3(8)	C(33)-C(32)-C(36)	108.9(7)
C(8)-C(7)-C(6)	105.2(8)	C(32)-C(33)-C(34)	108.3(7)
C(7)-C(8)-C(4)	109.4(8)	C(35)-C(34)-C(33)	106.4(7)
C(13)-C(9)-C(10)	109.8(5)	C(36)-C(35)-C(34)	108.3(7)
C(9)-C(10)-C(11)	107.2(6)	C(32)-C(36)-C(35)	108.0(6)
C(12)-C(11)-C(10)	108.4(5)	C(38)-C(37)-C(41)	108.5(5)
C(11)-C(12)-C(13)	108.1(5)	C(39)-C(38)-C(37)	108.1(5)
C(9)-C(13)-C(12)	106.5(5)	C(40)-C(39)-C(38)	108.2(5)
C(9)-C(13)-C(1)	130.1(5)	C(39)-C(40)-C(41)	109.1(5)
C(12)-C(13)-C(1)	123.3(5)	C(37)-C(41)-C(40)	106.1(5)
N(3)-C(15)-C(27)	121.3(5)	C(37)-C(41)-C(29)	132.7(5)
C(16)-C(15)-C(27)	129.8(5)	C(40)-C(41)-C(29)	121.2(5)
C(15)-C(16)-C(17)	107.0(5)		

3.2.8 Syntheses and Characterization of Copper Carbonyl Complexes of $Tp^{Fc,R}$.

The copper carbonyl complexes of hydrotris(pyrazolyl)borate ligands have been employed to investigate the electronic effects of the ligand on the metal center. TpCu(CO) complexes can easily be synthesized by metathesis of a copper halide and the appropriate Tp ligand (Scheme 3.8) under an atmosphere of CO.

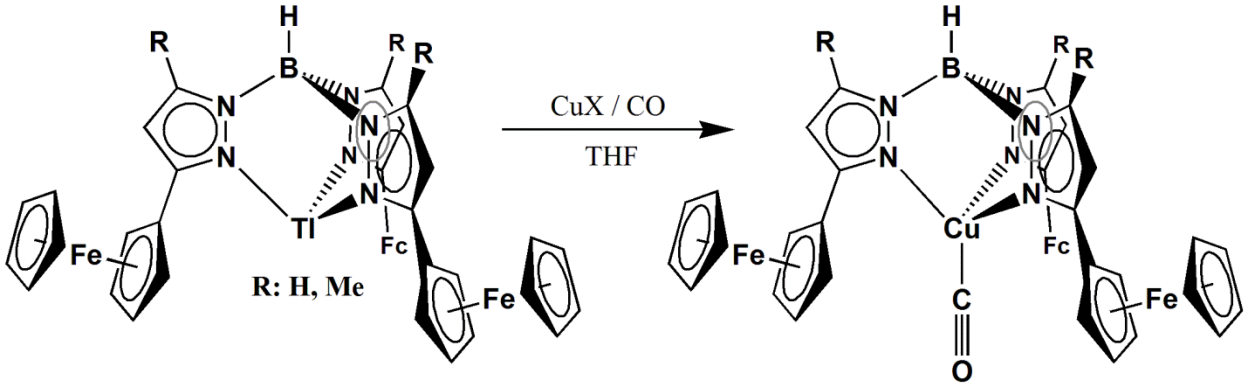

Scheme 3.8: Synthesis of the $Tp^{Fc}Cu(CO)$ (16) and $Tp^{Fc,Me}Cu(CO)$ (17).

$Tp^{Fc}Cu(CO)$ (**16**) was readily obtained through the metathesis of **7** with Cu(I) chloride or iodide in THF under an atmosphere of CO at room temperature. Subsequent work-up of the reaction mixture and recrystallization from THF, produced orange crystals of **16** in 55 % isolated yield. Its NMR spectrum is typical of a diamagnetic TpCu d^{10} complex with five pyrazole resonances signifying that the ligand remains symmetric. The X-ray structure determination revealed that **16** is a distorted tetrahedron (Figure 3.16).

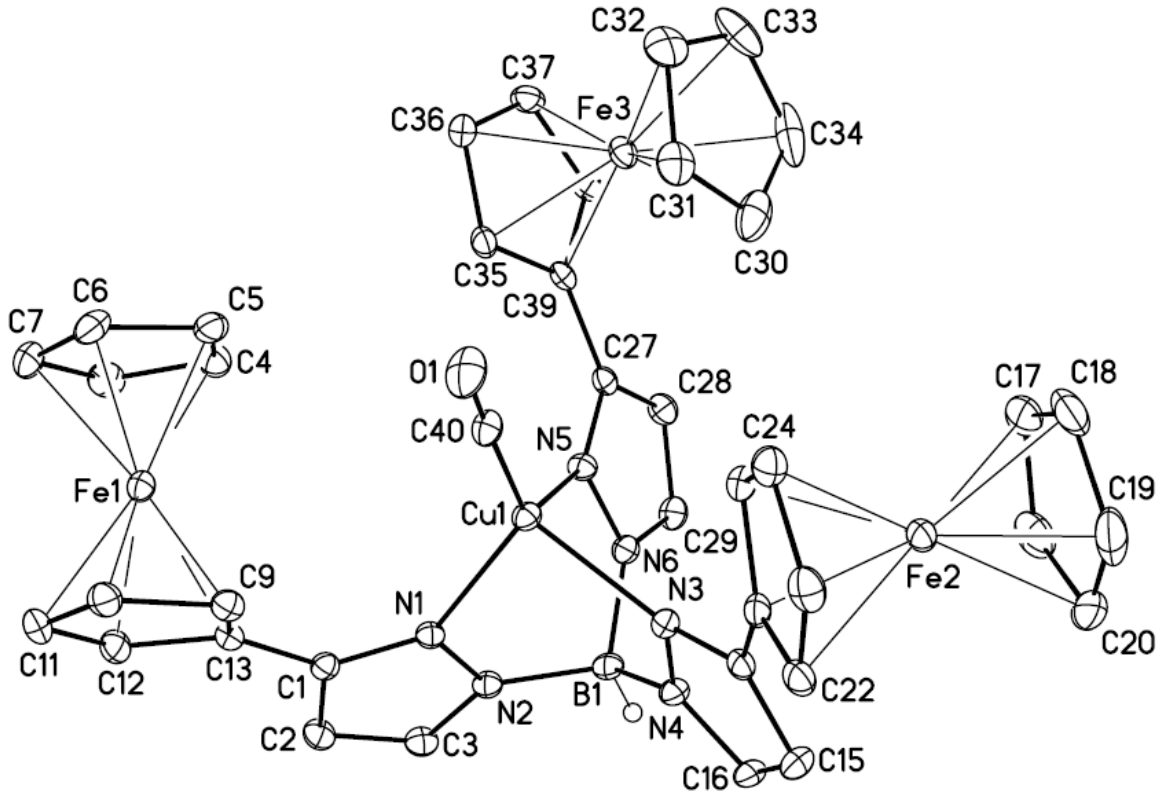

Figure 3.16: Molecular structure of $Tp^{Fc}Cu(CO)$ (16) at the 30% probability level. Hydrogen atoms (except the boron bound hydrogen, H1B) have been removed for clarity.

Table 3.10: Selected interatomic distances (Å) and angles (°) for $Tp^{Fc}Cu(CO)$ (16).

Distances (Å)

Cu(1)-C(40)	1.795(3)	C(11)-C(12)	1.427(3)
Cu(1)-N(1)	2.0654(19)	C(12)-C(13)	1.434(3)
Cu(1)-N(3)	2.082(2)	C(14)-C(15)	1.411(3)
Cu(1)-N(5)	2.085(2)	C(14)-C(26)	1.464(3)
O(1)-C(40)	1.129(3)	C(15)-C(16)	1.377(4)
B(1)-N(4)	1.548(3)	C(17)-C(18)	1.414(4)
B(1)-N(2)	1.547(3)	C(17)-C(21)	1.421(4)
B(1)-N(6)	1.549(3)	C(18)-C(19)	1.400(4)
N(1)-C(1)	1.347(3)	C(19)-C(20)	1.402(4)
N(1)-N(2)	1.375(2)	C(20)-C(21)	1.417(4)
N(2)-C(3)	1.346(3)	C(22)-C(23)	1.422(3)
N(3)-C(14)	1.348(3)	C(22)-C(26)	1.437(3)
N(3)-N(4)	1.371(3)	C(23)-C(24)	1.421(4)
N(4)-C(16)	1.347(3)	C(24)-C(25)	1.425(3)
N(5)-C(27)	1.347(3)	C(25)-C(26)	1.439(3)
N(5)-N(6)	1.369(3)	C(27)-C(28)	1.401(3)
N(6)-C(29)	1.346(3)	C(27)-C(39)	1.466(3)
C(1)-C(2)	1.410(3)	C(28)-C(29)	1.377(3)
C(1)-C(13)	1.473(3)	C(30)-C(34)	1.415(5)
C(2)-C(3)	1.378(3)	C(30)-C(31)	1.412(4)
C(4)-C(8)	1.412(4)	C(31)-C(32)	1.417(4)
C(4)-C(5)	1.424(4)	C(32)-C(33)	1.423(4)
C(5)-C(6)	1.424(4)	C(33)-C(34)	1.412(5)
C(6)-C(7)	1.424(4)	C(35)-C(36)	1.423(3)
C(7)-C(8)	1.418(4)	C(35)-C(39)	1.435(3)
C(9)-C(13)	1.432(3)	C(36)-C(37)	1.419(4)
C(9)-C(10)	1.437(3)	C(37)-C(38)	1.423(3)
C(10)-C(11)	1.420(4)	C(38)-C(39)	1.438(3)

Angles (°)

C(40)-Cu(1)-N(1)	126.19(10)	N(4)-B(1)-N(6)	108.46(19)
C(40)-Cu(1)-N(3)	115.63(10)	N(2)-B(1)-N(6)	108.87(19)
N(1)-Cu(1)-N(3)	94.61(8)	C(1)-N(1)-N(2)	106.47(18)
C(40)-Cu(1)-N(5)	128.54(10)	C(1)-N(1)-Cu(1)	140.94(16)
N(1)-Cu(1)-N(5)	90.66(8)	N(2)-N(1)-Cu(1)	111.38(13)
N(3)-Cu(1)-N(5)	92.00(8)	C(3)-N(2)-N(1)	109.83(19)
N(4)-B(1)-N(2)	110.1(2)	C(3)-N(2)-B(1)	128.7(2)

N(1)-N(2)-B(1)	121.39(18)	C(16)-C(15)-C(14)	105.4(2)
C(14)-N(3)-N(4)	106.79(18)	N(4)-C(16)-C(15)	108.6(2)
C(14)-N(3)-Cu(1)	139.93(16)	C(18)-C(17)-C(21)	108.2(3)
N(4)-N(3)-Cu(1)	111.71(14)	C(19)-C(18)-C(17)	107.6(3)
C(16)-N(4)-N(3)	109.9(2)	C(18)-C(19)-C(20)	108.9(3)
C(16)-N(4)-B(1)	129.9(2)	C(19)-C(20)-C(21)	108.0(3)
N(3)-N(4)-B(1)	120.19(18)	C(20)-C(21)-C(17)	107.2(3)
C(27)-N(5)-N(6)	106.23(18)	C(23)-C(22)-C(26)	108.2(2)
C(27)-N(5)-Cu(1)	141.42(16)	C(24)-C(23)-C(22)	108.4(2)
N(6)-N(5)-Cu(1)	111.01(14)	C(23)-C(24)-C(25)	108.3(2)
C(29)-N(6)-N(5)	109.85(19)	C(24)-C(25)-C(26)	108.0(2)
C(29)-N(6)-B(1)	129.2(2)	C(25)-C(26)-C(22)	107.2(2)
N(5)-N(6)-B(1)	120.79(18)	C(25)-C(26)-C(14)	128.5(2)
N(1)-C(1)-C(2)	109.8(2)	C(22)-C(26)-C(14)	124.4(2)
N(1)-C(1)-C(13)	124.7(2)	N(5)-C(27)-C(28)	110.2(2)
C(2)-C(1)-C(13)	125.4(2)	N(5)-C(27)-C(39)	122.8(2)
C(3)-C(2)-C(1)	105.1(2)	C(28)-C(27)-C(39)	126.8(2)
N(2)-C(3)-C(2)	108.8(2)	C(29)-C(28)-C(27)	104.9(2)
C(8)-C(4)-C(5)	107.7(2)	N(6)-C(29)-C(28)	108.8(2)
C(6)-C(5)-C(4)	108.1(2)	C(34)-C(30)-C(31)	108.3(3)
C(5)-C(6)-C(7)	107.6(2)	C(30)-C(31)-C(32)	107.9(3)
C(8)-C(7)-C(6)	107.9(2)	C(31)-C(32)-C(33)	107.8(3)
C(4)-C(8)-C(7)	108.6(2)	C(34)-C(33)-C(32)	107.9(3)
C(13)-C(9)-C(10)	108.2(2)	C(30)-C(34)-C(33)	108.0(3)
C(11)-C(10)-C(9)	107.9(2)	C(36)-C(35)-C(39)	108.6(2)
C(10)-C(11)-C(12)	108.4(2)	C(37)-C(36)-C(35)	108.1(2)
C(11)-C(12)-C(13)	108.2(2)	C(36)-C(37)-C(38)	108.2(2)
C(12)-C(13)-C(9)	107.4(2)	C(37)-C(38)-C(39)	108.4(2)
C(12)-C(13)-C(1)	123.8(2)	C(35)-C(39)-C(38)	106.7(2)
C(9)-C(13)-C(1)	128.3(2)	C(35)-C(39)-C(27)	128.6(2)
N(3)-C(14)-C(15)	109.4(2)	C(38)-C(39)-C(27)	124.6(2)
N(3)-C(14)-C(26)	122.8(2)	O(1)-C(40)-Cu(1)	175.4(2)
C(15)-C(14)-C(26)	127.8(2)		

3.2.9 Synthesis of $Tp^{Fc,Me}Cu(CO)$.

The copper carbonyl complex of the $Tp^{Fc,Me}$ ligand, $Tp^{Fc,Me}Cu(CO)$ (**17**) was synthesized by similar procedures as complex **16** by exposing a solution **8** and CuI in THF to an atmosphere of CO and was isolated in 49 % yield. The crystal structure (Figure 3.17) reveal four-coordinate copper center adopting a pseudo-tetrahedral geometry. The observed CO bond lengths of 1.118(5) Å for **17** is comparable to that of the $Tp^{Fc}Cu(CO)$ complex. Their CO stretching frequencies can be found and compared to other Tp ligands in this series in Table 3.14.

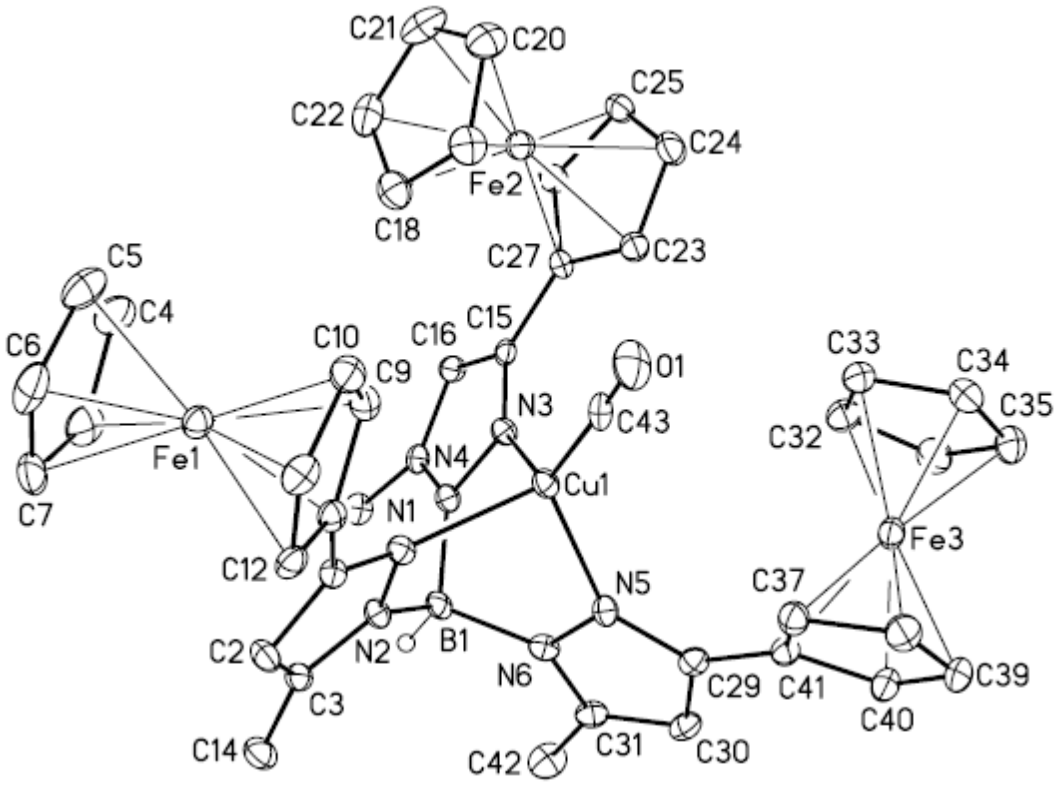

Figure 3.17: Molecular structure of $Tp^{Fc,Me}Cu(CO)$ (17) at the 30% probability level. Hydrogen atoms (except the boron bound hydrogen, H1B) have been removed for clarity.

Table 3.11: Selected interatomic distances (Å) and angles (°) for $Tp^{Fc,Me}Cu(CO)$ (17).

Distances (Å)

Cu(1)-C(43)	1.796(5)	C(12)-C(13)	1.425(6)
Cu(1)-N(5)	2.051(4)	C(15)-C(16)	1.400(6)
Cu(1)-N(1)	2.063(4)	C(15)-C(27)	1.469(6)
Cu(1)-N(3)	2.065(3)	C(16)-C(17)	1.377(6)
B(1)-N(4)	1.541(6)	C(17)-C(28)	1.494(6)
B(1)-N(2)	1.541(6)	C(18)-C(19)	1.410(7)
B(1)-N(6)	1.550(6)	C(18)-C(22)	1.417(7)
O(1)-C(43)	1.118(5)	C(19)-C(20)	1.413(7)
N(1)-C(1)	1.332(5)	C(20)-C(21)	1.395(7)
N(1)-N(2)	1.382(5)	C(21)-C(22)	1.412(7)
N(2)-C(3)	1.350(5)	C(23)-C(24)	1.416(6)
N(3)-C(15)	1.333(5)	C(23)-C(27)	1.421(6)
N(3)-N(4)	1.381(4)	C(24)-C(25)	1.404(6)
N(4)-C(17)	1.348(5)	C(25)-C(26)	1.421(6)
N(5)-C(29)	1.356(5)	C(26)-C(27)	1.427(6)
N(5)-N(6)	1.372(5)	C(29)-C(30)	1.396(6)
N(6)-C(31)	1.343(5)	C(29)-C(41)	1.465(6)
C(1)-C(2)	1.406(6)	C(30)-C(31)	1.376(6)
C(1)-C(13)	1.461(6)	C(31)-C(42)	1.489(6)
C(2)-C(3)	1.369(6)	C(32)-C(36)	1.408(7)
C(3)-C(14)	1.488(6)	C(32)-C(33)	1.409(7)
C(4)-C(5)	1.410(7)	C(33)-C(34)	1.414(6)
C(4)-C(8)	1.415(7)	C(34)-C(35)	1.420(7)
C(5)-C(6)	1.405(7)	C(35)-C(36)	1.404(7)
C(6)-C(7)	1.411(7)	C(37)-C(41)	1.417(6)
C(7)-C(8)	1.416(7)	C(37)-C(38)	1.417(6)
C(9)-C(10)	1.423(6)	C(38)-C(39)	1.427(7)
C(9)-C(13)	1.429(6)	C(39)-C(40)	1.402(6)
C(10)-C(11)	1.415(6)	C(40)-C(41)	1.429(6)
C(11)-C(12)	1.410(6)		

Angles (°)

C(43)-Cu(1)-N(5)	126.31(17)	N(1)-Cu(1)-N(3)	92.13(13)
C(43)-Cu(1)-N(1)	115.22(17)	N(4)-B(1)-N(2)	109.9(4)
N(5)-Cu(1)-N(1)	94.04(14)	N(4)-B(1)-N(6)	109.0(3)
C(43)-Cu(1)-N(3)	129.40(17)	N(2)-B(1)-N(6)	109.3(3)
N(5)-Cu(1)-N(3)	90.24(14)	C(1)-N(1)-N(2)	107.1(3)

C(1)-N(1)-Cu(1)	137.6(3)	C(16)-C(15)-C(27)	126.8(4)
N(2)-N(1)-Cu(1)	112.2(2)	C(17)-C(16)-C(15)	105.8(4)
C(3)-N(2)-N(1)	109.3(3)	N(4)-C(17)-C(16)	107.8(3)
C(3)-N(2)-B(1)	131.2(4)	N(4)-C(17)-C(28)	123.3(4)
N(1)-N(2)-B(1)	119.5(3)	C(16)-C(17)-C(28)	128.9(4)
C(15)-N(3)-N(4)	106.3(3)	C(19)-C(18)-C(22)	108.1(5)
C(15)-N(3)-Cu(1)	141.4(3)	C(18)-C(19)-C(20)	107.9(4)
N(4)-N(3)-Cu(1)	111.8(2)	C(21)-C(20)-C(19)	108.0(5)
C(17)-N(4)-N(3)	110.0(3)	C(20)-C(21)-C(22)	108.8(5)
C(17)-N(4)-B(1)	129.4(3)	C(21)-C(22)-C(18)	107.2(5)
N(3)-N(4)-B(1)	120.2(3)	C(24)-C(23)-C(27)	108.2(4)
C(29)-N(5)-N(6)	105.8(3)	C(25)-C(24)-C(23)	108.6(4)
C(29)-N(5)-Cu(1)	140.0(3)	C(24)-C(25)-C(26)	107.9(4)
N(6)-N(5)-Cu(1)	113.2(2)	C(25)-C(26)-C(27)	108.2(4)
C(31)-N(6)-N(5)	110.4(3)	C(23)-C(27)-C(26)	107.2(4)
C(31)-N(6)-B(1)	130.0(4)	C(23)-C(27)-C(15)	128.6(4)
N(5)-N(6)-B(1)	119.6(3)	C(26)-C(27)-C(15)	124.2(4)
N(1)-C(1)-C(2)	109.1(4)	N(5)-C(29)-C(30)	109.8(4)
N(1)-C(1)-C(13)	122.7(4)	N(5)-C(29)-C(41)	124.7(4)
C(2)-C(1)-C(13)	128.1(4)	C(30)-C(29)-C(41)	125.4(4)
C(3)-C(2)-C(1)	106.4(4)	C(31)-C(30)-C(29)	105.7(4)
N(2)-C(3)-C(2)	108.0(4)	N(6)-C(31)-C(30)	108.3(4)
N(2)-C(3)-C(14)	122.5(4)	N(6)-C(31)-C(42)	122.9(4)
C(2)-C(3)-C(14)	129.5(4)	C(30)-C(31)-C(42)	128.9(4)
C(5)-C(4)-C(8)	107.9(5)	C(36)-C(32)-C(33)	108.5(4)
C(6)-C(5)-C(4)	107.7(5)	C(32)-C(33)-C(34)	108.2(4)
C(5)-C(6)-C(7)	109.1(5)	C(33)-C(34)-C(35)	107.0(4)
C(6)-C(7)-C(8)	106.9(5)	C(36)-C(35)-C(34)	108.8(4)
C(4)-C(8)-C(7)	108.4(5)	C(35)-C(36)-C(32)	107.6(4)
C(10)-C(9)-C(13)	107.6(4)	C(41)-C(37)-C(38)	108.8(4)
C(11)-C(10)-C(9)	108.5(4)	C(37)-C(38)-C(39)	107.2(4)
C(12)-C(11)-C(10)	107.9(4)	C(40)-C(39)-C(38)	108.5(4)
C(11)-C(12)-C(13)	108.6(4)	C(39)-C(40)-C(41)	108.4(4)
C(12)-C(13)-C(9)	107.4(4)	C(37)-C(41)-C(40)	107.2(4)
C(12)-C(13)-C(1)	125.3(4)	C(37)-C(41)-C(29)	128.4(4)
C(9)-C(13)-C(1)	127.3(4)	C(40)-C(41)-C(29)	123.9(4)
N(3)-C(15)-C(16)	110.2(4)	O(1)-C(43)-Cu(1)	176.1(4)
N(3)-C(15)-C(27)	123.0(4)		

3.2.10 Synthesis of $Tp^{Fc,iPr**}Cu(CO)$ and $Tp^{Fc,iPr*}Cu(CO)$.

Although the Tl salts of the symmetric ligands of Tp^{Fc} and $Tp^{Fc,Me}$ led to the expected symmetric copper(I) carbonyl complexes in THF under an atmosphere of CO at room temperature, the $Tp^{Fc,iPr}$ ligand behaved quite differently. When $Tp^{Fc,iPr}$ Tl was reacted with CuI in the presence of CO in THF at room temperature and recrystallized from a cooled solution of pentane and diethylether (-30 °C), two distinct isomers were discernible in the ^{1}H NMR spectrum. However, the IR spectrum of is mixture only shows one CO stretching peak for both isomers at 2064 cm^{-1} and, therefore, the CO stretching frequencies of the regioisomers are most likely overlapping. X-ray quality crystals were grown from slow cooling of a saturated solution of **18** and **19** in pentane and diethylether. The X-ray structure determination revealed that **18** is a distorted tetrahedron (Fig. 3.18) with a doubly N-confused ligand. Compound **19** displays the same pseudo tetrahedral coordination geometry as **18**, however the isomerization of the Tp ligand has put only one of the *iso*-propyl groups in the 3-position on the pyrazolyl ring (Figure 3.19). In this case, the size of the CO co-ligand is smaller than that of either the iodide or the chloride. Therefore, the ligand has room to rearrange one or two pyrazolyl moieties generating the two regioisomers detected in the ^{1}H NMR spectrum.

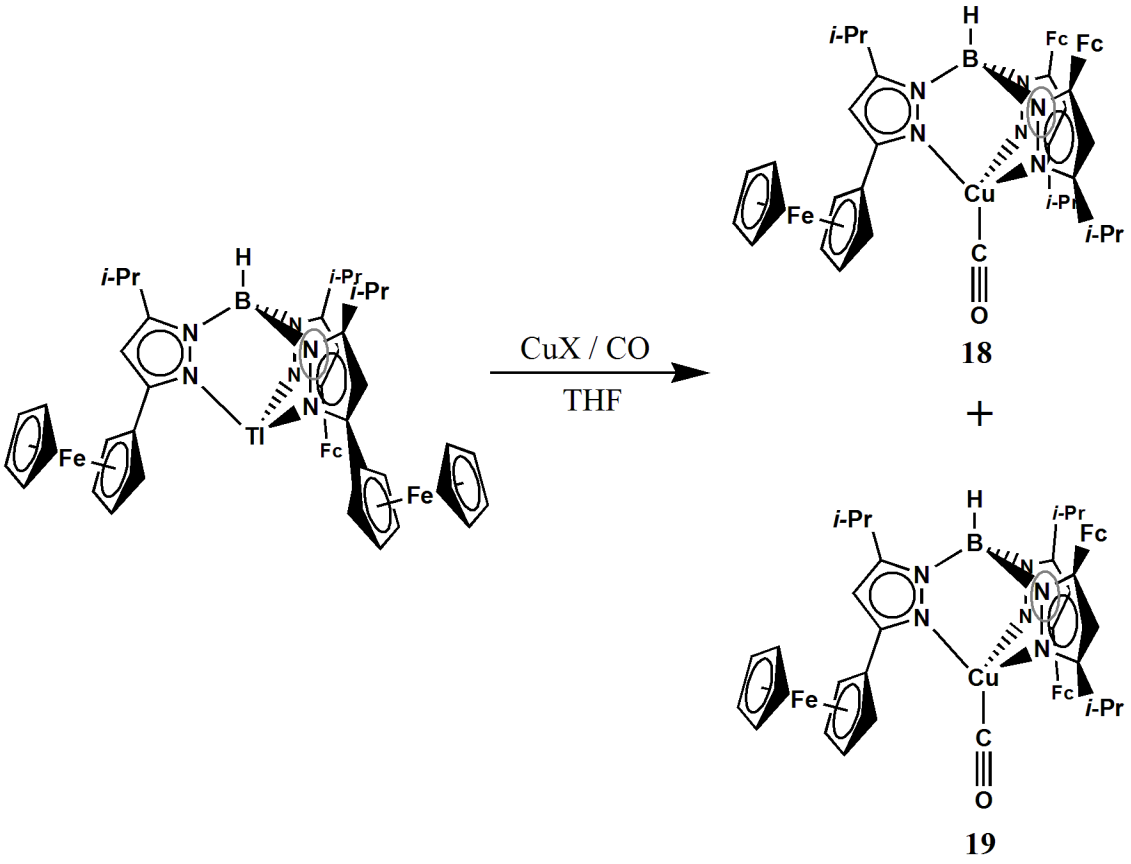

Scheme 3.9: Synthesis of $Tp^{Fc,iPr**}Cu(CO)$ (18) and $Tp^{Fc,iPr*}Cu(CO)$ (19).

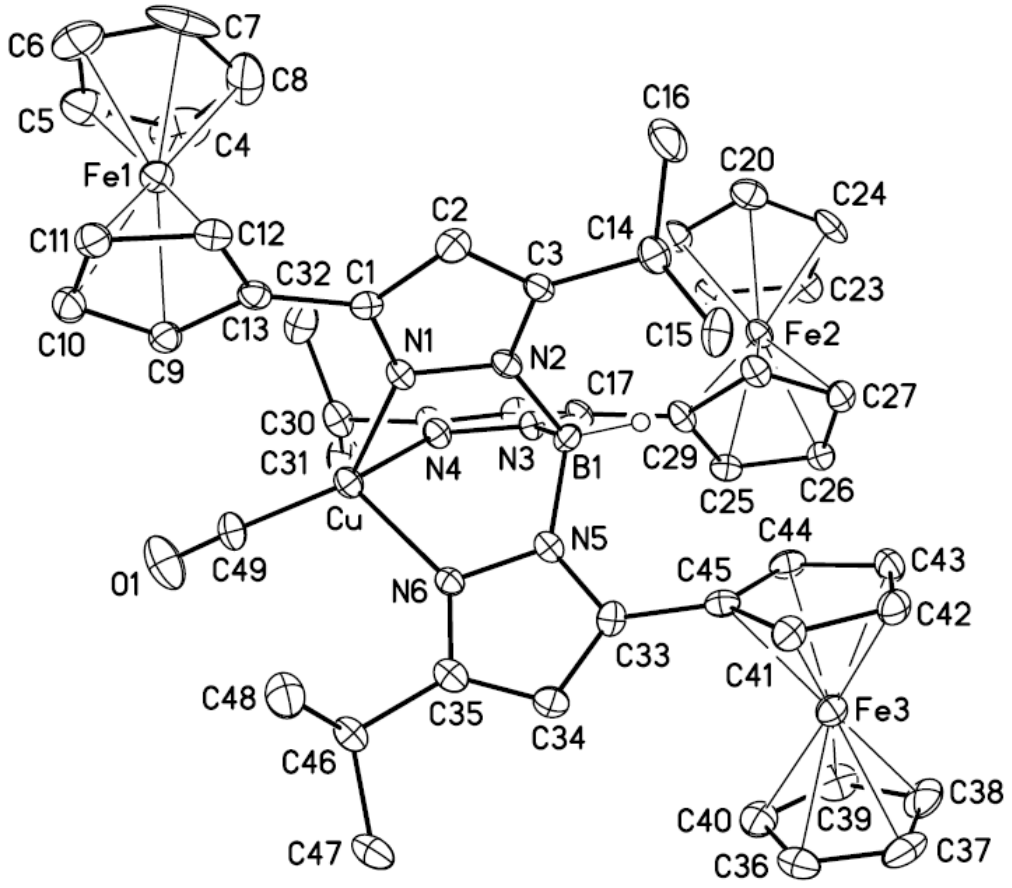

Figure 3.18: Molecular structure of $Tp^{Fc,iPr**}Cu(CO)$ (18) at the 30% probability level. Hydrogen atoms (except the boron bound hydrogen, H1B) have been removed for clarity.

Table 3.12: Selected interatomic distances (Å) and angles (°) for $Tp^{Fc,iPr**}Tl$ (18).

Distances (Å)

Cu-C(49)	1.786(10)	C(17)-C(18)	1.375(12)
Cu-N(6)	2.025(7)	C(17)-C(29)	1.473(12)
Cu-N(4)	2.035(7)	C(18)-C(19)	1.378(12)
Cu-N(1)	2.042(7)	C(19)-C(30)	1.501(12)
O(1)-C(49)	1.098(11)	C(20)-C(21)	1.421(14)
N(1)-C(1)	1.330(10)	C(20)-C(24)	1.437(15)
N(1)-N(2)	1.388(9)	C(21)-C(22)	1.464(15)
N(2)-C(3)	1.346(10)	C(22)-C(23)	1.426(14)
N(2)-B(1)	1.563(12)	C(23)-C(24)	1.422(14)
N(3)-C(17)	1.340(10)	C(25)-C(26)	1.391(13)
N(3)-N(4)	1.353(9)	C(25)-C(29)	1.417(12)
N(3)-B(1)	1.559(12)	C(26)-C(27)	1.388(13)
N(4)-C(19)	1.333(11)	C(27)-C(28)	1.383(12)
N(5)-C(33)	1.343(10)	C(28)-C(29)	1.416(12)
N(5)-N(6)	1.387(9)	C(30)-C(32)	1.517(15)
N(5)-B(1)	1.539(12)	C(30)-C(31)	1.548(14)
N(6)-C(35)	1.338(11)	C(33)-C(34)	1.374(12)
C(1)-C(2)	1.405(12)	C(33)-C(45)	1.453(12)
C(1)-C(13)	1.453(12)	C(34)-C(35)	1.375(13)
C(2)-C(3)	1.357(12)	C(35)-C(46)	1.501(13)
C(3)-C(14)	1.526(12)	C(36)-C(37)	1.368(15)
C(4)-C(5)	1.32(2)	C(36)-C(40)	1.393(15)
C(4)-C(8)	1.36(2)	C(37)-C(38)	1.429(16)
C(5)-C(6)	1.340(18)	C(38)-C(39)	1.342(15)
C(6)-C(7)	1.39(2)	C(39)-C(40)	1.393(15)
C(7)-C(8)	1.40(2)	C(41)-C(42)	1.398(13)
C(9)-C(10)	1.409(13)	C(41)-C(45)	1.441(12)
C(9)-C(13)	1.446(12)	C(42)-C(43)	1.422(13)
C(10)-C(11)	1.407(14)	C(43)-C(44)	1.403(13)
C(11)-C(12)	1.442(12)	C(44)-C(45)	1.410(12)
C(12)-C(13)	1.406(12)	C(46)-C(48)	1.530(14)
C(14)-C(15)	1.505(13)	C(46)-C(47)	1.533(15)
C(14)-C(16)	1.522(14)		

Angles (°)

C(49)-Cu-N(6)	117.0(4)	C(12)-C(13)-C(1)	123.9(8)
C(49)-Cu-N(4)	117.1(4)	C(9)-C(13)-C(1)	128.6(8)
N(6)-Cu-N(4)	95.7(3)	C(15)-C(14)-C(16)	110.3(9)
C(49)-Cu-N(1)	137.1(4)	C(15)-C(14)-C(3)	110.2(8)
N(6)-Cu-N(1)	88.6(3)	C(16)-C(14)-C(3)	111.5(8)
N(4)-Cu-N(1)	91.8(3)	N(3)-C(17)-C(18)	107.9(8)
C(1)-N(1)-N(2)	107.0(7)	N(3)-C(17)-C(29)	125.2(8)
C(1)-N(1)-Cu	140.7(6)	C(18)-C(17)-C(29)	126.3(8)
N(2)-N(1)-Cu	112.4(5)	C(17)-C(18)-C(19)	105.7(8)
C(3)-N(2)-N(1)	108.6(7)	N(4)-C(19)-C(18)	109.8(8)
C(3)-N(2)-B(1)	130.9(7)	N(4)-C(19)-C(30)	119.9(8)
N(1)-N(2)-B(1)	120.2(7)	C(18)-C(19)-C(30)	130.2(8)
C(17)-N(3)-N(4)	109.7(7)	C(21)-C(20)-C(24)	108.0(10)
C(17)-N(3)-B(1)	131.6(7)	C(20)-C(21)-C(22)	108.2(10)
N(4)-N(3)-B(1)	118.5(7)	C(23)-C(22)-C(21)	106.5(9)
C(19)-N(4)-N(3)	106.9(7)	C(22)-C(23)-C(24)	109.3(10)
C(19)-N(4)-Cu	137.0(6)	C(23)-C(24)-C(20)	108.0(9)
N(3)-N(4)-Cu	114.9(5)	C(26)-C(25)-C(29)	108.8(8)
C(33)-N(5)-N(6)	109.4(7)	C(27)-C(26)-C(25)	108.2(9)
C(33)-N(5)-B(1)	132.2(7)	C(26)-C(27)-C(28)	108.4(8)
N(6)-N(5)-B(1)	117.9(7)	C(27)-C(28)-C(29)	109.1(9)
C(35)-N(6)-N(5)	106.4(7)	C(25)-C(29)-C(28)	105.6(8)
C(35)-N(6)-Cu	138.5(6)	C(25)-C(29)-C(17)	124.4(8)
N(5)-N(6)-Cu	115.0(5)	C(28)-C(29)-C(17)	129.9(9)
N(1)-C(1)-C(2)	109.4(8)	C(19)-C(30)-C(32)	111.7(9)
N(1)-C(1)-C(13)	123.2(8)	C(19)-C(30)-C(31)	112.0(8)
C(2)-C(1)-C(13)	127.5(8)	C(32)-C(30)-C(31)	108.5(9)
C(3)-C(2)-C(1)	105.9(8)	N(5)-C(33)-C(34)	107.6(7)
N(2)-C(3)-C(2)	109.1(8)	N(5)-C(33)-C(45)	122.3(8)
N(2)-C(3)-C(14)	123.0(8)	C(34)-C(33)-C(45)	130.1(8)
C(2)-C(3)-C(14)	128.0(8)	C(35)-C(34)-C(33)	107.0(8)
C(5)-C(4)-C(8)	107.8(15)	N(6)-C(35)-C(34)	109.7(8)
C(4)-C(5)-C(6)	112.7(14)	N(6)-C(35)-C(46)	119.5(9)
C(5)-C(6)-C(7)	105.2(14)	C(34)-C(35)-C(46)	130.8(9)
C(6)-C(7)-C(8)	107.7(12)	C(37)-C(36)-C(40)	107.4(11)
C(4)-C(8)-C(7)	106.6(13)	C(36)-C(37)-C(38)	107.4(11)
C(10)-C(9)-C(13)	107.5(9)	C(39)-C(38)-C(37)	108.5(11)
C(11)-C(10)-C(9)	109.2(9)	C(38)-C(39)-C(40)	107.9(11)
C(10)-C(11)-C(12)	107.4(8)	C(36)-C(40)-C(39)	108.8(10)
C(13)-C(12)-C(11)	108.3(8)	C(42)-C(41)-C(45)	108.6(9)
C(12)-C(13)-C(9)	107.6(8)	C(41)-C(42)-C(43)	107.7(8)

C(44)-C(43)-C(42)	108.2(8)	C(35)-C(46)-C(47)	109.5(9)
C(43)-C(44)-C(45)	109.0(8)	C(48)-C(46)-C(47)	111.0(9)
C(44)-C(45)-C(41)	106.5(8)	O(1)-C(49)-Cu	176.1(10)
C(44)-C(45)-C(33)	129.4(8)	N(5)-B(1)-N(3)	110.8(7)
C(41)-C(45)-C(33)	124.1(8)	N(5)-B(1)-N(2)	107.9(7)
C(35)-C(46)-C(48)	110.8(8)	N(3)-B(1)-N(2)	109.6(7)

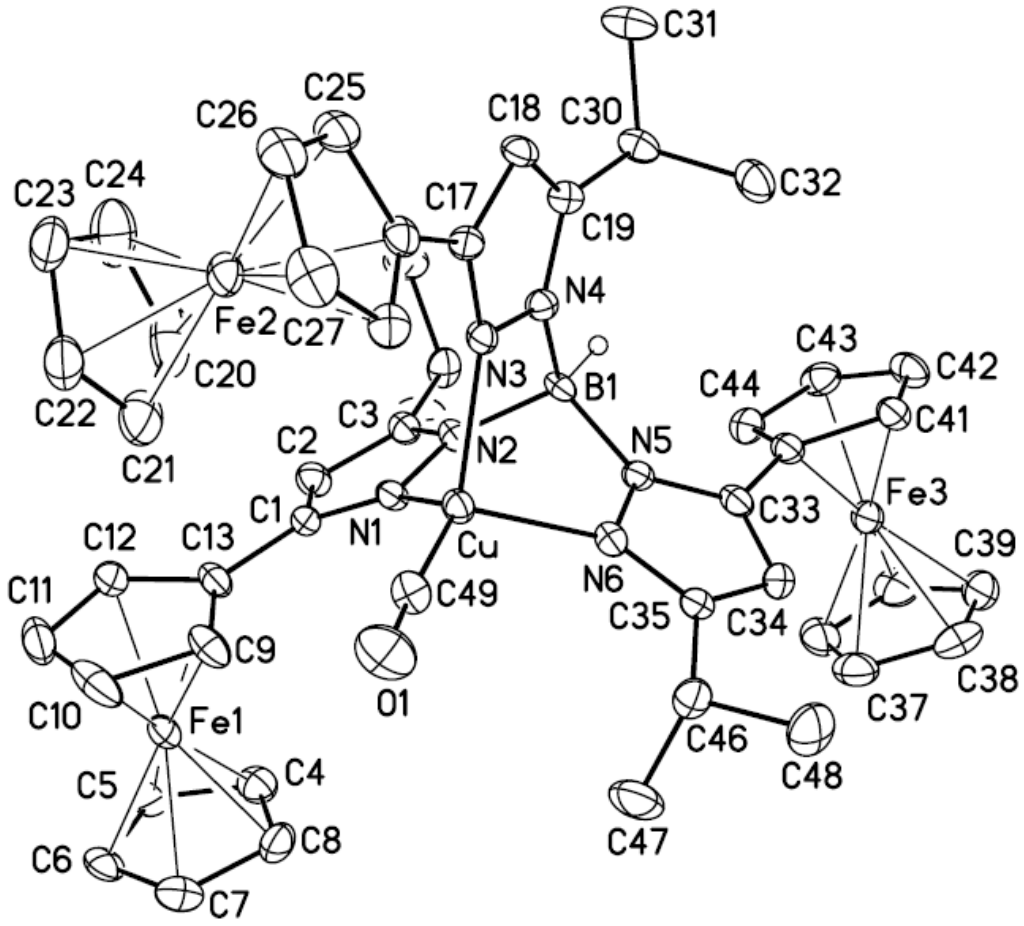

Figure 3.19: Molecular structure of $Tp^{Fc,iPr*}Cu(CO)$ (19) at the 30% probability level. Hydrogen atoms (except the boron bound hydrogen, H1B) have been removed for clarity.

Table 3.13: Selected interatomic distances (Å) and angles (°) for of $Tp^{Fc,iPr*}Cu(CO)$ (19).

Distances (Å)

Cu-C(49)	1.782(5)	C(18)-C(19)	1.367(6)
Cu-N(1)	2.038(4)	C(19)-C(30)	1.509(6)
Cu-N(3)	2.040(4)	C(20)-C(21)	1.390(10)
Cu-N(6)	2.046(4)	C(20)-C(24)	1.431(10)
B(1)-N(5)	1.544(6)	C(21)-C(22)	1.388(8)
B(1)-N(4)	1.552(6)	C(22)-C(23)	1.411(8)
B(1)-N(2)	1.553(6)	C(23)-C(24)	1.373(9)
N(1)-C(1)	1.332(6)	C(25)-C(26)	1.422(8)
N(1)-N(2)	1.389(5)	C(25)-C(29)	1.427(7)
N(2)-C(3)	1.351(6)	C(26)-C(27)	1.406(8)
N(3)-C(17)	1.334(5)	C(27)-C(28)	1.430(7)
N(3)-N(4)	1.374(5)	C(28)-C(29)	1.431(7)
N(4)-C(19)	1.352(5)	C(30)-C(32)	1.525(7)
N(5)-C(33)	1.340(5)	C(30)-C(31)	1.533(7)
N(5)-N(6)	1.369(5)	C(33)-C(34)	1.374(6)
N(6)-C(35)	1.323(6)	C(33)-C(45)	1.486(6)
O(1)-C(49)	1.119(5)	C(34)-C(35)	1.387(6)
C(1)-C(2)	1.388(6)	C(35)-C(46)	1.507(6)
C(1)-C(13)	1.463(6)	C(36)-C(37)	1.387(9)
C(2)-C(3)	1.369(6)	C(36)-C(40)	1.431(8)
C(3)-C(14)	1.512(6)	C(37)-C(38)	1.412(9)
C(4)-C(8)	1.406(8)	C(38)-C(39)	1.402(9)
C(4)-C(5)	1.413(7)	C(39)-C(40)	1.386(9)
C(5)-C(6)	1.406(8)	C(41)-C(42)	1.424(7)
C(6)-C(7)	1.384(7)	C(41)-C(45)	1.434(6)
C(7)-C(8)	1.423(8)	C(42)-C(43)	1.402(7)
C(9)-C(10)	1.422(7)	C(43)-C(44)	1.410(7)
C(9)-C(13)	1.433(7)	C(44)-C(45)	1.407(7)
C(10)-C(11)	1.403(9)	C(46)-C(48)	1.504(7)
C(11)-C(12)	1.410(8)	C(46)-C(47)	1.515(7)
C(12)-C(13)	1.413(7)	C(50)-C(51)	1.515(11)
C(14)-C(15)	1.508(7)	C(51)-C(52)	1.332(11)
C(14)-C(16)	1.520(7)	C(52)-C(53)	1.312(14)
C(17)-C(18)	1.410(6)	C(53)-C(54)	1.464(14)
C(17)-C(29)	1.462(6)		

Angles (°)

C(49)-Cu-N(1)	128.37(19)	C(10)-C(11)-C(12)	108.4(5)
C(49)-Cu-N(3)	126.0(2)	C(11)-C(12)-C(13)	108.9(6)
N(1)-Cu-N(3)	89.67(17)	C(12)-C(13)-C(9)	106.8(4)
C(49)-Cu-N(6)	116.63(19)	C(12)-C(13)-C(1)	125.3(5)
N(1)-Cu-N(6)	92.91(16)	C(9)-C(13)-C(1)	127.9(4)
N(3)-Cu-N(6)	94.02(16)	C(15)-C(14)-C(3)	111.6(4)
N(5)-B(1)-N(4)	109.3(4)	C(15)-C(14)-C(16)	112.0(4)
N(5)-B(1)-N(2)	110.3(3)	C(3)-C(14)-C(16)	110.7(4)
N(4)-B(1)-N(2)	109.1(4)	N(3)-C(17)-C(18)	110.1(4)
C(1)-N(1)-N(2)	106.1(4)	N(3)-C(17)-C(29)	124.5(4)
C(1)-N(1)-Cu	141.2(3)	C(18)-C(17)-C(29)	125.4(4)
N(2)-N(1)-Cu	112.4(3)	C(19)-C(18)-C(17)	105.6(4)
C(3)-N(2)-N(1)	109.3(4)	N(4)-C(19)-C(18)	107.9(4)
C(3)-N(2)-B(1)	130.4(4)	N(4)-C(19)-C(30)	122.6(4)
N(1)-N(2)-B(1)	120.2(4)	C(18)-C(19)-C(30)	129.1(4)
C(17)-N(3)-N(4)	106.0(4)	C(21)-C(20)-C(24)	106.6(6)
C(17)-N(3)-Cu	140.4(3)	C(22)-C(21)-C(20)	109.6(7)
N(4)-N(3)-Cu	113.1(3)	C(21)-C(22)-C(23)	107.0(6)
C(19)-N(4)-N(3)	110.3(4)	C(24)-C(23)-C(22)	109.0(6)
C(19)-N(4)-B(1)	130.2(4)	C(23)-C(24)-C(20)	107.9(7)
N(3)-N(4)-B(1)	119.2(3)	C(26)-C(25)-C(29)	107.3(5)
C(33)-N(5)-N(6)	108.7(4)	C(27)-C(26)-C(25)	109.7(5)
C(33)-N(5)-B(1)	133.0(4)	C(26)-C(27)-C(28)	107.0(5)
N(6)-N(5)-B(1)	117.8(3)	C(27)-C(28)-C(29)	108.5(5)
C(35)-N(6)-N(5)	107.5(4)	C(25)-C(29)-C(28)	107.4(4)
C(35)-N(6)-Cu	137.2(3)	C(25)-C(29)-C(17)	123.5(5)
N(5)-N(6)-Cu	115.1(3)	C(28)-C(29)-C(17)	129.1(4)
N(1)-C(1)-C(2)	110.3(4)	C(19)-C(30)-C(32)	109.2(4)
N(1)-C(1)-C(13)	122.5(4)	C(19)-C(30)-C(31)	110.2(4)
C(2)-C(1)-C(13)	127.1(4)	C(32)-C(30)-C(31)	110.3(4)
C(3)-C(2)-C(1)	106.3(4)	N(5)-C(33)-C(34)	108.5(4)
N(2)-C(3)-C(2)	107.9(4)	N(5)-C(33)-C(45)	123.2(4)
N(2)-C(3)-C(14)	123.7(4)	C(34)-C(33)-C(45)	128.2(4)
C(2)-C(3)-C(14)	128.2(4)	C(33)-C(34)-C(35)	105.5(4)
C(8)-C(4)-C(5)	108.3(5)	N(6)-C(35)-C(34)	109.7(4)
C(6)-C(5)-C(4)	107.5(5)	N(6)-C(35)-C(46)	121.1(4)
C(7)-C(6)-C(5)	108.8(5)	C(34)-C(35)-C(46)	128.8(4)
C(6)-C(7)-C(8)	108.3(5)	C(37)-C(36)-C(40)	108.4(6)
C(4)-C(8)-C(7)	107.1(5)	C(36)-C(37)-C(38)	107.5(6)
C(10)-C(9)-C(13)	108.0(5)	C(39)-C(38)-C(37)	108.3(6)
C(11)-C(10)-C(9)	107.8(5)	C(40)-C(39)-C(38)	108.5(6)

C(39)-C(40)-C(36)	107.3(6)	C(48)-C(46)-C(35)	111.4(4)
C(42)-C(41)-C(45)	106.8(4)	C(48)-C(46)-C(47)	110.4(5)
C(43)-C(42)-C(41)	109.1(4)	C(35)-C(46)-C(47)	110.8(4)
C(42)-C(43)-C(44)	107.5(5)	O(1)-C(49)-Cu	176.5(5)
C(45)-C(44)-C(43)	109.1(5)	C(52)-C(51)-C(50)	112.0(6)
C(44)-C(45)-C(41)	107.5(4)	C(53)-C(52)-C(51)	112.7(8)
C(44)-C(45)-C(33)	129.5(4)	C(52)-C(53)-C(54)	111.7(9)
C(41)-C(45)-C(33)	123.0(4)		

Table 3.14: CO stretching frequencies of known Tp^{R} and $Tp^{R,R}$ copper (I) carbonyl complexes.

Compound	vCO (cm^{-1})
$Tp^{iPr2}Cu(CO)$	2056[15]
$Tp^{tBu,Me}Cu(CO)$	2059[16]
$Tp^{Fc,Me}Cu(CO)$	2060
$Tp^{Fc}Cu(CO)$	2064
$Tp^{Fc,iPr}Cu(CO)$	2064[†]
$Tp^{tBu}Cu(CO)$	2069[17]
$Tp^{Ph2}Cu(CO)$	2080[18]
$Tp^{CF3}Cu(CO)$	2100[19]
$Tp^{(CF3)2}Cu(CO)$	2137[20]

[†]IR data taken as a mixture of regioisomers.

3.3 Conclusions

1,2 borotropic shifts are ubiquitous throughout the series of $Tp^{Fc,R}$ (R: H, Me, *i*-Pr) complexes. The thallium(I) salts of Tp^{Fc*} and $Tp^{Fc,Me*}$ undergo thermal isomerization above 220 °C to form the symmetric Tp^{Fc} and $Tp^{Fc,Me}$ ligands, respectively. This is reminiscent of the thermal isomerization found in the $Tp^{Ms}Tl$ system reported by Trofimenko.[8] However, the thallium(I) salt of the $Tp^{Fc,i\text{-}Pr}$ ligand undergoes thermal isomerization at 250 °C to form a mixture of three regioisomers detectable by ^1H NMR. This result suggests that the *iso*-propyl and ferrocenyl substituents have similar steric bulk and therefore can interchange their position on the pyrazolyl ring, similar to that of the $Tp^{iPr,Me}$ system.[5,6]

Salt metathese with cobalt(II) halides and the Tp^{Fc} and $Tp^{Fc,Me}$ ligands led to the isolation of the symmetric $Tp^{Fc}CoX$ and $Tp^{Fc,Me}CoX$ (X: Cl, I) complexes, respectively. Salt metathesis of the $Tp^{Fc,i\text{-}Pr}Tl$ and cobalt(II) iodide leads to the isolation of $Tp^{Fc,i\text{-}Pr}CoI$ as the only observable product. However, salt metathesis of $Tp^{Fc,i\text{-}Pr}Tl$ with cobalt(II) chloride leads to the isolation of an N-confused $Tp^{Fc,i\text{-}Pr*}CoCl$ complex. Moreover, the $Tp^{Fc,i\text{-}Pr}CoI$ complex is vulnerable to halide exchange in chloroform accompanied by borotropic rearrangement to the $Tp^{Fc,iPr*}CoCl$ complex at room temperature.

The salt metathesis of $Tp^{Fc}Tl$ and $Tp^{Fc,Me}Tl$ salts with copper(I) halides in the presence of CO results in the isolation of $Tp^{Fc}Cu(CO)$ and $Tp^{Fc,Me}Cu(CO)$, respectively. However, when $Tp^{Fc,iPr}Tl$ is reacted with copper(I) halides in the presence of CO, a mixture of two regioisomers, $Tp^{Fc,iPr*}Cu(CO)$ and $Tp^{Fc,iPr**}Cu(CO)$, are formed. Both of these isomers have been characterized by X-ray diffraction. With these results, it can be deduced that in the $Tp^{Fc,iPr}$ system the room temperature borotropic rearrangement is a result of a lack of steric difference between the *iso*-propyl and ferrocenyl groups coupled with the effect of the steric bulk of the co-ligand. The

smaller the co-ligand, such in the case of CO, the more allowance there is for rearrangement. However, in the case of the Tl salt of the ligand, the symmetric ligand is maintained at room temperature due to the large atomic radius of the Tl atom.

3.4 Experimental

All reactions were run under a nitrogen atmosphere, using standard glovebox and Schlenk techniques unless otherwise stated. Diethyl ether, pentane, tetrahydrofuran (THF), and toluene were dried by passing each solvent through activated alumina columns followed by a nitrogen purge to remove dissolved oxygen[21]. Organic chemicals were bought from Aldrich or Acros and inorganic chemicals were purchased from Strem. NMR spectra were obtained on Bruker AVIII-400 or AV 600 spectrometers and were referenced to the residual protons of the solvent (CD_2Cl_2, 5.32 ppm; $CDCl_3$, 7.27 ppm; C_6D_6, 7.15 ppm). ^{11}B NMR were referenced to $BF_3 \bullet Et_2O$ (0.0 ppm). FT-IR spectra were recorded on Matteson Alpha Centauri or Nicolet Magna-IR 560 spectrometers with a resolution of 4 cm^{-1}. X-ray crystallographic studies were conducted in the University of Delaware X-ray crystallographic facility. Elemental analyses were obtained from Robertson Microlit, Ledgewood, NJ 07852. Room-temperature molar magnetic susceptibilities (χ_m) in the solid state were determined using a Johnson Matthey magnetic susceptibility balance. They were corrected for diamagnetism using Pascal constants[22] and converted into effective magnetic moments (μ_{eff}).

3.4.1 Single crystal X-ray diffraction studies.

General considerations are given on page 57. No symmetry higher than triclinic was observed for **kla0006** (**14**), **kla0427** (**10**), **kla0428** (**9**), **kla0473** (**11**), **kla0502** (**15**)**, kla0075** (**19**), **kla0474** (**17**), **kla0497** (**16**), **kla0518** (**12**), **kla0262** (**7**) and **kla0243** (**8**). The systematic absences in the diffraction data were consistent with *C*2/*c* and *Cc* for **kla0040** (**13**) and, uniquely, for $P2_1/c$ for **kla0062** (**18**). Solution in the centrosymmetric space group option for non-unique cases yielded chemically reasonable and computationally stable results of refinement except for the isomorphic

kla0006 (**14**) and **kla0075** (**19**), which solved and refined only in *P*1. The absolute structure parameter in **kla0006** (**14**) and **kla0075** (**19**) refined to nil indicating the true hand of the data was established. Solvent molecules, one per compound molecule, were located in the asymmetric units for **kla0006** (**14**) (diethylether) and **kla0075** (**19**) (pentane). Cocrystallized tetrahydrofuran solvent molecules, 1.5 molecules per compound molecule, in **kla0040** (**13**) were found severely disordered and were treated as diffused contributions[23]. Borohydride H-atoms on **kla0006** (**14**), **kla0040** (**13**), **kla0427** (**10**), **kla0428** (**9**), **kla0075** (**19**) and **kla0243** (**8**) were located from the difference map and constrained to U_{iso} equal to 1.2 B-atom U_{eq}.

3.4.2 Hydrotris(3-ferrocenylpyrazolyl)borato-Thallium(I), TpFcTl, Thermal Isomerization of $Tp^{Fc*}Tl$ (1) to $Tp^{Fc}Tl$ (7).

A solid sample of $Tp^{Fc*}Tl$ was placed inside a round bottom flask and heated under vacuum at 220°C for 1 hour. The sample was allowed to cool to room temperature, quantitatively yielding the symmetric Tp^{Fc} ligand. ^{1}H NMR (400 MHz, $CDCl_3$): 7.62 (s, 3 H), 6.26 (s, 3 H), 4.57 (s, 6 H), 4.22 (s, 6 H), 4.03 (s, 15 H) ppm. ^{11}B NMR: -1.23 ppm. IR (KBR): 3090 (w), 2420 (w, B-H), 1549 (s), 1488 (s), 1424 (s), 1336 (s), 1204 (s), 1188 (s), 1045 (s) 1001 (s) 869 (s), 815 (s), 764 (m), 723 (s), 508 (w), 487 (s) cm^{-1}. Mp: 267 – 269 °C. Anal Calcd for $C_{39}H_{34}N_6BFe_3Tl$: C, 48.32; H, 3.53; N, 8.67. Found: C, 47.71; H, 3.26; N, 8.47.

3.4.3 Hydrotris(3-ferrocenyl-5-methylpyrazolyl)borato-Thallium(I), TpFc,MeTl, Thermal Isomerization of $Tp^{Fc,Me*}Tl$ (2) to $Tp^{Fc,Me}Tl$ (8).

A solid sample of $Tp^{Fc,Me*}Tl$ was placed inside a round bottom flask and heated under vacuum at 250°C for 1 hour. The sample was allowed to cool to room temperature, quantitatively yielding the symmetric $Tp^{Fc,Me}$ ligand. ^{1}H NMR (400 MHz, $CDCl_3$): 6.12 (s, 3 H), 4.59 (s, 6 H),

4.25 (s, 6 H), 4.11 (s, 15 H) 2.50 (s, 3 H) ppm. ^{11}B NMR: -7.84 ppm. IR (KBR): 3091 (m), 2917 (w), 2523 (w, B-H), 1559 (s), 1515 (s), 1425 (w), 1346 (s), 1318 (s), 1225 (s), 1179 (m), 1068 (m), 1000 (s), 973 (s), 882 (s), 644 (s), 507 (s) cm^{-1}. UV-vis (THF), λ_{max} (ϵ, M^{-1} cm^{-1}): 444 (517) nm. Mp: 285 – 287 °C. Anal Calcd for $C_{42}H_{40}N_6BFe_3Tl$: C, 49.87; H, 3.99; N, 8.31. Found: C, 49.30; H, 3.46; N, 8.47.

3.4.4 Iodo-hydrotris(3-ferrocenylpyrazolyl)borato-cobalt(II), Tp^{Fc}CoI (9).

0.5 g of Tp^{Fc}Tl (0.52 mmol) and 0.160 g of anhydrous CoI_2 (0.052 mmol) were dissolved in 100 mL of THF and allowed to stir overnight. The solution was filtered through a bed of Celite to remove TlI and the solvent evaporated. The green residue was triturated with pentanes and the solid collected on a frit. The solid was dissolved in a 50/50 mixture of pentanes and THF and the solution cooled -30 °C overnight. The resulting green crystalline solid was collected on a frit and washed with several portions of pentane and allowed to dry under vacuum yielding 0.35 g of Tp^{Fc}CoI (72 %). ^{1}H NMR (400 MHz, C_6D_6): 68.8 (br, 3 H), 30.5 (br, 3 H), 3.2 (br, 15 H), 3.0 (br, 6 H) 1.2 (br, 6 H) -20.0 (br, 1 H) ppm. IR (KBr): 3092 (w), 2924 (w), 2490 (w, B-H), 1732 (w), 1644 (w), 1548 (s), 1494 (m), 1340 (s), 1182 (w), 1105 (s), 1043 (w), 1000 (s), 871 (s), 818 (w), 773 (w), 503 (m), 454 (s) cm^{-1}. μ_{eff} = 4.2(1) μ_B (295 K). Mp: 195 – 197 °C. Anal Calcd for $C_{39}H_{34}N_6BFe_3CoI$: C, 49.26; H, 3.60; N, 8.84. Found: C, 49.30; H, 3.46; N, 8.13.

3.4.5 Chloro-hydrotris(3-ferrocenylpyrazolyl)borato-cobalt(II), Tp^{Fc}CoCl (10).

0.5 g of Tp^{Fc}Tl (0.52 mmol) and 0.070 g of anhydrous $CoCl_2$ (0.54 mmol) were dissolved in 100 mL of THF and allowed to stir overnight. The solution was filtered through a bed of Celite to remove TlI and the solvent evaporated. The green residue was triturated with pentanes and the solid collected on a frit. The solid was dissolved in a 50/50 mixture of pentanes and THF

and the solution cooled to -30 °C overnight. The resulting green crystalline solid was collected on a frit and washed with several portions of pentane and allowed to dry under vacuum yielding 0.3 g of $Tp^{Fc}CoCl$ (68 %). ^1H NMR (400 MHz, C_6D_6): 67.5 (br, 3 H), 33.5 (br, 3 H), 4.3 (br, 15 H), 3.4 (br, 6 H) 0.15 (br, 6 H) -17.8 (br, 1 H) ppm. IR (KBr): 3104 (s), 3093 (m), 2484 (w, B-H), 1546 (s), 1493 (s), 1433 (s), 1401 (s), 1382 (s), 1341 (s), 1182 (w), 1106 (s), 1042 (w), 1001 (s), 871 (s), 818 (w), 771 (s), 505 (m), 487 (s), 457 (s) cm^{-1}. μ_{eff} = 4.4(1) μ_B (295 K). Mp: 237 – 239 °C. Anal Calcd for $C_{39}H_{34}N_6BFe_3CoCl$: C, 54.50; H, 3.99; N, 9.78. Found: C, 54.42; H, 4.24; N, 9.52.

3.4.6 Iodo-hydrotris(3-ferrocenyl-5-methylpyrazolyl)borato-cobalt(II), $Tp^{Fc,Me}CoI$ (11).

A 500 mL round bottom flask charged with 8.0 g of $Tp^{Fc,Me}Tl$ (7.9 mmol), 2.5 g of anhydrous CoI_2 (8.1 mmol) and 300 mL of CH_2Cl_2 was refluxed for 1 hour under N_2 . The solution was allowed to cool to room temperature and filtered in air through a bed of Celite to remove TlI and unreacted starting materials. The volume of the solution was reduced to 50 mL and 50 mL of diethyl ether was added and cooled to 0 °C. The resulting green crystalline solid was collected on a frit and washed with several portions of pentane and allowed to dry under vacuum yielding 6.4 g of $Tp^{Fc,Me}CoI$ (81 %). ^1H NMR (400 MHz, C_6D_6): 73.1 (br, 3 H), 16.3 (br, 9 H), 3.7 (br, 15 H), 3.3 (br, 6 H) 1.3 (br, 6 H) -21.0 (br, 1 H) ppm. IR (KBr): 3098 (w), 2922 (w), 2540 (w, B-H), 1558 (s), 1469 (s), 1426 (s), 1364 (m), 1322 (s), 1184 (w), 1106 (s), 1058 (s), 1001 (s), 884 (s), 817 (w), 757 (s), 647 (m), 503 (m) cm^{-1}. UV-vis (THF), λ_{max} (ϵ, M^{-1} cm^{-1}): 431 (1010), 614 (357), 656 (575), 681 (525) nm. μ_{eff} = 4.3(1) μ_B (295 K). Mp: 246 – 248 °C. Anal Calcd for $C_{42}H_{40}N_6BFe_3CoI$: C, 50.80; H, 4.06; N, 8.46. Found: C, 50.29; H, 4.07; N, 8.23.

3.4.7 Chloro-hydrotris(3-ferrocenyl-5-methylpyrazolyl)borato-cobalt(II), $Tp^{Fc,Me}CoCl$ (12).

To a stirred solution of 3.2 g of $Tp^{Fc,Me}Tl$ (3.16 mmol) in 200 mL of CH_2Cl_2 was added 0.62 g of anhydrous $CoCl_2$ (4.78 mmol). The solution was refluxed for 1 hour, during which, the solution changed from orange to green and a colorless precipitate formed. The solution was allowed to cool to room temperature and filtered through a bed of Celite to remove TlCl and unreacted $CoCl_2$. The volume of the solution was reduced to 50 mL and 50 mL or diethyl ether was added and the solution cooled to 0 °C overnight. The resulting green solid was collected on a frit and washed with several portions of pentane and allowed to dry under vacuum yielding 2.125 g of $Tp^{Fc,Me}CoCl$ (75 %). ^1H NMR (400 MHz, C_6D_6): 72.4 (br, 3 H), 12.4 (br, 9 H), 6.4 (br, 6 H), 5.11 (br, 15 H) 3.6 (br, 6 H) -21.4 (br, 1 H) ppm. IR (KBr): 3097 (w), 2923 (w), 2539 (w, B-H), 1558 (s), 1469 (s), 1426 (s), 1364 (m), 1322 (s), 1183 (w), 1106 (s), 1058 (s), 1001 (s), 884 (s), 817 (w), 757 (s), 647 (m), 503 (m) cm^{-1}. $\mu_{eff} = 4.4(1)\ \mu_B$ (295 K). Mp: 255 – 257 °C. Anal Calcd for $C_{42}H_{40}N_6BFe_3CoCl$: C, 55.95; H, 4.47; N, 9.32. Found: C, 55.44; H, 4.96; N, 9.01.

3.4.8 Iodo-hydrotris(3-ferrocenyl-5-iso-propylpyrazolyl)borato-cobalt(II), $Tp^{Fc,iPr}CoI$ (13).

3 g of $Tp^{Fc,iPr}Tl$ (2.74 mmol) and 0.85 g of anhydrous CoI_2 (2.74 mmol) were dissolved in 150 mL of THF and allowed to stir overnight . The solution was filtered through a bed of Celite to remove TlI and the solvent evaporated. The crude product was washed with pentanes then recrystallized from a saturated solution of $Tp^{Fc,iPr}CoI$ in benzene and allowed to stand overnight. The resulting green crystalline solid was collected on a frit and washed with several portions of pentane and allowed to dry under vacuum yielding 2.1 g of $Tp^{Fc,iPr}CoI$ (71 %). ^1H NMR (400

MHz, C_6D_6): 74.5 (br, 3 H), 5.6 (br, 3 H), 3.1 (br, 18 H), 1.4 (br, 15 H), 0.5 (br, 6 H), 0.3 (br, 6) -22.0 (br, 1 H) ppm. IR (KBR): 3094 (w), 2963 (w), 2927 (w), 2870 (s), 2556 (w, B-H), 1652 (m), 1558 (s), 1506 (m), 1459 (w), 1397 (s), 1296 (s), 1171 (s), 1106 (s), 1001 (s), 897 (s), 814 (w), 738 (s), 703 (s), 644 (m) cm^{-1}. μ_{eff} = 4.3(1) μ_B (295 K). Mp: 229-231 °C. Anal Calcd for $C_{48}H_{52}N_6BFe_3CoI$: C, 53.52; H, 4.87; N, 7.80. Found: C, 53.86; H, 4.80; N, 7.69.

3.4.9 Chloro-hydrobis(3-ferrocenyl-5-iso-propylpyrazolyl)(3-iso-propyl-5-ferrocenylpyrazolyl)borato-cobalt(II), $Tp^{Fc,iPr*}CoCl$ (14).

To a stirred solution of 0.5 g of $Tp^{Fc,\ iPr}Tl$ (0.46 mmol) in 100 mL of THF, 0.06 g of anhydrous $CoCl_2$ (0.46 mmol). The solution was allowed to stir overnight, during which, the solution changed from orange to green and a colorless precipitate formed. The solution was filtered through a bed of Celite to remove TlCl and the THF removed under vacuum. The crude product was washed with pentane and dissolved in 20 mL of THF to which 20 mL of pentanes was layered and allowed to cool to -30 °C overnight. The resulting green solid was collected on a frit and washed with several portions of pentane and allowed to dry under vacuum yielding 0.34 g of $Tp^{Fc,\ iPr}CoCl$ (75 %). ^1H NMR (400 MHz, $CDCl_3$): 82.9 (s), 66.5 (s), 14.7 (br), 7.06 (s), 3.4 (br), 0.6 (s), 0.2 (s), -6.8 (s). IR (KBR): 3094 (w), 2963 (w), 2927 (w), 2870 (s), 2576 (w, B-H), 1652 (m), 1558 (s), 1506 (m), 1459 (w), 1397 (s), 1296 (s), 1171 (s), 1106 (s), 1001 (s), 897 (s), 814 (w), 738 (s), 703 (s), 644 (m) cm^{-1}. μ_{eff} = 4.4(1) μ_B (295 K). Mp: 174-176 °C (decomp.). Anal Calcd for $C_{48}H_{52}N_6BFe_3CoCl$: C, 58.49; H, 5.34; N, 8.53. Found: C, 57.50; H, 5.34; N, 8.29.

3.4.10 Room Temperature Conversion of $Tp^{Fc,iPr}CoI$ (13) to $Tp^{Fc,iPr*}CoCl$ (14).

Recrystallization by slow diffusion of pentanes into a saturated solution of $Tp^{Fc,iPr}CoI$ in $CHCl_3$ resulted in the quantitative conversion of $Tp^{Fc,i\text{-}Pr}CoI$ to $Tp^{Fc,i\text{-}Pr*}CoCl$ confirmed by ^1H NMR spectroscopy.

3.4.11 Carbonyl-hydrotris(3-ferrocenylpyrazolyl)borato-copper(I), $Tp^{Fc}Cu(CO)$ (16).

In a glovebox, 0.25 g (0.26 mmol) of $Tp^{Fc}Tl$ and 0.05 g (0.26 mmol) CuI were combined in an ampule equipped with a stir bar and dissolved in 20 mL of THF. The ampule was placed on a high vacuum line and freeze/pump/thawed 3 times. 1 atm of CO was introduced to the ampule and the reaction was allowed to stir overnight. The ampule was again freeze/pump/thawed three times to remove excess CO. The reaction was filtered and the THF concentrated to 10 mL and pentanes introduced via vapor phase diffusion, yielding orange crystalline material. The crystals were collected and washed with pentanes and dried under vacuum yielding 0.122 g (55 %) of the product. ^1H NMR (400 MHz, $CDCl_3$): 7.54 (s, 3 H), 6.24 (s, 3 H), 4.59 (s, 6 H), 4.23 (s, 6 H) 4.03 (s, 15 H) ppm. IR (KBR): 3092 (w), 2960 (s), 2922 (w), 2852 (w), 2463 (w, B-H), 2064 (s, υCO), 1549 (s), 1490 (s), 1400 (s), 1139 (s), 1259 (s), 1188 (s), 1044 (m), 871 (s), 814 (w), 722 (s), 504 (s) cm^{-1}. Mp: 210 – 214 °C. Anal Calcd for $C_{40}H_{34}N_6OBFe_3Cu$: C, 56.08; H, 4.00; N, 9.81. Found: C, 56.34; H, 4.12; N, 9.77.

3.4.12 Carbonyl-hydrotris(3-ferrocenyl-5-methylpyrazolyl)borato-copper(I), $Tp^{Fc,Me}Cu(CO)$ (17).

In a glovebox, 0.5 g of $Tp^{Fc,Me}Tl$ and 0.09 g CuI were combined in an ampule equipped with a stir bar and dissolved in 20 mL of THF. The ampule was placed on a high vacuum line and freeze/pump/thawed 3 times. 1 atm of CO was introduced to the ampule and the reaction was

allowed to stir overnight. The ampule was again freeze/pump/thawed three times to remove excess CO. The reaction was filtered and the THF concentrated to 10 mL and pentanes introduced via vapor phase diffusion yielding orange crystalline material. The crystals were collected and washed with pentanes and dried under vacuum yielding 0.216 g (49 %) of the product. ^{1}H NMR (400 MHz, CD_2Cl_2): 6.16 (s, 3 H), 4.57 (s, 6 H), 4.27 (s, 6 H), 4.11 (s, 15 H) 2.48 (s, 9 H) ppm. IR (KBR): 3096 (w), 2960 (w), 2922 (w), 2852 (w), 2517 (w, B-H), 2060 (s, υCO), 1635 (m), 1560 (s), 1428 (s), 1360 (m), 1261 (s), 1185 (s), 1106(s), 1023 (s), 882 (s), 810 (w), 645 (w), 505 (s) cm^{-1}. Mp: 236 – 238 °C. Anal Calcd for $C_{43}H_{40}N_6OBFe_3Cu$: C, 57.47; H, 4.49; N, 9.35. Found: C, 56.72; H, 4.43; N, 9.17.

3.4.13 Carbonyl-hydrobis(3-ferrocenyl-5-iso-propylpyrazolyl)(3-iso-propyl-5-ferrocenylpyrazolyl)borato-copper(I) and Carbonyl-hydrobis(3-iso-propyl-5-ferrocenylpyrazolyl)(3-ferrocenyl-5-iso-propylpyrazolyl)borato-copper(I), $Tp^{Fc,iPr*}Cu(CO)$ (19) and $Tp^{Fc,iPr**}Cu(CO)$ (18) .

In a glovebox, 0.5 g (0.46 mmol) of $Tp^{Fc,iPr}Tl$ and 0.065 g (0.46 mmol) CuI were combined in an ampule equipped with a stir bar and dissolved in 20 mL of THF. The ampule was placed on a high vacuum line and free/pump/thawed 3 times. 1 atm of CO was introduced to the ampule and the reaction was allowed to stir overnight. The ampule was again freeze/pump/thawed three times to remove excess CO. The reaction was filtered and the THF evaporated. The crude material was recrystallized from a 50/50 mixture of pentanes/diethylether in the freezer overnight at 0 °C. The orange crystals were collected on a frit, washed with pentanes and dried under vacuum yielding 0.27 g (60 %) of the product. ^{1}H NMR (400 MHz, $CDCl_3$): Isomer 1: 6.16 (s, 2 H), 6.12 (s, 1 H), 4.66 (s, 2 H), 4.60 (s, 4 H), 4.03 (s, 2 H), 4.00 (s, 4 H), 3.86 (s, 5 H), 3.84 (s, 10 H), 3.65 (m, 2 H), 2.99 (m, 1 H), 1.28 (d, J = 6.61 Hz, 6 H), 1.25

(d, J = 6.76 Hz, 12 H). Isomer 2: 6.26 (s, 2 H), 6.23 (s, 1 H), 4.60 (s, 2 H), 4.53 (s, 4 H), 4.10 (s, 4 H), 4.06 (s, 2 H), 3.91 (s, 10 H), 3.89 (s, 5 H), 3.65 (m, 1 H), 2.99 (m, 2 H), 1.21 (d, J = 6.73 Hz, 12 H), 1.16 (d, J = 6.91 Hz, 6 H). IR (KBR): 3094 (w), 2963 (w), 2927 (w), 2869 (s), 2539 (w, B-H), 2064 (w, υCO), 1652 (m), 1558 (s), 1506 (m), 1459 (w), 1397 (s), 1296 (s), 1171 (s), 1106 (s), 1001 (s), 895 (s), 872 (s), 810 (w), 745 (s), 706 (s), 652 (m) cm^{-1}. Mp: 160 – 164 °C. Anal Calcd for $C_{49}H_{52}N_6OBFe_3Cu$: C, 59.88; H, 5.33; N, 8.55. Found: C, 59.99; H, 5.40; N, 8.31.

3.5 References

1. Trofimenko, S. *Scorpionates*, **1999**, London: Imperial College Press.
2. Pettinari, C. *Scorpionates II: Chelating Borate Ligands,* **2008**, London: Imperial College Press.
3. Calabrese, J. C., Trofimenko, S., and Thompson, J. S., *J. Chem. Soc. Chem. Commun.,* **1986**, 1122.
4. Trofimenko, S., Calabrese, J. C., and Thompson, J. S., *Inorg. Chem.,* **1987**, *26*, 1507.
5. Cano, M., Heras, J. V., Jones, C. J., McCleverty, J. A., Trofimenko, S. *J. Chem. Soc. Dalton Trans*., **1990**, *9*, 3577.
6. Reinaud, O. M., Rheingold, A. L., and Theopold, K. H., *Inorg. Chem.*, **1994**, *33*, 2306.
7. Trofimenko, S., Calabrese, J. C., Kochi, J. K., Wolowiec, S., Hulsbergen, F. B., and Reedijk, J., *Inorg. Chem*., **1992**, *31*, 3943.
8. Rheingold, A. L., White, C. B., and Trofimenko, S., *Inorg. Chem*., **1993**, *32*, 3471.
9. Calabrese, J. C. and Trofimenko, S., *Inorg. Chem*., **1992**, *31*, 4810.
10. Han, R., Parkin, G., and Trofimenko, S., *Polyhedron*, **1995**, *14(3)*, 287.
11. Trofimenko, S.; Calabrese, J. C.; Domaille, P. J.; Thompson, J. S. *Inorg. Chem.,***1989**, *28*, 1091.
12. a) LeCloux, D. D., Keyes, M.C., Osawa, M., Renolds, V., Tolman, W. B., *Inorg. Chem*., **1994**, *33*, 6361.; b) Murtuza, S., Casagrande, O. L., Jordan, R. F., *Organometallics*, **2002**, *21*, 1882- 1890. c) Biagini, P., Calderazzo, F., Marchetti, F., Romano, A. M., Spera, S., *Organomet. Chem.*, **2006**, *691*, 4172.
13. Wiegand, B., Friend, C. M., *Chem. Rev*., **1992**, *92*, 491.

14. a) Albinati, A., Bovens, M., Rűegger, H., Venanzi, V. M., *Inorg. Chem*., **1997**, *36*, 5991.; b) Bucher, U. E., Currao, A., Nesper, R., Rűegger, H., Venanzi, V. M. and Younger, E., *Inorg. Chem*., **1995**, *34*, 66.

15. Kitajima, N., Fujisawa, K., Fujimoto, C., Moro-oka, Y., Hashimoto, S., Kitagawa T., Toriumi, K., Tatsumi, K. and Nakamura, A., *J. Am. Chem. Soc*., **1992**, *114*, 1277.

16. Kiani, S., Long, J. R. and Stavropoulos, P., *Inorg. Chim. Acta*, **1997**, *263*, 357.

17. Ruggiero, C. E., Carrier, S. M., Antholine, W. E., Whittaker, J. W., Cramer, C. J. and Tolman, W. B., *J. Am. Chem. Soc*., **1993**, *115*, 11285.

18. Imai, S., Fujisawa, K., Kobayashi, T, Shirasawa, N., Fujii, H., Yoshimura, T., Kitajima, N. and Moro-oka, Y., *Inorg. Chem*., **1998**, *37*, 3066.

19. Dias, H. V. R., Kim, H. J., Lu, H. L., Rajeshwar, K., Tacconi, N. R., Derecskei-Kovacs, A. and Marynick, D. S., *Organometallics*, **1996**, *15*, 2994.

20. Dias, H. V. R. and Lu, H. L., *Inorg. Chem.*, **1995**, *34*, 5380.

21. Pangborn, A. B.;Giardello, M. A. Grubbs, R. H. Rosen, R. K.; Timmers, F. J., *Organometallics*, **1996**, *15*, 1518.

22. Magnetic Properties of Coordination and Organometallic Transition Metal Compounds; Hellwege, K. H.; Hellwege, A. M., Ed.; Landolt-Börnstein Series; Springer-Verlag: Berlin, 1981; Vol. 11.

23. Squeeze, Platon: Spek, A. L., J. Appl. Cryst., 2003, *36*, 7.

Chapter 4

DIOXYGEN ACTIVATION BY LOW-VALENT $Tp^{Fc,Me}Co$ COMPLEXES

4.1 Introduction

Many Co(III) complexes are strong oxidizing agents[1].

$$Co^{3+}(aq) + e^- \longrightarrow Co^{2+}(aq) \quad E^o = 1.82\ V$$

Previous work in the Theopold group has led to the isolation of many interesting and novel Co oxygen compounds. From these studies, two kinds of intermediates have attracted our particular interest: the cobalt dioxygen complexes and the high-valent, cobalt oxo species. Metal dioxygen complexes can be classified into three groups, neutral dioxygen species, superoxides and peroxides. In the cases of superoxides and peroxides, the dioxygen ligand can bind in different ways to the metal (Scheme 4.1). Although the end-on binding motif is the most common, there are a few examples of side-on superoxide complexes.[2,3]

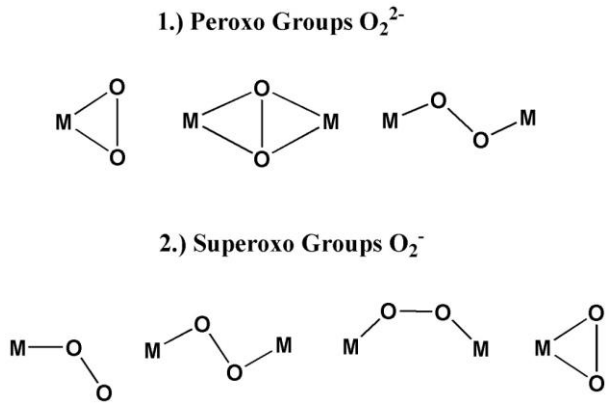

Scheme 4.1: Binding modes of O_2 to transition metals.[4]

Over the past two decades, the activation of dioxygen with cobalt complexes bearing sterically hindered tris(pyrazolyl)borate ligands has been well established by the Theopold lab; many of the resulting compounds have been subject to decomposition via hydrogen atom abstraction from the ligands. Specifically, when $Tp^{tBu,Me}Co(N_2)$ was exposed to oxygen the formation of a novel side-on superoxo species, $Tp^{tBu,Me}Co(O_2)$, was observed.[2a] When $Tp^{tBu,Me}Co(O_2)$ reacted with another equivalent of $Tp^{tBu,Me}CoN_2$, the only observable product is $Tp^{tBu,Me}CoOH$. This occurs presummably via hydrogen atom extraction from the tert-butyl groups on the ligand by a reactive '$Tp^{tBu,Me}Co{=}O$' species. The radical that is formed on the ligand then goes on to abstract a hydrogen atom from an external substrate. These results have encouraged us to synthesize new Tp ligands in which this type of decomposition can be eliminated or deterred.

The aim of this Chapter is to examine the reactivity of the cobalt(I) and cobalt(II) complexes bearing the novel $Tp^{Fc,Me}$ ligand towards O_2 for the isolation of a high-valent cobalt oxo species. Also described is the reactivity towards other oxidizing agents, specifically adamantly azide, for the isolation of a high-valent cobalt imido species.

4.2 Results and Discussion

4.2.1 Synthesis and Characterization of $Tp^{Fc,Me}CoNO_3$.

$TpMNO_3$ complexes have been utilized as precursors for the syntheses of many first-row transition metal hydroxide complexes.[5] $Tp^{Fc,Me}Tl$ was treated with $Co(NO_3)_2{\bullet}6H_2O$ in CH_2Cl_2 and allowed to stir over night. After workup, the product was recrystallized via vapor phase

diffusion of diethyl ether into a saturated solution of **20** in CH_2Cl_2, yielding orange-brown crystals in 65 % yield. The molecular structure (Figure 4.1) of **20** reveals a five-coordinate structure with the Tp bound $\boldsymbol{\kappa}^3$ to the Co metal center along with two oxygens of the nitrato group. However, the Co-O1 bond (1.986(3) Å) (Table 4.1) is significantly shorter than the Co-O2 bond of 2.334(3) Å due to the trans influence of N3. Similar Co-O bond distances are observed in complexes of the type $TpCoNO_3$ where the Tp ligand contains sterically hindered substituents.[6] For example, $Tp^{tBu}CoNO_3$[6a] features κ^2-coordination of the nitrate anion with significantly different Co-O bond distances (2.001(3) and 2.339(3) Å). Similarly, $Tp^{tBu,Me}CoNO_3$[6b] also displays different Co-O bond distances in the solid state consistent with **20** and $Tp^{tBu}CoNO_3$.

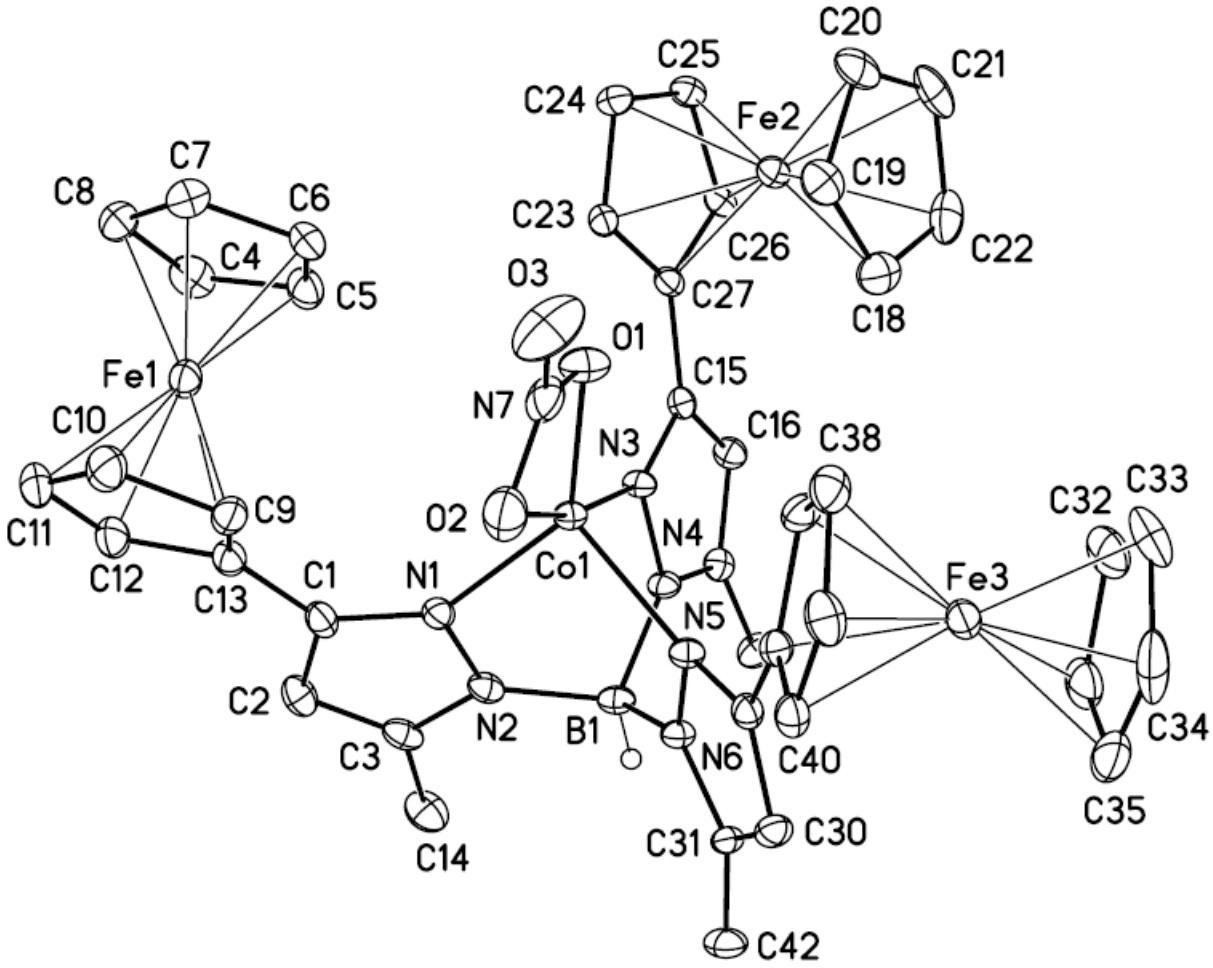

Figure 4.1: Molecular structure of $Tp^{Fc,Me}CoNO_3$ (20) at the 30% probability level. Hydrogen atoms (except the boron bound hydrogen, H1B) have been removed for clarity.

Table 4.1: Selected interatomic distances (Å) and angles (°) for $Tp^{Fc,Me}CoNO_3$ (20).

Distances (Å)

Co(1)-O(1)	1.986(3)	C(10)-C(11)	1.424(6)
Co(1)-N(5)	2.035(3)	C(11)-C(12)	1.420(6)
Co(1)-N(1)	2.044(3)	C(12)-C(13)	1.440(5)
Co(1)-N(3)	2.070(3)	C(15)-C(16)	1.402(5)
Co(1)-O(2)	2.334(3)	C(15)-C(27)	1.467(5)
B(1)-N(2)	1.547(5)	C(16)-C(17)	1.385(5)
B(1)-N(6)	1.545(5)	C(17)-C(28)	1.494(5)
B(1)-N(4)	1.562(5)	C(18)-C(19)	1.413(6)
N(1)-C(1)	1.348(5)	C(18)-C(22)	1.416(7)
N(1)-N(2)	1.393(4)	C(19)-C(20)	1.410(6)
N(2)-C(3)	1.346(5)	C(20)-C(21)	1.415(7)
N(3)-C(15)	1.347(5)	C(21)-C(22)	1.437(7)
N(3)-N(4)	1.382(4)	C(23)-C(27)	1.425(5)
N(4)-C(17)	1.351(5)	C(23)-C(24)	1.427(5)
N(5)-C(29)	1.347(5)	C(24)-C(25)	1.422(5)
N(5)-N(6)	1.379(4)	C(25)-C(26)	1.425(5)
N(6)-C(31)	1.356(5)	C(26)-C(27)	1.429(5)
N(7)-O(1)	1.224(5)	C(29)-C(30)	1.378(5)
N(7)-O(3)	1.239(5)	C(29)-C(41)	1.478(5)
N(7)-O(2)	1.276(5)	C(30)-C(31)	1.371(5)
C(1)-C(2)	1.398(6)	C(31)-C(42)	1.494(5)
C(1)-C(13)	1.473(6)	C(32)-C(33)	1.417(7)
C(2)-C(3)	1.374(6)	C(32)-C(36)	1.416(6)
C(3)-C(14)	1.505(5)	C(33)-C(34)	1.403(7)
C(4)-C(5)	1.410(6)	C(34)-C(35)	1.405(8)
C(4)-C(8)	1.412(7)	C(35)-C(36)	1.416(7)
C(5)-C(6)	1.416(6)	C(37)-C(38)	1.421(5)
C(6)-C(7)	1.421(6)	C(37)-C(41)	1.433(5)
C(7)-C(8)	1.415(6)	C(38)-C(39)	1.422(6)
C(9)-C(10)	1.429(6)	C(39)-C(40)	1.408(6)
C(9)-C(13)	1.434(6)	C(40)-C(41)	1.426(5)

Angles (°)

O(1)-Co(1)-N(5)	116.76(12)	N(5)-Co(1)-N(3)	93.79(12)
O(1)-Co(1)-N(1)	136.91(13)	N(1)-Co(1)-N(3)	91.70(12)
N(5)-Co(1)-N(1)	97.98(12)	O(1)-Co(1)-O(2)	58.42(13)
O(1)-Co(1)-N(3)	109.45(12)	N(5)-Co(1)-O(2)	89.94(12)

N(1)-Co(1)-O(2)	99.58(13)	C(11)-C(12)-C(13)	107.9(4)
N(3)-Co(1)-O(2)	167.52(12)	C(9)-C(13)-C(12)	107.6(4)
N(2)-B(1)-N(6)	110.2(3)	C(9)-C(13)-C(1)	129.5(4)
N(2)-B(1)-N(4)	108.9(3)	C(12)-C(13)-C(1)	122.7(4)
N(6)-B(1)-N(4)	108.9(3)	N(3)-C(15)-C(16)	109.4(3)
C(1)-N(1)-N(2)	106.2(3)	N(3)-C(15)-C(27)	124.2(3)
C(1)-N(1)-Co(1)	143.0(3)	C(16)-C(15)-C(27)	126.3(3)
N(2)-N(1)-Co(1)	109.8(2)	C(17)-C(16)-C(15)	106.5(3)
C(3)-N(2)-N(1)	109.5(3)	N(4)-C(17)-C(16)	107.2(3)
C(3)-N(2)-B(1)	129.3(3)	N(4)-C(17)-C(28)	123.9(3)
N(1)-N(2)-B(1)	121.1(3)	C(16)-C(17)-C(28)	128.9(4)
C(15)-N(3)-N(4)	106.4(3)	C(19)-C(18)-C(22)	108.6(4)
C(15)-N(3)-Co(1)	142.9(2)	C(18)-C(19)-C(20)	108.1(4)
N(4)-N(3)-Co(1)	109.7(2)	C(19)-C(20)-C(21)	108.4(4)
C(17)-N(4)-N(3)	110.5(3)	C(20)-C(21)-C(22)	107.7(4)
C(17)-N(4)-B(1)	129.2(3)	C(18)-C(22)-C(21)	107.2(4)
N(3)-N(4)-B(1)	120.0(3)	C(27)-C(23)-C(24)	108.0(3)
C(29)-N(5)-N(6)	106.3(3)	C(23)-C(24)-C(25)	108.2(3)
C(29)-N(5)-Co(1)	140.1(3)	C(26)-C(25)-C(24)	107.8(3)
N(6)-N(5)-Co(1)	110.2(2)	C(27)-C(26)-C(25)	108.2(3)
C(31)-N(6)-N(5)	109.2(3)	C(23)-C(27)-C(26)	107.7(3)
C(31)-N(6)-B(1)	130.2(3)	C(23)-C(27)-C(15)	128.6(3)
N(5)-N(6)-B(1)	120.5(3)	C(26)-C(27)-C(15)	123.7(3)
O(1)-N(7)-O(3)	122.1(4)	N(5)-C(29)-C(30)	109.9(3)
O(1)-N(7)-O(2)	116.8(4)	N(5)-C(29)-C(41)	121.7(3)
O(3)-N(7)-O(2)	121.0(4)	C(30)-C(29)-C(41)	128.3(3)
N(7)-O(1)-Co(1)	101.2(2)	C(31)-C(30)-C(29)	106.6(3)
N(7)-O(2)-Co(1)	83.4(2)	C(30)-C(31)-N(6)	107.9(3)
N(1)-C(1)-C(2)	109.6(4)	C(30)-C(31)-C(42)	129.7(3)
N(1)-C(1)-C(13)	125.3(4)	N(6)-C(31)-C(42)	122.4(4)
C(2)-C(1)-C(13)	125.0(4)	C(33)-C(32)-C(36)	108.2(4)
C(3)-C(2)-C(1)	106.3(4)	C(34)-C(33)-C(32)	107.6(5)
N(2)-C(3)-C(2)	108.4(4)	C(33)-C(34)-C(35)	108.8(5)
N(2)-C(3)-C(14)	122.6(4)	C(36)-C(35)-C(34)	108.0(5)
C(2)-C(3)-C(14)	129.0(4)	C(32)-C(36)-C(35)	107.4(5)
C(5)-C(4)-C(8)	108.4(4)	C(38)-C(37)-C(41)	107.7(3)
C(4)-C(5)-C(6)	108.0(4)	C(37)-C(38)-C(39)	107.9(4)
C(7)-C(6)-C(5)	107.8(4)	C(40)-C(39)-C(38)	108.6(4)
C(6)-C(7)-C(8)	107.9(4)	C(41)-C(40)-C(39)	108.1(4)
C(7)-C(8)-C(4)	107.9(4)	C(40)-C(41)-C(37)	107.6(3)
C(10)-C(9)-C(13)	107.8(4)	C(40)-C(41)-C(29)	124.2(3)
C(11)-C(10)-C(9)	108.2(4)	C(37)-C(41)-C(29)	128.1(3)
C(10)-C(11)-C(12)	108.4(4)		

4.2.2 Synthesis and Characterization of $Tp^{Fc,Me}CoOH$.

The previously reported $Tp^{tBu,Me}Co(O_2)$ has shown that the splitting dioxygen to form a putative metal oxo intermediate, when reacted with an equivalent of $Tp^{tBu,Me}Co(N_2)$, is plausible. However, this '$Tp^{tBu,Me}Co{=}O$' species undergoes hydrogen atom abstraction from either the ligand or external substrates to generate the corresponding hydroxide species.[2a] It seemed appropriate to independently synthesize the hydroxide complex, $Tp^{Fc,Me}CoOH$. After stirring a biphasic solution of $Tp^{Fc,Me}CoNO_3$ in CH_2Cl_2 and aqueous NaOH for 1 hour, the organic layer was separated and washed with several more portions of water and dried over Na_2SO_4. The solvent was removed and the residue was washed with pentane and recrystallized by slow diffusion of ether into a CH_2Cl_2 solution of **21**, yielding a brown crystalline material in 56 % yield. This complex can also be synthesized by the dropwise addition of a 1 M solution of n-Bu_4NOH in methanol to a solution of $Tp^{Fc,Me}CoI$ in THF at 0 °C in 54 % yield. The IR spectrum of **21** revealed a band at 3639 cm^{-1} which is characteristic of an O-H stretching frequency. **21** crystallizes in the triclinic space group P-1. The molecular structure of **21** (Figure 4.2) displays a four coordinate pseudo tetrahedral coordination geometry about the cobalt. This is similar to the structure observed in $Tp^{tBu,Me}CoOH$.[2a] The adaptation of a four coordinate geometry reinforces the notion that the $Tp^{Fc,Me}$ ligand can function as 'tetrahedral enforcers'. The Co-O bond distance (Table 4.2) is 1.892(4) Å.

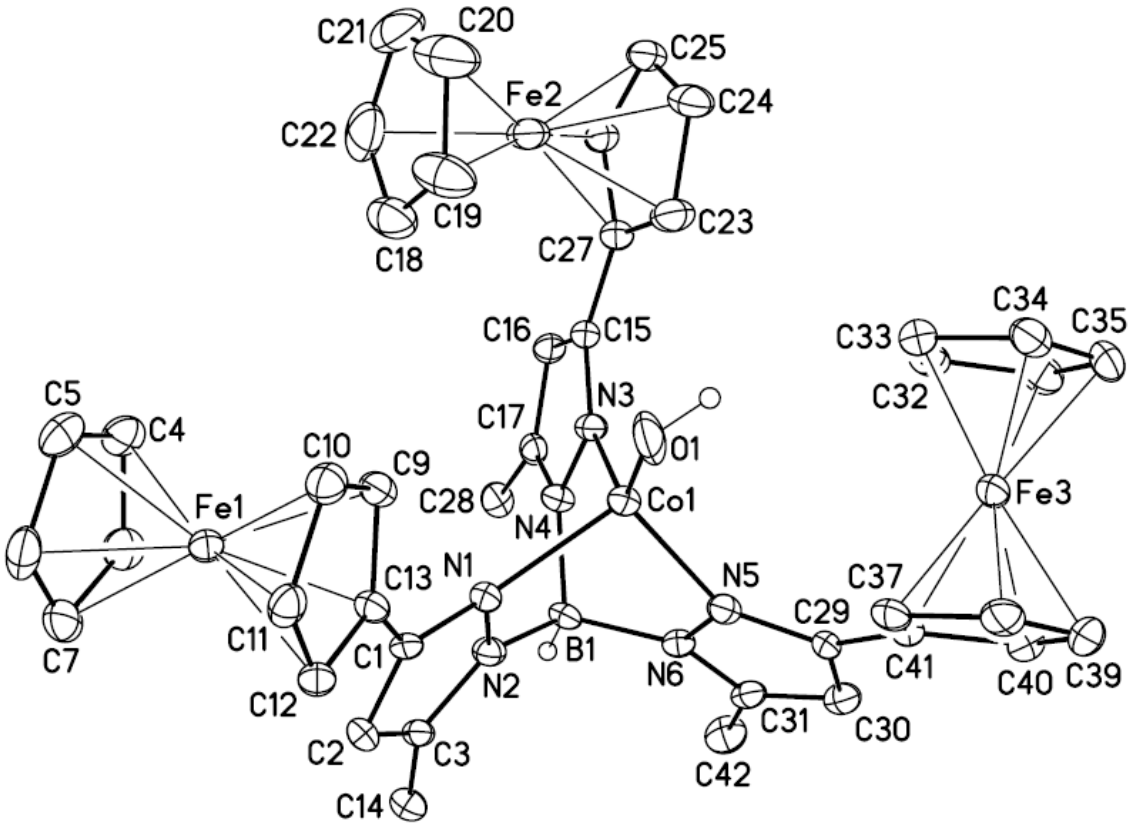

Figure 4.2: Molecular structure of $Tp^{Fc,Me}CoOH$ (21) at the 30% probability level. Hydrogen atoms (except the boron bound hydrogen, H1B, and the oxygen bound hydrogen, H1O) have been removed for clarity.

Table 4.2: Selected interatomic distances (Å) and angles (°) for $Tp^{Fc,Me}CoOH$ (21).

Distances (Å)

Co(1)-O(1)	1.892(4)	C(12)-C(13)	1.429(6)
Co(1)-N(5)	2.049(4)	C(15)-C(16)	1.406(6)
Co(1)-N(3)	2.057(4)	C(15)-C(27)	1.466(6)
Co(1)-N(1)	2.064(3)	C(16)-C(17)	1.382(6)
B(1)-N(2)	1.536(6)	C(17)-C(28)	1.490(6)
B(1)-N(6)	1.553(6)	C(18)-C(22)	1.388(9)
B(1)-N(4)	1.556(6)	C(18)-C(19)	1.399(8)
N(1)-C(1)	1.338(5)	C(19)-C(20)	1.401(8)
N(1)-N(2)	1.383(5)	C(20)-C(21)	1.388(10)
N(2)-C(3)	1.354(5)	C(21)-C(22)	1.425(9)
N(3)-C(15)	1.340(5)	C(23)-C(24)	1.422(6)
N(3)-N(4)	1.388(5)	C(23)-C(27)	1.425(7)
N(4)-C(17)	1.357(5)	C(24)-C(25)	1.398(7)
N(5)-C(29)	1.347(5)	C(25)-C(26)	1.428(7)
N(5)-N(6)	1.389(5)	C(26)-C(27)	1.427(6)
N(6)-C(31)	1.350(5)	C(29)-C(30)	1.388(6)
C(1)-C(2)	1.403(6)	C(29)-C(41)	1.468(6)
C(1)-C(13)	1.457(6)	C(30)-C(31)	1.390(6)
C(2)-C(3)	1.373(6)	C(31)-C(42)	1.493(6)
C(3)-C(14)	1.493(6)	C(32)-C(33)	1.411(7)
C(4)-C(5)	1.414(7)	C(32)-C(36)	1.423(7)
C(4)-C(8)	1.427(7)	C(33)-C(34)	1.416(6)
C(5)-C(6)	1.411(7)	C(34)-C(35)	1.404(7)
C(6)-C(7)	1.410(7)	C(35)-C(36)	1.437(7)
C(7)-C(8)	1.412(7)	C(37)-C(38)	1.419(6)
C(9)-C(13)	1.425(6)	C(37)-C(41)	1.434(6)
C(9)-C(10)	1.432(6)	C(38)-C(39)	1.437(7)
C(10)-C(11)	1.424(6)	C(39)-C(40)	1.420(7)
C(11)-C(12)	1.414(6)	C(40)-C(41)	1.436(6)

Angles (°)

O(1)-Co(1)-N(5)	124.09(15)	N(2)-B(1)-N(4)	110.0(4)
O(1)-Co(1)-N(3)	130.10(16)	N(6)-B(1)-N(4)	108.4(3)
N(5)-Co(1)-N(3)	92.37(14)	C(1)-N(1)-N(2)	106.8(3)
O(1)-Co(1)-N(1)	114.29(15)	C(1)-N(1)-Co(1)	138.9(3)
N(5)-Co(1)-N(1)	95.33(14)	N(2)-N(1)-Co(1)	111.4(2)
N(3)-Co(1)-N(1)	91.82(14)	C(3)-N(2)-N(1)	109.6(3)
N(2)-B(1)-N(6)	109.4(4)	C(3)-N(2)-B(1)	130.6(4)

N(1)-N(2)-B(1)	119.8(3)	C(17)-C(16)-C(15)	106.5(4)
C(15)-N(3)-N(4)	106.6(3)	N(4)-C(17)-C(16)	107.4(4)
C(15)-N(3)-Co(1)	141.8(3)	N(4)-C(17)-C(28)	123.3(4)
N(4)-N(3)-Co(1)	111.4(2)	C(16)-C(17)-C(28)	129.3(4)
C(17)-N(4)-N(3)	109.9(3)	C(22)-C(18)-C(19)	108.9(6)
C(17)-N(4)-B(1)	129.4(4)	C(18)-C(19)-C(20)	106.8(7)
N(3)-N(4)-B(1)	120.3(3)	C(21)-C(20)-C(19)	109.8(7)
C(29)-N(5)-N(6)	106.0(3)	C(20)-C(21)-C(22)	106.5(6)
C(29)-N(5)-Co(1)	141.5(3)	C(18)-C(22)-C(21)	108.0(7)
N(6)-N(5)-Co(1)	111.4(2)	C(24)-C(23)-C(27)	108.4(4)
C(31)-N(6)-N(5)	109.9(3)	C(25)-C(24)-C(23)	107.9(5)
C(31)-N(6)-B(1)	129.5(4)	C(24)-C(25)-C(26)	108.9(4)
N(5)-N(6)-B(1)	120.6(3)	C(27)-C(26)-C(25)	107.5(4)
N(1)-C(1)-C(2)	109.4(4)	C(23)-C(27)-C(26)	107.3(4)
N(1)-C(1)-C(13)	122.6(4)	C(23)-C(27)-C(15)	128.4(4)
C(2)-C(1)-C(13)	128.0(4)	C(26)-C(27)-C(15)	124.3(4)
C(3)-C(2)-C(1)	106.4(4)	N(5)-C(29)-C(30)	110.2(4)
N(2)-C(3)-C(2)	107.8(4)	N(5)-C(29)-C(41)	123.6(4)
N(2)-C(3)-C(14)	122.9(4)	C(30)-C(29)-C(41)	126.1(4)
C(2)-C(3)-C(14)	129.3(4)	C(29)-C(30)-C(31)	106.2(4)
C(5)-C(4)-C(8)	107.8(5)	N(6)-C(31)-C(30)	107.6(4)
C(6)-C(5)-C(4)	108.3(5)	N(6)-C(31)-C(42)	123.5(4)
C(7)-C(6)-C(5)	107.9(5)	C(30)-C(31)-C(42)	128.9(4)
C(6)-C(7)-C(8)	108.6(5)	C(33)-C(32)-C(36)	108.5(4)
C(7)-C(8)-C(4)	107.4(5)	C(32)-C(33)-C(34)	108.4(4)
C(13)-C(9)-C(10)	108.1(4)	C(35)-C(34)-C(33)	107.8(4)
C(11)-C(10)-C(9)	107.8(4)	C(34)-C(35)-C(36)	108.7(4)
C(12)-C(11)-C(10)	108.0(4)	C(32)-C(36)-C(35)	106.5(5)
C(11)-C(12)-C(13)	108.7(4)	C(38)-C(37)-C(41)	108.8(4)
C(9)-C(13)-C(12)	107.3(4)	C(37)-C(38)-C(39)	107.4(5)
C(9)-C(13)-C(1)	127.3(4)	C(40)-C(39)-C(38)	108.4(4)
C(12)-C(13)-C(1)	125.3(4)	C(39)-C(40)-C(41)	108.1(4)
N(3)-C(15)-C(16)	109.6(4)	C(37)-C(41)-C(40)	107.2(4)
N(3)-C(15)-C(27)	123.3(4)	C(37)-C(41)-C(29)	128.5(4)
C(16)-C(15)-C(27)	127.1(4)	C(40)-C(41)-C(29)	124.0(4)

4.2.3 Synthesis and Characterization of $Tp^{Fc,Me}Co(\eta^3\text{-}C_3H_5)$.

The usual synthesis of dioxygen complexes takes advantage of the reaction of low valent, substitutionally labile metal complexes, such as $Tp^{tBu,Me}Co(N_2)$. However, the reduction of $Tp^{Fc,Me}CoI$ with KC_8 or Mg turnings under N_2 resulted in the formation of several products. These compounds displayed similar solubility, making isolation by recrystallization difficult. The inability to cleanly reduce $Tp^{Fc,Me}CoI$ led to the investigation of alternative routes for the synthesis of formally Co(I) starting materials. It has been well documented that organocobalt complexes of the type $Tp^{tBu,Me}CoR$ and $PhTt^{tBu}CoR$ undergo clean carbonylation when they are exposed to CO, yielding $Tp^{tBu,Me}Co(CO)$[7] and $PhTt^{tBu}Co(CO)_2$,[8] respectively. When 2.2 equiv. of a 1.7 M solution of allyl magnesium chloride was added drop-wise to a solution of $Tp^{Fc,Me}CoCl$ in dioxane, an immediate color change from green to orange was observed. Subsequent work-up by filtration, removal of solvent and recrystallization from a cooled solution of **22** in THF followed by a second recrystallization of **22** in a 50/50 mixture of toluene and pentanes yields the title compound, **22**, in 61% yield as orange crystals. X-ray quality crystals were obtained by vapor diffusion of pentanes into a saturated solution of $Tp^{Fc,Me}Co(\eta^3\text{-allyl})$ in dioxane. **22** crystallized with three molecules of dioxane in the asymmetric unit. The most notable feature of the structure (Figure 4.3) is the η^3-allyl ligation leading to a square pyramidal Co(II) coordination geometry with two basal (N1 and N3) and one apical (N5) pyrazolyl arm. The effective magnetic moment of **22** is 2.5 μ_B. This suggests a low-spin (S = 1/2) state with one unpaired electron consistent with the square pyramidal geometry and the 17-electron configuration of **22**.[8]

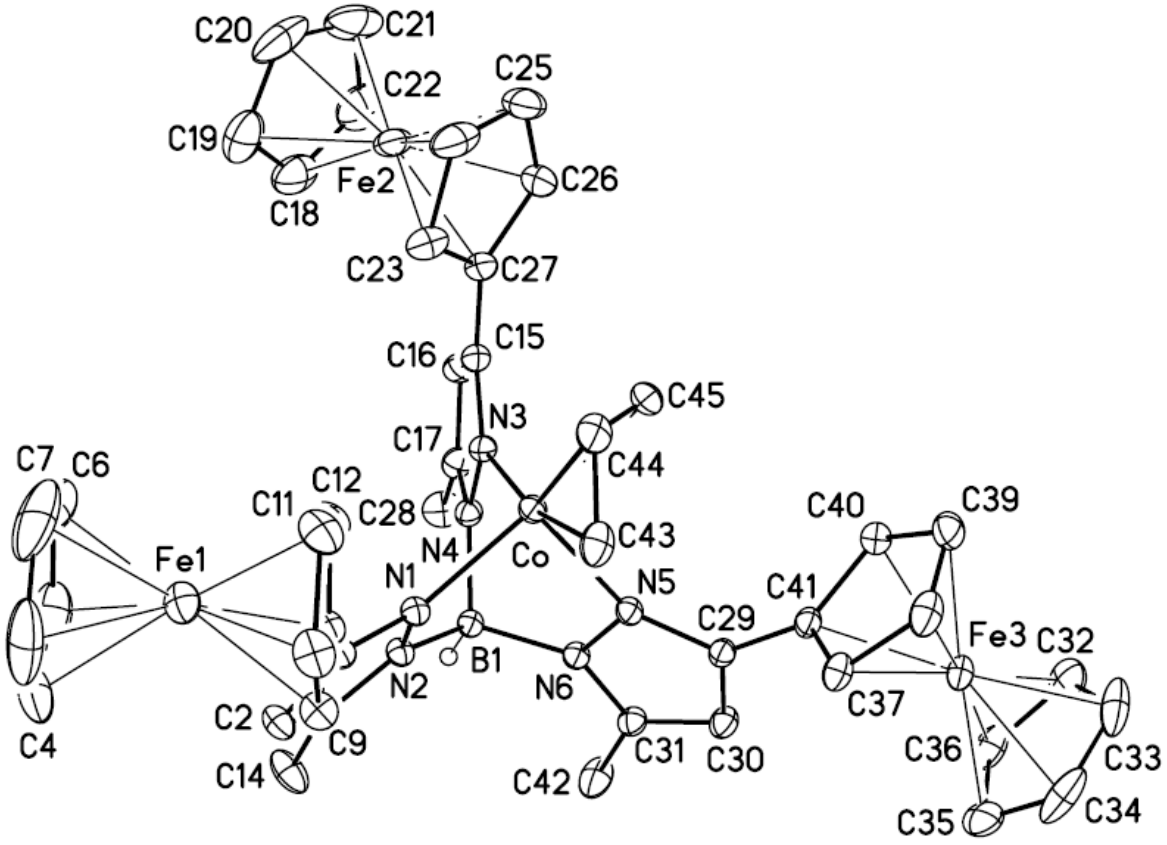

Figure 4.3: Molecular structure of $Tp^{Fc,Me}Co(\eta^3\text{-}C_3H_5)$ (22) at the 30% probability level. Hydrogen atoms (except the boron bound hydrogen, H1B) have been removed for clarity.

Table 4.3: Selected interatomic distances (Å) and angles (°) for $Tp^{Fc,Me}Co(\eta^3\text{-}C_3H_5)$ (22).

Distances (Å)

Co-C(44)	1.971(2)	C(12)-C(13)	1.422(3)
Co-N(3)	1.9955(18)	C(15)-C(16)	1.400(3)
Co-N(1)	2.0028(17)	C(15)-C(27)	1.461(3)
Co-C(45)	2.071(2)	C(16)-C(17)	1.373(3)
Co-C(43)	2.080(2)	C(17)-C(28)	1.492(3)
Co-N(5)	2.1982(17)	C(18)-C(19)	1.381(6)
B(1)-N(4)	1.536(3)	C(18)-C(22)	1.399(6)
B(1)-N(6)	1.537(3)	C(19)-C(20)	1.409(6)
B(1)-N(2)	1.545(3)	C(20)-C(21)	1.399(6)
N(1)-C(1)	1.341(3)	C(21)-C(22)	1.431(6)
N(1)-N(2)	1.370(2)	C(23)-C(24)	1.418(4)
N(2)-C(3)	1.354(3)	C(23)-C(27)	1.422(4)
N(3)-C(15)	1.343(3)	C(24)-C(25)	1.394(5)
N(3)-N(4)	1.375(2)	C(25)-C(26)	1.420(4)
N(4)-C(17)	1.355(3)	C(26)-C(27)	1.431(3)
N(5)-C(29)	1.349(3)	C(29)-C(30)	1.395(3)
N(5)-N(6)	1.374(2)	C(29)-C(41)	1.483(3)
N(6)-C(31)	1.355(3)	C(30)-C(31)	1.376(3)
C(1)-C(2)	1.400(3)	C(31)-C(42)	1.496(3)
C(1)-C(13)	1.471(3)	C(32)-C(36)	1.388(4)
C(2)-C(3)	1.374(3)	C(32)-C(33)	1.408(4)
C(3)-C(14)	1.494(3)	C(33)-C(34)	1.406(5)
C(4)-C(5)	1.379(5)	C(34)-C(35)	1.423(5)
C(4)-C(8)	1.397(6)	C(35)-C(36)	1.404(4)
C(5)-C(6)	1.382(5)	C(37)-C(38)	1.420(3)
C(6)-C(7)	1.421(6)	C(37)-C(41)	1.424(3)
C(7)-C(8)	1.402(7)	C(38)-C(39)	1.414(4)
C(9)-C(10)	1.422(3)	C(39)-C(40)	1.421(4)
C(9)-C(13)	1.426(3)	C(40)-C(41)	1.427(3)
C(10)-C(11)	1.411(4)	C(43)-C(44)	1.400(4)
C(11)-C(12)	1.428(3)	C(44)-C(45)	1.400(4)

Angles (°)

C(44)-Co-N(3)	127.55(9)	N(1)-Co-C(45)	169.34(9)
C(44)-Co-N(1)	129.03(10)	C(44)-Co-C(43)	40.31(11)
N(3)-Co-N(1)	89.14(7)	N(3)-Co-C(43)	167.85(9)
C(44)-Co-C(45)	40.44(11)	N(1)-Co-C(43)	100.52(9)
N(3)-Co-C(45)	98.03(9)	C(45)-Co-C(43)	71.43(11)

C(44)-Co-N(5)	118.98(8)	C(9)-C(13)-C(1)	124.4(2)
N(3)-Co-N(5)	89.70(7)	N(3)-C(15)-C(16)	109.8(2)
N(1)-Co-N(5)	91.10(6)	N(3)-C(15)-C(27)	121.3(2)
C(45)-Co-N(5)	96.80(9)	C(16)-C(15)-C(27)	128.8(2)
C(43)-Co-N(5)	97.39(8)	C(17)-C(16)-C(15)	106.1(2)
N(4)-B(1)-N(6)	108.95(16)	N(4)-C(17)-C(16)	107.7(2)
N(4)-B(1)-N(2)	109.20(16)	N(4)-C(17)-C(28)	122.8(2)
N(6)-B(1)-N(2)	109.28(16)	C(16)-C(17)-C(28)	129.5(2)
C(1)-N(1)-N(2)	106.34(16)	C(19)-C(18)-C(22)	109.7(4)
C(1)-N(1)-Co	137.26(14)	C(18)-C(19)-C(20)	108.1(4)
N(2)-N(1)-Co	116.39(12)	C(21)-C(20)-C(19)	107.8(4)
C(3)-N(2)-N(1)	109.97(16)	C(20)-C(21)-C(22)	108.1(4)
C(3)-N(2)-B(1)	130.24(17)	C(18)-C(22)-C(21)	106.3(4)
N(1)-N(2)-B(1)	119.73(16)	C(24)-C(23)-C(27)	108.0(3)
C(15)-N(3)-N(4)	106.28(17)	C(25)-C(24)-C(23)	108.7(3)
C(15)-N(3)-Co	136.08(15)	C(24)-C(25)-C(26)	108.3(3)
N(4)-N(3)-Co	116.54(12)	C(25)-C(26)-C(27)	107.9(3)
C(17)-N(4)-N(3)	110.02(17)	C(23)-C(27)-C(26)	107.1(2)
C(17)-N(4)-B(1)	130.88(18)	C(23)-C(27)-C(15)	126.8(2)
N(3)-N(4)-B(1)	119.09(16)	C(26)-C(27)-C(15)	126.2(2)
C(29)-N(5)-N(6)	105.61(16)	N(5)-C(29)-C(30)	110.13(18)
C(29)-N(5)-Co	141.68(14)	N(5)-C(29)-C(41)	121.95(18)
N(6)-N(5)-Co	112.18(12)	C(31)-C(30)-C(29)	106.29(18)
C(31)-N(6)-N(5)	110.72(16)	N(6)-C(31)-C(30)	107.26(18)
C(31)-N(6)-B(1)	129.41(17)	N(6)-C(31)-C(42)	123.37(19)
N(5)-N(6)-B(1)	119.85(16)	C(30)-C(31)-C(42)	129.4(2)
N(1)-C(1)-C(2)	110.03(18)	C(36)-C(32)-C(33)	107.7(3)
N(1)-C(1)-C(13)	122.49(19)	C(34)-C(33)-C(32)	108.3(3)
C(3)-C(2)-C(1)	105.66(19)	C(33)-C(34)-C(35)	107.7(2)
N(2)-C(3)-C(2)	107.98(18)	C(36)-C(35)-C(34)	106.9(3)
N(2)-C(3)-C(14)	123.06(19)	C(32)-C(36)-C(35)	109.4(3)
C(2)-C(3)-C(14)	129.0(2)	C(38)-C(37)-C(41)	108.3(2)
C(5)-C(4)-C(8)	108.7(4)	C(39)-C(38)-C(37)	108.0(2)
C(4)-C(5)-C(6)	108.6(3)	C(38)-C(39)-C(40)	108.2(2)
C(5)-C(6)-C(7)	107.9(4)	C(39)-C(40)-C(41)	108.0(2)
C(8)-C(7)-C(6)	107.1(4)	C(37)-C(41)-C(40)	107.41(19)
C(4)-C(8)-C(7)	107.7(4)	C(37)-C(41)-C(29)	125.79(19)
C(10)-C(9)-C(13)	108.2(2)	C(40)-C(41)-C(29)	126.8(2)
C(11)-C(10)-C(9)	108.0(2)	C(44)-C(43)-Co	65.67(13)
C(10)-C(11)-C(12)	108.3(2)	C(43)-C(44)-C(45)	119.9(2)
C(13)-C(12)-C(11)	107.9(2)	C(43)-C(44)-Co	74.02(13)
C(12)-C(13)-C(9)	107.59(19)	C(45)-C(44)-Co	73.63(14)
C(12)-C(13)-C(1)	127.9(2)	C(44)-C(45)-Co	65.94(13)

4.2.4 Reaction of $Tp^{Fc,Me}Co(\eta^3\text{-}C_3H_5)$ (22) with CO; Synthesis of $Tp^{Fc,Me}Co(CO)$.

Heating a solution of **22** under 1 atm of CO at 60 °C for one hour resulted in a color change from orange to yellow. After three freeze/pump/thaw cycles, the solution had changed from yellow to green (Scheme 4.2). After subsequent work-up, compound **23** could be isolated in 85 % yield as green crystals. The IR spectrum revealed a band at 1949 cm^{-1}, which was assigned as a CO stretching frequency; this is slightly higher than the CO stretching frequency of 1942 cm^{-1} observed in $Tp^{tBu,Me}Co(CO)$ and comparable with other known $Tp^{R,R'}Co(CO)$ complexes (Table 4.4). The effective magnetic moment of **23** in the solid state measured $\mu_{eff} = 3.2(1)\ \mu_B$. This value is consistent with the presence of two unpaired electrons; the ground state of this 16-electron d^8 complex is a triplet (S=1), much like that of $Tp^{tBu,Me}Co(CO)$[9], $Tp^{iPr,Me}Co(CO)$[10]and $Tp^{Np}Co(CO)$.[11]

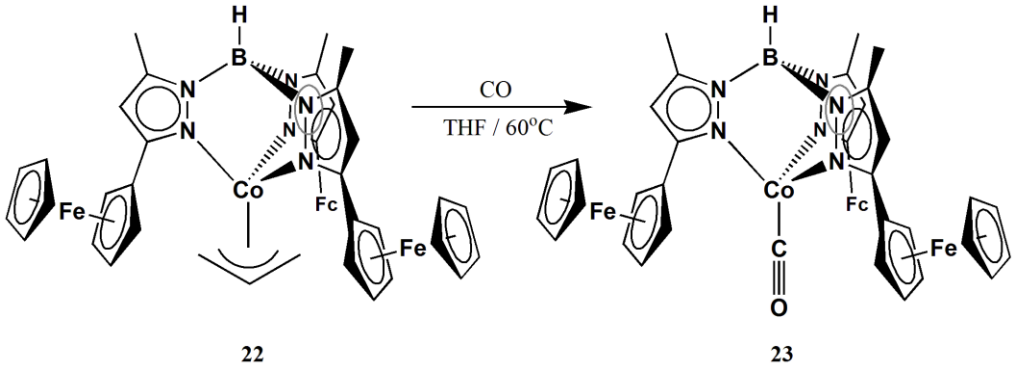

22 23

Scheme 4.2: Synthesis of $Tp^{Fc,Me}Co(CO)$ (23).

Compound	νCO (cm^{-1})
$Tp^{tBu,Me}Co(CO)$[9]	1942
$Tp^{tBu}Co(CO)$[10]	1946
$Tp^{iPr,Me}Co(CO)$[10]	1946
$Tp^{Fc,Me}Co(CO)$	1949
$Tp^{Np}Co(CO)$[11]	1950

Table 4.4: Comparison Co-CO stretching frequencies for known TpCo(CO) complexes.

X-ray quality crystals of **23** were grown by vapor phase diffusion of pentanes into a saturated solution of **23** in THF. Compound **23** crystallized in the triclinic space group P-1. The molecular structure (Figure 4.4) shows that **23** adopts a four coordinate 'bent' geometry in which the CO fragment deviates 22.3° from the B-Co axis (Table 4.5). This 'α-angle' (Scheme 4.3) is smaller than that of the previously reported $Tp^{Np}Co(CO)$, which had an α-angle of 26.6°, suggesting that the pocket created by the ferrocenyl moieties is more constrained than that of Tp^{Np}. It is important to note that this distortion of the CO moiety from the B-Co axis is electronically driven;[11] however, the degree to which it deviates from this axis is influenced by sterics.

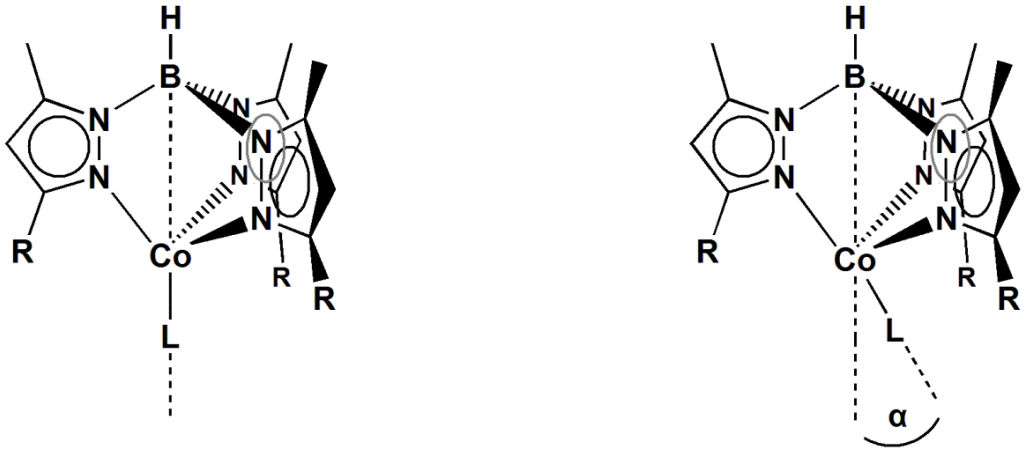

Scheme 4.3: α-angle determination from X-ray crystal structures.

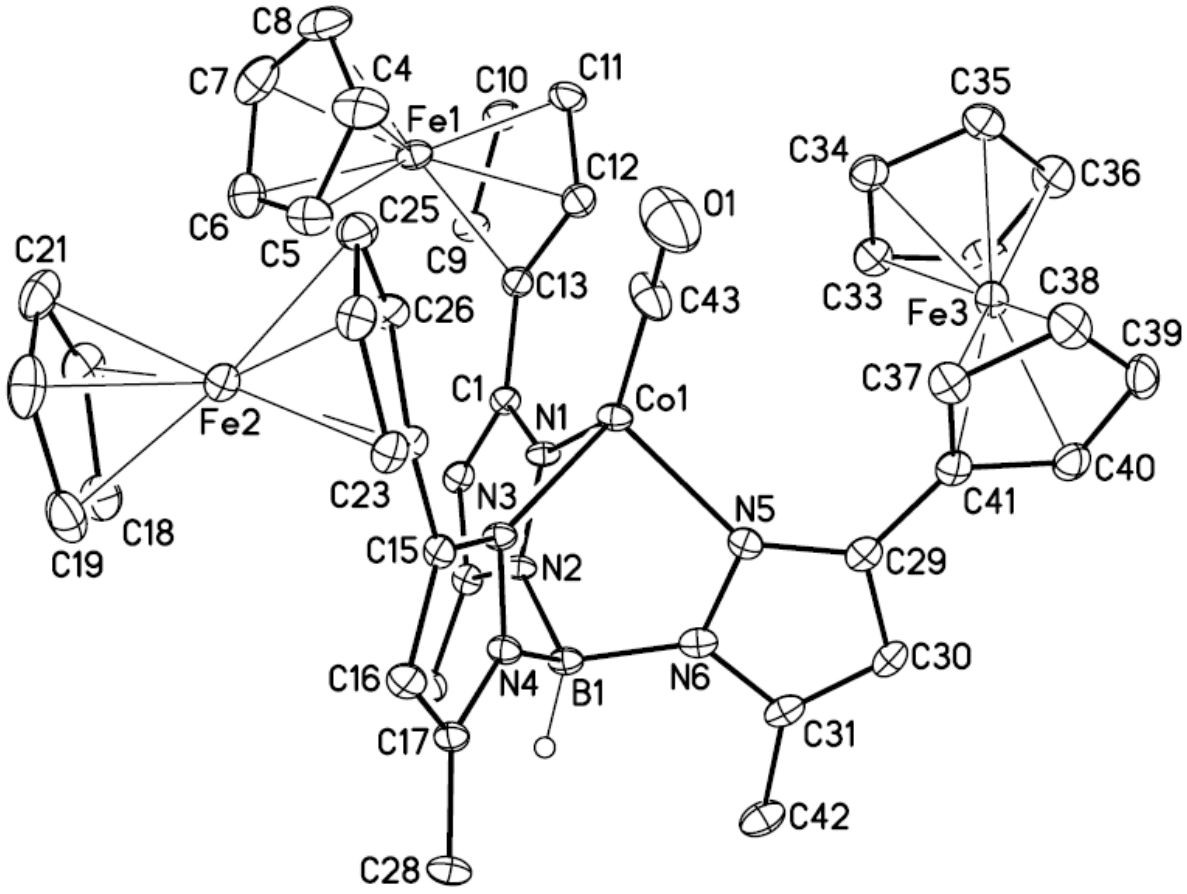

Figure 4.4: Molecular structure of $Tp^{Fc,Me}Co(CO)$ (23) at the 30% probability level. Hydrogen atoms (except the boron bound hydrogen, H1B) have been removed for clarity.

Table 4.5: Selected interatomic distances (Å) and angles (°) for $Tp^{Fc,Me}Co(CO)$ (23).

Distances (Å)

Co(1)-C(43)	1.777(5)	C(12)-C(13)	1.428(7)
Co(1)-N(1)	2.037(4)	C(15)-C(16)	1.407(6)
Co(1)-N(3)	2.063(3)	C(15)-C(27)	1.470(6)
Co(1)-N(5)	2.070(4)	C(16)-C(17)	1.373(6)
B(1)-N(6)	1.540(6)	C(17)-C(28)	1.508(6)
B(1)-N(4)	1.543(6)	C(18)-C(22)	1.413(7)
B(1)-N(2)	1.557(6)	C(18)-C(19)	1.429(8)
O(1)-C(43)	1.124(6)	C(19)-C(20)	1.420(8)
N(1)-C(1)	1.340(5)	C(20)-C(21)	1.415(8)
N(1)-N(2)	1.379(5)	C(21)-C(22)	1.417(7)
N(2)-C(3)	1.351(6)	C(23)-C(24)	1.421(6)
N(3)-C(15)	1.332(5)	C(23)-C(27)	1.426(6)
N(3)-N(4)	1.388(5)	C(24)-C(25)	1.417(7)
N(4)-C(17)	1.346(5)	C(25)-C(26)	1.439(6)
N(5)-C(29)	1.350(6)	C(26)-C(27)	1.435(6)
N(5)-N(6)	1.382(5)	C(29)-C(30)	1.402(6)
N(6)-C(31)	1.360(5)	C(29)-C(41)	1.472(6)
C(1)-C(2)	1.405(6)	C(30)-C(31)	1.382(7)
C(1)-C(13)	1.464(6)	C(31)-C(42)	1.491(6)
C(2)-C(3)	1.385(6)	C(32)-C(33)	1.415(7)
C(3)-C(14)	1.491(6)	C(32)-C(36)	1.430(8)
C(4)-C(5)	1.414(8)	C(33)-C(34)	1.422(7)
C(4)-C(8)	1.432(8)	C(34)-C(35)	1.425(7)
C(5)-C(6)	1.418(8)	C(35)-C(36)	1.411(7)
C(6)-C(7)	1.405(8)	C(37)-C(38)	1.426(7)
C(7)-C(8)	1.410(9)	C(37)-C(41)	1.439(7)
C(9)-C(13)	1.426(6)	C(38)-C(39)	1.416(8)
C(9)-C(10)	1.428(6)	C(39)-C(40)	1.422(7)
C(10)-C(11)	1.408(7)	C(40)-C(41)	1.432(6)
C(11)-C(12)	1.423(6)		

Angles (°)

C(43)-Co(1)-N(1)	144.6(2)	N(6)-B(1)-N(4)	109.8(4)
C(43)-Co(1)-N(3)	106.7(2)	N(6)-B(1)-N(2)	108.1(3)
N(1)-Co(1)-N(3)	92.18(14)	N(4)-B(1)-N(2)	109.6(3)
C(43)-Co(1)-N(5)	116.0(2)	C(1)-N(1)-N(2)	107.3(3)
N(1)-Co(1)-N(5)	91.61(14)	C(1)-N(1)-Co(1)	139.3(3)
N(3)-Co(1)-N(5)	93.64(14)	N(2)-N(1)-Co(1)	113.1(3)

C(3)-N(2)-N(1)	109.9(3)	C(17)-C(16)-C(15)	105.8(4)
C(3)-N(2)-B(1)	130.3(4)	N(4)-C(17)-C(16)	108.2(4)
N(1)-N(2)-B(1)	119.5(3)	N(4)-C(17)-C(28)	122.7(4)
C(15)-N(3)-N(4)	106.3(3)	C(16)-C(17)-C(28)	129.0(4)
C(15)-N(3)-Co(1)	139.0(3)	C(22)-C(18)-C(19)	108.1(5)
N(4)-N(3)-Co(1)	112.1(2)	C(20)-C(19)-C(18)	107.1(5)
C(17)-N(4)-N(3)	109.7(3)	C(21)-C(20)-C(19)	108.7(5)
C(17)-N(4)-B(1)	130.5(4)	C(20)-C(21)-C(22)	107.7(5)
N(3)-N(4)-B(1)	119.7(3)	C(18)-C(22)-C(21)	108.4(5)
C(29)-N(5)-N(6)	106.2(3)	C(24)-C(23)-C(27)	107.9(4)
C(29)-N(5)-Co(1)	141.0(3)	C(25)-C(24)-C(23)	109.2(4)
N(6)-N(5)-Co(1)	111.4(3)	C(24)-C(25)-C(26)	107.1(4)
C(31)-N(6)-N(5)	109.9(4)	C(27)-C(26)-C(25)	108.1(4)
C(31)-N(6)-B(1)	129.0(4)	C(23)-C(27)-C(26)	107.6(4)
N(5)-N(6)-B(1)	121.1(3)	C(23)-C(27)-C(15)	124.8(4)
N(1)-C(1)-C(2)	108.9(4)	C(26)-C(27)-C(15)	127.6(4)
N(1)-C(1)-C(13)	123.0(4)	N(5)-C(29)-C(30)	110.1(4)
C(2)-C(1)-C(13)	128.2(4)	N(5)-C(29)-C(41)	125.0(4)
C(3)-C(2)-C(1)	106.6(4)	C(30)-C(29)-C(41)	124.8(4)
N(2)-C(3)-C(2)	107.3(4)	C(31)-C(30)-C(29)	105.9(4)
N(2)-C(3)-C(14)	123.6(4)	N(6)-C(31)-C(30)	107.9(4)
C(2)-C(3)-C(14)	129.1(4)	N(6)-C(31)-C(42)	123.1(4)
C(5)-C(4)-C(8)	106.7(6)	C(30)-C(31)-C(42)	129.0(4)
C(4)-C(5)-C(6)	109.1(5)	C(33)-C(32)-C(36)	107.7(5)
C(7)-C(6)-C(5)	107.4(5)	C(32)-C(33)-C(34)	108.5(5)
C(6)-C(7)-C(8)	108.8(5)	C(33)-C(34)-C(35)	107.5(5)
C(7)-C(8)-C(4)	108.1(5)	C(36)-C(35)-C(34)	108.4(5)
C(13)-C(9)-C(10)	108.5(4)	C(35)-C(36)-C(32)	107.9(4)
C(11)-C(10)-C(9)	108.1(4)	C(38)-C(37)-C(41)	108.3(4)
C(10)-C(11)-C(12)	108.0(4)	C(39)-C(38)-C(37)	107.8(5)
C(11)-C(12)-C(13)	108.8(4)	C(38)-C(39)-C(40)	108.7(4)
C(9)-C(13)-C(12)	106.7(4)	C(39)-C(40)-C(41)	108.2(5)
C(9)-C(13)-C(1)	124.8(4)	C(40)-C(41)-C(37)	107.0(4)
C(12)-C(13)-C(1)	128.5(4)	C(40)-C(41)-C(29)	123.6(4)
N(3)-C(15)-C(16)	110.0(4)	C(37)-C(41)-C(29)	129.0(4)
N(3)-C(15)-C(27)	123.0(4)	O(1)-C(43)-Co(1)	175.6(6)
C(16)-C(15)-C(27)	127.0(4)		

4.2.5 Reaction of $Tp^{Fc,Me}Co(CO)$ (23) with CO.

Depending on the CO pressure, the $Tp^{Fc,Me}Co$ moiety binds one or two carbonyl ligands. This is most apparent in the ^{1}H-NMR spectrum. Exposure of a solution of **23** to 1 atm of CO at room temperature resulted in a color change from green to yellow. The ^{1}H-NMR revealed a shift in the resonances towards the diamagnetic region (Figure 4.5). This is consistent with the appearance of an 18-electron, $Tp^{Fc,Me}Co(CO)_2$ species.

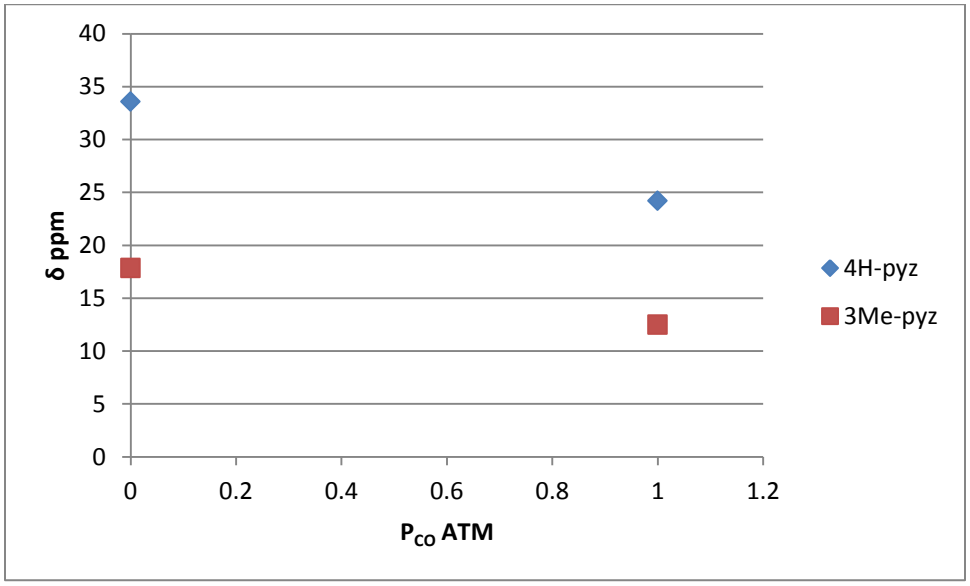

Figure 4.5: Chemical shifts of the 3-Me and 4-H pyrazolyl positions of the $Tp^{Fc,Me}Co$ moiety under CO pressure.

$$\textbf{(1)}\quad Tp^{Fc,Me}Co(CO) + CO \underset{k_{-1}}{\overset{k_1}{\rightleftharpoons}} Tp^{Fc,Me}Co(CO)_2, \quad K_{eq} = \frac{[Tp^{Fc,Me}Co(CO)_2]}{[Tp^{Fc,Me}Co(CO)][CO]}$$

In the presence of 1 atmosphere of CO, the actual chemical shifts of the mixture are population weighted averages of these extremes between the $Tp^{Fc,Me}Co(CO)$ and $Tp^{Fc,Me}Co(CO)_2$ species. These data along with the solubility data for CO in benzene (7.17 mM under 1 atm of CO at

room temperature)[12] and the chemical shifts for known diamagnetic species of the $Tp^{Fc,Me}$ ligand (i.e., $Tp^{Fc,Me}Tl$) allowed for the determination of the equilibrium constant, K_{eq} (eq. 1). The calculated K_{eq}, K_{eq} (298 K) = 69(1) (See experimental), suggests that under one atmosphere of CO at room temperature the equilibrium favors the $Tp^{Fc,Me}Co(CO)$ species. In comparison, the K_{eq} for the $Tp^{iPr,Me}Co(CO)$ / $Tp^{iPr,Me}Co(CO)_2$ system is K_{eq} (298 K) = 1.001.[13] Several attempts to crystallize $Tp^{Fc,Me}Co(CO)_2$ under an atmosphere of CO only resulted in the isolation of the mono carbonyl species. The susceptibility to ligand loss due to bond weakening can be attributed to the steric encumbrance of the cobalt by the $Tp^{Fc,Me}$ ligand.

4.2.6 Reaction of $Tp^{Fc,Me}Co(CO)$ (23) with O_2; Synthesis of $Tp^{Fc,Me}Co(O_2)$.

Exposure of a dilute solution of **23** (1 mg/mL) in THF to 1 atm of O_2 resulted in an immediate color change from green to brown. Subsequent work-up revealed the near quantitative conversion of **23** to $Tp^{Fc,Me}Co(O_2)$ (**24**). The overlayed IR spectra (Figure 4.6) showed the disappearance of the CO stretching frequency at 1949 cm^{-1} and the appearance of a new band at 954 cm^{-1} which is lower than would be expected for a transition metal superoxo ($\upsilon_{OO} \approx 1050 – 1200cm^{-1}$) yet higher than that of a metal peroxo stretching frequency ($\upsilon_{OO} \approx 800 – 930\ cm^{-1}$).[14] This result is very similar to the O_2 stretching frequency of 961 cm^{-1} found for $Tp^{tBu,Me}Co(O_2)$.[2a] To further characterize this O_2 complex, **23** was exposed to $^{18}O_2$. The estimated vibrational frequency for ^{18}O-^{18}O in **24** can be calculated using equation 2.

$$(2) \quad \frac{\upsilon_B}{\upsilon_A} = \frac{\sqrt{\mu_A}}{\sqrt{\mu_B}}$$

Where υ_B is the vibrational frequency expected for X-(^{18}O-^{18}O), υ_A is the observed vibrational frequency for X-(^{16}O-^{16}O), μ_A is the reduced mass (equation 3) for X-(^{16}O-^{16}O), and μ_B is the reduced mass for X-(^{18}O-^{18}O).

$$(3) \quad \mu = \frac{m1m2}{m1 + m2}$$

After substituting the masses of the two atoms for m_1 and m_2 into equation 2 to obtain μ; the calculated vibrational frequency (υ_B) of X-(^{18}O-^{18}O) can be obtained by rearrangement of equation 2. The calculated vibrational frequency for ^{18}O-^{18}O in $Tp^{Fc,Me}Co(^{18}O_2)$ is 901 cm^{-1}. The IR spectrum of this complex, $Tp^{Fc,Me}Co(^{18}O_2)$, exhibited an ^{18}O-^{18}O stretching frequency of 902 cm^{-1}, which is consistent with the calculated stretching frequency.

Crystals of air-stable compound **24** were grown by vapor diffusion of diethyl ether into a saturated solution of **24** in CH_2Cl_2. The molecular structure (Figure 4.7) shows that the oxygen is bound in a side-on fashion, reminiscent of its $Tp^{tBu,Me}Co(O_2)$ analog.[2a] Compound **24** has an apparent O-O bond length of 1.229(4) Å. This bond distance is significantly shorter than what is suggested by the IR stretching frequency (~ 1.4 Å).[14] Close inspection of the ORTEP plot of **24** revealed that the oxygen atoms appear to have elongated thermal elipsoids, suggesting that they are suffering from some sort of positional disorder. A low temperature data collection was done in an attempt to elucidate the O-O bond distance. In the $Tp^{tBu,Me}Co(O_2)$ system, when X-ray crystallographic analysis was done at room temperature, the oxygen atoms suffer from disorder. However, structural analysis based on data collected at a lower temperature (90 K) revealed an increase in the O-O bond length from 1.262(8) Å (295 K)[2a] to 1.378(3) Å (90 K).[15] This is due to the librational motion in the molecule which is reduced at lower temperatures. However, low

temperature data collection (90 K) on **24** revealed no apparent elongation of the O-O bond at 1.235(4) Å (Figure A3.2). Therefore, **24** suffers from a positional disorder which is brought upon by the larger binding pocket that is afforded by the Fc-substituents than that of the $Tp^{tBu,Me}$ analog. From the IR stretching frequency, it can be deduced that the O-O bond distance should be approximately 1.4 Å.[14] When the O-O bond distance is constrained to this distance and the structure refined, a second disordered position is observed with a refined O-O distance of 1.377(19) Å (Figure A3.3-A3.5). However, the elongated thermal ellipsoids on this model suggest that additional positions of the O_2 fragment cannot be discounted. The effective magnetic moment of **24** is 3.71(3) μ_B is consistent with antiferromagnetic coupling of the metal ion (S=3/2) and the superoxide ligand (S=1/2).[16] This results in a triplet (S=1) ground state for **24**. The observed moment in **24** is also consistent with the magnetic moment of the analogous $Tp^{tBu,Me}Co(O_2)$ of 3.88 μ_B.[2a]

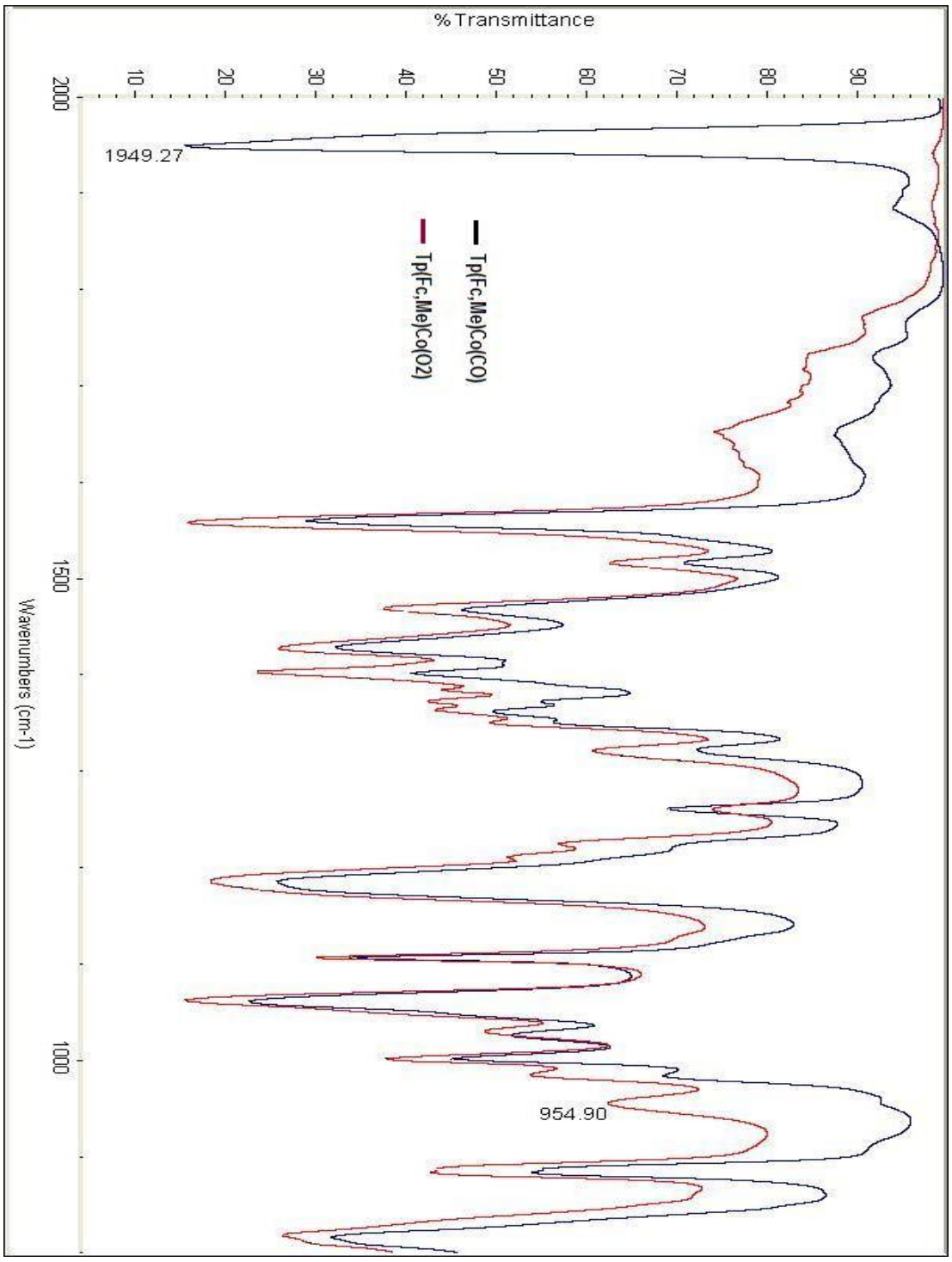

Figure 4.6: IR spectral overlay of $Tp^{Fc,Me}Co(CO)$ (23) and $Tp^{Fc,Me}(O_2)$ (24).

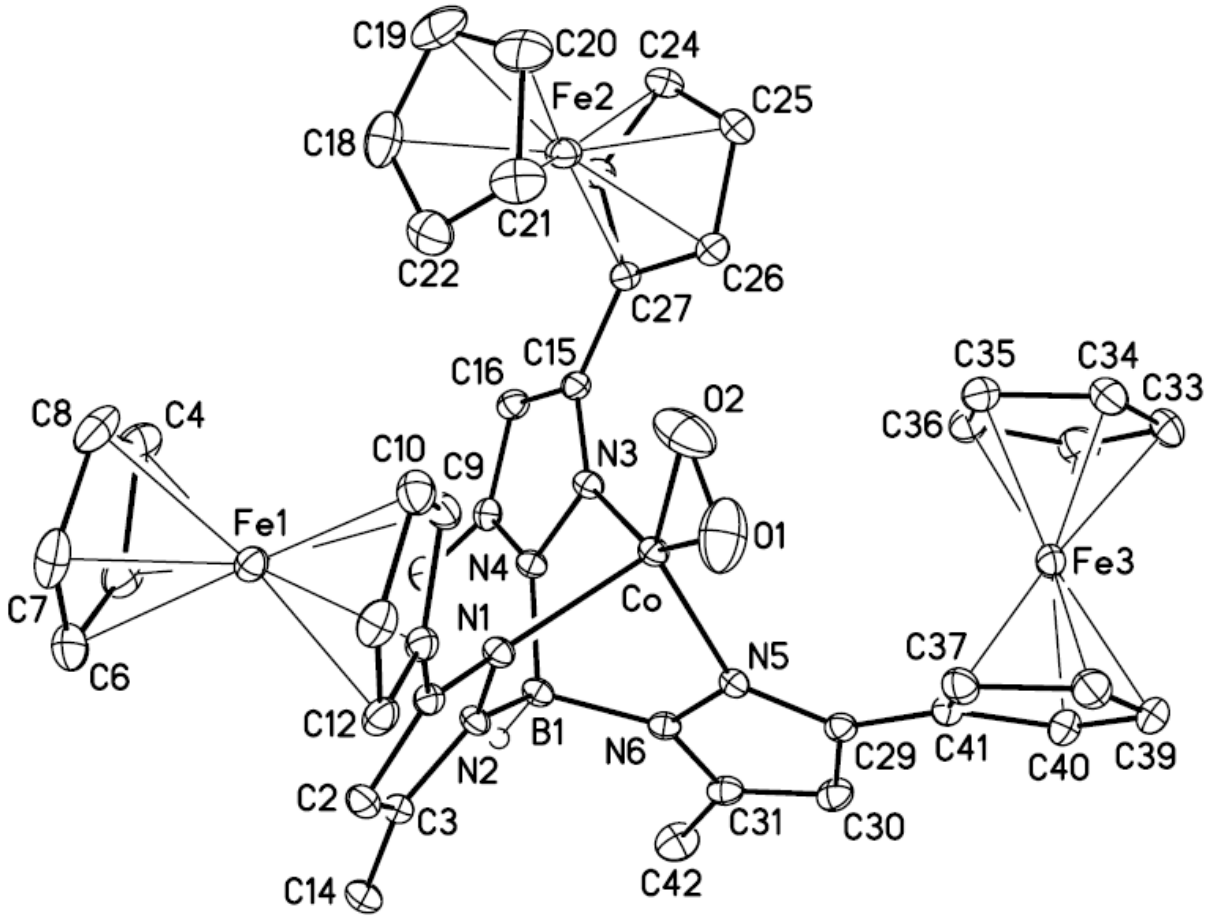

Figure 4.7: Molecular structure of $Tp^{Fc,Me}Co(O_2)$ (24) at the 30% probability level. Hydrogen atoms (except the boron bound hydrogen, H1B) have been removed for clarity.

Table 4.6: Selected interatomic distances (Å) and angles (°) for $Tp^{Fc,Me}Co(O_2)$ (24).

Distances (Å)

Co-O(1)	1.829(2)	C(11)-C(12)	1.417(3)
Co-O(2)	1.850(2)	C(12)-C(13)	1.433(3)
Co-N(3)	2.0267(18)	C(15)-C(16)	1.402(3)
Co-N(5)	2.0494(17)	C(15)-C(27)	1.465(3)
Co-N(1)	2.0657(17)	C(16)-C(17)	1.376(3)
B(1)-N(2)	1.543(3)	C(17)-C(28)	1.498(3)
B(1)-N(6)	1.543(3)	C(18)-C(19)	1.428(5)
B(1)-N(4)	1.550(3)	C(18)-C(22)	1.410(4)
O(1)-O(2)	1.229(4)	C(19)-C(20)	1.413(5)
N(1)-C(1)	1.343(3)	C(20)-C(21)	1.417(4)
N(1)-N(2)	1.376(2)	C(21)-C(22)	1.412(4)
N(2)-C(3)	1.345(3)	C(23)-C(24)	1.419(3)
N(3)-C(15)	1.346(3)	C(23)-C(27)	1.430(3)
N(3)-N(4)	1.381(2)	C(24)-C(25)	1.416(4)
N(4)-C(17)	1.348(3)	C(25)-C(26)	1.428(3)
N(5)-C(29)	1.347(3)	C(26)-C(27)	1.431(3)
N(5)-N(6)	1.378(2)	C(29)-C(30)	1.395(3)
N(6)-C(31)	1.347(3)	C(29)-C(41)	1.463(3)
C(1)-C(2)	1.399(3)	C(30)-C(31)	1.377(3)
C(1)-C(13)	1.465(3)	C(31)-C(42)	1.488(3)
C(2)-C(3)	1.378(3)	C(32)-C(36)	1.418(4)
C(3)-C(14)	1.494(3)	C(32)-C(33)	1.424(4)
C(4)-C(8)	1.417(4)	C(33)-C(34)	1.413(4)
C(4)-C(5)	1.418(4)	C(34)-C(35)	1.422(3)
C(5)-C(6)	1.417(4)	C(35)-C(36)	1.426(4)
C(6)-C(7)	1.412(4)	C(37)-C(38)	1.431(3)
C(7)-C(8)	1.413(4)	C(37)-C(41)	1.434(3)
C(9)-C(10)	1.423(3)	C(38)-C(39)	1.425(4)
C(9)-C(13)	1.431(3)	C(39)-C(40)	1.418(4)
C(10)-C(11)	1.423(3)	C(40)-C(41)	1.445(3)

Angles (°)

O(1)-Co-O(2)	39.03(12)	O(1)-Co-N(1)	103.93(10)
O(1)-Co-N(3)	151.96(12)	O(2)-Co-N(1)	114.18(9)
O(2)-Co-N(3)	113.25(11)	N(3)-Co-N(1)	91.70(7)
O(1)-Co-N(5)	110.32(10)	N(5)-Co-N(1)	93.34(7)
O(2)-Co-N(5)	141.22(11)	N(2)-B(1)-N(6)	108.95(17)
N(3)-Co-N(5)	91.49(7)	N(2)-B(1)-N(4)	109.90(17)

N(6)-B(1)-N(4)	108.28(17)	C(9)-C(13)-C(1)	128.12(19)
O(2)-O(1)-Co	71.41(16)	N(3)-C(15)-C(16)	109.42(18)
O(1)-O(2)-Co	69.56(15)	N(3)-C(15)-C(27)	124.84(19)
C(1)-N(1)-N(2)	106.24(16)	C(16)-C(15)-C(27)	125.72(19)
C(1)-N(1)-Co	137.92(15)	C(17)-C(16)-C(15)	106.26(19)
N(2)-N(1)-Co	112.50(12)	N(4)-C(17)-C(16)	107.89(19)
C(3)-N(2)-N(1)	110.18(17)	N(4)-C(17)-C(28)	122.97(19)
C(3)-N(2)-B(1)	130.41(18)	C(16)-C(17)-C(28)	129.1(2)
N(1)-N(2)-B(1)	119.32(16)	C(19)-C(18)-C(22)	107.7(3)
C(15)-N(3)-N(4)	106.42(17)	C(20)-C(19)-C(18)	107.7(3)
C(15)-N(3)-Co	140.46(15)	C(19)-C(20)-C(21)	108.2(3)
N(4)-N(3)-Co	112.78(13)	C(20)-C(21)-C(22)	107.9(3)
C(17)-N(4)-N(3)	110.01(17)	C(21)-C(22)-C(18)	108.4(3)
C(17)-N(4)-B(1)	129.48(17)	C(24)-C(23)-C(27)	108.5(2)
N(3)-N(4)-B(1)	120.19(17)	C(25)-C(24)-C(23)	108.0(2)
C(29)-N(5)-N(6)	106.36(17)	C(24)-C(25)-C(26)	108.3(2)
C(29)-N(5)-Co	139.59(15)	C(27)-C(26)-C(25)	108.0(2)
N(6)-N(5)-Co	112.95(12)	C(26)-C(27)-C(23)	107.20(19)
C(31)-N(6)-N(5)	110.00(18)	C(26)-C(27)-C(15)	129.2(2)
C(31)-N(6)-B(1)	130.10(18)	C(23)-C(27)-C(15)	123.6(2)
N(5)-N(6)-B(1)	119.89(16)	N(5)-C(29)-C(30)	109.54(19)
N(1)-C(1)-C(2)	109.75(19)	N(5)-C(29)-C(41)	125.10(19)
N(1)-C(1)-C(13)	123.23(19)	C(30)-C(29)-C(41)	125.3(2)
C(2)-C(1)-C(13)	126.99(19)	C(31)-C(30)-C(29)	106.29(19)
C(3)-C(2)-C(1)	105.93(19)	N(6)-C(31)-C(30)	107.80(19)
N(2)-C(3)-C(2)	107.87(19)	N(6)-C(31)-C(42)	123.0(2)
N(2)-C(3)-C(14)	122.7(2)	C(30)-C(31)-C(42)	129.2(2)
C(2)-C(3)-C(14)	129.4(2)	C(36)-C(32)-C(33)	107.4(2)
C(8)-C(4)-C(5)	108.0(2)	C(34)-C(33)-C(32)	108.5(2)
C(4)-C(5)-C(6)	107.9(2)	C(35)-C(34)-C(33)	108.2(2)
C(7)-C(6)-C(5)	107.9(2)	C(34)-C(35)-C(36)	107.4(2)
C(6)-C(7)-C(8)	108.4(2)	C(32)-C(36)-C(35)	108.5(2)
C(4)-C(8)-C(7)	107.8(2)	C(38)-C(37)-C(41)	108.0(2)
C(10)-C(9)-C(13)	108.2(2)	C(37)-C(38)-C(39)	108.0(2)
C(11)-C(10)-C(9)	107.6(2)	C(40)-C(39)-C(38)	108.6(2)
C(12)-C(11)-C(10)	108.8(2)	C(39)-C(40)-C(41)	107.9(2)
C(11)-C(12)-C(13)	107.8(2)	C(37)-C(41)-C(40)	107.5(2)
C(12)-C(13)-C(9)	107.56(19)	C(37)-C(41)-C(29)	129.0(2)
C(12)-C(13)-C(1)	124.2(2)	C(40)-C(41)-C(29)	123.2(2)

4.2.7 Reaction of $Tp^{Fc,Me}Co(\eta^3\text{-}C_3H_5)$ with O_2.

When **22** was exposed to O_2 in C_6D_6 an immediate color change from orange to green to brown occured. The ^1H NMR of the reaction revealed a mixture of two products, with $Tp^{Fc,Me}CoOH$ (**21**) and $Tp^{Fc,Me}CoO_2$ (**24**) in a 10:1 ratio. The proposed mechanism for this reaction follows two possible pathways (scheme 4.4). In the first, the insertion of dioxygen into the Co-allyl bond leads to the formation of a putative $Tp^{Fc,Me}CoOOC_3H_5$ species. $Tp^{Fc,Me}CoOOC_3H_5$ then undgoes O-O bond homolysis to form a putative '$Tp^{Fc,Me}Co{=}O$' species which abstracts a hydrogen atom to form **21**. The second pathway involves ligation of O_2 with the expulsion of an allyl radical to form **24.** In a similar vein, a solid sample of **22** was exposed to oxygen for 2 days. After removal of excess O_2, C_6D_6 was added to the sample. ^1H NMR spectroscopy revealed that the $Tp^{Fc,Me}Co$ system formed once again **21** along with trace amounts of **24**. IR spectroscopy revealed no incorporation of deuterium in the case of **21** which indicates that the abstracted hydrogen does not come from solvent in the solid state reaction. Also, hydrogen atom abstraction does not appear to occur from the ligand which is apparent in the ^1H NMR. This would suggest that hydrogen is being abstracted from the organic fragment, 'OC_3H_5', which is formed during the course of the reaction.

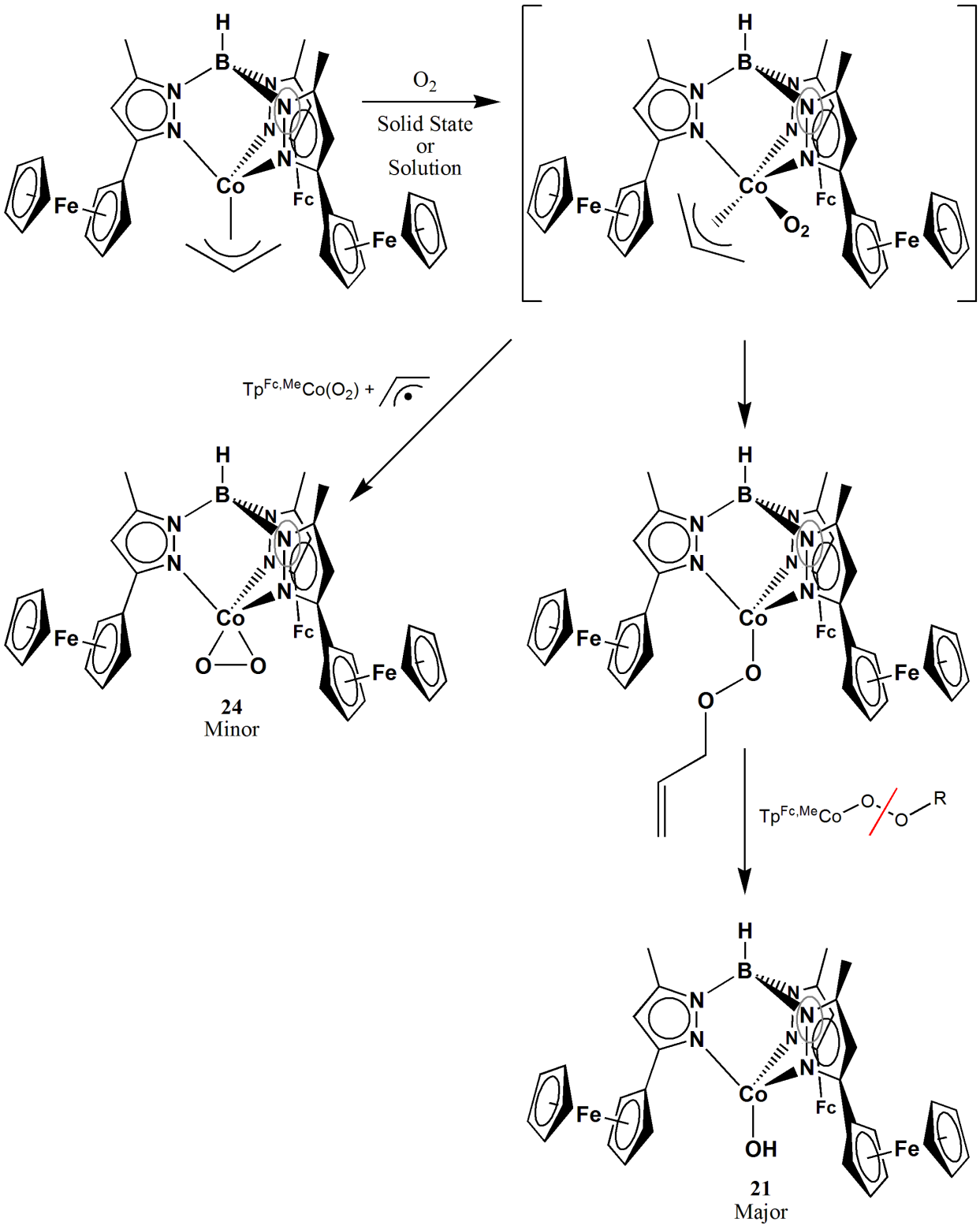

Scheme 4.4: Reaction of $Tp^{Fc,Me}Co(\eta^3\text{-allyl})$ (22) with O_2.

To gather support for the formation of a $Tp^{Fc,Me}CoOOC_3H_5$ intermediate , several low-temperature UV-Vis experiments were run. When **22** was exposed to excess oxygen at -78 °C, several new peaks appeared at 601 nm and 648 nm, respectively, along with an increase of absorbance at 450 nm (Figure 4.8). These new features of the spectrum persisted at this temperature. However, when the solution was warmed up to -15 °C, a decrease in the

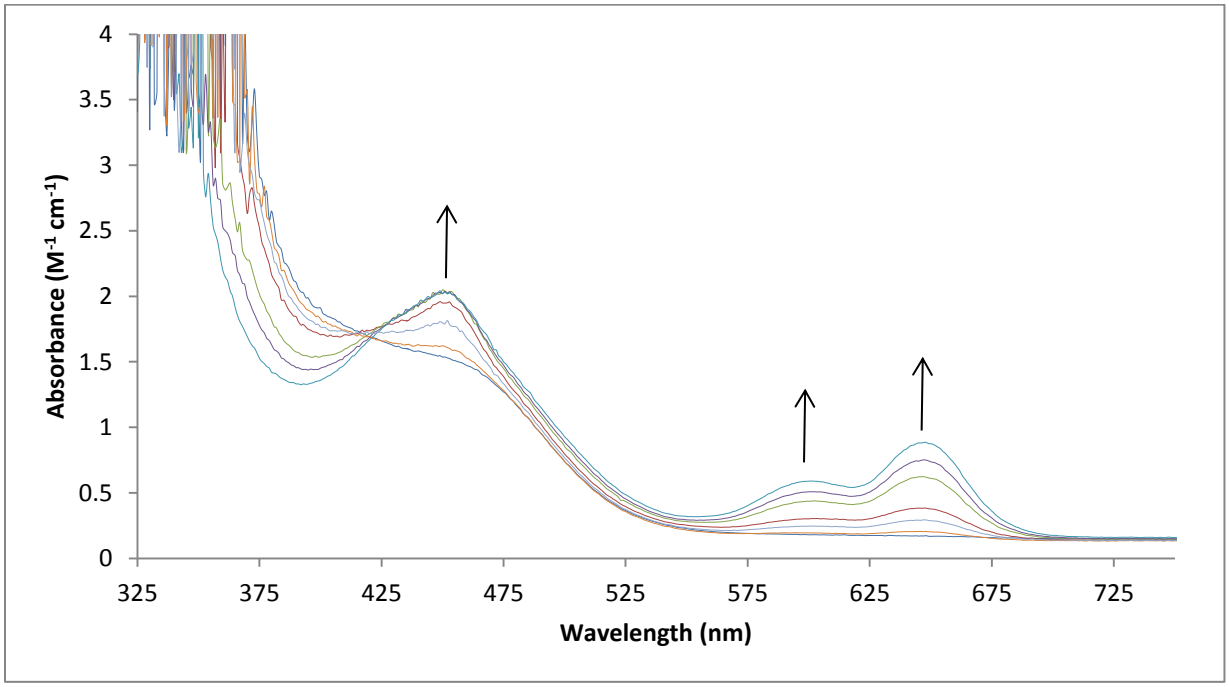

Figure 4.8: Time-dependent change of the UV-Vis spectra during the reaction of 22 with O_2 in THF (0.11 mM) at -78 °C. Scans repeated with a cycle time of 0.1 min.

absorbance at 450 nm was observed along with the appearance of new peaks at 592 nm and 670 nm (Figure 4.9). The resulting spectrum is consistent with the UV-Vis spectrum that was recorded for **21** (Figure A3.6). A more compelling argument for the existence of an allyl-peroxo intermediate comes from the low-temperature reaction of **21** with cumyl hydroperoxide. Alkyl-peroxo species have been postulated as intermediates in the $Tp^{iPr2}Co$ system when $[Tp^{iPr2}Co(\mu\text{-}OH)]_2$ was exposed to alkyl hydroperoxides.[17] The putative alkyl-peroxide undergoes O-O bond

homolysis accompanied by hydrogen atom extraction from the tertiary position of the *iso*-propyl arm to yield a metallocyclic alkoxide. By switching to the $Tp^{tBu,iPr}$ ligand, a stable alkylperoxide was synthesized and structurally characterized.[17]

The UV-Vis spectrum of the reaction of $Tp^{Fc,Me}CoOH$ with $Ph(Me)_2COOH$ (Figure 4.10) shows an increase in the absorbance at 450 nm along with the appearance of peaks at 607 nm and 651 nm. This was similar to the peaks observed for the reaction of **22** and O_2. Likewise, upon warm-up to room temperature, this cumyl-peroxide underwent O-O bond homolysis which led to the final product of **21**. This evidence suggests that the formation of a $Tp^{Fc,Me}CoOOR$ species followed by O-O bond homolysis is a plausible pathway to the formation of **21** in the reaction of **22** with O_2.

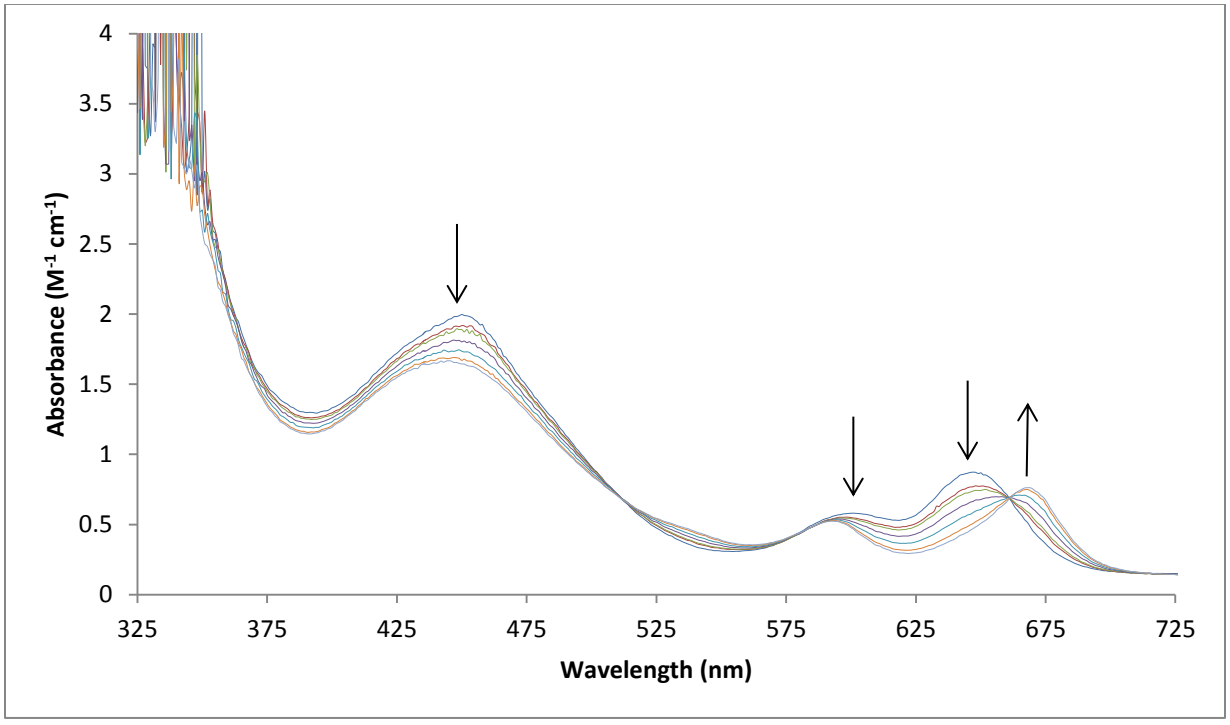

Figure 4.9: Time-dependent change of the UV-Vis spectra during the reaction of 22 with O_2 in THF (1.1 mM) from -78 °C to -15 °C. Scans repeated with a cycle time of 0.1 min.

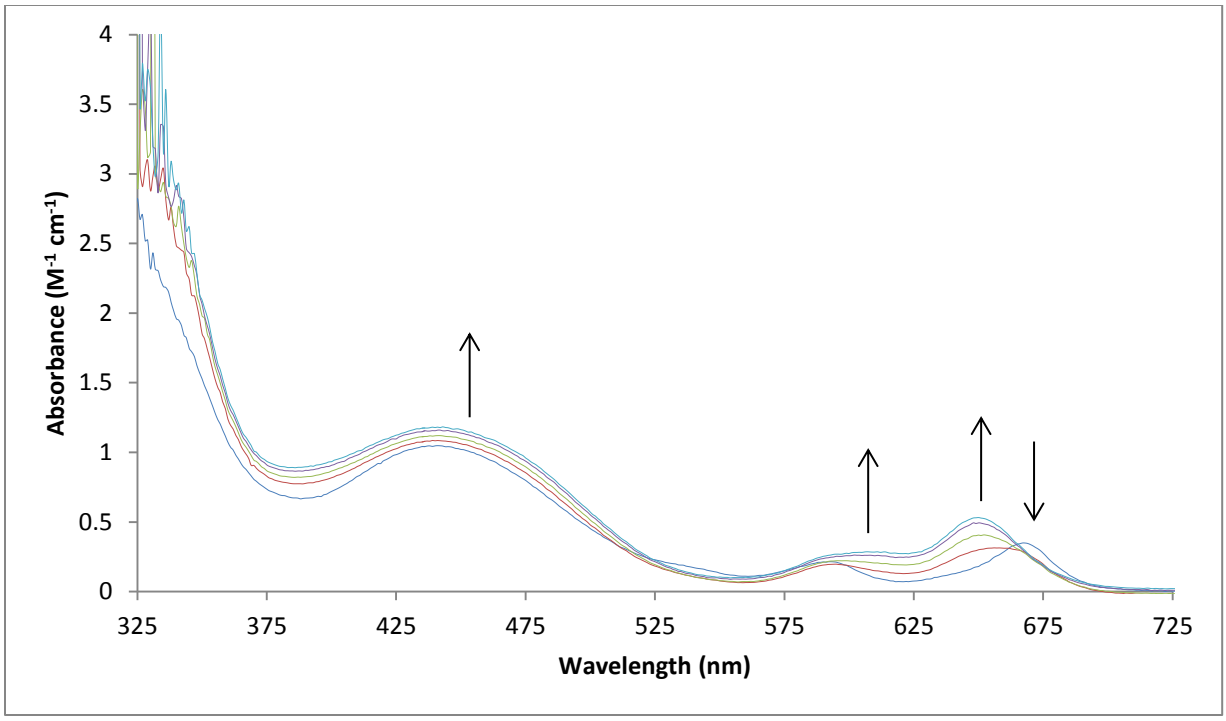

Figure 4.10: Time-dependent change of the UV-Vis spectra during the reaction of 21 with $Ph(Me)_2COOH$ in THF (1.1 mM) at -78 °C. Scans repeated with a cycle time of 0.1 min.

4.2.8 Synthesis and Characterization of $Tp^{Fc,Me}CoNAd$.

Absent an isolable metal oxo complex, the isolation of a stable isoelectronic imido complex, $Tp^{Fc,Me}Co{=}NR$, became of interest (Scheme 4.5).

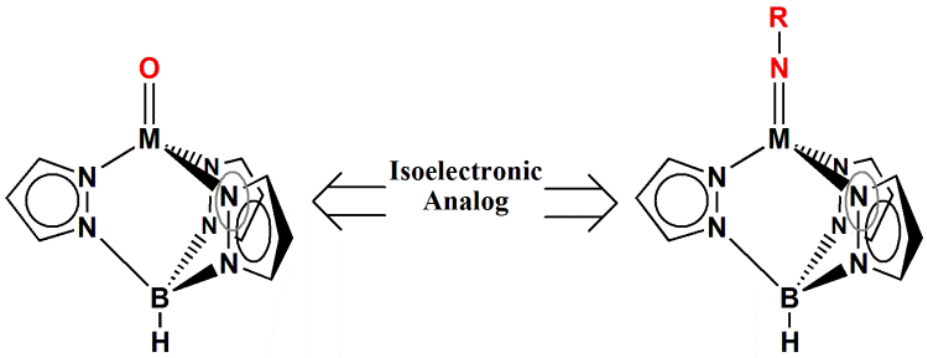

Scheme 4.5: Relationship between the metal-oxo and metal-imido species.

Although previous work in the Theopold group has shown several examples of terminal cobalt imido complexes, late transition metal imido species remain rare.[18] This can be attributed to a lack of empty d orbitals available for π donation from the NR^{2-} ligand. Aside from their role as an isoelectronic model for terminal oxo species, the principal interest in synthesizing these compounds is that the terminally bound functionality may be transferred to unreactive substrates such as olefins or C-H bonds.[19] The isolation of $Tp^{Fc,Me}$CoNR also provides a platform to directly compare the thermal stability of the metal imido complexes on the $Tp^{Fc,Me}$ ligand with its higher C-H bond strength to that of the $Tp^{tBu,Me}$ ligand system.

A solution of $Tp^{Fc,Me}$CoI was stirred with an equal molar amount of N_3Ad in THF. 1 equiv. of KC_8 was added and the solution immediately changed color from green to orange with concomitant evolution of N_2 gas. The solution was allowed to stir for 45 minutes and then filtered. The solvent was removed and the residue triturated with pentanes and dried. The resulting orange solid was recrystallized by layering pentanes on a THF solution of **25,** allowing a 31 % yield of **25**. The ^{1}H NMR spectrum of this diamagnetic complex, which is expected for a low spin Co^{3+}, d^6, S = 0 complex, shows a set of eight resonances, five of which were attributed to the Tp ligand and three of which are assigned to the adamantyl group. High temperature (100 °C) ^{1}H-NMR done in benzene-d_6 revealed no apparent shifts of the resonances of **25** towards the paramagnetic region suggesting that unlike its $Tp^{tBu,Me}$ analog, **25** does not exhibit spin crossover behavior up to 100 °C. X-ray quality crystals were grown from a saturated solution of **25** in benzene layered with pentane. The molecular structure of **25** (Figure 4.11), which crystallizes in the triclinic spacegroup P-1 with 2.5 molecules of benzene in the asymmetric unit, showed the Tp ligand bound κ^3 to the metal center with the fourth coordination site occupied by the NAd^{2-} ligand in a pseudo tetrahedral coordination geometry. The Co-N bond distances is 1.644(5) Å

(Table 4.7), which is slightly shorter than that of the $Tp^{tBu,Me}$CoNAd (Co-N bond distances of 1.655(2) Å.[20]

An unexpected result occured when $Tp^{Fc,Me}$CoI was reduced in the presence of excess N_3Ad (3 equivalents). The formation of $Tp^{Fc,Me}CoN_4Ad_2$ (**26**) was achieved via coupling of a N_3Ad molecule with $Tp^{Fc,Me}$CoNAd. Notably, **26** also can be prepared by reacting **25** with N_3Ad. The molecular structure of **26** shows one of the pyrazolyl arms has decoordinated to accommodate the bulky N_4Ad_2 ligand (Figure 4.12). The N-N bond distances of 1.309(3) Å (N7-N8), 1.348(3) Å (N8-N9), and 1.307(3) (N9-N10) Å suggests that the N_4Ad_2 fragment is formally a neutral tetraazadiene ligand and that the metal center is formally Co(I) (Table 4.8). However, the effective magnetic moment of 4.08(3) μ_B measured in benzene-d_6 (Evans method) suggests a Co(II) species with three unpaired electrons in solution. Subsequent thermal (heating in C_6D_6 at 100 °C overnight) and irradiation reactions (THF, 254 nm, 1 hr) with **26** showed no decomposition to form a $Tp^{Fc,Me}Co(NAd)_2$ species. **26** is stable at room temperature in air for days before finally decomposing to the hydroxo complex, **21**.

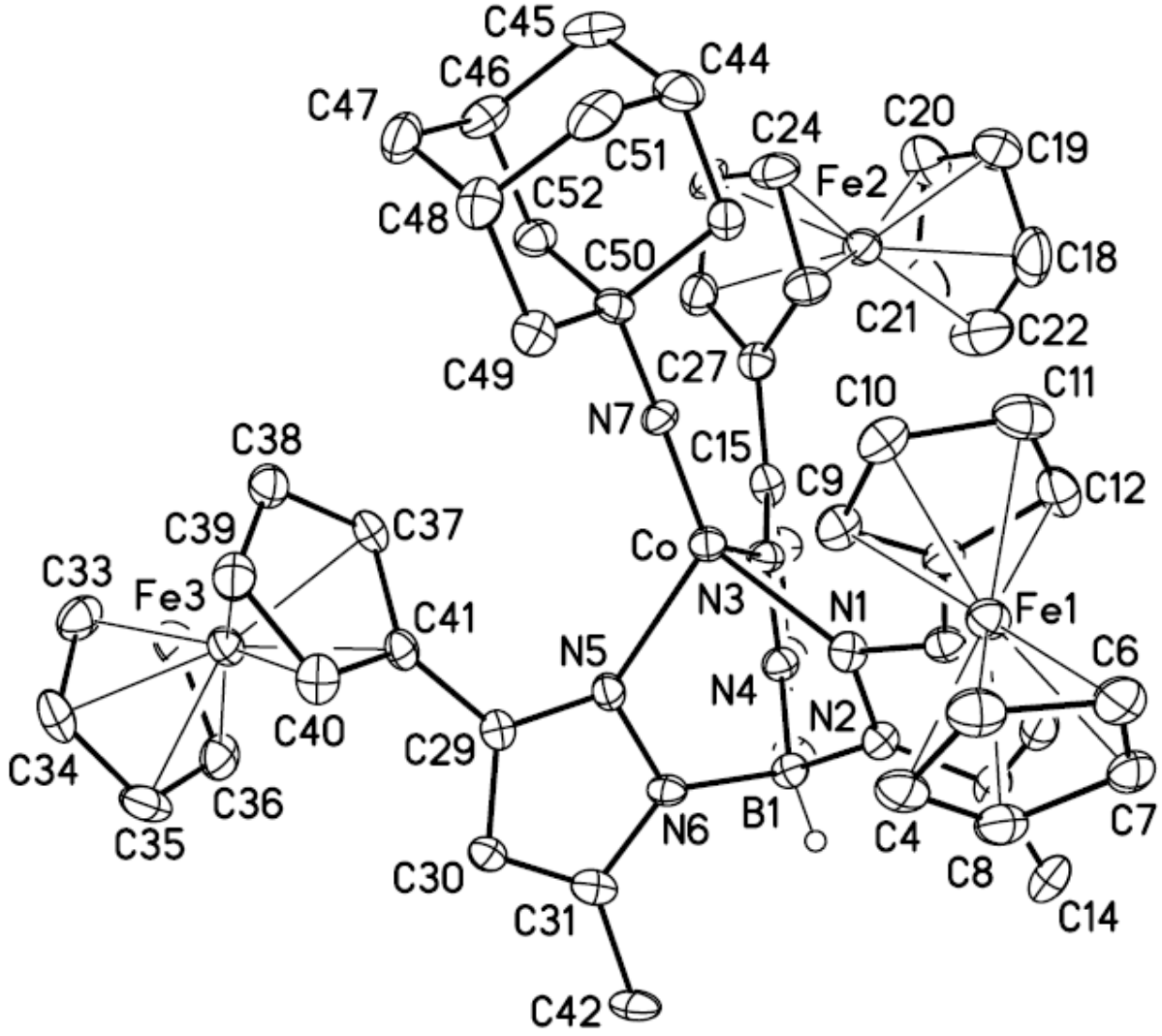

Figure 4.11: Molecular structure of $Tp^{Fc,Me}$CoNAd (25) at the 30% probability level. Hydrogen atoms (except the boron bound hydrogen, H1B) have been removed for clarity.

Table 4.7: Selected interatomic distances (Å) angles (°) for $Tp^{Fc,Me}$CoNAd (26).

Distances (Å)

Co-N(7)	1.644(5)	C(18)-C(19)	1.395(13)
Co-N(5)	2.002(6)	C(19)-C(20)	1.387(12)
Co-N(1)	2.006(6)	C(20)-C(21)	1.403(14)
Co-N(3)	2.021(6)	C(21)-C(22)	1.393(17)
B(1)-N(6)	1.532(9)	C(23)-C(27)	1.417(10)
B(1)-N(2)	1.541(10)	C(23)-C(24)	1.427(10)
B(1)-N(4)	1.554(9)	C(24)-C(25)	1.408(11)
N(1)-C(1)	1.344(9)	C(25)-C(26)	1.424(11)
N(1)-N(2)	1.383(7)	C(26)-C(27)	1.416(10)
N(2)-C(3)	1.348(8)	C(29)-C(30)	1.403(9)
N(3)-C(15)	1.348(8)	C(29)-C(41)	1.483(9)
N(3)-N(4)	1.366(7)	C(30)-C(31)	1.352(10)
N(4)-C(17)	1.349(9)	C(31)-C(42)	1.510(10)
N(5)-C(29)	1.337(8)	C(32)-C(33)	1.384(11)
N(5)-N(6)	1.386(7)	C(32)-C(36)	1.401(11)
N(6)-C(31)	1.364(8)	C(33)-C(34)	1.413(11)
N(7)-C(50)	1.417(8)	C(34)-C(35)	1.409(12)
C(1)-C(2)	1.405(9)	C(35)-C(36)	1.408(11)
C(1)-C(13)	1.460(9)	C(37)-C(41)	1.425(10)
C(2)-C(3)	1.355(10)	C(37)-C(38)	1.427(10)
C(3)-C(14)	1.497(10)	C(38)-C(39)	1.407(11)
C(4)-C(5)	1.409(10)	C(39)-C(40)	1.407(10)
C(4)-C(8)	1.435(10)	C(40)-C(41)	1.434(9)
C(5)-C(6)	1.405(11)	C(43)-C(44)	1.537(10)
C(6)-C(7)	1.403(11)	C(43)-C(50)	1.542(9)
C(7)-C(8)	1.407(10)	C(44)-C(51)	1.541(11)
C(9)-C(10)	1.399(10)	C(44)-C(45)	1.548(11)
C(9)-C(13)	1.417(10)	C(45)-C(46)	1.537(11)
C(10)-C(11)	1.408(11)	C(46)-C(47)	1.514(11)
C(11)-C(12)	1.416(11)	C(46)-C(52)	1.523(10)
C(12)-C(13)	1.449(10)	C(47)-C(48)	1.523(11)
C(15)-C(16)	1.382(10)	C(48)-C(51)	1.516(11)
C(15)-C(27)	1.461(10)	C(48)-C(49)	1.546(10)
C(16)-C(17)	1.374(10)	C(49)-C(50)	1.545(9)
C(17)-C(28)	1.505(10)	C(50)-C(52)	1.552(9)
C(18)-C(22)	1.382(18)		

Angles (°)

N(7)-Co-N(5)	125.5(3)	C(9)-C(10)-C(11)	108.7(7)
N(7)-Co-N(1)	126.8(3)	C(10)-C(11)-C(12)	107.5(7)
N(5)-Co-N(1)	88.9(2)	C(11)-C(12)-C(13)	108.6(7)
N(7)-Co-N(3)	126.0(3)	C(9)-C(13)-C(12)	105.6(6)
N(5)-Co-N(3)	88.8(2)	C(9)-C(13)-C(1)	129.1(7)
N(1)-Co-N(3)	88.6(2)	C(12)-C(13)-C(1)	124.9(7)
N(6)-B(1)-N(2)	108.6(6)	N(3)-C(15)-C(16)	109.5(7)
N(6)-B(1)-N(4)	107.4(6)	N(3)-C(15)-C(27)	122.3(6)
N(2)-B(1)-N(4)	107.9(6)	C(16)-C(15)-C(27)	128.2(7)
C(1)-N(1)-N(2)	105.3(5)	C(17)-C(16)-C(15)	106.7(7)
C(1)-N(1)-Co	134.9(5)	N(4)-C(17)-C(16)	107.3(6)
N(2)-N(1)-Co	117.7(4)	N(4)-C(17)-C(28)	121.7(7)
C(3)-N(2)-N(1)	110.5(6)	C(16)-C(17)-C(28)	130.9(7)
C(3)-N(2)-B(1)	132.0(6)	C(22)-C(18)-C(19)	110.0(12)
N(1)-N(2)-B(1)	117.5(5)	C(22)-C(18)-Fe(2)	70.3(6)
C(15)-N(3)-N(4)	106.3(6)	C(19)-C(18)-Fe(2)	70.3(6)
C(15)-N(3)-Co	134.2(5)	C(20)-C(19)-C(18)	107.4(10)
N(4)-N(3)-Co	117.4(4)	C(19)-C(20)-C(21)	107.1(10)
C(17)-N(4)-N(3)	110.2(6)	C(22)-C(21)-C(20)	109.5(12)
C(17)-N(4)-B(1)	132.0(6)	C(18)-C(22)-C(21)	106.1(11)
N(3)-N(4)-B(1)	117.8(6)	C(27)-C(23)-C(24)	108.1(7)
C(29)-N(5)-N(6)	106.0(5)	C(25)-C(24)-C(23)	107.9(7)
C(29)-N(5)-Co	135.0(5)	C(24)-C(25)-C(26)	108.0(7)
N(6)-N(5)-Co	117.7(4)	C(27)-C(26)-C(25)	108.2(7)
C(31)-N(6)-N(5)	109.3(6)	C(26)-C(27)-C(23)	107.7(7)
C(31)-N(6)-B(1)	132.9(6)	C(26)-C(27)-C(15)	124.7(7)
N(5)-N(6)-B(1)	117.7(5)	C(23)-C(27)-C(15)	127.6(7)
C(50)-N(7)-Co	178.7(5)	N(5)-C(29)-C(30)	110.0(6)
N(1)-C(1)-C(2)	109.9(6)	N(5)-C(29)-C(41)	123.4(6)
N(1)-C(1)-C(13)	121.7(6)	C(30)-C(29)-C(41)	126.6(6)
C(2)-C(1)-C(13)	128.3(7)	C(31)-C(30)-C(29)	106.4(6)
C(3)-C(2)-C(1)	106.3(7)	C(30)-C(31)-N(6)	108.2(6)
N(2)-C(3)-C(2)	108.0(7)	C(30)-C(31)-C(42)	130.8(7)
N(2)-C(3)-C(14)	122.6(7)	N(6)-C(31)-C(42)	121.0(7)
C(2)-C(3)-C(14)	129.4(7)	C(33)-C(32)-C(36)	109.7(8)
C(5)-C(4)-C(8)	105.9(7)	C(32)-C(33)-C(34)	107.0(8)
C(6)-C(5)-C(4)	109.7(8)	C(35)-C(34)-C(33)	108.4(8)
C(7)-C(6)-C(5)	107.7(7)	C(36)-C(35)-C(34)	107.4(7)
C(6)-C(7)-C(8)	108.2(7)	C(32)-C(36)-C(35)	107.4(7)
C(7)-C(8)-C(4)	108.5(7)	C(41)-C(37)-C(38)	107.7(7)
C(10)-C(9)-C(13)	109.6(7)	C(39)-C(38)-C(37)	108.2(7)

C(40)-C(39)-C(38)	108.6(7)	C(46)-C(47)-C(48)	109.8(6)
C(39)-C(40)-C(41)	108.2(7)	C(51)-C(48)-C(47)	110.0(7)
C(37)-C(41)-C(40)	107.3(6)	C(51)-C(48)-C(49)	108.5(6)
C(37)-C(41)-C(29)	127.0(6)	C(47)-C(48)-C(49)	110.3(6)
C(40)-C(41)-C(29)	125.7(6)	C(50)-C(49)-C(48)	109.5(6)
C(44)-C(43)-C(50)	110.5(6)	N(7)-C(50)-C(43)	109.7(6)
C(43)-C(44)-C(51)	109.0(6)	N(7)-C(50)-C(49)	110.4(6)
C(43)-C(44)-C(45)	108.6(6)	C(43)-C(50)-C(49)	108.3(6)
C(51)-C(44)-C(45)	108.9(7)	N(7)-C(50)-C(52)	110.1(6)
C(46)-C(45)-C(44)	109.5(6)	C(43)-C(50)-C(52)	108.2(6)
C(47)-C(46)-C(52)	111.2(7)	C(49)-C(50)-C(52)	110.0(6)
C(47)-C(46)-C(45)	109.3(7)	C(48)-C(51)-C(44)	110.2(6)
C(52)-C(46)-C(45)	109.0(6)	C(46)-C(52)-C(50)	109.5(6)

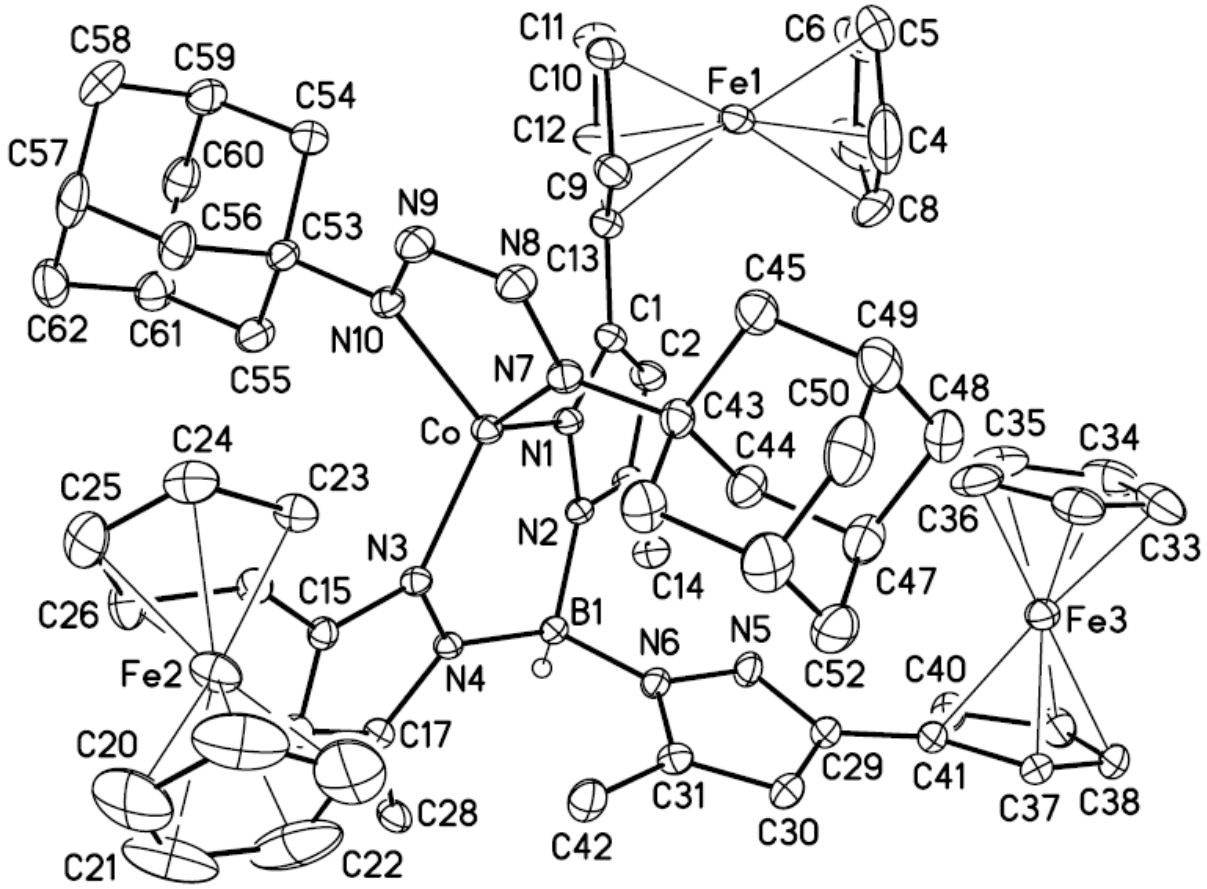

Figure 4.12: Molecular structure of $Tp^{Fc,Me}CoN_4Ad_2$ (26) at the 30% probability level. Hydrogen atoms (except the boron bound hydrogen, H1B) have been removed for clarity.

Table 4.8: Selected interatomic distances (Å) and angles (°) for $Tp^{Fc,Me}CoN_4Ad_2$ (26).

Distances (Å)

Co-N(7)	1.9242(19)	C(17)-C(28)	1.496(3)
Co-N(10)	1.9374(18)	C(18)-C(22)	1.417(7)
Co-N(1)	1.9732(18)	C(18)-C(19)	1.440(7)
Co-N(3)	1.9821(18)	C(19)-C(20)	1.359(6)
B(1)-N(4)	1.540(3)	C(20)-C(21)	1.356(6)
B(1)-N(2)	1.557(3)	C(21)-C(22)	1.341(7)
B(1)-N(6)	1.557(3)	C(23)-C(24)	1.418(3)
N(1)-C(1)	1.350(3)	C(23)-C(27)	1.424(3)
N(1)-N(2)	1.384(2)	C(24)-C(25)	1.402(4)
N(2)-C(3)	1.355(3)	C(25)-C(26)	1.417(4)
N(3)-C(15)	1.346(3)	C(26)-C(27)	1.425(3)
N(3)-N(4)	1.385(2)	C(29)-C(30)	1.394(3)
N(4)-C(17)	1.354(3)	C(29)-C(41)	1.470(3)
N(5)-C(29)	1.329(3)	C(30)-C(31)	1.376(3)
N(5)-N(6)	1.374(2)	C(31)-C(42)	1.497(3)
N(6)-C(31)	1.369(3)	C(32)-C(36)	1.397(5)
N(7)-N(8)	1.309(3)	C(32)-C(33)	1.411(4)
N(7)-C(43)	1.488(3)	C(33)-C(34)	1.398(5)
N(8)-N(9)	1.348(3)	C(34)-C(35)	1.422(5)
N(9)-N(10)	1.307(3)	C(35)-C(36)	1.415(5)
N(10)-C(53)	1.485(3)	C(37)-C(41)	1.421(3)
C(1)-C(2)	1.389(3)	C(37)-C(38)	1.419(4)
C(1)-C(13)	1.471(3)	C(38)-C(39)	1.415(4)
C(2)-C(3)	1.375(3)	C(39)-C(40)	1.430(4)
C(3)-C(14)	1.489(3)	C(40)-C(41)	1.426(4)
C(4)-C(5)	1.418(5)	C(43)-C(44)	1.529(3)
C(4)-C(8)	1.437(8)	C(43)-C(45)	1.533(3)
C(5)-C(6)	1.392(5)	C(43)-C(46)	1.535(3)
C(6)-C(7)	1.370(5)	C(44)-C(47)	1.548(4)
C(7)-C(8)	1.374(8)	C(45)-C(49)	1.551(4)
C(9)-C(13)	1.421(3)	C(46)-C(51)	1.553(4)
C(9)-C(10)	1.423(4)	C(47)-C(52)	1.516(4)
C(10)-C(11)	1.403(4)	C(47)-C(48)	1.524(4)
C(11)-C(12)	1.414(4)	C(48)-C(49)	1.526(4)
C(12)-C(13)	1.430(3)	C(49)-C(50)	1.514(5)
C(15)-C(16)	1.396(3)	C(50)-C(51)	1.525(5)
C(15)-C(27)	1.465(3)	C(51)-C(52)	1.526(4)
C(16)-C(17)	1.377(3)	C(53)-C(55)	1.524(3)

C(53)-C(56)	1.530(3)	C(57)-C(62)	1.525(4)
C(53)-C(54)	1.541(3)	C(58)-C(59)	1.528(4)
C(54)-C(59)	1.534(4)	C(59)-C(60)	1.530(4)
C(55)-C(61)	1.538(3)	C(60)-C(61)	1.520(4)
C(56)-C(57)	1.545(4)	C(61)-C(62)	1.524(4)
C(57)-C(58)	1.524(4)		

Angles (°)

N(7)-Co-N(10)	78.53(8)	N(1)-C(1)-C(13)	123.8(2)
N(7)-Co-N(1)	118.66(8)	C(2)-C(1)-C(13)	126.6(2)
N(10)-Co-N(1)	119.87(8)	C(3)-C(2)-C(1)	106.6(2)
N(7)-Co-N(3)	123.63(8)	N(2)-C(3)-C(2)	108.1(2)
N(10)-Co-N(3)	117.56(8)	N(2)-C(3)-C(14)	123.8(2)
N(1)-Co-N(3)	99.72(7)	C(2)-C(3)-C(14)	128.0(2)
N(4)-B(1)-N(2)	113.74(18)	C(5)-C(4)-C(8)	105.5(4)
N(4)-B(1)-N(6)	111.00(18)	C(6)-C(5)-C(4)	107.2(4)
N(2)-B(1)-N(6)	109.39(18)	C(7)-C(6)-C(5)	110.4(4)
C(1)-N(1)-N(2)	106.74(17)	C(6)-C(7)-C(8)	107.6(5)
C(1)-N(1)-Co	132.08(15)	C(7)-C(8)-C(4)	109.2(4)
N(2)-N(1)-Co	121.04(13)	C(13)-C(9)-C(10)	108.2(2)
C(3)-N(2)-N(1)	109.10(17)	C(11)-C(10)-C(9)	108.5(2)
C(3)-N(2)-B(1)	125.15(18)	C(10)-C(11)-C(12)	107.9(2)
N(1)-N(2)-B(1)	125.23(17)	C(11)-C(12)-C(13)	108.7(3)
C(15)-N(3)-N(4)	106.66(17)	C(9)-C(13)-C(12)	106.7(2)
C(15)-N(3)-Co	132.29(15)	C(9)-C(13)-C(1)	130.1(2)
N(4)-N(3)-Co	120.21(13)	C(12)-C(13)-C(1)	123.2(2)
C(17)-N(4)-N(3)	109.10(17)	N(3)-C(15)-C(16)	109.78(19)
C(17)-N(4)-B(1)	124.83(18)	N(3)-C(15)-C(27)	123.0(2)
N(3)-N(4)-B(1)	125.21(17)	C(16)-C(15)-C(27)	127.2(2)
C(29)-N(5)-N(6)	106.13(18)	C(17)-C(16)-C(15)	106.0(2)
C(31)-N(6)-N(5)	109.96(18)	N(4)-C(17)-C(16)	108.47(19)
C(31)-N(6)-B(1)	136.15(19)	N(4)-C(17)-C(28)	122.6(2)
N(5)-N(6)-B(1)	112.75(17)	C(16)-C(17)-C(28)	128.8(2)
N(8)-N(7)-C(43)	112.02(18)	C(22)-C(18)-C(19)	105.2(4)
N(8)-N(7)-Co	116.13(15)	C(20)-C(19)-C(18)	106.7(4)
C(43)-N(7)-Co	131.84(15)	C(21)-C(20)-C(19)	109.9(5)
N(7)-N(8)-N(9)	114.81(18)	C(22)-C(21)-C(20)	109.6(5)
N(10)-N(9)-N(8)	114.69(18)	C(21)-C(22)-C(18)	108.5(4)
N(9)-N(10)-C(53)	111.83(17)	C(24)-C(23)-C(27)	108.5(2)
N(9)-N(10)-Co	115.78(15)	C(25)-C(24)-C(23)	107.8(2)
C(53)-N(10)-Co	132.36(14)	C(24)-C(25)-C(26)	108.8(2)
N(1)-C(1)-C(2)	109.4(2)	C(25)-C(26)-C(27)	107.8(2)

C(23)-C(27)-C(26)	107.1(2)	C(52)-C(47)-C(44)	108.7(2)
C(23)-C(27)-C(15)	128.5(2)	C(48)-C(47)-C(44)	108.5(2)
C(26)-C(27)-C(15)	124.4(2)	C(47)-C(48)-C(49)	109.6(2)
N(5)-C(29)-C(30)	110.9(2)	C(50)-C(49)-C(48)	111.2(3)
N(5)-C(29)-C(41)	119.5(2)	C(50)-C(49)-C(45)	108.7(3)
C(30)-C(29)-C(41)	129.6(2)	C(48)-C(49)-C(45)	109.2(2)
C(31)-C(30)-C(29)	105.9(2)	C(49)-C(50)-C(51)	110.2(2)
N(6)-C(31)-C(30)	107.1(2)	C(50)-C(51)-C(52)	110.6(3)
N(6)-C(31)-C(42)	125.3(2)	C(50)-C(51)-C(46)	108.1(3)
C(30)-C(31)-C(42)	127.6(2)	C(52)-C(51)-C(46)	108.3(2)
C(36)-C(32)-C(33)	108.2(3)	C(47)-C(52)-C(51)	110.7(3)
C(34)-C(33)-C(32)	108.3(3)	N(10)-C(53)-C(55)	107.40(18)
C(33)-C(34)-C(35)	107.8(3)	N(10)-C(53)-C(56)	111.69(19)
C(36)-C(35)-C(34)	107.5(3)	C(55)-C(53)-C(56)	109.5(2)
C(32)-C(36)-C(35)	108.1(3)	N(10)-C(53)-C(54)	109.73(19)
C(41)-C(37)-C(38)	108.4(2)	C(55)-C(53)-C(54)	109.2(2)
C(39)-C(38)-C(37)	108.2(2)	C(56)-C(53)-C(54)	109.3(2)
C(38)-C(39)-C(40)	107.9(2)	C(59)-C(54)-C(53)	109.2(2)
C(41)-C(40)-C(39)	107.9(2)	C(53)-C(55)-C(61)	110.1(2)
C(37)-C(41)-C(40)	107.6(2)	C(53)-C(56)-C(57)	109.0(2)
C(37)-C(41)-C(29)	126.9(2)	C(58)-C(57)-C(62)	110.2(2)
C(40)-C(41)-C(29)	125.5(2)	C(58)-C(57)-C(56)	109.5(2)
N(7)-C(43)-C(44)	107.71(18)	C(62)-C(57)-C(56)	109.4(2)
N(7)-C(43)-C(45)	112.4(2)	C(57)-C(58)-C(59)	109.1(2)
C(44)-C(43)-C(45)	109.1(2)	C(58)-C(59)-C(60)	109.5(2)
N(7)-C(43)-C(46)	108.28(19)	C(58)-C(59)-C(54)	109.6(2)
C(44)-C(43)-C(46)	109.6(2)	C(60)-C(59)-C(54)	109.7(2)
C(45)-C(43)-C(46)	109.7(2)	C(61)-C(60)-C(59)	109.7(2)
C(43)-C(44)-C(47)	109.9(2)	C(62)-C(61)-C(60)	109.5(2)
C(43)-C(45)-C(49)	108.8(2)	C(62)-C(61)-C(55)	109.2(2)
C(43)-C(46)-C(51)	109.4(2)	C(60)-C(61)-C(55)	109.3(2)
C(52)-C(47)-C(48)	110.3(2)	C(61)-C(62)-C(57)	109.5(2)

4.2.9 Thermal Stability of $Tp^{Fc,Me}CoNAd$ (25).

Unlike $Tp^{tBu,Me}CoNAd$, which undergoes a clean thermal decomposition at 40 °C over the course 10 days,[20] the $Tp^{Fc,Me}CoNAd$ remains intact for days in benzene at 60 °C under vacuum or in the presence of ethylene (Figure A3.2). However, when a solution of **25** was heated at 100 °C in solution, the appearance of new paramagnetic resonances was observed (Figure A3.9). The $Tp^{Fc,Me}$ ligand has shown the ability to undergo thermal isomerization when complexed with Co. Thus the possibility of thermal rearrangement of the Tp ligand cannot be discounted in the case of **25**. After several days, compound **25** may be thermally isomerized to the $Tp^{Fc,Me*}CoNAd$ (Scheme 4.6) complex, which then decomposes (presumably *via* H-atom abstraction from the methyl group) after prolonged periods at elevated temperatures (~100 °C). However, attempts to isolate the product of this reaction have been unsuccessful.

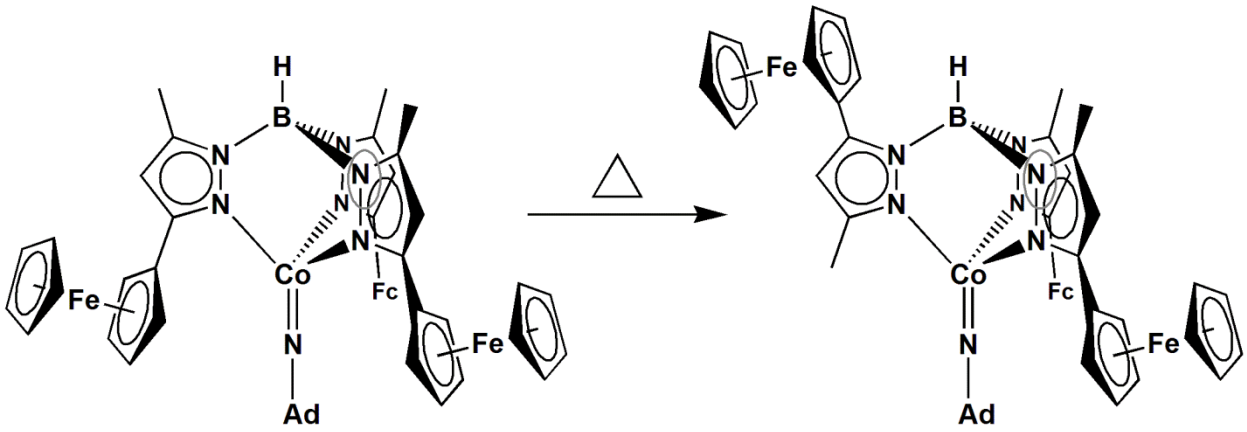

Scheme 4.6: Thermal isomerization of $Tp^{Fc,Me}CoNAd$ to $Tp^{Fc,Me*}CoNAd$.

4.3 Conclusions

The preparation of low-valent (Co(I) and Co(II)) $Tp^{Fc,Me}Co$ complexes has been achieved. Metathesis of $Tp^{Fc,Me}CoI$ with allyl Grignard yields $Tp^{Fc,Me}Co(\eta^3\text{-allyl})$, which is a

useful starting material for reactivity with O_2 and CO. When exposed to O_2, $Tp^{Fc,Me}Co(\eta^3\text{-allyl})$ underwent insertion of O_2 into the Co allyl bond to form a putative $Tp^{Fc,Me}CoOOC_3H_5$ complex which underwent bond homolysis to form $Tp^{Fc,Me}CoOH$ and $Tp^{Fc,Me}CoO_2$ in both the solid state and solution. When $Tp^{Fc,Me}Co(\eta^3\text{-allyl})$ is exposed to CO at 60 °C in THF, $Tp^{Fc,Me}Co(CO)$ can be isolated. $Tp^{Fc,Me}Co(CO)$ reacts with O_2 at room temperature to cleanly convert to $Tp^{Fc,Me}CoO_2$ in low concentrations (1 mg/mL). This is important to prevent the formation of the carbonate, $[Tp^{Fc,Me}Co]_2(\mu\text{-}CO_3)$ (FigureA3.10-$[Tp^{Fc,Me}Co]_2(\mu\text{-}CO_3)(H_2O)$), species which is obtained in the reaction of $Tp^{Fc,Me}Co(CO)$ with O_2 at high concentrations of $Tp^{Fc,Me}Co(CO)$.

The reduction of $Tp^{Fc,Me}CoI$ with KC8 in the presence of N_3Ad generated $Tp^{Fc,Me}CoNAd$. The thermal stability of $Tp^{Fc,Me}CoNAd$ is significantly greater than that of the analogous, $Tp^{tBu,Me}CoNAd$. Unlike $Tp^{tBu,Me}CoNAd$, $Tp^{Fc,Me}CoNAd$ remained stable in solution at 60 °C for days. However, at temperatures exceeding 100 °C, $Tp^{Fc,Me}CoNAd$ decomposed to unidentified products. Also, the $Tp^{Fc,Me}$ ligand allowed for the isolation of $Tp^{Fc,Me}CoN_4Ad_2$ when $Tp^{Fc,Me}CoI$ is reduced in the presence of excess N_3Ad.

The high C-H bond strength of the Fc substituents on Tp ligands may allow for the isolation of reactive products which suffer ligand decomposition in the parent $Tp^{t\text{-}Bu,Me}$ system. However, thermal isomerization still remains a problem in the $Tp^{Fc,Me}$ system which might be overcome by the employment of a Tp^{Fc2} ligand.

4.4 Experimental

All reactions were run under a nitrogen atmosphere using standard glovebox and Schlenk techniques unless otherwise stated. Diethyl ether, pentane, tetrahydrofuran (THF), and toluene were distilled over Na or K-benzophenone ketyl under nitrogen atmosphere or by passing the solvent through activated alumina columns followed by a nitrogen purge to remove dissolved oxygen.[21] Organic chemicals were bought from Aldrich or Acros and inorganic chemicals were purchased from Strem. NMR spectra were obtained on a Bruker AVIII-400 or AV 600 spectrometer and were referenced to the residual protons of the solvent (CD_2Cl_2, 5.32 ppm; $CDCl_3$, 7.24 ppm; C_6D_6, 7.15 ppm). FT-IR spectra were recorded on Matteson Alpha Centauri or Nicolet Magna-IR 560 spectrometers with a resolution of 4 cm^{-1}. X-ray crystallographic studies were conducted in the University of Delaware X-ray crystallographic facility. Elemental analyses were obtained fromRobertson Microlit, Ledgewood, NJ 07852. Room-temperature molar magnetic susceptibilities (χ_m) in the solid state were determined using a Johnson Matthey magnetic susceptibility balance. They were corrected for diamagnetism using Pascal constants[22] and converted into effective magnetic moments (μ_{eff}). Solution magnetic susceptibilities were determined by the Evans method.[23]

4.4.1 Single crystal X-ray diffraction studies.

General considerations are given on page 57. The systematic absences in the diffraction data were consistent with *C*2/*c* and *Cc* for **kla0304** (**22**). No symmetry higher than triclinic was observed for the other structures. Solution in the centrosymmetric space group option yielded chemically reasonable and computationally stable results of refinement. Solvent molecules were located in the asymmetric unit for **kla0290** (**25**) (2.5 benzene per compound molecule) and

kla0304 (**22**) (three 1,4-dioxane per compound molecule). Two molecules of cocrystallized 1,4-dioxane in **kla0304** (**22**) were found disordered in two positions, treated with equal atomic displacement parameters for chemically equivalent disordered contributions, with refined site occupancy ratios of 60/40 and 52/48. Rigid bond restraints on U_{ij} were applied to all atoms in **kla0265** (**26**), and all cocrystallized solvent molecules. Borohydride H-atoms on **kla0265** (**26**), **kla0315** (**24**), and **kla0317** (**23**) were located from the difference map and constrained to U_{iso} equal to 1.2 B-atom U_{eq}.

4.4.2 Nitrato-hydrotris(3-ferrocenyl-5-methylpyrazolyl)borato-cobalt(II), $Tp^{Fc,Me}CoNO_3$ (20).

1.0 g of $Tp^{Fc,Me}Tl$ (0.99 mmol) and 0.3 g of $Co(NO_3)_2 \bullet 6H_2O$ (1.03 mmol) were dissolved in 100 mL of CH_2Cl_2 and refluxed for one hour. The brownish orange solution was allowed to cool to room temperature and filtered through a bed of Celite and the solvent evaporated. The brown residue was triturated with pentanes and the solid collected on a frit. The crude product was recrystallized by vapor diffusion of diethylether into a saturated solution of **20** in CH_2Cl_2 . The resulting brownish-orange crystalline solid was collected on a frit and washed with several portions of pentane and allowed to dry under vacuum yielding 0.61 g of $Tp^{Fc,Me}CoNO_3$ (66 %). ^{1}H NMR (400 MHz, CD_2Cl_2): 69.2 (br, 3 H), 19.3 (br, 9 H), 8.4 (br, 6 H), 3.5 (br, 6 H), 2.7 (br, 15 H) ppm. IR (KBr): 3093 (s), 2963 (s), 2924 (s), 2544 (w, υ_{B-H}), 1836 (w), 1650 (w), 1532 (s), 1468 (s), 1429 (s), 1372 (m), 1322 (s), 1272 (w), 1222 (s), 1181 (w), 1106 (s), 1059 (w), 1026 (s), 999 (w), 883 (s), 646 (m), 503 (m), 438 (s) cm^{-1}. μ_{eff} = 4.2(1) μ_B (295 K). Mp: 274 °C (decomp.). Anal Calcd for $C_{42}H_{40}N_7O_3BFe_3Co$: C, 54.35; H, 4.34; N, 10.56. Found: C, 53.93; H, 4.47; N, 10.32.

4.4.3 Hydroxo-hydrotris(3-ferrocenyl-5-methylpyrazolyl)borato-cobalt(II), $Tp^{Fc,Me}CoOH$ (21).

Method 1: 0.72 mL of a 1M solution of n-butylammonium hydroxide was added drop-wise to a stirred solution 0.5 g $Tp^{Fc,Me}CoCl$ (0.55 mmol) in 20 mL of CH_2Cl_2. An immediate color change from green to brown occurred along with the formation of a colorless precipitate. After 12 hours of stirring, the solution was filtered through Celite and the solvent removed under vacuum. The resulting brown solid was placed in a frit and was washed with a small portion of water, followed by several small portions of methanol, and dried. The solid dissolved in 10 mL of CH_2Cl_2 and allowed to crystallize via vapor-phase diffusion of diethyl ether yielding 0.32 g of $Tp^{Fc,Me}CoOH$ (54 %).

Method 2: In a 100 mL round bottom equipped with a stir bar, 0.465 g of $Tp^{Fc,Me}CoNO_3$ (0.5 mmol) was dissolved in 25 mL of CH_2Cl_2. 50 mL of a 0.05 M solution of NaOH in water was added and the solution was allowed to stir for 2 hours. The organic layer was separated from the aqueous layer and washed with several portions of water (3 x 50 mL). The organic solution was dried over Na_2SO_4 and filtered. The solvent was removed and the brown residue triturated with pentanes and collected on a frit. The solid was dissolved in 20 mL of a 50/50 mixture of CH_2Cl_2 and diethylether and left at 0°C over night. The brownish orange crystals were collected and washed with pentanes and dried under vacuum yielding 0.25 g (56 %) of the desired product. ^1H NMR (400 MHz, CD_2Cl_2): 64.8 (br, 3 H), 14.2 (br, 9 H), 4.31 (br, 6 H), 3.28 (br, 6 H), 0.16 (br, 15 H) ppm. IR (KBr): 3639 (w, υ_{O-H}), 3096 (w), 2957 (w), 2923 (s), 2853 (w), 2774 (s), 2533 (w, υ_{B-H}), 1560 (s), 1469 (s), 1430 (s), 1402 (w), 1320 (s), 1182 (w), 1106 (s), 1060 (w), 1020 (s), 1000 (s), 886 (s), 810 (w), 785 (s), 645 (s), 573 (s) cm^{-1}. UV-vis (THF), λ_{max} (ϵ, M^{-1}

cm^{-1}): 453 (1127), 592 (493), 670 (652) nm. μ_{eff} = 3.9(1) μ_B (295 K). Mp: 274 – 276 °C. Anal Calcd for $C_{42}H_{41}N_6OBFe_3Co$: C, 57.12; H, 4.68; N, 9.52. Found: C, 57.06; H, 4.76; N, 9.23.

4.4.4 η3-Allyl-hydrotris(3-ferrocenyl-5-methylpyrazolyl)borato-cobalt(II), $Tp^{Fc,Me}Co(\eta^3\text{-}C_3H_5)$ (22).

0.72 mL of a 1.7 M solution of allylmagnesium chloride in THF was added drop-wise to a stirred solution 0.5 g $Tp^{Fc,Me}CoCl$ (0.55 mmol) in 50 mL of 1,4-dioxane. After 12 hours of stirring, a color change from green to orange had occurred, along with the formations of a colorless precipitate. The solution was filtered through Celite and the solvent removed under vacuum and gentle heating. The residue was dissolved in a minimum amount of THF and recrystallized at -30°C overnight. The resulting orange solid was collected on a frit and dissolved in 10 mL of toluene and 10 mL of pentane was carefully layered on top. The solution was allowed to cool to -30 °C. After 2 days, the resulting orange solid was collected on a frit, washed with pentane and dried under vacuum yielding 0.32 g of $Tp^{Fc,Me}Co(\eta^3\text{-}C_3H_5)$ (64 %). ^{1}H NMR (400 MHz, C_6D_6): 19.0 (br, 9 H), 10.1 (br, 3 H), 5.9 (br, 6 H), 3.3 (br, 6 H), 2.6 (br, 15 H) ppm. IR (KBr): 3092 (w), 2922 (w), 2854 (w), 2520 (w, $\upsilon_{B\text{-}H}$), 1772 (m), 1652 (m), 1558 (s), 1516 (s), 1421 (m), 1398 (s), 1260 (s), 1192 (w), 1106 (s), 1062 (s), 1001 (s), 814 (w), 782 (s), 502 (m), 467 (w) cm^{-1}. UV-vis (THF), λ_{max} (ϵ, M^{-1} cm^{-1}): 431 (1132) nm. μ_{eff} = 2.5(1) μ_B (295 K). Mp: 195 - 197 °C (decomp.). Anal Calcd for $C_{45}H_{45}N_6BFe_3Co\bullet 2C_4H_8O$: C, 60.55; H, 5.85; N, 7.99. Found: C, 61.18; H, 4.91; N, 7.67.

4.4.5 Carbonyl-hydrotris(3-ferrocenyl-5-methylpyrazolyl)borato-cobalt(I), $Tp^{Fc,Me}Co(CO)$ (23).

In a glove box, an ampule equipped with a stir bar was charged with 0.5 g of $Tp^{Fc,Me}Co(\eta^3\text{-}C_3H_5)$ (0.55 mmol) and 20 mL of toluene. The ampule was brought out of the box and placed on a high vacuum line and freeze/pump/thawed 3 times. 1 atmosphere of CO was added to the ampule and the reaction was heated at 75 °C for one hour, during which time, a color change from orange to yellow occurred. The solution was freeze/pumped/thawed (3x) to remove excess CO where upon a green precipitate formed. The solution was brought back into the glove box and the yellow-green product collected on a frit. The solid was washed with pentane and dried in *vacuo* yielding 0.37 (75 %) of the product. A second crop was collected from the concentrated and cooled toluene mother liquor. Total yield 0.42 g (85 % yield). ^1H NMR (400 MHz, C_6D_6): 33.4 (br, 3 H), 17.8 (br, 9 H), 4.3 (br, 6 H), 0.1 (br, 15 H) ppm. IR (KBr): 3093 (w), 2959 (w), 2923 (s), 2854 (w), 2528 (w, $\upsilon_{B\text{-}H}$), 1949 (s, $\upsilon_{C\text{-}O}$), 1560 (s), 1516 (s), 1467 (s), 1428 (s), 1401 (s), 1361 (m), 1185 (w), 1106 (s), 1060 (s), 1001 (s), 883 (s), 815 (w), 784 (s), 646 (m) cm^{-1}. $\mu_{eff} = 3.2(1)\ \mu_B$ (295 K). Mp: 279 - 281 °C (decomp.). Mass Spectrum (LIFDI) m/z, (%): 898.072, (100, M^+). Anal Calcd for $C_{43}H_{40}N_6OBFe_3Co$: C, 57.63; H, 4.72; N, 9.38. Found: C, 56.69; H, 4.06; N, 9.04.

4.4.6 Calculation of K_{eq} for the reaction of $Tp^{Fc,Me}Co(CO)$ (23) with CO.

To a solution of **23** in benzene-d_6 in a J. Young tube, one atm of CO was added. The relative concentrations of $Tp^{Fc,Me}Co(CO)$ and $Tp^{Fc,Me}Co(CO)_2$ were calculated from the ratio of the proton shifts of the resulting ^1H NMR compared to the proton shifts known for $Tp^{Fc,Me}Co(CO)$ and $Tp^{Fc,Me}Tl$.

$$K_{eq} = \frac{[Tp^{Fc,Me}Co(CO)_2]}{[Tp^{Fc,Me}Co(CO)][CO]}$$

$$K_{eq} = \frac{1}{2 \times 0.00717}$$

$$K_{eq} = 69.69$$

4.4.7 Superoxo-(3-ferrocenyl-5-methylpyrazolyl)borato-cobalt(II), $Tp^{Fc,Me}Co(O_2)$ (24).

In a glove box under an inert atmosphere, an ampule equipped with a stir bar was charged with 50 mg of $Tp^{Fc,Me}Co(\eta^3\text{-}C_3H_5)$ (0.05 mmol) and 50 mL of THF. The ampule was brought out of the box and placed on a high vacuum line and freeze/pump/thawed three times and 1 atmosphere of CO was added to the ampule. After heating for one hour, the reaction was cooled to room temperature and freeze/pump/thawed one time. 1 atmosphere of O_2 was introduced and an immediate color change from yellow-green to brown occurred. The solution was allowed to stir for 1 hr. The solution was freeze/pump/thawed three times to remove excess O_2. The solution was filtered in air and the solvent removed. The crude brown solid was recrystallized by vapor phase diffusion of ether into a solution of $Tp^{Fc,Me}CoO_2$ in CH_2Cl_2. The resulting brown crystals were collected on a frit, washed with pentane and dried under vacuum yielding 42 mg (86 %) of the product. ^{1}H NMR (400 MHz, CD_2Cl_2): 32.2 (br, 9 H), 27.1 (br, 1 H), 17.6 (br, 3 H), 3.69 (br, 6 H), 1.15 (br, 15 H), -2.01 (br, 6 H) ppm. IR (KBr): 3094 (w), 2923 (w), 2852 (s), 2534 (w, $\upsilon_{B\text{-}H}$), 1558 (s), 1469 (s) 1427 (s), 1403 (s), 1372 (m), 1321 (s), 1185 (w), 1106 (s), 1000 (s), 954 (w,$\upsilon_{16O\text{-}16O}$), 902 (w, $\upsilon_{18O\text{-}18O}$), 883 (s), 817 (w), 759 (s), 505 (m) cm^{-1}. μ_{eff} = 3.71(3) μ_B (298 K, benzene-d_6). Mp: 235- 240 °C (decomp.). Mass Spectrum (LIFDI) m/z, (%): 898.0696, (100, M^+). Anal Calcd for $C_{42}H_{40}N_6O_2BFe_3Co$: C, 56.17; H, 4.49; N, 9.36. Found: C, 55.27; H, 4.36; N, 9.07.

4.4.8 Adamantylimido-hydrotris(3-ferrocenyl-5-methylpyrazolyl)borato-cobalt(III), $Tp^{Fc,Me}CoNAd$ (25).

To a solution of 0.2 g of $Tp^{Fc,Me}CoI$ (0.2 mmol) and 0.035 g of azidoadamantane (0.2 mmol) in 20 mL of THF, 0.030 g of KC_8 (0.22 mmol) was added. An immediate color change from green to orange occurred along with a concomitant evolution of N_2 gas. The solution was allowed to stir for 30 minutes and then filtered through a plug of Celite. The volume of THF was reduced by half and placed into a 20 mL scintillation vial. Pentane was carefully layered on top of the THF and the vial placed into the freezer at -30 °C. After 24 hours, orange crystals had formed and were collected on a frit and washed with pentane yielding 80 mg (37 %) of the product. ^{1}H NMR (400 MHz, C_6D_6): 6.43 (br, 3 H), 5.03 (br, 6 H), 4.03 (br, 6 H), 3.92 (br, 15 H), 2.17 (br, 9 H), 1.75 (br, 6 H), 1.56 (br, 6 H), 1.04 (br, 3 H) ppm. IR (KBr): 3095 (w), 2907 (w), 2522 (w, B-H), 1560 (s), 1516 (s), 1426 (s), 1364 (m), 1322 (s), 1185 (w), 1106 (s), 1060 (s), 1001 (s), 884 (s), 816 (w), 757 (s), 647 (m), 504 (m) cm^{-1}. UV-vis (THF), λ_{max} (ϵ, M^{-1} cm^{-1}): 419 (703), 592 (21), 670 (92), 779 (115) nm. Mp: 148 -152°C (decomp). Anal Calcd for $C_{52}H_{55}N_7BFe_3Co$: C, 61.51; H, 5.46; N, 9.66. Found: C, 61.56; H, 5.74; N, 9.16.

4.4.9 Diadamantyltetraazadiene-hydrotris(3-ferrocenyl-5-methylpyrazolyl)borato-cobalt(II), $Tp^{Fc,Me}CoN_4Ad_2$ (26).

To a solution of 0.1 g of $Tp^{Fc,Me}CoI$ (0.1 mmol) in 20 mL of THF and 52 mg of azidoadamantane (0.3 mmol), 15 mg of KC_8 (0.11 mmol) was added. An immediate color change from green to orange occurred along with a concomitant evolution of N_2 gas. The solution was allowed to stir for 30 minutes and then filtered through a plug of Celite. The volume of THF was reduced by half and placed into a 20 mL scintillation vial. Pentane was carefully layered on top of the THF and the vial placed into the freezer at -30 °C. After 24 hours, reddish-

orange crystals had formed and were collected on a frit and washed with pentane yielding 50 mg mg (42 %) of the product. ^{1}H NMR (400 MHz, C_6D_6): 46.5 (br), 7.95 (br), 7.34 (br), 4.7 (s), 1.69 (br), 0.96 (s), -1.89 (s), -3.70 (s), -4.06(s), -4.89 (s), -7.35 (s), -9.91 (s), -9.36 (s), -18.48 (br), -19.13 (d). IR (KBr): 3099 (w), 2898 (w), 2848 (s), 2487 (w, υ_{B-H}), 1559 (s), 1469 (s), 1426 (s), 1364 (m), 1322 (s), 1183 (w), 1106 (s), 1068 (s), 1001 (s), 884 (s), 885 (w), 786 (s), 647 (m), 503 (m) cm^{-1}. Mp: 244 - 247 °C. μ_{eff} = 4.08(3) μ_B (298 K, benzene-d_6). Anal Calcd for $C_{62}H_{70}N_{10}BFe_3Co$: C, 62.44; H, 5.92; N, 11.75. Found: C, 62.69; H, 6.17; N, 11.06

4.5 References

1. Cotton, F. A.; Wilkinson, G. *Advanced Inorganic Chemistry* John Wiley and Sons Inc.; New York. **1988**, 5th Edition, 724.
2. a) Egan, J. W. J.; Haggerty, B. S.; Rheingold, A. L.; Sendlinger, S. C.; Theopold, K. H., *J. Am. Chem. Soc.* **1990,** 112, 2445.; b) Qin, K.; Incarvito, C. D.; Rheingold, A. L.; Theopold, K. H., *J. Am. Chem. Soc.* **2002,** *124*, 14008.
3. a) Fujisawa, K.; Tanaka, M.; Moro-oka, Y.; Kitajima, N. *J. Am. Chem. Soc.*, **1994**, *116*, 12079.; b) Chen, P.; Root, D. E.; Campochiaro, C.; Fujisawa, K.; Salomon, E. I. *J. Am. Chem. Soc.* **2003**, *125*, 466.; c) Zhang, X.; Loppnow, G. R.; McDonald, R.; Takats, J. *J. Am. Chem. Soc.* **1995**, *117*, 7828.
4. a) Cotton, F. A.; Wilkinson, G.; Murillo, C. A.; Bochmann, M (**1999**) *Advanced Inorganic Chemistry* 6th edition, New York: John Wiley & Sons, Inc. b) Lewis, E. A. and Tolman, W. B., Chem. Rev., **2004**, *104*, 1047.
5. Kitajima, N., Hikichi, S., Tanaka, M. and Moro-oka, Y., *JACS*, **1993**, *115*, 5496.
6. a.) Han, R., Parkin, G., *J. Am. Chem. Soc*., **1991**, *113*, 9707. b.) Thyagarajan, S., Doctoral Dissertation, University of Delaware, **2003**.
7. Jewson, J. D., Liable-Sands, L. M., Yap, G. P. A., Rheingold, A. L. and Theopold, K. H., *Organometallics*, **1999**, *18*, 300.
8. DuPont, J. A., Coxey, M. B., Schebler, P. J., Incarvito, C. D., Dougherty, W. G., Yap, G. P. A., Rheingold, A. L. and Riordan, C. G., *Organometallics*, **2007**, *26*, 971.
9. Egan, J. W., Personal Communication, University of Delaware.

10. Detrich, J. L., Doctoral Dissertation, University of Delaware, **1996**.

11. Detrich, J. L., Konečnỳ, R., Vetter, W. M., Doren, D., Rheingold, A. L. and Theopold, K. H., *J. Am. Chem. Soc*., **1996**, *118*, 1703.

12. Fogg, P. G. T., Gerrard, W., *Solubility of Gases in Liquids*, Wiley: Chichester, **1991**, 278.

13. Dietrich, J. L., Reinaud, O. M., Rheingold, A. L. and Theopold, K. H., *J. Am. Chem. Soc.,* **1995**, *117*, 11745.

14. Cramer, C. J., Tolman, W.B., Theopold, K. H. and Rheingold, A.L., *PNAS*, **2003**, 3635.

15. Bogadi, R., Coppens, P. Personal Communication.

16. Cheung, S. K., Grimes, C. J., Wong, J., Reed, C. A., *J. Am. Chem.Soc*. **1976**, *98*, 5028.

17. Hikichi, S., Komatsuzaki, H., Akita, M. and Moro-oka, Y., *J. Am. Chem. Soc*., **1998**, *120*, 4699.

18. For examples see: a) Glueck, D. S., Hollander, F. J., Bergman, R. G., *J. Am. Chem. Soc*. **1989**, *111*, 2719.; b) Glueck, D. S., Wu, J. X., Hollander, F. J., Bergman, R. G., *J. Am. Chem. Soc*. **1991**, *113*, 2041.; c) Mindiola, D. J., Hillhouse, G. L., *J. Am. Chem. Soc*. **2001**, 123, 4623; d) Jenkins, D. M., Betley, T. A., Peters, J. C., *J. Am. Chem. Soc*. **2002**, *124*, 11 238; e) Betley, T. A., Peters, J. C., *J. Am. Chem. Soc*. **2003**, *125*, 10782.; f) X. Dai, P. Kapoor, T. H. Warren, *J. Am. Chem. Soc.* **2004**, *126*, 4798. g) King, E. R., Sazama, G. T. and Betley, T. A., *J. Am. Chem. Soc*. **2012**, *134*, 17858.

19. Nugent, W. A.; Mayer, J. M. Metal−Ligand Multiple Bonds; Wiley: New York, 1988.

20. Shay, D. T., Yap, G. P. A., Zakharov, L. N., Rheingold, A. L. and Theopold, K. H., Angew. Chem. Int. Ed., **2005**, *44*, 1508.

21. Pangborn, A. B., Giardello, M. A., Grubbs, R. H., Rosen, R. K., Timmers, F. J., *Organometallic*, **1996**, *15*, 1518.

22. Magnetic Properties of Coordination and Organometallic Transition Metal Compounds; Hellwege, K. H., Hellwege, A. M., Ed., Landolt-Börnstein Series; Springer-Verlag: Berlin, **1981**; Vol. 11.

23. Evans, D. F., *J. Chem. Soc*., **1959**, 2003. A correction for the superconducting solenoidal field must be made, see: Live, D. H., Chan, S. I., *Anal. Chem.*, **1970**, *42*, 791.

Appendix A

PERMISSIONS GRANTED

All figures reused in the abstract of this dissertation were done with permission from the copyright holders.

Figure 1.1:

“Springer and the original publisher (Structure and Bonding, 142, 2011, page 20, Electronic Structures of Oxo-Metal Ions, Jay R. Winkler and Harry B. Gray, figure 1, original copyright notice) is given to the publication in which the material was originally published, by adding; with kind permission from Springer Science and Business Media.”

Figure 1.2:

"Reprinted (adapted) with permission from (O’Halloran, K. P., Zhao, C., Ando, N. S.; Schultz, A. J.; Koetzle, T. F., Piccoli, P. M. B., Hedman, B.; Hodgson, K. O., Bobyr, E.; Kirk, M. L., Knottenbelt, S., Depperman, E. C., Stein, B., Anderson, T. M.; Cao, R., Geletii, Y. V., Hardcastle, K. I., Musaev, D. G., Neiwert, W. A., Fang, X.; Morokuma, K., Wu, S., Kögerler, P., Hill, C. L., *Inorg. Chem*. **2012**, *51*, 7025.). Copyright (2012) American Chemical Society."

Figure 1.3:

Molecular structure of $Ir^{v}(O)(mes)_3$ was generated from the cif file obtained from the Cambridge Structural Database (CSD).[1]

A.1 Supplimental Material for Chapter 2

Table A1.1 displayes the percentage of the sphere shielded by the ligand, G(L), and the equivalent cone angle (ECA) corresponding to the solid angle of the ligand, Omega (L), for all ligands in prepared in this dissertation.[2] All calculations were done using Solid-G software. The G(L) and ECA for $Tp^{tBu,Me}Tl$ were calculated from literature values.[3]

Table A1.1: Calculated G(L) and ECA for $RTp^{Fc,R}Tl$ compounds.

Compound	G(L)	ECA (°)
$Tp^{Fc*}Tl$	59.99	203.05
$Tp^{Fc}Tl$ (Ch. 2)	64.57	213.89
$Tp^{Fc,Me*}Tl$	59.41	75.08
$Tp^{Fc,Me}Tl$ (Ch. 2)	65.99	217.30
$Tp^{Fc,iPr}Tl$	58.91	200.53
$Tp^{CF3,Fc}Tl$	50.08	180.18
$PhTp^{Fc}Tl$	55.99	193.75
$Tp^{tBu,Me}Tl$	55.88	193.50

All torsion angles were calculated by SHELXL following the conventions defined by Allen & Rogers.[4] Torsion angles were calculated from three interatomic vectors of four atom positions from the N atom proximal to the Tl atom to the ferrocenyl Fe atom (Figure A1.1). In the cases of N-confusion, torsion angles were calculated from three interatomic vectors of four atom positions from the N atom distal to the Tl atom to the ferrocenyl Fe atom. Clockwise rotation of the Fc moiety relative to the pyrazolyl ring was assigned a positive torsion angle and counter clockwise rotation was assigned a negative torsion angle. The torsion angles for each complex have been arranged from largest (most positive) to the smallest (most negative) angle (Table Al.1). As these complexes are chiral, racemix mixtures exist within the crystals with complementary angles (different signs).

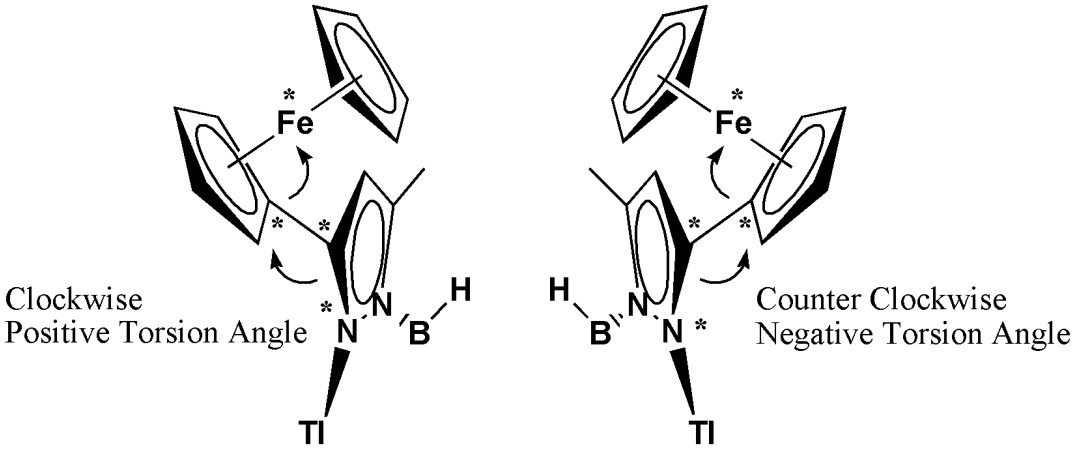

Figure A1.1: Torsion angle calculation for RTp^{Fc,R}Tl compounds.

Table A1.2: Torsion angles for $RTp^{Fc,R}Tl$ compounds.

Compound	Angle 1 (°)	Angle 2 (°)	Angle 3 (°)
$Tp^{Fc*}Tl$	93.5(6)	76.7(5)	-108.2(5)
$Tp^{Fc,Me*}Tl$	122.14(19)	98.1(2)	49.3(3)
$Tp^{Fc,iPr}Tl$	96.7(5)	96.7(5)	96.7(5)
$Tp^{CF3,Fc}Tl$	169.3(4)	143.7(5)	143.2(4)
$PhTp^{Fc}Tl$	133.5(3)	115.3(3)	-73.4(4)

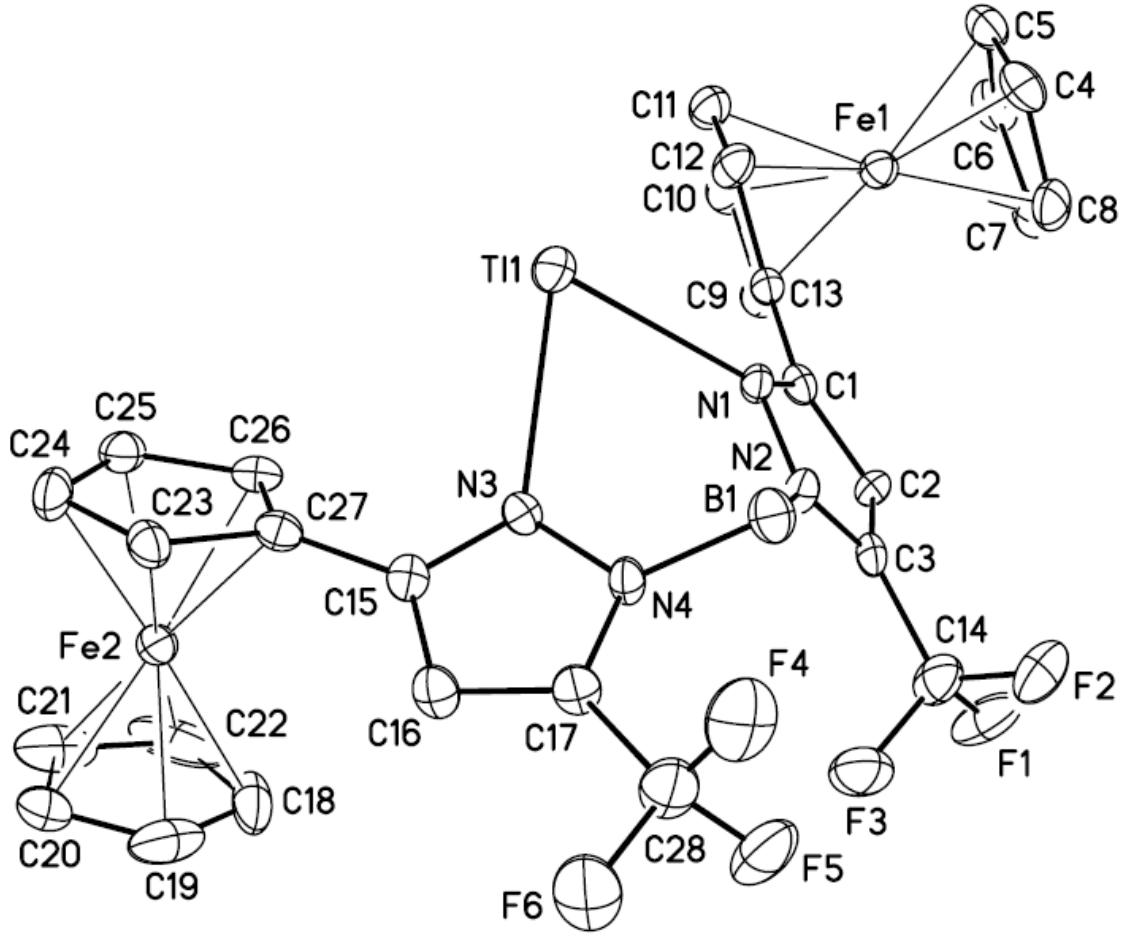

Figure A1.2: Molecular structure of $Bp^{CF3,Fc}Tl$ at 30% probability level. Hydrogen atoms have been removed for clarity.

Table A1.3: Selected interatomic distances (Å) and bond angles (°) for $Bp^{Fc,CF3}Tl$.

Distances (Å)

Tl(1)-N(1)	2.578(5)	C(4)-C(5)	1.417(9)
Tl(1)-N(3)	2.593(5)	C(5)-C(6)	1.400(9)
B(1)-N(2)	1.553(8)	C(6)-C(7)	1.427(9)
B(1)-N(4)	1.565(8)	C(7)-C(8)	1.393(9)
Cl(1)-C(29)	1.713(8)	C(9)-C(10)	1.396(9)
Cl(2)-C(29)	1.734(8)	C(9)-C(13)	1.427(8)
Cl(3)-C(29)	1.726(7)	C(10)-C(11)	1.430(9)
F(1)-C(14)	1.339(7)	C(11)-C(12)	1.422(8)
F(2)-C(14)	1.340(8)	C(12)-C(13)	1.417(8)
F(3)-C(14)	1.313(8)	C(15)-C(16)	1.404(8)
F(4)-C(28)	1.352(9)	C(15)-C(27)	1.461(8)
F(5)-C(28)	1.312(8)	C(16)-C(17)	1.357(8)
F(6)-C(28)	1.334(8)	C(17)-C(28)	1.490(9)
N(1)-C(1)	1.348(7)	C(18)-C(19)	1.357(12)
N(1)-N(2)	1.345(6)	C(18)-C(22)	1.458(14)
N(2)-C(3)	1.355(7)	C(19)-C(20)	1.346(11)
N(3)-C(15)	1.343(7)	C(20)-C(21)	1.327(12)
N(3)-N(4)	1.360(6)	C(21)-C(22)	1.367(13)
N(4)-C(17)	1.357(7)	C(23)-C(27)	1.421(8)
C(1)-C(2)	1.407(8)	C(23)-C(24)	1.428(9)
C(1)-C(13)	1.468(8)	C(24)-C(25)	1.398(9)
C(2)-C(3)	1.395(8)	C(25)-C(26)	1.425(8)
C(3)-C(14)	1.496(9)	C(26)-C(27)	1.436(8)
C(4)-C(8)	1.402(9)		

Angles (°)

N(1)-Tl(1)-N(3)	76.54(15)	C(17)-N(4)-B(1)	131.8(5)
N(2)-B(1)-N(4)	110.0(5)	N(3)-N(4)-B(1)	118.6(5)
C(1)-N(1)-N(2)	107.8(5)	N(1)-C(1)-C(2)	110.9(5)
C(1)-N(1)-Tl(1)	130.0(4)	N(1)-C(1)-C(13)	120.0(5)
N(2)-N(1)-Tl(1)	118.0(3)	C(2)-C(1)-C(13)	129.0(5)
N(1)-N(2)-C(3)	108.3(5)	C(3)-C(2)-C(1)	102.3(5)
N(1)-N(2)-B(1)	118.6(5)	N(2)-C(3)-C(2)	110.6(6)
C(3)-N(2)-B(1)	133.0(6)	N(2)-C(3)-C(14)	123.1(6)
C(15)-N(3)-N(4)	106.9(5)	C(2)-C(3)-C(14)	126.3(6)
C(15)-N(3)-Tl(1)	128.7(4)	C(8)-C(4)-C(5)	107.2(6)
N(4)-N(3)-Tl(1)	118.8(3)	C(6)-C(5)-C(4)	108.6(7)
C(17)-N(4)-N(3)	108.6(5)	C(5)-C(6)-C(7)	107.4(7)

C(8)-C(7)-C(6)	107.7(7)	N(4)-C(17)-C(28)	122.8(6)
C(7)-C(8)-C(4)	109.2(7)	C(16)-C(17)-C(28)	127.1(6)
C(10)-C(9)-C(13)	108.6(6)	C(19)-C(18)-C(22)	106.4(8)
C(9)-C(10)-C(11)	108.9(6)	C(18)-C(19)-C(20)	109.1(9)
C(12)-C(11)-C(10)	106.4(6)	C(21)-C(20)-C(19)	109.4(9)
C(13)-C(12)-C(11)	109.2(6)	C(20)-C(21)-C(22)	110.6(9)
C(12)-C(13)-C(9)	106.9(5)	C(21)-C(22)-C(18)	104.4(8)
C(12)-C(13)-C(1)	126.7(6)	C(27)-C(23)-C(24)	108.3(6)
C(9)-C(13)-C(1)	126.4(6)	C(25)-C(24)-C(23)	108.5(6)
F(3)-C(14)-F(1)	107.4(6)	C(24)-C(25)-C(26)	108.1(6)
F(3)-C(14)-F(2)	107.2(6)	C(25)-C(26)-C(27)	108.3(6)
F(1)-C(14)-F(2)	105.7(6)	C(23)-C(27)-C(26)	106.9(6)
F(3)-C(14)-C(3)	113.5(6)	C(23)-C(27)-C(15)	125.8(6)
F(1)-C(14)-C(3)	109.9(6)	C(26)-C(27)-C(15)	127.2(6)
F(2)-C(14)-C(3)	112.6(6)	F(5)-C(28)-F(6)	107.1(7)
N(3)-C(15)-C(16)	110.2(5)	F(5)-C(28)-F(4)	107.2(7)
N(3)-C(15)-C(27)	121.3(5)	F(6)-C(28)-F(4)	106.1(6)
C(16)-C(15)-C(27)	128.5(6)	F(5)-C(28)-C(17)	114.6(6)
C(17)-C(16)-C(15)	104.5(5)	F(6)-C(28)-C(17)	109.4(6)
N(4)-C(17)-C(16)	109.9(6)	F(4)-C(28)-C(17)	112.0(6)

Table A1.4: Crystal data and structure refinement for $Bp^{Fc}Tl$.

Identification code	klat914
Empirical formula	C30 H32 B Fe2 N4 O Tl
Formula weight	791.47
Temperature	200(2) K
Wavelength	0.71073 Å
Crystal system, space group	Monoclinic, P n
Unit cell dimensions	a = 5.757(2) Å alpha = 90 deg. b = 18.061(7) Å beta = 99.120(5) deg. c = 13.559(5) Å gamma = 90 deg.
Volume	1392.0(9) $Å^3$
Z, Calculated density	2, 1.888 Mg/m^3
Absorption coefficient	6.834 mm^{-1}
F(000)	772
Crystal size	0.352 x 0.190 x 0.089 mm
Theta range for data collection	2.255 to 28.266 deg.
Limiting indices	-7<=h<=7, -24<=k<=24, -18<=l<=18
Reflections collected / unique	18050 / 6683 [R(int) = 0.0305]
Completeness to theta = 25.000	99.7 %
Absorption correction	Semi-empirical from equivalents
Max. and min. transmission	1.000000 and 0.551762
Refinement method	Full-matrix least-squares on F^2
Data / restraints / parameters	6683 / 2 / 358
Goodness-of-fit on F^2	0.714
Final R indices [I>2sigma(I)]	R1 = 0.0176, wR2 = 0.0429
R indices (all data)	R1 = 0.0182, wR2 = 0.0435
Absolute structure parameter	0.012(3)
Extinction coefficient	n/a
Largest diff. peak and hole	0.318 and -0.977 e. $Å^{-3}$

Table A1.5: Crystal data and structure refinement for $Tp^{Fc*}Tl$ (1).

Identification code	kla0004
Empirical formula	C39 H34 B Fe3 N6 Tl
Formula weight	969.45
Temperature	200(2) K
Wavelength	0.71073 Å
Crystal system, space group	Monoclinic, P2(1)/c
Unit cell dimensions	a = 7.4998(18) Å alpha = 90 deg. b = 23.030(5) Å beta = 94.731(4) deg. c = 19.904(5) Å gamma = 90 deg.
Volume	3426.2(14) $Å^3$
Z, Calculated density	4, 1.879 Mg/m^3
Absorption coefficient	5.973 mm^{-1}
F(000)	1896
Crystal size	0.30 x 0.16 x 0.15 mm
Theta range for data collection	1.77 to 28.31 deg.
Limiting indices	-9<=h<=9, -30<=k<=30, -26<=l<=26
Reflections collected / unique	45959 / 8482 [R(int) = 0.1085]
Completeness to theta = 25.00	100.0 %
Absorption correction	Semi-empirical from equivalents
Max. and min. transmission	0.4718 and 0.2682
Refinement method	Full-matrix least-squares on F^2
Data / restraints / parameters	8482 / 0 / 454
Goodness-of-fit on F^2	1.010
Final R indices [I>2sigma(I)]	R1 = 0.0453, wR2 = 0.0771
R indices (all data)	R1 = 0.0833, wR2 = 0.0874
Largest diff. peak and hole	1.641 and -0.656 $e.Å^{-3}$

Table A1.6: Crystal data and structure refinement for $Tp^{Fc,Me*}Tl$ (2).

Identification code	kla0244
Empirical formula	C44 H46 B Fe3 N6 O S Tl
Formula weight	1089.66
Temperature	200(2) K
Wavelength	0.71073 Å
Crystal system, space group	Triclinic, P-1
Unit cell dimensions	a = 11.5633(7) Å alpha = 71.3780(10) deg. b = 13.6431(8) Å beta = 77.6110(10) deg. c = 14.3940(9) Å gamma = 71.2460(10) deg.
Volume	2021.8(2) $Å^3$
Z, Calculated density	2, 1.790 Mg/m^3
Absorption coefficient	5.124 mm^{-1}
F(000)	1080
Crystal size	0.46 x 0.18 x 0.07 mm
Theta range for data collection	1.50 to 27.46 deg.
Limiting indices	-14<=h<=14, -17<=k<=17, -18<=l<=18
Reflections collected / unique	26541 / 9228 [R(int) = 0.0236]
Completeness to theta = 25.00	100.0 %
Absorption correction	Semi-empirical from equivalents
Max. and min. transmission	0.7318 and 0.2025
Refinement method	Full-matrix least-squares on F^2
Data / restraints / parameters	9228 / 0 / 519
Goodness-of-fit on F^2	1.030
Final R indices [I>2sigma(I)]	R1 = 0.0197, wR2 = 0.0520
R indices (all data)	R1 = 0.0211, wR2 = 0.0528
Largest diff. peak and hole	1.329 and -0.739 $e.Å^{-3}$

Table A1.7: Crystal data and structure refinement for $Tp^{Fc,iPr}Tl$ (3).

Identification code	klat967
Empirical formula	C48 H52 B Fe3 N6 Tl
Formula weight	1095.69
Temperature	200(2) K
Wavelength	0.71073 Å
Crystal system, space group	Rhombohedral, R-3
Unit cell dimensions	a = 21.384(3) Å alpha = 90 deg. b = 21.384(3) Å beta = 90 deg. c = 16.938(4) Å gamma = 120 deg.
Volume	6708(2) $Å^3$
Z, Calculated density	6, 1.627 Mg/m^3
Absorption coefficient	4.587 mm^{-1}
F(000)	3276
Crystal size	0.23 x 0.18 x 0.12 mm
Theta range for data collection	1.90 to 28.29 deg.
Limiting indices	-28<=h<=28, -28<=k<=28, -22<=l<=22
Reflections collected / unique	25697 / 3712 [R(int) = 0.1293]
Completeness to theta = 25.00	100.0 %
Absorption correction	Semi-empirical from equivalents
Max. and min. transmission	0.6159 and 0.4133
Refinement method	Full-matrix least-squares on F^2
Data / restraints / parameters	3712 / 0 / 181
Goodness-of-fit on F^2	1.003
Final R indices [I>2sigma(I)]	R1 = 0.0473, wR2 = 0.0854
R indices (all data)	R1 = 0.0868, wR2 = 0.0988
Largest diff. peak and hole	0.890 and -0.713 e. $Å^{-3}$

Table A1.8: Crystal data and structure refinement for $Tp^{CF3,Fc}Tl$ (4).

Identification code	kla0226
Empirical formula	C42 H31 B F9 Fe3 N6 Tl
Formula weight	1173.46
Temperature	200(2) K
Wavelength	0.71073 Å
Crystal system, space group	Triclinic, P-1
Unit cell dimensions	a = 10.6673(16) Å alpha = 95.653(3) deg. b = 11.2558(17) Å beta = 90.620(3) deg. c = 18.130(3) Å gamma = 110.879(2) deg.
Volume	2021.6(5) $Å^3$
Z, Calculated density	2, 1.928 Mg/m^3
Absorption coefficient	5.111 mm^{-1}
F(000)	1140
Crystal size	0.25 x 0.13 x 0.09 mm
Theta range for data collection	1.13 to 27.48 deg.
Limiting indices	-13<=h<=13, -14<=k<=14, -23<=l<=23
Reflections collected / unique	21596 / 9222 [R(int) = 0.0549]
Completeness to theta = 25.00	99.8 %
Absorption correction	Semi-empirical from equivalents
Max. and min. transmission	0.6451 and 0.3557
Refinement method	Full-matrix least-squares on F^2
Data / restraints / parameters	9222 / 30 / 569
Goodness-of-fit on F^2	1.010
Final R indices [I>2sigma(I)]	R1 = 0.0489, wR2 = 0.0937
R indices (all data)	R1 = 0.0801, wR2 = 0.1046
Largest diff. peak and hole	1.293 and -0.639 $e.Å^{-3}$

Table A1.9: Crystal data and structure refinement for $PhTp^{Fc}Tl$ (5).

Identification code	kla0030
Empirical formula	C45 H38 B Fe3 N6 Tl
Formula weight	1045.54
Temperature	200(2) K
Wavelength	0.71073 Å
Crystal system, space group	Monoclinic, P2(1)/c
Unit cell dimensions	a = 11.8715(17) Å alpha = 90 deg. b = 13.821(2) Å beta = 102.049(3) deg. c = 23.992(4) Å gamma = 90 deg.
Volume	3849.9(10) $Å^3$
Z, Calculated density	4, 1.804 Mg/m^3
Absorption coefficient	5.323 mm^{-1}
F(000)	2056
Crystal size	0.34 x 0.32 x 0.19 mm
Theta range for data collection	1.71 to 28.29 deg.
Limiting indices	-15<=h<=15, -18<=k<=18, -31<=l<=31
Reflections collected / unique	32774 / 9508 [R(int) = 0.0489]
Completeness to theta = 25.00	99.8 %
Absorption correction	Semi-empirical from equivalents
Max. and min. transmission	0.4376 and 0.2678
Refinement method	Full-matrix least-squares on F^2
Data / restraints / parameters	9508 / 0 / 505
Goodness-of-fit on F^2	1.026
Final R indices [I>2sigma(I)]	R1 = 0.0360, wR2 = 0.0697
R indices (all data)	R1 = 0.0552, wR2 = 0.0758
Largest diff. peak and hole	1.194 and -0.701 $e.Å^{-3}$

Table A1.10: Crystal data and structure refinement for $Bp^{Fc,CF3}Tl$.

Identification code	kla0223
Empirical formula	C29 H22 B Cl3 F6 Fe2 N4 Tl
Formula weight	973.74
Temperature	199(2) K
Wavelength	0.71073 Å
Crystal system, space group	Monoclinic, C2/c
Unit cell dimensions	a = 28.983(8) Å alpha = 90 deg. b = 11.245(3) Å beta = 97.013(4) deg. c = 20.015(5) Å gamma = 90 deg.
Volume	6474(3) A^3
Z, Calculated density	8, 1.998 Mg/m^3
Absorption coefficient	6.160 mm^{-1}
F(000)	3736
Crystal size	0.18 x 0.13 x 0.06 mm
Theta range for data collection	2.05 to 27.54 deg.
Limiting indices	-37<=h<=37, -14<=k<=14, -22<=l<=25
Reflections collected / unique	29450 / 7437 [R(int) = 0.0919]
Completeness to theta = 25.00	100.0 %
Absorption correction	Semi-empirical from equivalents
Max. and min. transmission	0.7088 and 0.3969
Refinement method	Full-matrix least-squares on F^2
Data / restraints / parameters	7437 / 0 / 415
Goodness-of-fit on F^2	1.061
Final R indices [I>2sigma(I)]	R1 = 0.0478, wR2 = 0.0752
R indices (all data)	R1 = 0.0987, wR2 = 0.0882
Largest diff. peak and hole	0.873 and -0.793 $e.Å^{-3}$

A.2 Supplimental Material for Chapter 3

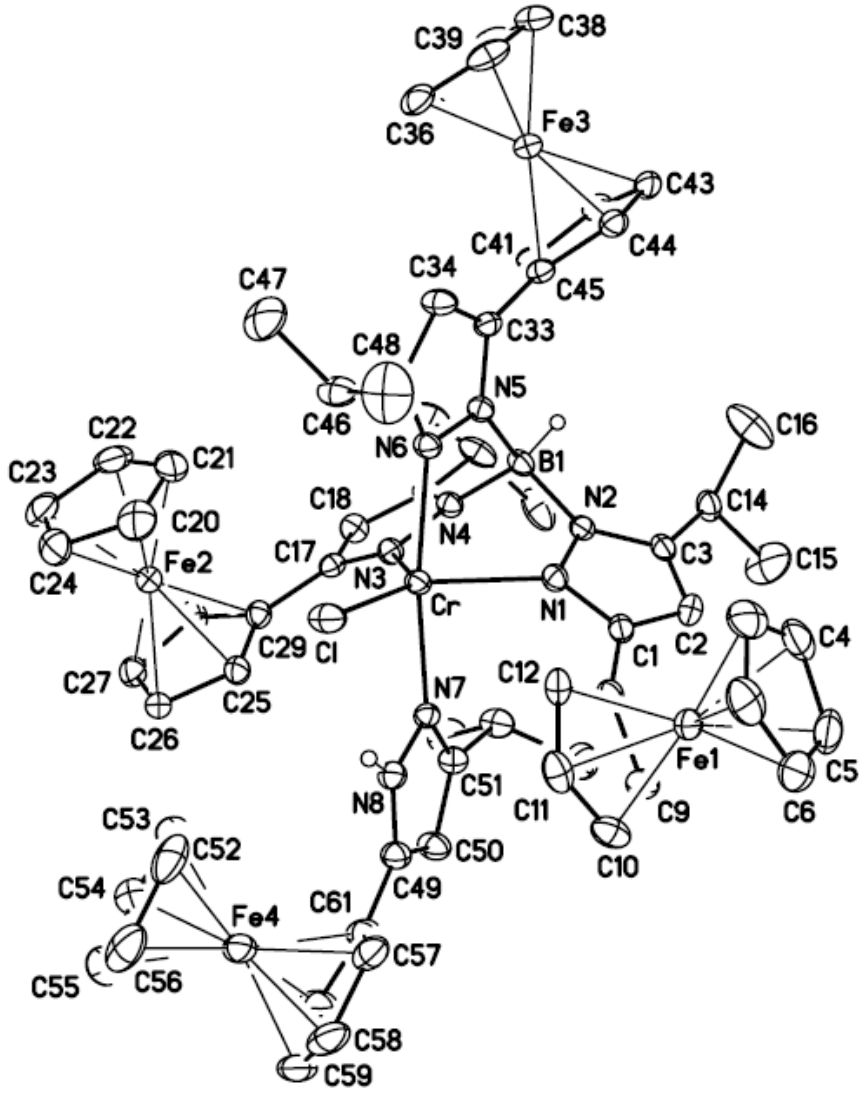

Figure A2.1: Molecular structure of $Tp^{Fc,iPr*}CrCl(Pz^{Fc,iPr}H)$ at the 30% probability level. Hydrogen atoms (except the boron bound hydrogen, H1B) have been removed for clarity.

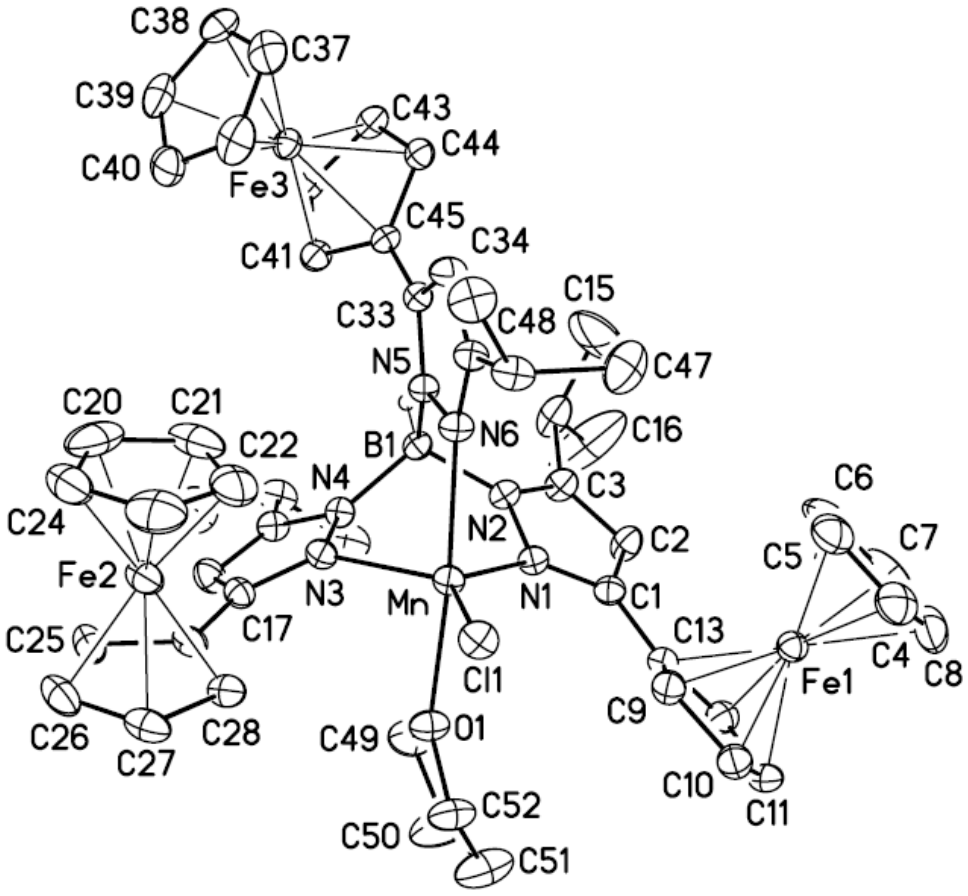

Figure A2.2: Molecular structure of $Tp^{Fc,iPr*}MnCl(THF)$ at the 30% probability level. Hydrogen atoms (except the boron bound hydrogen, H1B) have been removed for clarity.

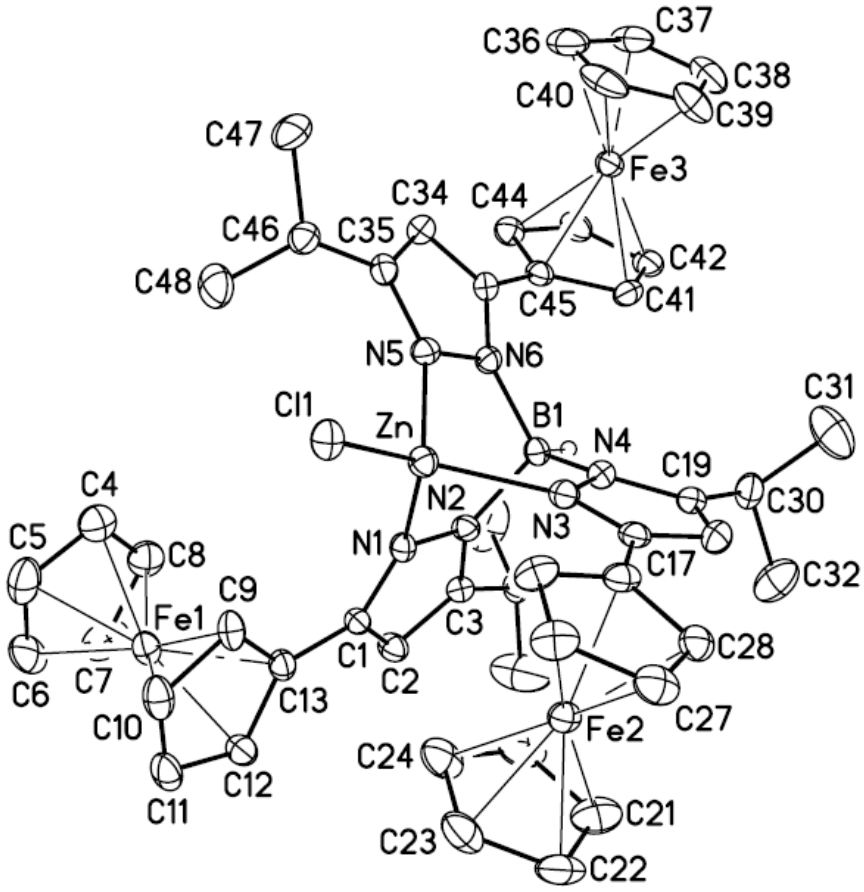

Figure A2.3: Molecular structure of $Tp^{Fc,iPr*}ZnCl$ at the 30% probability level. Hydrogen atoms (except the boron bound hydrogen, H1B) have been removed for clarity.

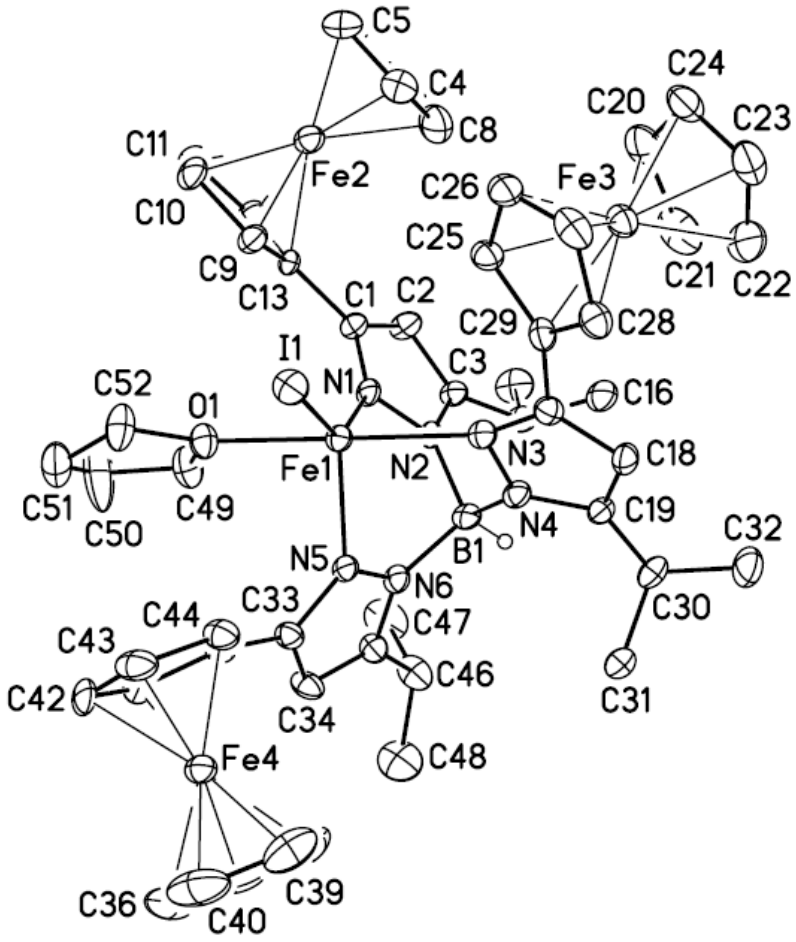

Figure A2.4: Molecular structure of $Tp^{Fc,iPr}FeI(THF)$ at the 30% probability level. Hydrogen atoms (except the boron bound hydrogen, H1B) have been removed for clarity.

All torsion angles were calculated by SHELXL following the conventions defined by Allen & Rogers.[4] Torsion angles were calculated from three interatomic vectors of four atom positions from the N atom proximal to the M atom to the ferrocenyl Fe atom (Figure A2.5). In the cases of N-confusion, torsion angles were calculated from three interatomic vectors of four atom positions from the N atom distal to the M atom to the ferrocenyl Fe atom. Clockwise rotation of the Fc moiety relative to the pyrazolyl ring was assigned a positive torsion angle and counter clockwise rotation was assigned a negative torsion angle. The torsion angles for each complex have been arranged from largest (most positive) to the smallest (most negative) angle (Table A2.1).

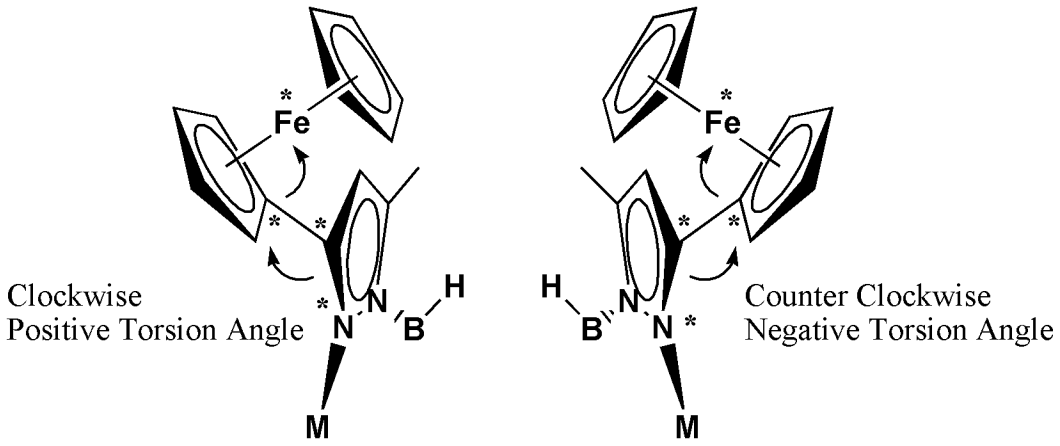

Figure A2.5: Torsion angle calculation for $Tp^{Fc,R}M$ compounds.

Table A2.1: Torsion angles for $Tp^{Fc,R}M$ compounds.

Compound	Angle 1 (°)	Angle 2 (°)	Angle 3 (°)
$Tp^{Fc}Tl$	79.0(4)	73.2(4)	-114.2(3)
$Tp^{Fc}CoI$	95.4(4)	71.5(6)	-122.3(4)
$Tp^{Fc}CoCl$	88.5(3)	73.9(3)	-118.21(8)
$Tp^{Fc}Cu(CO)$	87.6(3)	71.5(3)	-120.7(2)
$Tp^{Fc,Me}Tl$	73.9(4)	70.7(5)	-109.9(4)
$Tp^{Fc,Me}CoI$	85.7(3)	74.1(4)	-122.9(3)
$Tp^{Fc,Me}CoCl$	83.5(3)	73.8(3)	-117.5(2)
$Tp^{Fc,Me}Cu(CO)$	83.0(5)	71.5(6)	-119.1(4)
$Tp^{Fc,iPr}CoI$	128.5(4)	123.7(4)	-116.0(4)
$Tp^{Fc,iPr*}CoCl$	137.3(4)	107.5(5)	64.4(6)
$Tp^{Fc,iPr*}Cu(CO)$	138.6(4)	110.4(5)	61.9(6)
$Tp^{Fc,iPr**}Cu(CO)$	139.5(8)	137.4(7)	106.0(9)

Table A2.2: Crystal data and structure refinement for $Tp^{Fc}Tl$ (7).

Identification code	kla0136
Empirical formula	C73 H62 B Cl12 Fe6 N6 Tl
Formula weight	1998.96
Temperature	200(2) K
Wavelength	0.71073 A
Crystal system, space group	Trigonal, R -3 :H
Unit cell dimensions	a = 26.65(3) A alpha = 90 deg. b = 26.65(3) A beta = 90 deg. c = 18.78(2) A gamma = 120 deg.
Volume	11550(31) A^3
Z, Calculated density	6, 1.724 Mg/m^3
Absorption coefficient	3.646 mm^{-1}
F(000)	5928
Crystal size	0.242 x 0.137 x 0.083 mm
Theta range for data collection	2.071 to 27.499 deg.
Limiting indices	-34<=h<=34, -34<=k<=34, -24<=l<=24
Reflections collected / unique	50056 / 5876 [R(int) = 0.2832]
Completeness to theta = 25.000	99.9 %
Absorption correction	Semi-empirical from equivalents
Max. and min. transmission	0.7456 and 0.6158
Refinement method	Full-matrix least-squares on F^2
Data / restraints / parameters	5876 / 0 / 282
Goodness-of-fit on F^2	1.014
Final R indices [I>2sigma(I)]	R1 = 0.0989, wR2 = 0.2466
R indices (all data)	R1 = 0.1984, wR2 = 0.3143
Extinction coefficient	n/a
Largest diff. peak and hole	2.147 and -1.552 $e.A^{-3}$

Table A2.3: Crystal data and structure refinement for $Tp^{Fc,Me}Tl$ (8).

Identification code	kla0243
Empirical formula	C42 H40 B Fe3 N6 Tl
Formula weight	1011.53
Temperature	200(2) K
Wavelength	0.71073 A
Crystal system, space group	Triclinic, P-1
Unit cell dimensions	a = 13.0542(7) A alpha = 108.3310(10) deg. b = 13.1951(7) A beta = 106.4350(10) deg. c = 13.3690(7) A gamma = 109.8410(10) deg.
Volume	1850.07(17) A^3
Z, Calculated density	2, 1.816 Mg/m^3
Absorption coefficient	5.535 mm^{-1}
F(000)	996
Crystal size	0.18 x 0.14 x 0.06 mm
Theta range for data collection	1.78 to 27.51 deg.
Limiting indices	-16<=h<=16, -17<=k<=17, -17<=l<=17
Reflections collected / unique	24505 / 8491 [R(int) = 0.0354]
Completeness to theta = 25.00	100.0 %
Absorption correction	Semi-empirical from equivalents
Max. and min. transmission	0.7324 and 0.4408
Refinement method	Full-matrix least-squares on F^2
Data / restraints / parameters	8491 / 0 / 484
Goodness-of-fit on F^2	1.012
Final R indices [I>2sigma(I)]	R1 = 0.0289, wR2 = 0.0599
R indices (all data)	R1 = 0.0367, wR2 = 0.0639
Largest diff. peak and hole	1.337 and -0.428 $e.A^{-3}$

Table A2.4: Crystal data and structure refinement for $Tp^{Fc}CoI$ (9).

Identification code	kla0428
Empirical formula	C39 H34 B Co Fe3 I N6
Formula weight	950.91
Temperature	200(2) K
Wavelength	0.71073 A
Crystal system, space group	Triclinic, P -1
Unit cell dimensions	a = 12.402(3) A alpha = 111.475(4) deg. b = 12.433(3) A beta = 113.079(4) deg. c = 13.719(3) A gamma = 95.079(4) deg.
Volume	1743.2(7) A^3
Z, Calculated density	2, 1.812 Mg/m^3
Absorption coefficient	2.616 mm^{-1}
F(000)	946
Crystal size	0.187 x 0.122 x 0.095 mm
Theta range for data collection	1.794 to 27.582 deg.
Limiting indices	-16<=h<=16, -16<=k<=16, -17<=l<=17
Reflections collected / unique	23374 / 8046 [R(int) = 0.0667]
Completeness to theta = 25.000	100.0 %
Absorption correction	Semi-empirical from equivalents
Max. and min. transmission	0.7456 and 0.6836
Refinement method	Full-matrix least-squares on F^2
Data / restraints / parameters	8046 / 0 / 463
Goodness-of-fit on F^2	1.001
Final R indices [I>2sigma(I)]	R1 = 0.0454, wR2 = 0.0842
R indices (all data)	R1 = 0.0746, wR2 = 0.0967
Extinction coefficient	n/a
Largest diff. peak and hole	0.648 and -0.795 $e.A^{-3}$

Table A2.5: Crystal data and structure refinement for $Tp^{Fc}CoCl$ (10).

Identification code	kla0427
Empirical formula	C39 H34 B Cl Co Fe3 N6
Formula weight	859.46
Temperature	200(2) K
Wavelength	0.71073 A
Crystal system, space group	Triclinic, P -1
Unit cell dimensions	a = 12.382(3) A alpha = 111.536(3) deg. b = 12.439(3) A beta = 111.956(3) deg. c = 13.495(3) A gamma = 97.765(3) deg.
Volume	1701.5(6) A^3
Z, Calculated density	2, 1.678 Mg/m^3
Absorption coefficient	1.852 mm^{-1}
F(000)	874
Crystal size	0.428 x 0.421 x 0.250 mm
Theta range for data collection	1.827 to 27.791 deg.
Limiting indices	-16<=h<=16, -16<=k<=16, -17<=l<=17
Reflections collected / unique	22439 / 7959 [R(int) = 0.0257]
Completeness to theta = 25.000	99.9 %
Absorption correction	Semi-empirical from equivalents
Max. and min. transmission	0.7456 and 0.6158
Refinement method	Full-matrix least-squares on F^2
Data / restraints / parameters	7959 / 0 / 463
Goodness-of-fit on F^2	1.038
Final R indices [I>2sigma(I)]	R1 = 0.0286, wR2 = 0.0705
R indices (all data)	R1 = 0.0362, wR2 = 0.0748
Extinction coefficient	n/a
Largest diff. peak and hole	0.423 and -0.271 $e.A^{-3}$

Table A2.6: Crystal data and structure refinement for $Tp^{Fc,Me}CoI$ (11).

Identification code	kla0473
Empirical formula	C42 H40 B Co Fe3 I N6
Formula weight	992.99
Temperature	200(2) K
Wavelength	0.71073 A
Crystal system, space group	Triclinic, P -1
Unit cell dimensions	a = 13.1097(9) A alpha = 105.4450(10) deg. b = 13.4283(9) A beta = 111.4820(10) deg. c = 13.4608(10) A gamma = 107.2710(10) deg.
Volume	1908.9(2) A^3
Z, Calculated density	2, 1.728 Mg/m^3
Absorption coefficient	2.393 mm^{-1}
F(000)	994
Crystal size	0.482 x 0.250 x 0.176 mm
Theta range for data collection	1.752 to 27.690 deg.
Limiting indices	-16<=h<=17, -16<=k<=17, -17<=l<=17
Reflections collected / unique	25708 / 8861 [R(int) = 0.0417]
Completeness to theta = 25.000	100.0 %
Absorption correction	Semi-empirical from equivalents
Max. and min. transmission	0.7456 and 0.5934
Refinement method	Full-matrix least-squares on F^2
Data / restraints / parameters	8861 / 0 / 490
Goodness-of-fit on F^2	1.031
Final R indices [I>2sigma(I)]	R1 = 0.0331, wR2 = 0.0724
R indices (all data)	R1 = 0.0455, wR2 = 0.0786
Extinction coefficient	n/a
Largest diff. peak and hole	0.451 and -0.600 $e.A^{-3}$

Table A2.7: Crystal data and structure refinement for $Tp^{Fc,Me}CoCl$ (12).

Identification code	kla0518
Empirical formula	C42 H40 B Cl Co Fe3 N6
Formula weight	901.54
Temperature	200(2) K
Wavelength	0.71073 A
Crystal system, space group	Triclinic, P -1
Unit cell dimensions	a = 13.0248(19) A alpha = 106.920(2) deg. b = 13.3161(19) A beta = 109.622(2) deg. c = 13.4371(19) A gamma = 108.091(2) deg.
Volume	1872.3(5) A^3
Z, Calculated density	2, 1.599 Mg/m^3
Absorption coefficient	1.687 mm^1
F(000)	922
Crystal size	0.415 x 0.332 x 0.106 mm
Theta range for data collection	1.793 to 27.629 deg.
Limiting indices	-16<=h<=16, -17<=k<=17, -17<=l<=17
Reflections collected / unique	25211 / 8677 [R(int) = 0.0370]
Completeness to theta = 25.000	100.0 %
Absorption correction	Semi-empirical from equivalents
Max. and min. transmission	0.7456 and 0.6334
Refinement method	Full-matrix least-squares on F^2
Data / restraints / parameters	8677 / 0 / 490
Goodness-of-fit on F^2	1.037
Final R indices [I>2sigma(I)]	R1 = 0.0368, wR2 = 0.0901
R indices (all data)	R1 = 0.0508, wR2 = 0.0979
Extinction coefficient	n/a
Largest diff. peak and hole	0.722 and -0.409 $e.A^{-3}$

Table A2.8: Crystal data and structure refinement for $Tp^{Fc,iPr}CoI$ (13).

Identification code	kla0040s
Empirical formula	C54 H64 B Co Fe3 I N6 O1.50
Formula weight	1185.30
Temperature	200(2) K
Wavelength	0.71073 A
Crystal system, space group	Monoclinic, C2/c
Unit cell dimensions	a = 46.517(9) A alpha = 90 deg. b = 9.480(3) A beta = 90.822(6) deg. c = 23.174(7) A gamma = 90 deg.
Volume	10218(4) A^3
Z, Calculated density	8, 1.541 Mg/m^3
Absorption coefficient	1.804 mm^{-1}
F(000)	4840
Crystal size	0.19 x 0.15 x 0.04 mm
Theta range for data collection	1.76 to 26.00 deg.
Limiting indices	-57<=h<=53, -11<=k<=11, -28<=l<=28
Reflections collected / unique	44008 / 10043 [R(int) = 0.0659]
Completeness to theta = 25.00	99.9 %
Absorption correction	Semi-empirical from equivalents
Max. and min. transmission	0.9281 and 0.7302
Refinement method	Full-matrix least-squares on F^2
Data / restraints / parameters	10043 / 0 / 550
Goodness-of-fit on F^2	1.027
Final R indices [I>2sigma(I)]	R1 = 0.0483, wR2 = 0.1128
R indices (all data)	R1 = 0.0685, wR2 = 0.1229
Largest diff. peak and hole	1.921 and -0.956 $e.A^{-3}$

Table A2.9: Crystal data and structure refinement for $Tp^{Fc,iPr*}CoCl$ (14).

Identification code	kla0006
Empirical formula	C52 H62 B Cl Co Fe3 N6 O
Formula weight	1059.82
Temperature	200(2) K
Wavelength	0.71073 A
Crystal system, space group	Triclinic, P1
Unit cell dimensions	a = 10.361(3) A alpha = 65.456(4) deg. b = 10.833(3) A beta = 71.075(5) deg. c = 12.697(4) A gamma = 81.803(5) deg.
Volume	1226.3(6) A^3
Z, Calculated density	1, 1.435 Mg/m^3
Absorption coefficient	1.301 mm^{-1}
F(000)	551
Crystal size	0.20 x 0.19 x 0.15 mm
Theta range for data collection	1.84 to 28.30 deg.
Limiting indices	-13<=h<=13, -14<=k<=14, -16<=l<=16
Reflections collected / unique	16745 / 11986 [R(int) = 0.0423]
Completeness to theta = 25.00	100.0 %
Absorption correction	Semi-empirical from equivalents
Max. and min. transmission	0.8308 and 0.7837
Refinement method	Full-matrix least-squares on F^2
Data / restraints / parameters	11986 / 3 / 597
Goodness-of-fit on F^2	1.014
Final R indices [I>2sigma(I)]	R1 = 0.0611, wR2 = 0.0899
R indices (all data)	R1 = 0.0966, wR2 = 0.0988
Absolute structure parameter	-0.006(14)
Largest diff. peak and hole	1.031 and -0.501 $e.A^{-3}$

Table A2.10: Crystal data and structure refinement for $Tp^{Fc,Me*}CoI$ (15).

Identification code	kla0502
Empirical formula	C42 H40 B Co Fe3 I N6
Formula weight	992.99
Temperature	200(2) K
Wavelength	0.71073 A
Crystal system, space group	Triclinic, P -1
Unit cell dimensions	a = 11.049(3) A alpha = 65.560(3) deg. b = 14.013(3) A beta = 70.566(3) deg. c = 14.758(4) A gamma = 77.988(3) deg.
Volume	1955.0(8) A^3
Z, Calculated density	2, 1.687 Mg/m^3
Absorption coefficient	2.337 mm^{-1}
F(000)	994
Crystal size	0.266 x 0.193 x 0.068 mm
Theta range for data collection	1.779 to 27.524 deg.
Limiting indices	-14<=h<=14, -18<=k<=18, -19<=l<=19
Reflections collected / unique	24866 / 8954 [R(int) = 0.0748]
Completeness to theta = 25.000	99.9 %
Absorption correction	Semi-empirical from equivalents
Max. and min. transmission	0.7456 and 0.5748
Refinement method	Full-matrix least-squares on F^2
Data / restraints / parameters	8954 / 0 / 490
Goodness-of-fit on F^2	1.035
Final R indices [I>2sigma(I)]	R1 = 0.0541, wR2 = 0.1172
R indices (all data)	R1 = 0.0987, wR2 = 0.1335
Extinction coefficient	n/a
Largest diff. peak and hole	0.974 and -1.553 $e.A^{-3}$

Table A2.11: Crystal data and structure refinement for $Tp^{Fc}Cu(CO)$ (16).

Identification code	kla0497
Empirical formula	C40 H34 B Cu Fe3 N6 O
Formula weight	856.63
Temperature	200(2) K
Wavelength	0.71073 A
Crystal system, space group	Triclinic, P -1
Unit cell dimensions	a = 12.428(5) A alpha = 111.125(6) deg. b = 12.469(5) A beta = 111.014(6) deg. c = 13.499(5) A gamma = 99.408(6) deg.
Volume	1715.6(11) A^3
Z, Calculated density	2, 1.658 Mg/m^3
Absorption coefficient	1.899 mm^{-1}
F(000)	872
Crystal size	0.421 x 0.338 x 0.148 mm
Theta range for data collection	1.815 to 27.443 deg.
Limiting indices	-15<=h<=16, -16<=k<=16, -17<=l<=17
Reflections collected / unique	22774 / 7807 [R(int) = 0.0381]
Completeness to theta = 25.000	100.0 %
Absorption correction	Semi-empirical from equivalents
Max. and min. transmission	0.7456 and 0.6335
Refinement method	Full-matrix least-squares on F^2
Data / restraints / parameters	7807 / 0 / 469
Goodness-of-fit on F^2	1.020
Final R indices [I>2sigma(I)]	R1 = 0.0332, wR2 = 0.0747
R indices (all data)	R1 = 0.0460, wR2 = 0.0815
Extinction coefficient	n/a
Largest diff. peak and hole	0.378 and -0.362 $e.A^{-3}$

Table A2.12: Crystal data and structure refinement for $Tp^{Fc,Me}Cu(CO)$ (17).

Identification code	kla0474
Empirical formula	C43 H40 B Cu Fe3 N6 O
Formula weight	898.71
Temperature	200(2) K
Wavelength	0.71073 A
Crystal system, space group	Triclinic, P -1
Unit cell dimensions	a = 13.158(5) A alpha = 107.447(7) deg. b = 13.255(5) A beta = 110.750(7) deg. c = 13.373(5) A gamma = 107.084(7) deg.
Volume	1859.8(13) A^3
Z, Calculated density	2, 1.605 Mg/m^3
Absorption coefficient	1.756 mm^{-1}
F(000)	920
Crystal size	0.181 x 0.110 x 0.046 mm
Theta range for data collection	1.802 to 27.688 deg.
Limiting indices	-17<=h<=17, -17<=k<=17, -17<=l<=17
Reflections collected / unique	24549 / 8622 [R(int) = 0.0819]
Completeness to theta = 25.000	100.0 %
Absorption correction	Semi-empirical from equivalents
Max. and min. transmission	0.7456 and 0.6075
Refinement method	Full-matrix least-squares on F^2
Data / restraints / parameters	8622 / 0 / 499
Goodness-of-fit on F^2	1.027
Final R indices [I>2sigma(I)]	R1 = 0.0551, wR2 = 0.1172
R indices (all data)	R1 = 0.1077, wR2 = 0.1355
Extinction coefficient	n/a
Largest diff. peak and hole	0.679 and -0.935 $e.A^{-3}$

Table A2.13: Crystal data and structure refinement for $Tp^{Fc,iPr**}Cu(CO)$ (18).

Identification code	kla0062a
Empirical formula	C49 H52 B Cu Fe3 N6 O
Formula weight	982.87
Temperature	200(2) K
Wavelength	0.71073 A
Crystal system, space group	Monoclinic, P2(1)/c
Unit cell dimensions	a = 22.714(6) A alpha = 90 deg. b = 10.306(3) A beta = 118.884(4) deg. c = 22.775(6) A gamma = 90 deg.
Volume	4668(2) A^3
Z, Calculated density	4, 1.399 Mg/m^3
Absorption coefficient	1.406 mm^{-1}
F(000)	2032
Crystal size	0.48 x 0.30 x 0.23 mm
Theta range for data collection	2.04 to 25.00 deg.
Limiting indices	-27<=h<=26, -12<=k<=12, -27<=l<=27
Reflections collected / unique	35809 / 8203 [R(int) = 0.1405]
Completeness to theta = 25.00	99.8 %
Absorption correction	Semi-empirical from equivalents
Max. and min. transmission	0.7409 and 0.5495
Refinement method	Full-matrix least-squares on F^2
Data / restraints / parameters	8203 / 0 / 556
Goodness-of-fit on F^2	1.028
Final R indices [I>2sigma(I)]	R1 = 0.0783, wR2 = 0.2064
R indices (all data)	R1 = 0.1504, wR2 = 0.2681
Largest diff. peak and hole	2.516 and -0.479 $e.A^{-3}$

Table A2.14: Crystal data and structure refinement for $Tp^{Fc,iPr*}Cu(CO)$ (19).

Identification code	kla0075
Empirical formula	C54 H63 B Cu Fe3 N6 O
Formula weight	1054.00
Temperature	200(2) K
Wavelength	0.71073 A
Crystal system, space group	Triclinic, P1
Unit cell dimensions	a = 10.362(10) A alpha = 65.079(16) deg. b = 10.861(10) A beta = 71.812(17) deg. c = 12.651(12) A gamma = 81.823(17) deg.
Volume	1227(2) A^3
Z, Calculated density	1, 1.427 Mg/m^3
Absorption coefficient	1.343 mm^{-1}
F(000)	549
Crystal size	0.38 x 0.29 x 0.27 mm
Theta range for data collection	1.85 to 28.44 deg.
Limiting indices	-13<=h<=13, -14<=k<=14, -16<=l<=16
Reflections collected / unique	16811 / 12065 [R(int) = 0.0402]
Completeness to theta = 25.00	100.0 %
Absorption correction	Semi-empirical from equivalents
Max. and min. transmission	0.7099 and 0.6329
Refinement method	Full-matrix least-squares on F^2
Data / restraints / parameters	12065 / 3 / 606
Goodness-of-fit on F^2	1.002
Final R indices [I>2sigma(I)]	R1 = 0.0568, wR2 = 0.0983
R indices (all data)	R1 = 0.0845, wR2 = 0.1097
Absolute structure parameter	-0.006(13)
Largest diff. peak and hole	0.881 and -0.378 $e.A^{-3}$

A.3 Supplimental Material for Chapter 4

All torsion angles were calculated by SHELXL following the conventions defined by Allen & Rogers.[4] Torsion angles were calculated from three interatomic vectors of four atom positions from the N atom proximal to the Co atom to the ferrocenyl Fe atom (Figure A3.1). Clockwise rotation of the Fc moiety relative to the pyrazolyl ring was assigned a positive torsion angle and counter clockwise rotation was assigned a negative torsion angle. The torsion angles for each complex have been arranged from largest (most positive) to the smallest (most negative) angle (Table A3.1).

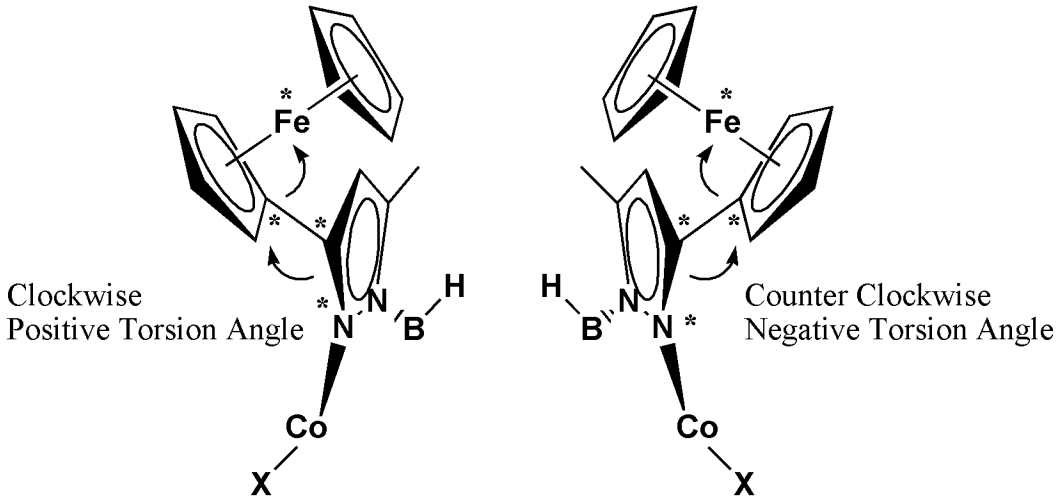

Figure A3.1: Torsion angle calculation for $Tp^{Fc,R}CoX$ compounds.

Table A3.1: Torsion angles for $Tp^{Fc,Me}CoX$ compounds.

Compound	Angle 1 (°)	Angle 2 (°)	Angle 3 (°)
$Tp^{Fc,Me}CoNO_3$	86.2(4)	70.1(5)	-121.3(3)
$Tp^{Fc,Me}CoOH$	84.0(5)	71.6(6)	-118.4(4)
$Tp^{Fc,Me}Co(\eta^3\text{-}C_3H_5)$	177.79(15)	137.72(19)	-141.38(18)
$Tp^{Fc,Me}Co(CO)$	83.9(5)	68.9(6)	-118.9(4)
$Tp^{Fc,Me}Co(O_2)$	81.9(3)	69.9(3)	-116.3(2)
$Tp^{Fc,Me}CoNAd$	136.3(6)	129.6(6)	127.3(6)
$Tp^{Fc,Me}CoN_4Ad_2$	127.2(2)	66.7(3)	-121.4(2)

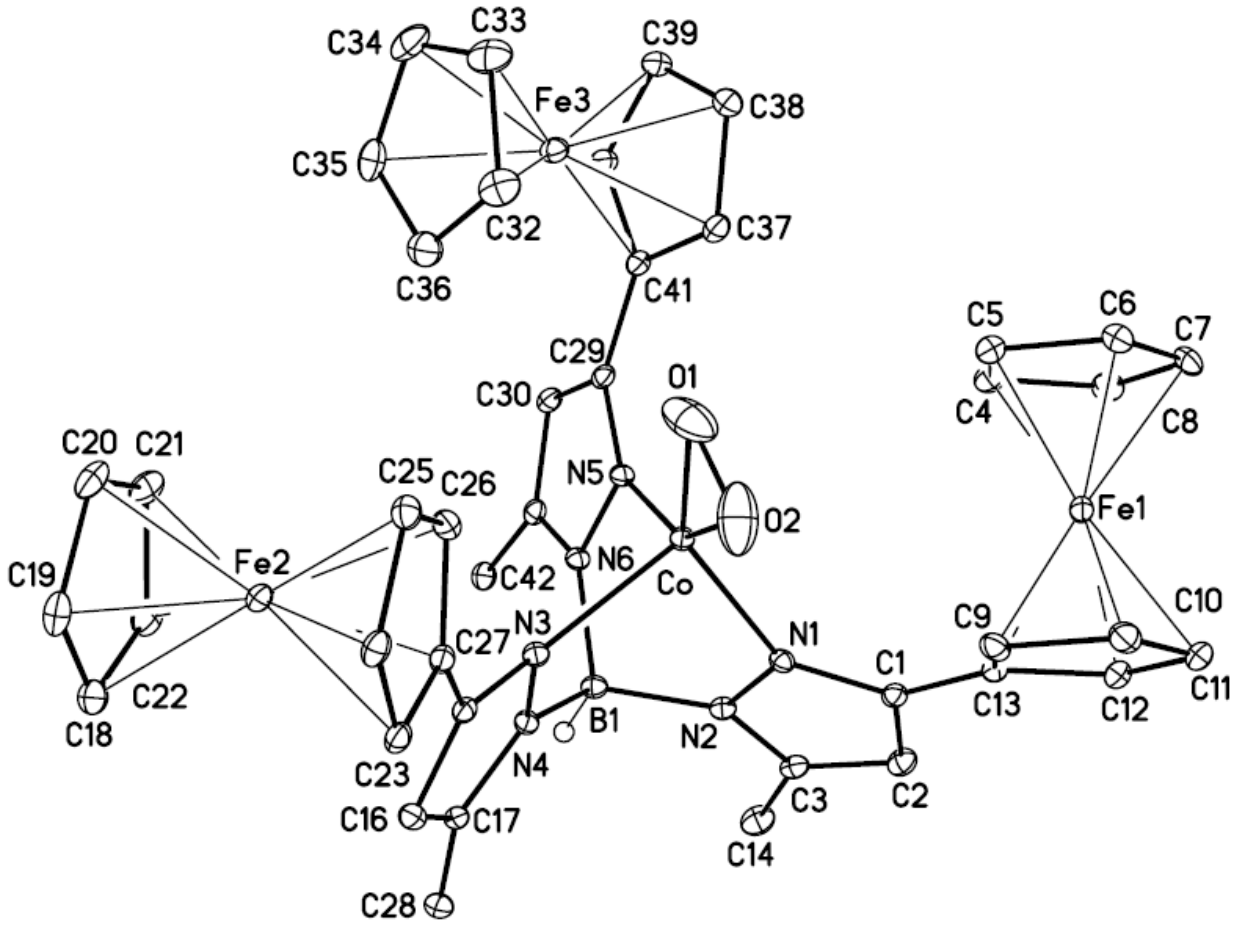

Figure A3.2: Molecular structure of $Tp^{Fc,Me}Co(O_2)$ (24) at the 30% probability level at 90K. Hydrogen atoms (except the boron bound hydrogen, H1B) have been removed for clarity.

Table A3.2: Selected interatomic distances (Å) and angles (°) for $Tp^{Fc,Me}Co(O_2)$ (24) at 90K.

Distances (Å)

Co-O(2)	1.830(3)	C(11)-C(12)	1.419(4)
Co-O(1)	1.855(2)	C(12)-C(13)	1.440(3)
Co-N(5)	2.027(2)	C(15)-C(16)	1.405(3)
Co-N(1)	2.049(2)	C(15)-C(27)	1.464(3)
Co-N(3)	2.070(2)	C(16)-C(17)	1.380(3)
B(1)-N(4)	1.542(3)	C(17)-C(28)	1.492(3)
B(1)-N(2)	1.546(3)	C(18)-C(19)	1.423(4)
B(1)-N(6)	1.557(3)	C(18)-C(22)	1.427(4)
O(1)-O(2)	1.235(4)	C(19)-C(20)	1.430(4)
N(1)-C(1)	1.350(3)	C(20)-C(21)	1.424(4)
N(1)-N(2)	1.379(3)	C(21)-C(22)	1.428(4)
N(2)-C(3)	1.351(3)	C(23)-C(24)	1.420(3)
N(3)-C(15)	1.345(3)	C(23)-C(27)	1.438(3)
N(3)-N(4)	1.382(3)	C(24)-C(25)	1.429(4)
N(4)-C(17)	1.349(3)	C(25)-C(26)	1.432(3)
N(5)-C(29)	1.350(3)	C(26)-C(27)	1.436(3)
N(5)-N(6)	1.384(3)	C(29)-C(30)	1.406(3)
N(6)-C(31)	1.349(3)	C(29)-C(41)	1.461(3)
C(1)-C(2)	1.400(3)	C(30)-C(31)	1.379(3)
C(1)-C(13)	1.466(3)	C(31)-C(42)	1.495(3)
C(2)-C(3)	1.379(4)	C(32)-C(36)	1.422(4)
C(3)-C(14)	1.484(3)	C(32)-C(33)	1.427(4)
C(4)-C(8)	1.421(4)	C(33)-C(34)	1.417(5)
C(4)-C(5)	1.435(4)	C(34)-C(35)	1.432(4)
C(5)-C(6)	1.424(4)	C(35)-C(36)	1.427(4)
C(6)-C(7)	1.420(4)	C(37)-C(38)	1.428(4)
C(7)-C(8)	1.431(4)	C(37)-C(41)	1.440(4)
C(9)-C(10)	1.432(4)	C(38)-C(39)	1.427(4)
C(9)-C(13)	1.440(3)	C(39)-C(40)	1.426(4)
C(10)-C(11)	1.438(4)	C(40)-C(41)	1.437(3)

Angles (°)

O(2)-Co-O(1)	39.14(14)	O(2)-Co-N(3)	103.74(12)
O(2)-Co-N(5)	152.02(14)	O(1)-Co-N(3)	113.21(10)
O(1)-Co-N(5)	113.27(12)	N(5)-Co-N(3)	91.73(8)
O(2)-Co-N(1)	110.54(12)	N(1)-Co-N(3)	93.17(8)
O(1)-Co-N(1)	142.20(12)	N(4)-B(1)-N(2)	108.76(19)
N(5)-Co-N(1)	91.38(8)	N(4)-B(1)-N(6)	109.63(19)

N(2)-B(1)-N(6)	108.03(19)	C(9)-C(13)-C(1)	128.5(2)
O(2)-O(1)-Co	69.36(17)	N(3)-C(15)-C(16)	109.7(2)
O(1)-O(2)-Co	71.49(18)	N(3)-C(15)-C(27)	123.1(2)
C(1)-N(1)-N(2)	106.13(19)	C(16)-C(15)-C(27)	127.1(2)
C(1)-N(1)-Co	139.56(17)	C(17)-C(16)-C(15)	105.8(2)
N(2)-N(1)-Co	113.25(14)	N(4)-C(17)-C(16)	108.1(2)
C(3)-N(2)-N(1)	110.2(2)	N(4)-C(17)-C(28)	122.5(2)
C(3)-N(2)-B(1)	129.8(2)	C(16)-C(17)-C(28)	129.4(2)
N(1)-N(2)-B(1)	119.99(19)	C(19)-C(18)-C(22)	107.9(2)
C(15)-N(3)-N(4)	106.33(19)	C(18)-C(19)-C(20)	108.1(2)
C(15)-N(3)-Co	137.98(16)	C(21)-C(20)-C(19)	107.9(2)
N(4)-N(3)-Co	112.30(14)	C(20)-C(21)-C(22)	108.0(2)
C(17)-N(4)-N(3)	109.99(19)	C(18)-C(22)-C(21)	108.0(2)
C(17)-N(4)-B(1)	130.1(2)	C(24)-C(23)-C(27)	107.8(2)
N(3)-N(4)-B(1)	119.82(19)	C(23)-C(24)-C(25)	109.0(2)
C(29)-N(5)-N(6)	106.45(19)	C(24)-C(25)-C(26)	107.2(2)
C(29)-N(5)-Co	140.17(17)	C(25)-C(26)-C(27)	108.4(2)
N(6)-N(5)-Co	113.01(14)	C(26)-C(27)-C(23)	107.5(2)
C(31)-N(6)-N(5)	110.13(19)	C(26)-C(27)-C(15)	128.3(2)
C(31)-N(6)-B(1)	129.4(2)	C(23)-C(27)-C(15)	124.0(2)
N(5)-N(6)-B(1)	120.21(19)	N(5)-C(29)-C(30)	109.2(2)
N(1)-C(1)-C(2)	109.7(2)	N(5)-C(29)-C(41)	124.8(2)
N(1)-C(1)-C(13)	125.0(2)	C(30)-C(29)-C(41)	126.0(2)
C(2)-C(1)-C(13)	125.2(2)	C(31)-C(30)-C(29)	106.5(2)
C(3)-C(2)-C(1)	106.2(2)	N(6)-C(31)-C(30)	107.7(2)
N(2)-C(3)-C(2)	107.8(2)	N(6)-C(31)-C(42)	122.9(2)
N(2)-C(3)-C(14)	122.9(2)	C(30)-C(31)-C(42)	129.4(2)
C(2)-C(3)-C(14)	129.4(2)	C(36)-C(32)-C(33)	108.0(3)
C(8)-C(4)-C(5)	108.3(2)	C(34)-C(33)-C(32)	108.1(3)
C(6)-C(5)-C(4)	107.9(2)	C(33)-C(34)-C(35)	108.2(3)
C(7)-C(6)-C(5)	107.7(2)	C(36)-C(35)-C(34)	107.6(3)
C(6)-C(7)-C(8)	108.8(2)	C(32)-C(36)-C(35)	108.1(3)
C(4)-C(8)-C(7)	107.3(2)	C(38)-C(37)-C(41)	108.1(2)
C(10)-C(9)-C(13)	107.7(2)	C(39)-C(38)-C(37)	108.4(2)
C(9)-C(10)-C(11)	108.1(2)	C(40)-C(39)-C(38)	107.8(2)
C(12)-C(11)-C(10)	108.2(2)	C(39)-C(40)-C(41)	108.7(2)
C(11)-C(12)-C(13)	108.2(2)	C(40)-C(41)-C(37)	107.0(2)
C(12)-C(13)-C(9)	107.7(2)	C(40)-C(41)-C(29)	123.7(2)
C(12)-C(13)-C(1)	123.5(2)	C(37)-C(41)-C(29)	129.3(2)

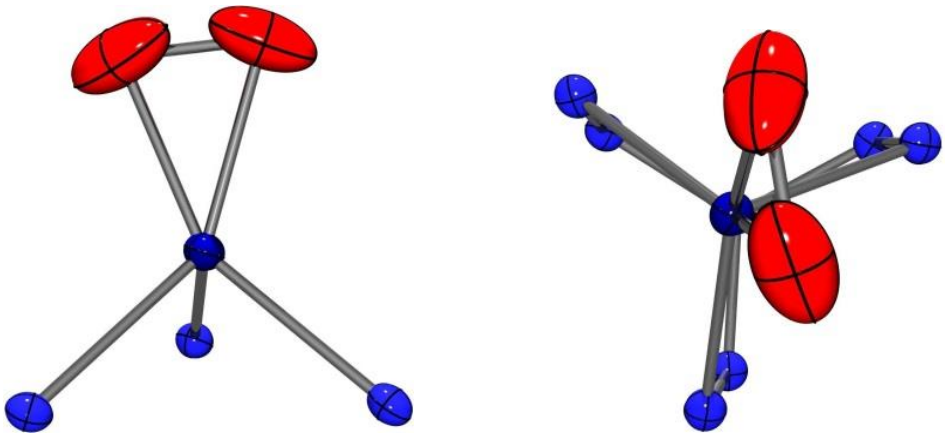

Figure A3.3: Side view (left) and top view (right) of disordered oxygens of the $Tp^{Fc,Me}Co(O_2)$ (24) at 90 K.

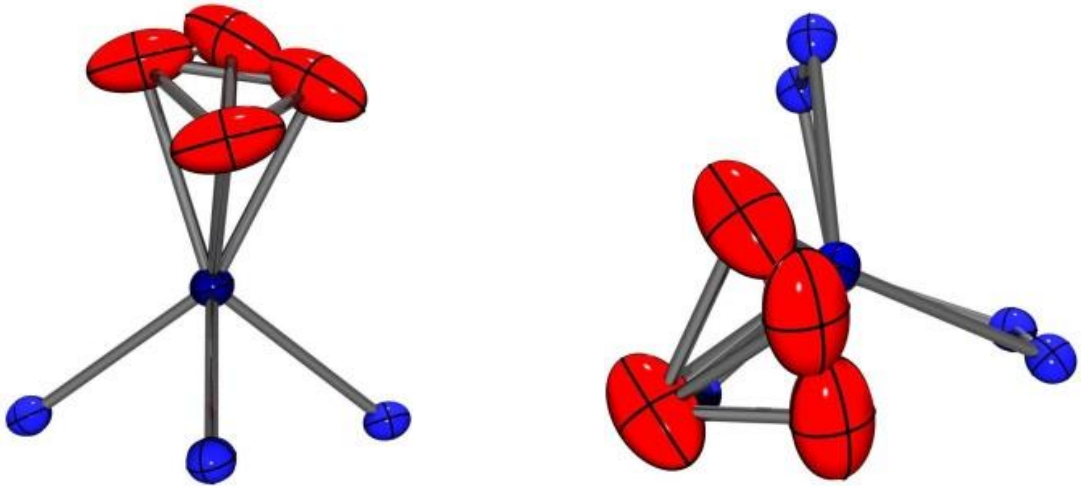

Figure A3.4: Side view (left) and top view (right) of the modeled positional disorder of the oxygens of the $Tp^{Fc,Me}Co(O_2)$ (24) at 90 K with an O-O distance 1.40 Å and 1.377(19) Å. This disorder exists in a 83/17 population percentage.

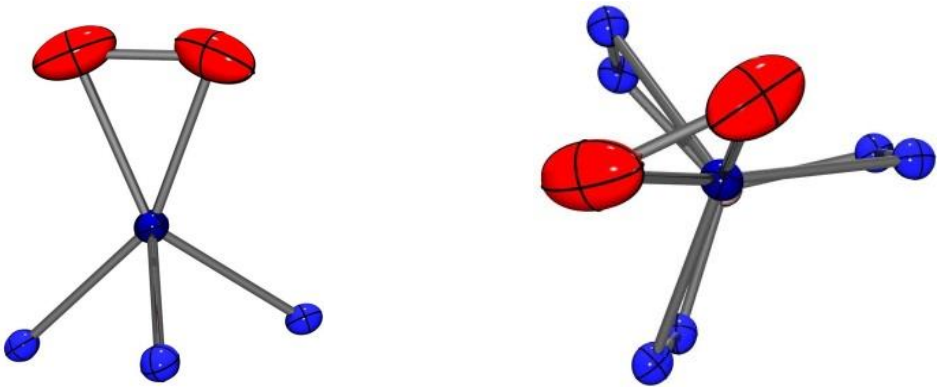

Figure 3A.5: Side view (left) and top view (right) of the constrained oxygens of the $Tp^{Fc,Me}Co(O_2)$ (24) at 90 K.

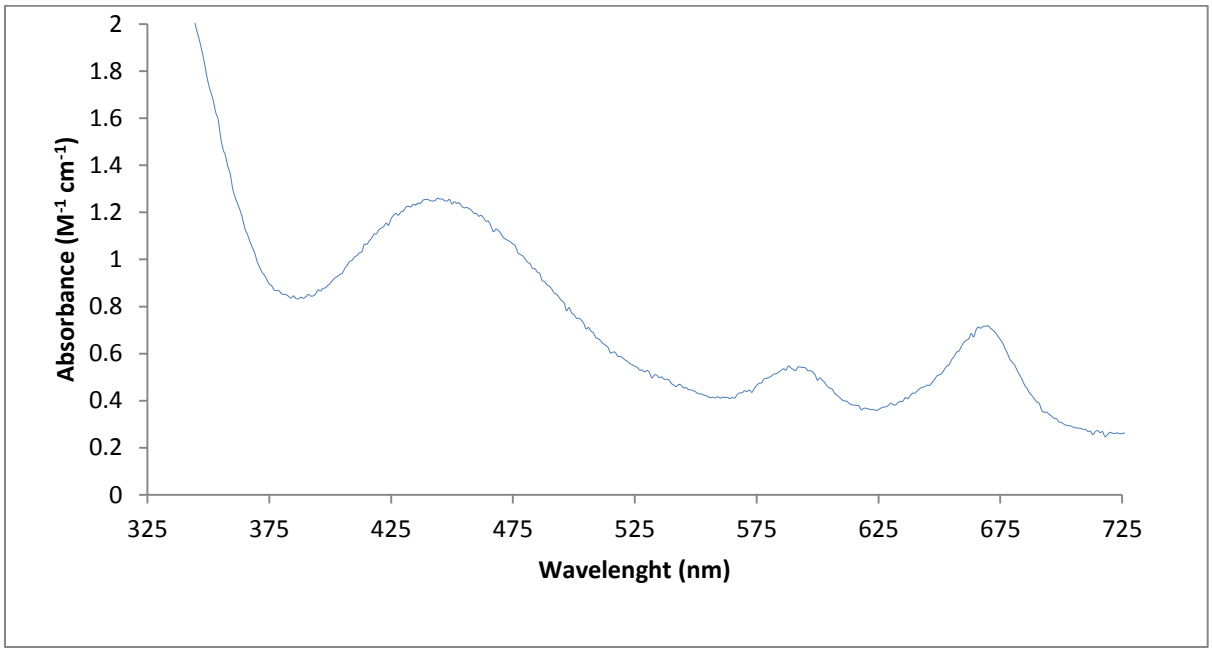

Figure A3.6: UV-Vis spectrum of 21 in THF (1.1 mM) at RT.

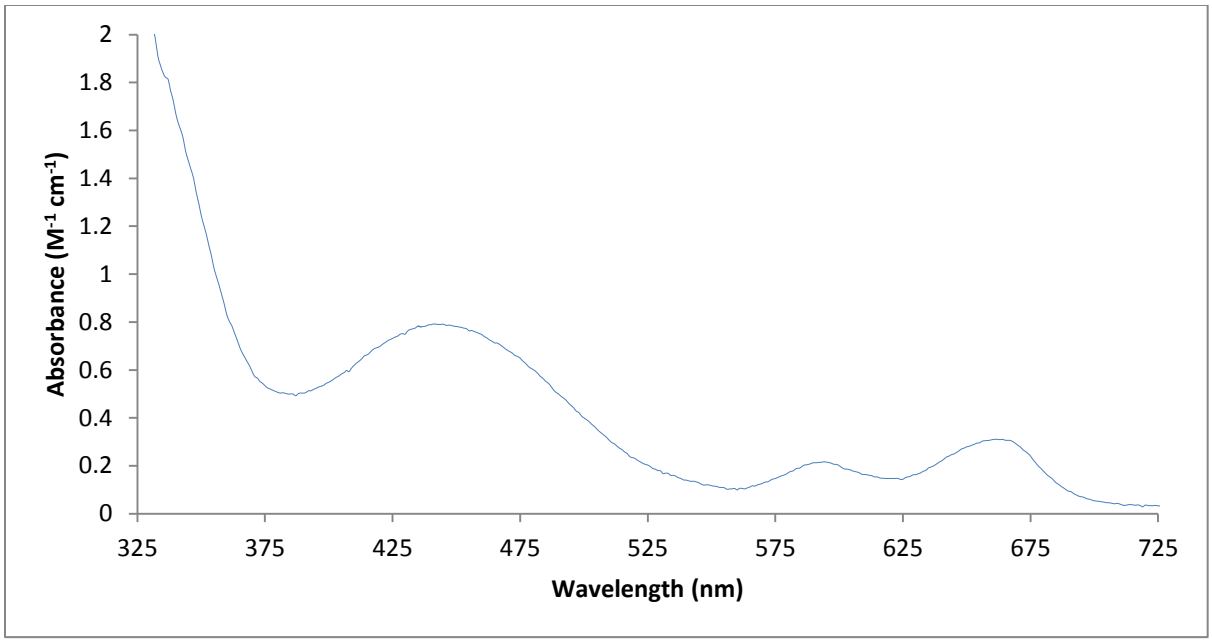

Figure A3.7: UV-Vis spectrum after warm up of the reaction of 21 with $Ph(Me)_2COOH$ in THF (1.1 mM) at -78 °C.

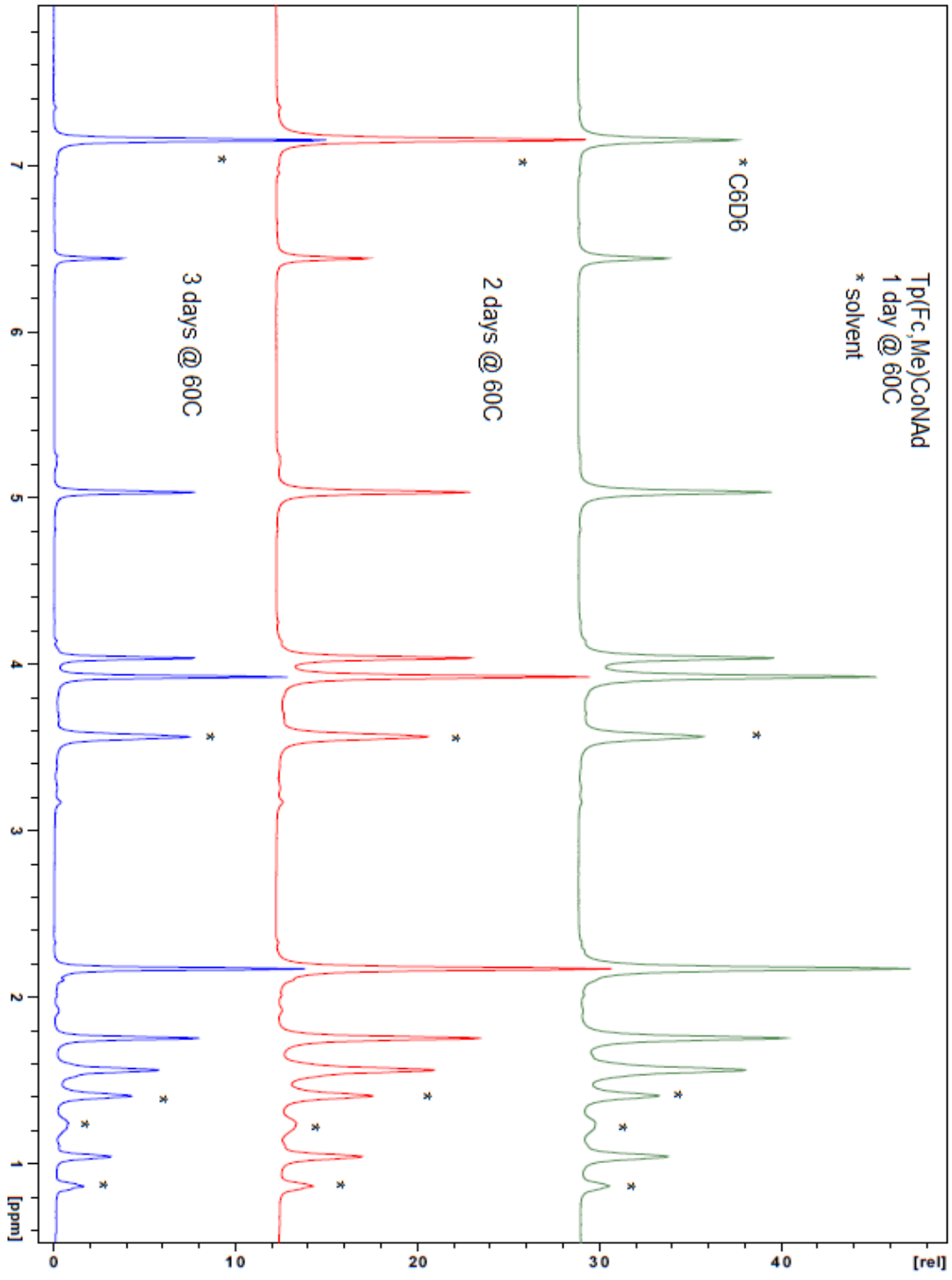

Figure A3.8: Thermal stability of $Tp^{Fc,Me}$CoNAd with THF and pentane solvent in C_6D_6 at 60 °C.

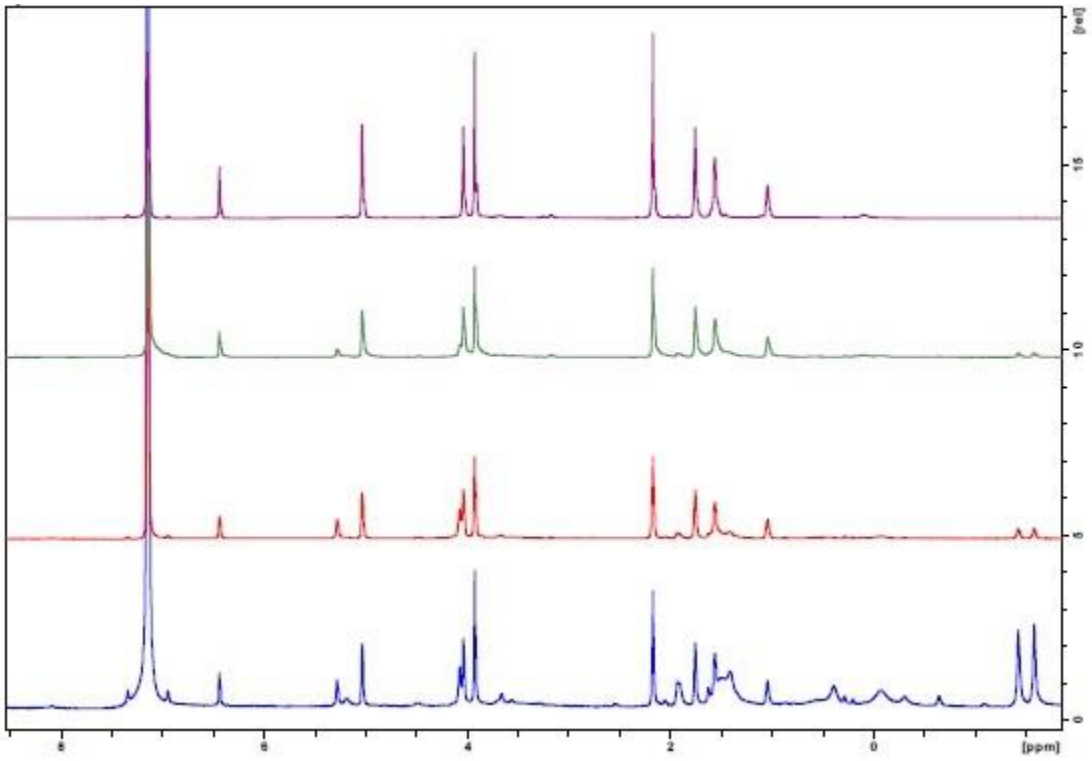

Figure A3.9: Thermal stability of $Tp^{Fc,Me}CoNAd$ in C_6D_6 at 100 °C.

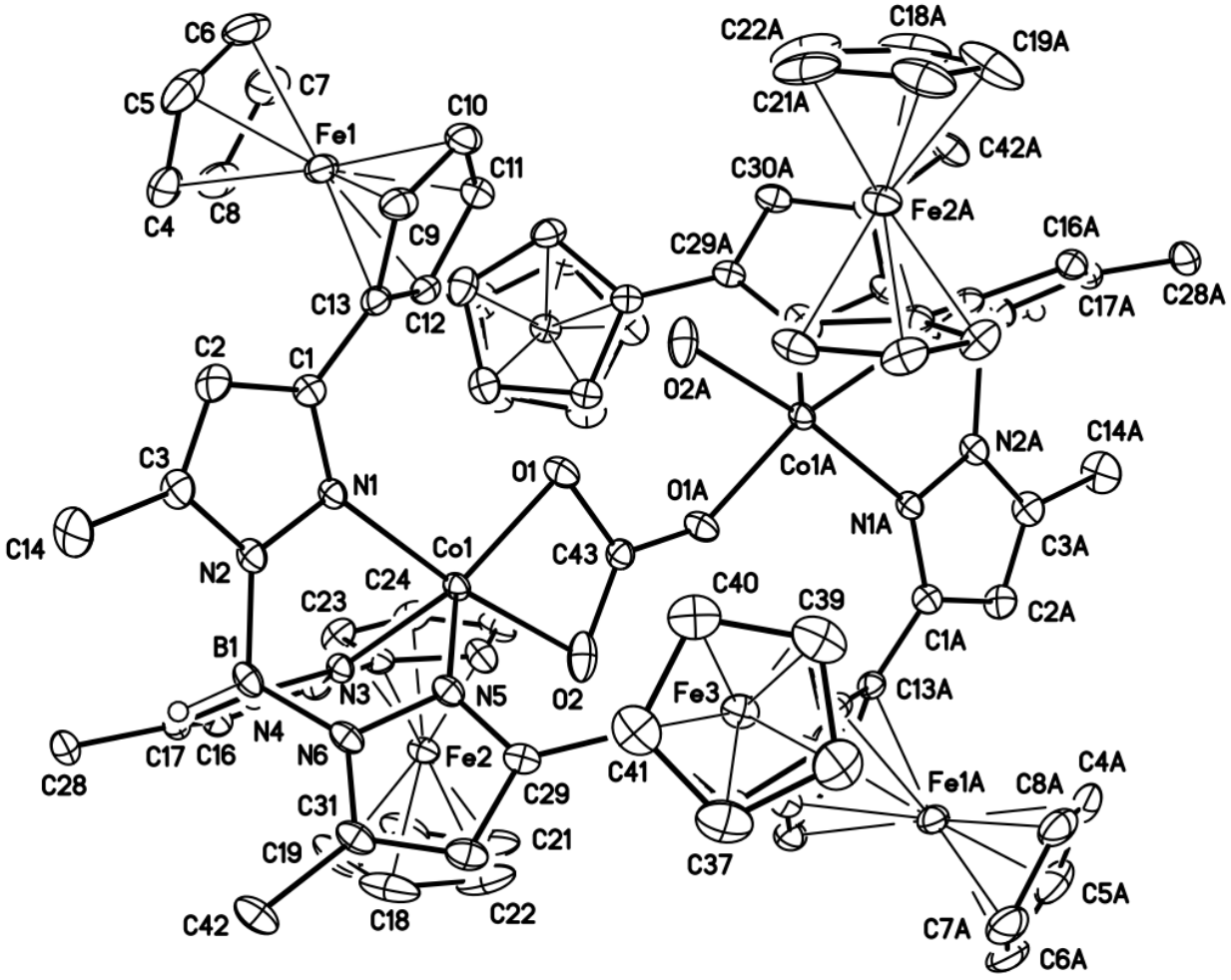

Figure A3.10: Molecular structure of $[Tp^{Fc,Me}Co]_2(\mu\text{-}CO_3)(H_2O)$ at the 30% probability level. Hydrogen atoms (except the boron bound hydrogen, H1B) have been removed for clarity.

Table A3.3: Crystal data and structure refinement for $Tp^{Fc,Me}CoNO_3$ (20).

Identification code	kla0528
Empirical formula	C42 H40 B Co Fe3 N7 O3
Formula weight	928.10
Temperature	200(2) K
Wavelength	0.71073 A
Crystal system, space group	Triclinic, P -1
Unit cell dimensions	a = 13.3463(12) A alpha = 112.443(2) deg. b = 13.3541(12) A beta = 107.111(2) deg. c = 13.4012(12) A gamma = 105.800(2) deg.
Volume	1899.4(3) A^3
Z, Calculated density	2, 1.623 Mg/m^3
Absorption coefficient	1.604 mm^{-1}
F(000)	950
Crystal size	0.409 x 0.236 x 0.129 mm
Theta range for data collection	1.773 to 27.571 deg.
Limiting indices	-17<=h<=17, -17<=k<=17, -17<=l<=17
Reflections collected / unique	25409 / 8735 [R(int) = 0.0663]
Completeness to theta = 25.000	100.0 %
Absorption correction	Semi-empirical from equivalents
Max. and min. transmission	0.7456 and 0.6413
Refinement method	Full-matrix least-squares on F^2
Data / restraints / parameters	8735 / 0 / 517
Goodness-of-fit on F^2	0.850
Final R indices [I>2sigma(I)]	R1 = 0.0484, wR2 = 0.1259
R indices (all data)	R1 = 0.0806, wR2 = 0.1546
Extinction coefficient	n/a
Largest diff. peak and hole	0.512 and -0.460 $e.A^{-3}$

Table A3.4: Crystal data and structure refinement for $Tp^{Fc,Me}CoOH$ (21).

Identification code	kla0467
Empirical formula	C42 H41 B Co Fe3 N6 O
Formula weight	883.10
Temperature	200(2) K
Wavelength	0.71073 A
Crystal system, space group	Triclinic, P -1
Unit cell dimensions	a = 13.095(5) A alpha = 107.623(5) deg. b = 13.284(5) A beta = 110.279(5) deg. c = 13.438(5) A gamma = 107.456(5) deg.
Volume	1863.2(11) A3
Z, Calculated density	2, 1.574 Mg/m^3
Absorption coefficient	1.626 mm^{-1}
F(000)	906
Crystal size	0.355 x 0.305 x 0.157 mm
Theta range for data collection	1.889 to 27.670 deg.
Limiting indices	-16<=h<=17, -17<=k<=17, -17<=l<=17
Reflections collected / unique	24122 / 8608 [R(int) = 0.0642]
Completeness to theta = 25.000	99.9 %
Absorption correction	Semi-empirical from equivalents
Max. and min. transmission	0.7456 and 0.6344
Refinement method	Full-matrix least-squares on F^2
Data / restraints / parameters	8608 / 0 / 490
Goodness-of-fit on F^2	1.037
Final R indices [I>2sigma(I)]	R1 = 0.0568, wR2 = 0.1362
R indices (all data)	R1 = 0.0951, wR2 = 0.1566
Extinction coefficient	n/a
Largest diff. peak and hole	1.656 and -0.839 $e.A^{-3}$

Table A3.5: Crystal data and structure refinement for $Tp^{Fc,Me}Co(\eta^3\text{-}C_3H_5)$ (22).

Identification code	kla0304
Empirical formula	C57 H69 B Co Fe3 N6 O6
Formula weight	1171.47
Temperature	200(2) K
Wavelength	0.71073 A
Crystal system, space group	Monoclinic, C 2/c
Unit cell dimensions	a = 33.152(4) A alpha = 90 deg. b = 10.7340(11) A beta = 111.958(2) deg. c = 32.920(4) A gamma = 90 deg.
Volume	10865(2) A^3
Z, Calculated density	8, 1.432 Mg/m^3
Absorption coefficient	1.141 mm^{-1}
F(000)	4888
Crystal size	0.556 x 0.480 x 0.236 mm
Theta range for data collection	1.487 to 27.516 deg.
Limiting indices	-42<=h<=42, -13<=k<=13, -42<=l<=42
Reflections collected / unique	63118 / 12453 [R(int) = 0.0510]
Completeness to theta = 25.000	99.9 %
Absorption correction	Semi-empirical from equivalents
Max. and min. transmission	0.7456 and 0.6573
Refinement method	Full-matrix least-squares on F^2
Data / restraints / parameters	12453 / 438 / 660
Goodness-of-fit on F^2	1.029
Final R indices [I>2sigma(I)]	R1 = 0.0392, wR2 = 0.1062
R indices (all data)	R1 = 0.0495, wR2 = 0.1131
Extinction coefficient	n/a
Largest diff. peak and hole	0.847 and -0.455 $e.A^{-3}$

Table A3.6: Crystal data and structure refinement for $Tp^{Fc,Me}Co(CO)$ (23).

Identification code	kla0317
Empirical formula	C43 H40 B Co Fe3 N6 O
Formula weight	894.10
Temperature	200(2) K
Wavelength	0.71073 A
Crystal system, space group	Triclinic, P -1
Unit cell dimensions	a = 13.123(5) A alpha = 107.565(6) deg. b = 13.256(5) A beta = 110.927(6) deg. c = 13.424(5) A gamma = 106.935(6) deg.
Volume	1859.0(12) A^3
Z, Calculated density	2, 1.597 Mg/m^3
Absorption coefficient	1.631 mm^{-1}
F(000)	916
Crystal size	0.352 x 0.214 x 0.126 mm
Theta range for data collection	1.803 to 27.201 deg.
Limiting indices	-16<=h<=16, -16<=k<=16, -17<=l<=17
Reflections collected / unique	15947 / 8143 [R(int) = 0.0614]
Completeness to theta = 25.000	99.6 %
Absorption correction	Semi-empirical from equivalents
Max. and min. transmission	0.7455 and 0.5151
Refinement method	Full-matrix least-squares on F^2
Data / restraints / parameters	8143 / 0 / 502
Goodness-of-fit on F^2	1.013
Final R indices [I>2sigma(I)]	R1 = 0.0667, wR2 = 0.1695
R indices (all data)	R1 = 0.0860, wR2 = 0.1918
Extinction coefficient	n/a
Largest diff. peak and hole	1.838 and -1.075 $e.A^{-3}$

Table A3.7: Crystal data and structure refinement for $Tp^{Fc,Me}Co(O_2)$ (24).

Identification code	kla0315
Empirical formula	C42 H40 B Co Fe3 N6 O2
Formula weight	898.09
Temperature	200(2) K
Wavelength	0.71073 A
Crystal system, space group	Triclinic, P-1
Unit cell dimensions	a = 13.0662(7) A alpha = 107.7150(10) deg. b = 13.2260(7) A beta = 109.4380(10) deg. c = 13.3755(7) A gamma = 108.3280(10) deg.
Volume	1840.62(17) A^3
Z, Calculated density	2, 1.620 Mg/m^3
Absorption coefficient	1.649 mm^{-1}
F(000)	920
Crystal size	0.46 x 0.29 x 0.06 mm
Theta range for data collection	1.81 to 27.49 deg.
Limiting indices	-16<=h<=16, -17<=k<=17, -17<=l<=17
Reflections collected / unique	23864 / 8412 [R(int) = 0.0215]
Completeness to theta = 25.00	100.0 %
Absorption correction	Semi-empirical from equivalents
Max. and min. transmission	0.9075 and 0.5169
Refinement method	Full-matrix least-squares on F^2
Data / restraints / parameters	8412 / 0 / 502
Goodness-of-fit on F^2	1.006
Final R indices [I>2sigma(I)]	R1 = 0.0327, wR2 = 0.0862
R indices (all data)	R1 = 0.0378, wR2 = 0.0905
Largest diff. peak and hole	0.746 and -0.737 $e.A^{-3}$

Table A3.8: Crystal data and structure refinement for $Tp^{Fc,Me}CoNAd$ (25).

Identification code	kla0290
Empirical formula	C67 H70 B Co Fe3 N7
Formula weight	1210.59
Temperature	200(2) K
Wavelength	0.71073 A
Crystal system, space group	Triclinic, P-1
Unit cell dimensions	a = 12.601(5) A alpha = 83.513(10) deg. b = 14.977(7) A beta = 75.164(9) deg. c = 16.457(7) A gamma = 74.051(9) deg.
Volume	2884(2) A^3
Z, Calculated density	2, 1.394 Mg/m^3
Absorption coefficient	1.071 mm^{-1}
F(000)	1262
Crystal size	0.26 x 0.09 x 0.06 mm
Theta range for data collection	1.28 to 27.58 deg.
Limiting indices	-16<=h<=16, -19<=k<=19, -21<=l<=21
Reflections collected / unique	38061 / 13311 [R(int) = 0.1810]
Completeness to theta = 25.00	100.0 %
Absorption correction	Semi-empirical from equivalents
Max. and min. transmission	0.9346 and 0.7675
Refinement method	Full-matrix least-squares on F^2
Data / restraints / parameters	13311 / 111 / 685
Goodness-of-fit on F^2	0.848
Final R indices [I>2sigma(I)]	R1 = 0.0787, wR2 = 0.1632
R indices (all data)	R1 = 0.2078, wR2 = 0.2447
Largest diff. peak and hole	0.562 and -0.523 $e.A^{-3}$

Table A3.9: Crystal data and structure refinement for $Tp^{Fc,Me}CoN_4Ad_2$ (26).

Identification code	kla0265
Empirical formula	C62 H70 B Co Fe3 N10
Formula weight	1192.57
Temperature	200(2) K
Wavelength	0.71073 A
Crystal system, space group	Triclinic, P-1
Unit cell dimensions	a = 12.9344(11) A alpha = 93.352(2) deg. b = 13.8880(12) A beta = 111.443(2) deg. c = 16.8925(15) A gamma = 97.223(2) deg.
Volume	2784.0(4) A^3
Z, Calculated density	2, 1.423 Mg/m^3
Absorption coefficient	1.109 mm^{-1}
F(000)	1244
Crystal size	0.16 x 0.11 x 0.07 mm
Theta range for data collection	1.49 to 26.37 deg.
Limiting indices	-16<=h<=16, -17<=k<=17, -21<=l<=21
Reflections collected / unique	34142 / 11391 [R(int) = 0.0331]
Completeness to theta = 25.00	99.9 %
Absorption correction	Semi-empirical from equivalents
Max. and min. transmission	0.9294 and 0.8442
Refinement method	Full-matrix least-squares on F^2
Data / restraints / parameters	11391 / 447 / 700
Goodness-of-fit on F^2	1.017
Final R indices [I>2sigma(I)]	R1 = 0.0380, wR2 = 0.0868
R indices (all data)	R1 = 0.0564, wR2 = 0.0952
Largest diff. peak and hole	0.541 and -0.545 $e.A^{-3}$

References

1. Allen, F. H. and Rogers, D., *Acta. Cryst. B.*, **1969**, *25*, 1326.
2. Guzei, I. A., Wendt, M., *Dalton Trans*., **2006**, 3991
3. Yoon, K., and Parkin, G., *Polyhedron*, **1995**, *6*. 811.
4. Allen, F. H., *Acta Cryst*., **2002**, *B58*, 380.